SPLIT ATTRACTOR FLOW TREES AND BLACK HOLE ENTROPY IN TYPE II STRING THEORY

Thomas WYDER

Supervisor:
Prof. Dr. W. Troost, K.U. Leuven

Members of the
Examination Committee:
Prof. Dr. D. Bollé, K.U. Leuven, president
Prof. Dr. F. Denef, K.U. Leuven / Harvard University
Prof. Dr. M. Fannes, K.U. Leuven
Prof. Dr. M. Reineke, Bergische Universität Wuppertal
Prof. Dr. S. Vandoren, Universiteit Utrecht
Prof. Dr. A. Van Proeyen, K.U. Leuven

Dissertation presented in
partial fulfilment of the
requirements for the
degree of Doctor of
Science

October 2009

ISBN 978-90-8649-290-9
D/2009/10.705/68

Contents

Introduction

Readers scan these first words of my Ph.D. thesis with different intentions. Therefore, the author's first statements are meant to help the reader find (at best) what he might be looking for. Three parts of this thesis should be accessible to any non-expert. These are:

1. *The introduction*: in this part, the author explains the general context of his research, in two segments. First, the field of research called 'string theory' is sketched. This is followed by a short orientation on the topic of 'black holes'. The introduction is rounded off by a short overview of the content of this thesis, allowing the reader to decide, whether, and if he answers this question to himself affirmatively, to which part he would like to turn to continue reading. The introduction should allow any reader to understand the topic of this Ph.D. and put the title of the thesis in context. It should serve as a layman's guide to the first two main chapters of this thesis.

2. *The conclusions*: while the more specialized reader will find separate and more scientific introductions, summaries and discussions at the beginning and at the end of each chapter, the conclusions as a separate section are intended to be far more accessible. In particular, they consist of a short description of the research performed during the author's Ph.D. studies, using a metaphor. Namely, the type of research on black holes in string theory will be compared to studying genomes in microbiology. The analogies are sometimes far from perfect, but they do allow to transport some intuition on the author's work with relative ease. The concluding discussion is meant as a layman's guide to chapters 3-5 of this thesis.

3. *The part of the appendix titled 'Dutch summary'*: finally, there is a short description of the content of this thesis in Dutch. This parallels many explanations put forward in the introduction and the conclusions, but is briefer. However, it enjoys the fact of being written in another beautiful language, as the title suggests.

The main part of this Ph.D. thesis consists of five chapters. Three (chapters 1-3) introduce the context in which the research of the author has been performed. These first three chapters appear in the order of increasing specialization. Two (chapters 4 and 5) describe the author's main research results.

Finally, some minimal reading suggestions are given for expert readers with various backgrounds to take shortcuts to the most interesting parts of this thesis. The sections and chapters indicated below are suggested *in addition to the chapter introductions and*

summaries / overviews given at the beginning / end of each main chapter as well as the concluding discussion.

- A physicist working in a field different from string theory is advised to read: 1.1, 2.1, 2.3, 2.4.2 – 2.4.4, 3.3. This should allow some understanding of the core chapter of this thesis: 4.

- A string theorist familiar with the field of research in general, but not with the specific techniques used in these studies, is suggested to read: 2.1 – 2.3, 2.4.2 – 2.4.4, 3.3, followed by chapters 4 and 5.

- An expert familiar with the techniques used in this thesis can of course move on to chapters 4 and 5, immediately.

- A reader with interest in the connection of the author's results to algebraic geometry will find the results of interest in chapter 4. Sections 2.1, 2.3, 2.4.2 - 2.4.4 and 3.3 should provide some background on the physics involved. The appendix A.1 should clarify notation and the use of some mathematical concepts involved.

As was mentioned before, this introduction will be rounded off with a detailed overview (in more technical terms) over the content of this thesis. This overview precedes two sections, written for a more general public, one on 'string theory' and one on 'black holes'.

String theory as a candidate for a quantum theory of all four forces

It does not seem misplaced to name the historic phenomenon of unification as well as the inner consistency, simplicity paired with abstraction, and the connected mathematical elegance as an incitement for string theorists. Unification in theoretical physics can be followed back through the centuries. It denotes the ascription of different phenomena to common laws of nature. As an example, consider how electricity and magnetism, which were understood as two independent physical phenomena for a long time, were both explained by the laws of electromagnetism, in the second half of the 19th century. With some hesitation one might summarize nowadays' stand of unification of theories in theoretical physics as follows:

- *The microcosmos*: The three forces (amongst which electromagnetism) governing 'the very small' are described by quantum field theories. Particles acquire the interpretation of propagating disturbances of quantum fields, and all particles are divided into two fundamental categories: fermions, with a half-integer spin (an inner quantum mechanical angular momentum); e.g. an electron, and bosons, with an integer spin; e.g. a photon. This fundamental division in two parts might to the aesthete be perceived as disturbing, if he would like 'everything to be of the same make'.

- *The macrocosmos*: The weakest force, gravity, becomes the only relevant force on large scales. Gravity is described by general relativity theory, founded by Albert Einstein, in 1915.

One would like to have a theory, doing justice, at the same time to gravity and the macrocosmos, as well as the microcosmos and therefore the other three forces.

It seems fair to say that the majority of physicists accept, according to the findings from general relativity theory, that our universe contains black holes. Indirect evidence for the actual existence of many such objects has now been found, and it is a widely held belief, that galaxies contain super-massive black holes at their centers. Black holes are extremely massive, thus gravity is important, but they are also dense enough (implying a high energy density), that quantum effects must not be neglected, at least near the core of the matter making up a black hole. To describe them properly, a theory of quantum gravity, or maybe of all four forces is unavoidable. Black holes will be the topic of the next section.

Another central idea which dates from around the beginning of the 1970's is supersymmetry. Supersymmetry relates one partner-boson to every fermion and vice versa. It therefore provides for a common origin of the two sorts of particles. Furthermore, supersymmetry also implies many other desirable (and some undesirable) virtues, both from the viewpoint of theory and experiment, and supersymmetry is also one of the main points under investigation of the projects begun at CERN. String theory automatically involves supersymmetry for inner consistency and plays an unchallenged role in most research studies within string theory. Experiments on supersymmetry may also be understood as indicators for string theory.

If one were to try and use one sentence to separate string theory from 'pre-string' physics, it would be the paradigm shift from a point-particle to the string, from a zero- to a one-dimensional object. All particles, no matter how different they might seem, arise as different vibrational modes of a string, much in the way different tones are produced on a violin string. This underlines beautifully their common origin. As it turned out in 1995 however, the string lost the fundamental role it had just gained. String theory naturally incorporates objects of various dimensions, called p-branes (objects with p space dimensions, and one time dimension, as they travel through time). A 0-brane is a point particle, a 1-brane is a string, but these are just special cases of p-branes. The latter can be understood as generalizations of particles (or strings) of an arbitrary dimension. To be explicit, this means that one can also come across 2-branes, 3-branes, etc. Just like a charged point particle, also a p-brane can be charged (in a more general way). Such branes will become important when modeling black holes in string theory.

At this point, no further attempt will be made to explain string theory more explictly, but the author will rather try to give a very short character sketch of the field of research, hoping to give a broad audience a flavor of the type of activity a string theorist might be involved in. The reader can find more explicit explanations on the basics of string theory in the first section of chapter 1.

Character sketch of the research field of string theory

It would be incorrect to imagine string theory as a uniform field of research. Rather, string theory stands for a conglomeration of research on a large number of (strictly speaking) distinct theories, which reflects the fact that the field is at an early stage of development. This structural condition seems worthy of being communicated. These distinct 'sub-theories' of string theory come in a wide variety. Some are four-dimensional, others are six-dimensional (theories with any number of dimension are involved at some point), while some of them just describe a subspectrum of the physical states. Nevertheless, and this is the beauty of it, all of these theories have a lot in common. First of all, they center around the notions of dynamical strings and more generally, branes. More fundamentally, they are all believed to describe aspects of one big fundamental theory, called 'M-theory'. In neat accordance with this interpretation, it is often the case that specific questions or problems in the field not only allow, but often demand analysis in different 'pictures'. These different pictures might be provided by different theories, or within a theory, to use a more technical phrase, in different 'duality frames'. While one of these pictures might emblaze and simplify one aspect of a problem, it might cloud another aspect. Another picture (theory or duality frame) might reverse the role of these two aspects. Sometimes, the same phenomenon can be investigated from different points of view, often leading to remarkable and even spooky validations. At times, this fate can be a source of deep fulfilment, whereas at other times, this kind of 'patchwork approach' might be highly disturbing to the physicist, as it sets boundaries to his striving for order and setting a clear frame of analysis. With great pleasure, the author might right now refer to this phenomenon as the wonderful waggishness inherent to the quest for quantum gravity. To summarize, it seems a good first approach to imagine the field of research as taking peeps through little windows at phenomena in M-theory (by means on occasion of doing inhumanly complicated and sometimes interminable calculations).

A bridge between string theory and reality: compactification

One fact that appears strange to many people upon initial confrontation with string theory is, that they require to be ten-dimensional for their inner consistency. In fact, M-theory even requires to be eleven-dimensional. What is meant by requiring a dimensionality for inner consistency? The reader can imagine calculating the volume of a ball in three dimensions and calculating the surface of a circle in two dimensions. This is an example of two analagous calculations, but working in a different number of dimensions. The type of calculations that is referred to in the following, is much more complicated, but to give a bold picture: if one chooses anything different from ten (or eleven) dimensions, calculations become senseless, because they just yield infinities. Now, given that our universe has ten or eleven dimensions, one has to make contact with 'reality', in the sense of a four-dimensional spacetime universe. Generally, what one does, is to choose six (or seven) dimensions very small and compact, and four large dimensions. The four large dimensions (three space dimensions and one time dimension) are perceived in one's daily life, but there are also

'extra dimensions'. Probably, it might sound a bit misguiding to the layman to speak of extra dimensions. Rather, these 'extra dimensions' stand for 'internal, extra degrees of freedom'. To gain some intuition on such an extra degree of freedom, the layman may think of an elementary particle, e.g. an electron. Such an electron has an inner quantum mechanical angular momentum, namely the spin, which can take on different values. The direction in which the spin 'points' is not in spacetime however, but it is an inner degree of freedom. One might just say that it points into a direction of an extra dimension. One of the key messages of the previous passage is that these degrees of freedom arise in the same way as spacetime dimensions in string theory, they are of a common origin.

The sticking point of quantum gravity: black holes

Increasingly, a string theorist is confronted with political and social pressure to make verifiable predictions, if he wants to maintain that he is a visionary physicist and not a careless mathematician. It is hard to know, how close any experimental verification of string theoretical predictions lies. In any case, researchers are called to concretize their qualitative descriptions of primordial cosmology and of black holes. It is clear that these two physical systems are the playground in which a theory of quantum gravity has to be put to a test. In this thesis, black holes are set as a landmark.

Black holes: the most dense assemblies of matter in our universe

Black holes were discovered during the First World War by Karl Schwarzschild, as solutions to Einstein's equations of general relativity. General relativity describes gravity as the curvature of spacetime. In particular, a massive object forces the space surrounding it to curve. The term 'black hole' refers to an area in spacetime, that is populated by such a dense congregation of matter, that space is so strongly curved, that no object can escape this region anymore. This also applies to light, the fastest moving entity in the universe. Because light does not escape, the objects appear black, hence the name 'black holes'. Matter can fall into a black hole, and there is a certain point of 'no-return': the event horizon of a black hole.

Black holes are believed to be the final phase in the life cycle of very massive stars [1]. This shall be briefly described. A star is a luminous plasma held together by gravity, is of course tremendously hot, and can be pictured as a huge nuclear power plant performing nuclear fusion. In order to do this, it consumes 'fuel' (the fuel is used to perform nuclear fusion): hydrogen and later on in the life cycle, heavier elements. As long as there is fuel left, the star resides in an equilibrium. This equilibrium can be pictured as the cancellation of the effects induced by gravity, which tries to 'pull the matter closer together', and of the pressure, as it is a gigantic active 'engine', 'trying to push the matter further apart'. Put very simply, when a star runs out of fuel, there is no pressure left to counteract gravity. A star will start to collapse, and it depends on the original mass, what the end stadium of

[1] Our star, the sun, is too light and will never become a black hole.

the star will be. The heavier stars perform gigantic explosions called supernovae, of which some have been observed, but this will be left out in the following discussion.

- When the matter of the star is squeezed, atoms are squashed and electrons become free. The pressure of the resulting gas of electrons becomes the dominant counterforce to gravity. If the electron gas pressure is strong enough, the star can reach an equilibrium state called a *white dwarf*. The upper limit for the total (original) mass of the star lies somewhere around $M \approx 1.4 M_\odot$ – a bit less than one and a half times the mass of our sun [2].

- For heavier stars, the gravitational collaps will not stop at an equilibrium called a white dwarf. Rather, the star continues to collapse, and a new equilibrium might be reached, where the role of the electrons is taken over by the neutrons. This equilibrium is called a *neutron star* or a *pulsar*.

- If the star is too massive, the gravity is also too strong for the neutron star equilibrium. At present there is no knowledge of any denser 'plasma' than the one thought to be found in a neutron star, and upon further gravitational contraction, one does not expect to reach another equilibrium. In this case, the most resounding gravitational collapse takes place, presumably leading to a black hole. The resulting object continues an ongoing collapse in 'on itself' and disappears behind an event horizon, shielding it off from the outside.

Based on (indirect) experimental observation, there are by now several 'candidates', which are widely believed to be black holes. An example for such indirect observations is given by a star, that behaves as though it were a member of a double star system, but one cannot see its partner. This might be because the partner was once a star, but is now a black hole. Apart from the double star systems, there is also the fact that a black hole that acquires new matter, also referred to as an 'active black hole', will produce distinct radiation, and such radiation has been observed. This is no proof that the radiation stems from a black hole, but the black hole is a model predicting data that has been measured. If black holes exist, they come in a variety. Some are super-massive black holes in centers of galaxies (galaxies are generically believed to harbor super-massive black holes at their center), some of them are black holes in stellar mass range.

The amount of information contained by a black hole and the microscopic explanation using geometries of extra dimensions

Probably every reader will have heard of Schrödinger's cat. The purpose of this absurd invention is allow everyone to easily understand and remember one of the key principles in any theory that is 'quantum'. According to the mainstream 'Kopenhagener' interpretation of quantum theories, a quantum object lives in a superposition of more than one state. In the case of Schrödinger's cat, the cat is alive and dead, until someone measures, whether

[2] $M_\odot$ is a symbol which is commonly used to denote the mass of our sun.

the cat is dead. The wavefunction of the cat consists of a part 'alive' and a part 'dead', each possibly weighted by a probability (say 90% and 10% probability, so if one had one hundred cats one would statistically find 90 of the cats alive). A wavefunction is a sum of possible 'states' of a system weighted with their probabilities. One more concept is of interest in this context. In the case of the cat, the cat can be in two possible states. This means that before measuring whether the cat is dead or alive, one lacks some information: there is an uncertainty as to the state of the cat. In physics, this is called 'entropy' of the system. This leads to the discussion of what a black hole is as an object in quantum gravity.

In the Seventies of the 20th century, Stephen Hawking and collaborators made the prediction, that the amount of uncertainty adhering to a black hole is proportional to the area of the event horizon [3]. This uncertainty is the counterpart to the amount of information contained in a black hole, and receives the term 'entropy' in physics. But the 'classical' picture of a black hole is just a black 'ball' without any complexion. An important goal of a theory of quantum gravity, is to explain this entropy microscopically. The possible number of states in which a black hole could reside is a measure for the amount of uncertainty, of entropy. For any given area of the event horizon, one would thus like to explain this number by finding all possible 'microstates' of the black hole. In string theory, this has been done for some (supersymmetric) black holes. The general paradigm is to model black holes by wrapping various extended objects, called D-branes around extra dimensions, in such a manner, that the whole assembly of branes is perceived as a point-like object from a four-dimensional point of view. By assembling enough branes, one can model a black hole. The number of possibilities to realize such a black hole from a four-dimensional point of view with these branes, explains the entropy.

Split attractor flow trees

The concept 'split attractor flow trees' appearing in the title of this thesis needs some explanation. Having said that one models black holes in string theory by wrapping branes (several branes) around extra dimensions, this allows to explain, that (a certain class of) black holes very strongly restrict the geometry of extra dimensions. In fact, to model a black hole, one can choose the form and size of the geometry of extra dimensions at infinite distance of such a black hole, but the black hole then imposes a particular geometry, all the way from infinite distance until the event horizon of the black hole. If one chooses a slightly different geometry at infinite distance of the black hole, the black hole again dictates a specific, but slightly different geometry all the way from infinite distance up to the event horizon. The geometry at the event horizon however remains unchanged. There are certain physical fields that 'measure' this geometry, and their values are driven to attractor values. One therefore speaks of the 'black hole attractor mechanism'. Should one

[3] As a side remark: the fact that the amount of uncertainty grows with the surface and not with the volume might be seen as a cue to the concept of 'holography', that appears to be distilling into one of the most fundamental characteristics of string theory.

depict these fields, in dependence of a radial coordinate in spacetime (a simple black hole is radially symmetric), the values of these fields form a line (in the space of possible field values), starting at the chosen value at infinity, and ending at the attractor point. This line can also be referred to as a 'single flow'.

It turns out also that black holes with more than one center, so-called 'multi-centered black holes' are of great importance in string theory. Such multi-centered black holes are bound states of black holes. A similar attractor mechanism also holds for these black holes, but the line, starting at a given background for the geometry chosen at infinite distance of the (multi-centered) black hole, splits (maybe more than once). There is one 'end branch' for each center, terminating at the corresponding attractor point. For each center, the attractor point describes ('form or size' of) the geometry of the extra dimension at the event horizon. This depiction of the fields measuring the geometries are called split attractor flow trees, and they have been conjectured to be an existence criterion for multi-centered black holes. Taking a small jump ahead, note that a special class of multi-centered black holes (or more generally bound states) play an important role in this thesis. They will receive the interpretation of chromosomes of a black hole in the metaphor developed for the research performed by the author, in the concluding discussion. This remark underlines the crucial importance of split attractor flow trees and multi-centered black holes for the present work.

To conclude the introductory explanations on the topic of these thesis, let it be said that this thesis studies black holes in (type II) string theory, using split attractor flow trees.

Content of this thesis

The first three out of five main chapters set the stage within string theory for the research performed by the author, which is presented in the last two main chapters. Before presenting the content of these chapters, for the sake of completeness, let it be mentioned, that there is an appendix, in which conventions, notation and mathematical definitions used in this thesis are gathered. The appendix also contains some lengthy, technical research results, to which there will be references in the main text when they come into play. The last part of the appendix is a layman's guide to the content of this thesis in Dutch. As a general aid to communicate the central line of thought presented, short summaries (and sometimes outlooks) are included at the end of each chapter, placing the chapter into the bigger context of the thesis as a whole.

- Chapter 1 presents the general framework of this thesis: type II string theory compactifications, with focus on the most prominent choice of a Calabi-Yau manifold for the 'extra dimensions'. The latter is discussed both from a worldvolume and from a supergravity spacetime perspective. The last part of the chapter discusses the BPS[4] D-brane content and more generally the BPS spectrum of these theories.

[4]The word 'BPS' stands short for Bogomolnyi–Prasad–Sommerfeld and should in this context be read as supersymmetric and mass equal to charge (in some units).

- Chapter 2 gathers the relevant information on black holes, realized in the setting introduced in chapter one. The BPS black hole attractor mechanism is introduced. Building upon this, one of the most important tools of this thesis can be explained: split attractor flow trees. Split attractor flow trees as an existence criterion for multi-centered black holes, and more generally, for BPS bound states in type II string theory, reach their full glory in the split attractor flow conjecture. Finally, entropy of black holes is briefly discussed.

- Chapter 3 presents some basics and moreover some relevant features of topological string theory, which owes its connection to this thesis to a stunning conjecture that appeared in 2004, by Ooguri, Strominger and Vafa, known under the name 'OSV-conjecture'. Topological string theory computes invariants counting BPS states on Calabi-Yau manifolds, which can be used to enumerate black hole microstates for certain study models.

- Chapter 4 presents the results on enumerating mixed ensembles of D-brane states on various Calabi-Yau manifolds modeled as hypersurfaces in weighted projective spaces. In many aspects this research can be seen as a low-charge counterpart to studying black hole microstates. Various exact results on elliptic genera are presented, including some corrections to previous studies performed by other researchers. Additionally, a refinement for the index enumerating BPS bound states is proposed. This index, although at this point still lacking a mathematical definition, is presumably a refinement of the index proposed in [1], giving a more refined physical picture associated to the wall-crossing formula of Kontsevich and Soibelman, [2]. As elliptic genera are determined exclusively from polar states through modularity, non-trivial checks can be performed on a couple of non-polar states, yielding strong evidence that the performed calculations are correct. In addition, the results provide additional evidence for a strong version of the split attractor flow conjecture. A part of the results presented in this chapter has been published in [3], together with Andrés Collinucci, while another part has been published in [4], together with Walter Van Herck.

- Chapter 5 presents the research performed by the author in collaboration with Joris Raeymakers, Bert Vercnocke and Walter Van Herck, published in [5]. The first part of the chapter contains a short explanation of some basic facts on the fuzzball program on black holes in string theory, which, in addition to the previous material, should allow the reader to understand the context of research. The research relates the framework of 4d black holes and of the research presented in chapter 4 to 5d fuzzball geometries.

- Finally, there is a short chapter called 'concluding discussion', in which a metaphor is developed to elucidate the context and the findings of the research described in this thesis. Namely, it draws analogies between the studying of black hole microstates in string theory, and the studying of genomes in microbiology. Some analogies are

by no means perfect, but the author nevertheless believes, this metaphor can be a valuable source of inspiration, and hopefully serve as a memorable allegory.

Chapter 1

String theory compactifications

As pointed out in the introduction, string theory refers to a conglomeration of research attempting to formulate a consistent theory of quantum gravity, or even more broadly, of a unified theory of all forces, which might well be valid up all the way to the Planck scale, $E_P \approx 1.2 \cdot 10^{19}\text{GeV}/c^2$. The basic starting point of all this research, separating it from pre-string theories of fundamental physics is the fact that one treats one-dimensional objects, strings, instead of points as the basic building blocks of the universe. Historically, the field of string theory was founded around the beginning of the seventies of the 20th Century. One of the important early discoveries was a miraculous anomaly cancellation mechanism, [6]. The first fifteen years of research were centered around the study of string quantum mechanics, governed by a field theory living on the string worldsheet, the surface a string sweeps out as time evolves. After this initial period of 'string quantum mechanics', it turned out that other extended objects, going under the notion of branes, play an important role, questioning and eventually relativizing this aforementioned fundamental role of the string. Therefore, to borrow a custom which recently seems to have become fashionable amongst physicists, one might from todays' perspective call 'string theory' a historical misnomer, and rather speak of 'brane theory'.

In this chapter, the relevant part (for this thesis) of the web of strings and branes is presented, arising in the different consistent superstring theories. By web of strings and branes the variegated zoo of various objects is meant, with different worldvolume dimensionality, present in the different theories. In addition, some common dualities between different theories will be stated, some of which will be used later on in this thesis, and have been and are specifically used in the research performed by the author. As a next step, compactification of string theory to four dimensions is discussed. The most common choices for the internal space dimensions are either a six-torus, T^6 (this type of compactification is at the base of the research presented in chapter 5), a Calabi-Yau twofold times a two-torus. $K3 \times T^2$, or a compact Calabi-Yau (CY) threefold X (as will be at the basis of the presentations on the OSV-conjecture in chapter 3 and the research presented in chapter 4). The emphasis in this chapter will be on the case involving a CY 3-fold X. This will be done by taking a quick glance at the worldsheet perspective on a string theory compactification. In a second step, the spacetime physics associated to such a compactifi-

cation is highlighted. In order to do that, the classical low-energy approximation to type II string theories, type II supergravities is presented, starting in ten spacetime dimensions, followed by a discussion of compactification, which is realized as Kaluza-Klein reduction and truncation.

As the research presented in the later chapters takes place in four and to a lesser extent in five spacetime dimensions within type II string theory, the focus will be on the very powerful, so-called special geometry inherent to four-dimensional supergravity theories. This sets the stage to investigate supersymmetric black holes preserving part of the supersymmetry retained after compactification, which are the center of attention in chapter 2. The last part of this chapter gathers the foundations on D-branes and of their complementary realization as p-brane solutions to supergravity theories, which will be used at various occasions further on in this thesis. Finally, as announced in the introduction, the reader can find a very brief summary of some key thoughts presented in this chapter in the last subsection, including some pointers to later topics, embedding this chapter in the more global context of the thesis as a whole.

1.1 The web of strings and branes

The thread is picked up at the point in recent research history called the 'first superstring revolution', which dates back to 1985. The realization which theories of strings allow anomaly cancellation, rendering them consistent, led to the puzzling number of exactly five different superstring theories. For anomaly cancellation to hold, these five superstring theories all require a 10D spacetime, and they are named as follows:

- **Type I string theory:**
  unoriented open strings with $\mathcal{N} = 1$ supersymmetry in $D = 10$, $SO(32)$ gauge group,

- **Type IIA string theory:**
  oriented closed and open strings, $\mathcal{N} = 2$ supersymmetry in $D = 10$, non-chiral massless fermions,

- **Type IIB string theory:**
  oriented closed and open strings, $\mathcal{N} = 2$ supersymmetry in $D = 10$, chiral massless fermions,

- **Type $SO(32)$ heterotic string theory:**
  hybrid form of left-moving $\mathcal{N} = 2$ and right-moving $\mathcal{N} = 1$ supersymmetry in $D = 10$, fermions partly replaced with scalar fields, gauge group $SO(32)$,

- **Type $E8 \otimes E8$ heterotic string theory:**
  hybrid form of left-moving $\mathcal{N} = 2$ and right-moving $\mathcal{N} = 1$ supersymmetry in $D = 10$, gauge group $E8 \otimes E8$.

The state of art, that one was left with five seemingly different choices for a consistent theory of quantum gravity (or possibly of all forces) was highly inconvenient. There seemed to be no apparent deeper reason to which theory should be the correct one. This era came to an end with the 'second superstring revolution' in 1995, a huge turning point in the development of string theory. Namely, Edward Witten conjectured the five different superstring theories to be related by dualities and each to describe different limits of one big underlying theory, given the name M-theory. How did this conjecture come about?

As the perturbative analysis of string theories reveals, the massless sectors of each of these five 10D string theories consists of a very specific and constrained set of bosonic and fermionic fields. These massless degrees of freedom can be described, at least classically and at low energy, by 10D supergravity theories. At the same time, it had been previously discovered in 1978, [7], that there is an $\mathcal{N} = 1$ supergravity theory in $D = 11$, involving fields with spin up to 2. Such a theory preserves 32 supercharges, and is maximal in the sense that – also in lower dimensions – introducing more supercharges forces to include higher spin fields. In this sense, this supergravity can be seen as the tip of an iceberg and seems to be a special theory of supergravity; it has been conjectured to be the classical description of the physics governing the zero modes of M-theory (although not much information is available on this theory itself), in analogy to the relation of 10D supergravity theories to critical (10D) string theories. Figure 1.1 pictures the relation between these different theories.

Classical supergravity theories have been studied very carefully over the last decades. Of significant importance within this pursuit is the concept of dimensional reduction, which will be discussed in more detail, shortly. The main idea is to choose some dimensions very small, 'wound up', or, put differently, 'compactified', and see how to effectively describe the higher dimensional theory at low energies, as observed from the lower dimensional point of view. An important step was the realization that $\mathcal{N} = 1, D = 11$ supergravity leads to a maximal (maximal in the sense of maximal supersymmetry) supergravity theory in 10D upon dimensional reduction, choosing the eleventh direction to be a tiny circle, also referred to as the M-theory circle. This 10D theory is type IIA supergravity, a classical low energy limit of type IIA string theory. The reader gets the bigger idea: M-theory is thought to reduce to type IIA string theory upon compactification on a circle. This connection illustrates another phenomenon typical for the whole field of research: the beautiful geometrization / higher dimensional interpretation of various concepts. One of them is the strength of the string coupling of type IIA string theory, which is interpreted as the size of the M-theory circle. Thus, upon compactification on a very small circle, the perturbative string theory description of type IIA becomes an accurate approximative description of M-theory. At the same time, the very small circle allows the massive field modes obtained upon the dimensional reduction of 11D supergravity to be neglected: this is the truncation to the massless type IIA supergravity (to the reader unfamiliar with this jargon: these concepts will be explained in more detail, shortly). In this sense, the five superstring theories are interpreted as different perturbative expansions of a unique vacuum of M-theory, whereas the $\mathcal{N} = 1, D = 11$ supergravity is interpreted as a classical

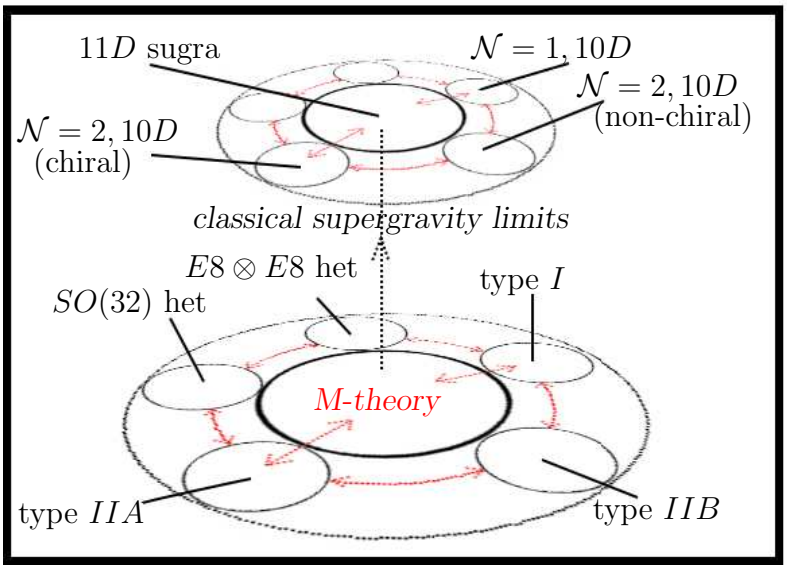

Figure 1.1: **M-theory, superstring theories and 11D/10D supergravity**: This figure represents the relation of various theories to a putative 11D fundamental quantum theory of all forces called M-theory. Upon taking certain limits, this theory is thought to be described by one of the five possible superstring theories, which are interrelated by dualities (indicated by the dotted red arrows). The classical low energy limits describing the massless modes of these theories are thought to be supergravity theories (the upper layer in the figure). 11D supergravity can be dimensionally reduced and related to type II or heterotic supergravity theories. These 10D supergravity theories support various duality relations (also indicated with dotted red arrows), which can be interpreted as a test ground for the dualities in the full underlying theories (the lower layer in the figure), or, put differently, allowing to peak into the relations between the quantum field theories of strings and branes, theories of immense complexity. Note that there are also supergravity theories associated to the heterotic string theories, which were not labeled in order to avoid cluttering of the figure.

theory describing the massless fields of the fundamental theory in eleven dimensions. Also $E_8 \times E_8$-heterotic string theory is believed to be a low-energy limit of M-theory, obtained by compactifying on an interval I, leaving an external ten-dimensional space. By virtue of more dualities, all string theories are conjecturally related to M-theory.

This idea of dualities led physicists to probe non-perturbative features of string theory, by mapping an untractable problem in the non-perturbative regime of a theory to a dual picture, where one would e.g. be at weak coupling and possess techniques to tackle the dual formulation. In the meantime, many intriguing tests of these dualities have been performed, sometimes yielding spectacularly different but completely consistent points of view of the same physical problem and its solution. An example of such a duality is *mirror symmetry* between type IIA string theory compactified on a Calabi-Yau threefold X and type IIB string theory compactified on the 'mirror' Calabi-Yau Y. These two compactified string theories are believed to describe the same physics.

Another important realization, which penetrated the world of research starting around 1995, was already pointed at. Namely, strings are not the only degrees of freedom in string theory. Strings are 1-dimensional objects, which sweep out a 2-dimensional 'world volume' as time evolves. More generally, string and M-theory contain p-dimensional objects, sweeping out a $(p+1)$-dimensional world volume. Such an object is called a p-brane. This concept contains the string as a special case, the 1-brane, and also the point-particle, the 0-brane. More specifically, the concept of a D-brane, a Dirichlet-brane, appears when studying perturbative worldsheet string theory. Open strings can satisfy boundary conditions of the form

$$\begin{aligned} n^a \partial_a X^\mu &= 0 \qquad \mu = 0, ..., p\,, \\ X^i &= c^i \qquad i = p+1, ..., 9\,, \end{aligned}$$

where the c^i are constants, and n^a is a normal vector to the surface $X^i = c^i$ in 10D spacetime. The $X^D = (X^\mu, X^i)$ $(D = 0, ..., 9)$ are bosonic worldsheet fields, and with this boundary conditions, naturally split up into coordinates X^μ given the interpretation of lying in the directions of the worldvolume of the brane, and coordinates normal to the brane, X^i. The coordinates normal to the brane are constant (as long as the brane is not treated dynamically), and are interpreted as end points of open strings. Furthermore, Polchinski discovered in 1995, [8] that D-branes carry charge under gauge fields. Depending on the specific charge of such a brane, or more specifically, on which sector of string theory the massless degree of freedom interpreted as a (generalized) gauge field (to which such a brane couples) lives, one speaks of a NS-p-brane or a Dp-brane, or, very generally, of a mixed type (p, q)-brane, [9]. Furthermore, there are also so–called instantonic branes (if the whole worldvolume lies in spacelike directions), referred to as S-branes, [10], where 'S' stands for 'spacelike'. The branes in M-theory are referred to as M-branes: the (electric) M2-brane and the (magnetic, dual) M5-brane.

This sets the stage to start discussing string theory as a perturbative, compactified theory, choosing six compact dimensions and four non-compact dimensions (space-time), much in the way that string theory was perceived in the eighties and beginning of the nineties of the 20th Century. As the following section is not essential for an understanding of the main topics in this thesis, the reader may decide to skip it. Note however that the introduction to topological string theory in chapter 3 will build upon this section, and the discussion of 5 will be based on some of the introduced concepts.

1.2 String theory compactified on a Calabi-Yau manifold

As mentioned before, string theory was originally studied as a 2D quantum field theory on the worldsheet, containing worldsheet bosons as well as fermions. This thesis uses type II string theory, and only this case will be analyzed in the following. The classical local superconformal symmetry translates into a superconformal quantum symmetry, and it is

required that the left- and right-moving central charges have to be equal to $c = 15$. This is also sometimes denoted as a $\mathcal{N} = (2, 2)$ supersymmetric field theory with $c_L = c_R = 15$ (or $\mathcal{N} = 2, c = 15$ for short). A first, if modest step to make contact with 'everyday physics' is to assume that four of the ten space-time dimensions are large, whereas the other six are assumed to be 'wound-up' and tiny. For now, the case will be discussed when the theory is a product of a $\mathcal{N} = 2, c = 6$ theory for the external space-time part, and a $\mathcal{N} = 2, c = 9$ part for the internal compact dimensional part. The former theory can be realized as a theory of two complex bosons and superpartners, where the bosons are interpreted as the four real space-time coordinates. The interest for this thesis however lies in the internal theory, as a modification of this part of the theory leads to the so-called 'twisting' of the ordinary $\mathcal{N} = 2$ superconformal algebra, which is a good topic by which to familiarize the reader with topological string theory. This will be discussed in chapter 3.

The $\mathcal{N} = 2$ superconformal algebra is built out of the energy momentum tensor $T(z)$ and two weight 3/2 supercurrents $G^+(z)$ and $G^-(z)$, which automatically also enforces inclusion of an additional $U(1)$ current $J(z)$. One can expand these operators into their Laurent modes according to

$$T(z) = \sum_{n\in\mathbb{Z}} \frac{L_n}{z^{n+2}}, \qquad G(z) = \sum_{n\in\mathbb{Z}} \frac{G^{\pm}_{n\pm a}}{z^{n\pm a+3/2}}, \qquad J(z) = \sum_{n\in\mathbb{Z}} \frac{J_n}{z^{n+1}}, \tag{1.1}$$

which allows the expression of the algebra as

$\mathcal{N} = 2$ superconformal algebra
$[L_m, L_n] = (m-n)L_{m+n} + \frac{c}{12}m(m^2-1)\delta_{m+n,0}$
$[L_m, G^{\pm}_{n\pm a}] = (\frac{m}{2} - (n \pm a))G^{\pm}_{n+m\pm a}$
$[L_m, J_n] = -nJ_{m+n}$
$[J_m, G^{\pm}_{n\pm a}] = \pm G^{\pm}_{n+m\pm a}$
$[J_m, J_n] = \frac{c}{3}m\delta_{m+n,0}$
$\{G^{\pm}_{m+a}, G^{\pm}_{n-a}\} = 2L_{m+n} + (m-n+2a)J_{m+n} + \frac{c}{3}((m+a)^2 - \frac{1}{4})\delta_{m+n,0}$

where the central charge will be chosen as $c = 9$ in this case, according to preceding remarks. The parameter $0 \leq a < 1$ controls the boundary conditions of the fermionic currents. This can be seen from $z \to e^{2\pi i}z$, which implies $G^{\pm} \to -e^{\mp 2\pi i a}G^{\pm}$. Algebras with different choices for a are related via spectral flow. If a is chosen integer, one speaks of Ramond boundary conditions, if a is chosen half-integer, one speaks of Neveu-Schwarz boundary conditions.

There are several examples of theories with $\mathcal{N} = 2$ superconformal symmetry, and the different conformal field theories related to string theory are often closely connected. It is interesting to choose a non-linear sigma model realization of the worldsheet superstring with a curved Riemannian manifold as a background. Such a non-linear sigma model governs maps $\phi : \Sigma \to X$ from the worldsheet Σ to a target manifold X, which will now be assumed to be a complex Riemannian manifold. In order for an action of such a non-linear sigma model to possess $(2, 2)$ supersymmetry, it is conveniently constructed using a superspace formalism, in schematic form $S \approx \int d^2z d^4\theta K(\Phi^i, \bar{\Phi}^i)$. In this form it is easy to

prove that the target space manifold X has to be a Kähler manifold (defined in A.1 of the appendix). The reader can follow this closely in [11]. Furthermore, by calculating the β-function for the metric one obtains something proportional to the Ricci tensor, at lowest order. This is thus a possibility to discover that the conformal symmetry requires X to be a Calabi-Yau manifold, which is by definition a Kähler manifold allowing a Ricci-flat metric.

Non-linear sigma model realization of $\mathcal{N} = 2$ superconformal worldsheet theory

An explicit realization of an $\mathcal{N} = 2$ superconformal worldsheet theory will be discussed briefly: a non-linear sigma model. The interest will lie in two global symmetries known as *R-symmetries*. In particular, it will be shown that they are only present both after quantizing the theory when choosing a Calabi-Yau manifold as a target space. These symmetries are at the basis of defining the so-called topological twist, leading to topological field theories (and eventually string theories). This will be discussed in chapter 3.

Coordinates $(z, \bar{z})$ will be chosen on the worldsheet Σ, and (ϕ^i) $(i = 1, 2, 3)$ on the 3-complex dimensional target space X. This means that the manifold can be described by a family of charts $\{U_\alpha, \phi^i_\alpha, \phi^{\bar{i}}_\alpha\}$, such that transition functions do not mix the holomorphic and anti-holomorphic coordinates, i.e. on an intersection $U_\alpha \cap U_\beta$ one has $\phi^i_\alpha = \phi^i_\alpha(\phi^1_\beta, \ldots, \phi^3_\beta)$ and $\phi^{\bar{i}}_\alpha = \phi^{\bar{i}}_\alpha(\phi^{\bar{1}}_\beta, \ldots, \phi^{\bar{3}}_\beta)$. One can hence decompose the fields appearing in the action according to

$$\phi^I = \{\phi^i, \phi^{\bar{i}}\}, \quad \psi^I_\pm = \{\psi^i_\pm, \psi^{\bar{i}}_\pm\}\,, \quad \text{and} \quad g^{IJ} = \{g^{i\bar{j}}, g^{\bar{i}j}\}\,. \tag{1.2}$$

Stating that the geometry of X is 'complex' means that that a splitting of indices into barred and unbarred indices is consistent throughout all patches of X. One also wants the supersymmetry transformations to respect the complex structure of X, thus one has to require that the metric on X be such that parallel transport of vectors preserves the decomposition $TX = T^{1,0}X \oplus T^{0,1}X$. Metrics that satisfy this condition are called *Kähler* metrics. The (supersymmetric) action for this non-linear sigma model realization of an $\mathcal{N} = (2, 2)$ superconformal field theory reads

$$\begin{aligned} S \;=\; & \int_\Sigma d^2z \,\big(\frac{1}{2}\, g^{i\bar{j}}\, \partial_z\phi^i\, \partial_{\bar{z}}\phi^{\bar{j}} + \frac{1}{2}\, g^{\bar{i}j}\, \partial_z\phi^{\bar{i}}\, \partial_{\bar{z}}\phi^j \\ & + i\, g_{\bar{i}j}\, \psi^{\bar{i}}_-\, D_z\, \psi^j_- + i\, g_{\bar{i}j}\, \psi^{\bar{i}}_+\, D_{\bar{z}}\, \psi^j_+ + \frac{1}{4}\, R_{i\bar{j}k\bar{l}}\, \psi^i_+\, \psi^{\bar{j}}_+\, \psi^k_-\, \psi^{\bar{l}}_-\,\big)\,, \end{aligned} \tag{1.3}$$

where $D_{\bar{z}}\psi^i_+ = \partial_{\bar{z}}\psi^I_+ + \partial_{\bar{z}}\phi^j \Gamma^i_{jk}\psi^k_+$ (and analogous for D_z).

The superalgebra

The supersymmetry generators $Q_\pm$ and $\overline{Q}_\pm$ are defined such that a total supersymmetry variation is expressed as follows:

$$\delta = i\,\alpha_-\, Q_+ + i\,\alpha_+\, Q_- + i\,\tilde{\alpha}_-\, \overline{Q}_+ + i\,\tilde{\alpha}_+\, \overline{Q}_-\,. \tag{1.4}$$

These generators obey the following anti-commutation relations[1]:

$$\{Q_\pm, \overline{Q}_\pm\} = P \pm H \,, \tag{1.5}$$

where P and H are the Euclidean versions of the generators of space and time translations.

Recall that the action (1.3) is referred to as $\mathcal{N} = (2,2)$ supersymmetric, because there are two holomorphic and two anti-holomorphic SUSY parameters. The spinors and SUSY transformation parameters are sections of the following bundles:

$$\begin{aligned}
\psi_+^i &\in \Gamma(\Sigma, K^{1/2} \otimes \Phi^*(T^{1,0}X)) \,, \quad \psi_+^{\bar{i}} \in \Gamma(\Sigma, K^{1/2} \otimes \Phi^*(T^{0,1}X)) \,, \\
\psi_-^i &\in \Gamma(\Sigma, \overline{K^{1/2}} \otimes \Phi^*(T^{1,0}X)) \,, \quad \psi_-^{\bar{i}} \in \Gamma(\Sigma, \overline{K^{1/2}} \otimes \Phi^*(T^{0,1}X)) \,, \\
\alpha_+ \,, \tilde{\alpha}_+ &\in \Gamma(\Sigma, K^{1/2}) \,, \\
\alpha_- \,, \tilde{\alpha}_- &\in \Gamma(\Sigma, \overline{K^{1/2}}) \,,
\end{aligned} \tag{1.6}$$

where $K^{1/2}$ and $\overline{K^{1/2}}$ can loosely be referred to as the 'square root' of the canonical, $K = \overline{T^{(1,0)}\Sigma} = T^{(0,1)}\Sigma$, and the anti-canonical bundle, $\overline{K} = \overline{T^{(0,1)}\Sigma} = T^{(1,0)}\Sigma$. More specifically, these spin bundles have transition functions which are elements of $U(1)$ and square to elements, which are transition functions of K and $\overline{K}$.

Classical and quantum R-symmetry

Now that the supersymmetry of the sigma model has been established, let two additional global symmetries be stated, that this theory enjoys. These symmetries go by the name of *vector R-symmetry* and *axial R-symmetry*, whose generators will be denoted by F_V and F_A, respectively. These two symmetries act on the fermions only, and are defined as follows:

$$\begin{aligned}
e^{i\,\alpha\,F_V} \{\psi_\pm^i, \psi_\pm^{\bar{i}}\} &\mapsto \{e^{-i\,\alpha}\,\psi_\pm^i, e^{i\,\alpha}\,\psi_\pm^{\bar{i}}\} \,, \\
e^{i\,\alpha\,F_A} \{\psi_\pm^i, \psi_\pm^{\bar{i}}\} &\mapsto \{e^{\mp i\,\alpha}\,\psi_\pm^i, e^{\pm i\,\alpha}\,\psi_\pm^{\bar{i}}\} \,.
\end{aligned} \tag{1.7}$$

Finally, one can write the commutation relations with the supersymmetry generators:

$$\begin{aligned}
[F_V, Q_\pm] &= \quad Q_\pm \,, \\
[F_V, \overline{Q}_\pm] &= -\overline{Q}_\pm \,, \\
[F_A, Q_\pm] &= \pm Q_\pm \,, \\
[F_A, \overline{Q}_\pm] &= \mp \overline{Q}_\pm \,.
\end{aligned} \tag{1.8}$$

Having defined the R-symmetries (1.7) of the classical action (1.3), the question arises whether they are symmetries of the full quantum theory. This question will be answered by carefully defining the measure of the path integral. In order to do this, the basis of the fermions is changed to 'momentum' space. For simplicity, spacetime indices are suppressed and the fermions are written as $\psi_\pm$ and $\overline{\psi}_\pm$. The ψ_- will be decomposed into eigenspinors

[1] Only non-vanishing relations are written.

of the $D_{\bar{z}}D_z$ operator. If one denotes the eigenvalues as λ_n, then one can write the spinor as follows:

$$\psi_- = \sum_{n=0}^{\infty} \sum_{\alpha} c_{n,\alpha} {\psi_-}^{(n,\alpha)} , \tag{1.9}$$

where the n labels the eigenvalue and the α labels the degeneracy of that eigenvalue. One can split up this sum into zero and non-zero modes

$$\psi_- = \sum_{\alpha} c_{0,\alpha} {\psi_-}^{(0,\alpha)} + \sum_{n=1}^{\infty} \sum_{\alpha} c_{n,\alpha} {\psi_-}^{(n,\alpha)} , \tag{1.10}$$

where $\lambda_0 = 0$. Notice that a zero mode of $D_{\bar{z}}D_z$ is necessarily annihilated by D_z. Suppose there is a ψ_- such that $D_{\bar{z}}D_z\psi_- = 0$. Then, one can take the complex conjugate of that solution, $\overline{\psi}_+$, and compute the following

$$\begin{aligned} 0 &= -\int \overline{\psi}_+ \, D_{\bar{z}}D_z\psi_- = +\int D_{\bar{z}}\overline{\psi}_+ \, D_z\psi_- \\ &= +\int \left(D_z\psi_-\right)^* D_z\psi_- \geq 0 , \end{aligned} \tag{1.11}$$

where the last inequality is saturated if and only if $D_z\psi_- = 0$.
One can similarly make a decomposition of $\overline{\psi}_-$ into eigenspinors of the same operator, and $\overline{\psi}_+$ and ψ_+ into eigenvectors of $D_zD_{\bar{z}}$. Having made this change of basis, one can rewrite the fermionic measure of the path integral roughly as follows:

$$\Big(\prod_{\alpha} d{\psi_+}^{(0,\alpha)}\Big)\Big(\prod_{\alpha} d{\psi_-}^{(0,\alpha)}\Big)\Big(\prod_{\alpha} d\overline{\psi}_+{}^{(0,\alpha)}\Big)\Big(\prod_{\alpha} d\overline{\psi}_-{}^{(0,\alpha)}\Big) \times (\text{nonzero modes}) . \tag{1.12}$$

In this basis, the action will look like

$$S \sim \sum_{n,m\neq 0} \sum_{\alpha,\beta}^{\infty} \left(\overline{\psi}_+^{(n,\alpha)} \, D_{\bar{z}} \, \psi_+^{(m,\beta)} + \overline{\psi}_-^{(n,\alpha)} \, D_z \, \psi_-^{(m,\beta)}\right) . \tag{1.13}$$

The point now is that the zero modes do not appear in the action, because they have been killed by the corresponding operator. This means that the Grassmann integration over these modes will go unsaturated, i.e. we will have integrals of the form $\int d\psi \cdot 1 = 0$. So the whole path integral will vanish unless one adds some fermions to the integrand. The question is: how many fermions of each kind does one have to add? If it turns out that one had to add the same amount of fermions for each kind, say ℓ, then non-vanishing correlators for this theory will look like this:

$$\langle \psi_+^1 \ldots \psi_+^l \, \psi_-^1 \ldots \psi_-^l \, \overline{\psi}_+^1 \ldots \overline{\psi}_+^l \overline{\psi}_-^1 \ldots \overline{\psi}_-^l \rangle . \tag{1.14}$$

Such a correlator has neutral R_V and R_A charge, so no anomaly is present. If, however, the number of zero modes of the different kinds of operators differ, then there will be an

anomaly. So one needs to count the (difference in) zero modes. First of all, one notes that the number ℓ_+ of ψ_+ zero modes is equal to the number of $\overline{\psi}_-$ zero modes. This follows from the fact that

$$\left(D_{\bar{z}}\psi_+\right)^* = D_z\overline{\psi}_- \,. \tag{1.15}$$

Similarly, the number ℓ_- of ψ_- zero modes equals the number of $\overline{\psi_+}$ zero modes. This means that the non-vanishing correlator will have neutral R_V charge, because there is an equal number of barred and unbarred spinors.
Now, it is time to know the difference $\ell_+ - \ell_-$. The space of sections of $K^{1/2}\otimes\Phi^*(T^{(1,0)})$ (i.e. ψ_+ spinors) that are annihilated by D_z is denoted in the language of sheaf cohomology as $H^0(K^{1/2}\otimes\Phi^*(T^{(1,0)}))$. The Riemann-Roch theorem yields information about this space by stating that, given a bundle E on a complex n-dimensional space Y, the following relation holds:

$$\sum_{i=0}^{n}(-1)^i \dim(H^i(E)) = \int_Y \mathrm{ch}(E)\,\mathrm{td}(Y)\,. \tag{1.16}$$

On the left hand side, $H^i(E)$ means $(0,i)$-forms taking values in E that are in the kernel of a covariantized $D_{\bar{z}}$ operator, modulo elements in the image of this operator. On the right hand side, ch and td stand for the Chern character and Todd class of the bundles in their argument. In this case, the alternating sum terminates at the first cohomology

$$\sum_{i=0}^{n}(-1)^n \dim(H^i(E)) = \dim(H^0) - \dim(H^1)\,. \tag{1.17}$$

H^0 was what was sought, and now what remains is its difference with H^1. One can use what is known as *Serre duality*, which states the following:

$$H^i(E) = H^{n-i}(K\otimes\overline{E})^*\,, \tag{1.18}$$

where $\overline{E}$ is the dual bundle, and the * means 'dual vector space'. In this case, this means

$$H^1(K^{1/2}\otimes\Phi^*(T^{(1,0)}X)) = H^0(K\otimes\overline{K^{1/2}}\otimes\Phi^*(T^{(0,1)}X))^* = H^0(K^{1/2}\otimes\Phi^*(T^{(0,1)}X))^*\,. \tag{1.19}$$

This is the dual to the space of $\overline{\psi}_+$'s, so its dimension is just ℓ_-. In other words, the Riemann-Roch theorem (1.16) already yields the difference $\ell_+ - \ell_-$. So let the right hand side be computed. First, one needs $\mathrm{ch}(K^{1/2}\otimes\Phi^*(T^{(1,0)}X))$, and one can simplify this by using the rule that the Chern character of a tensor product bundle equals the product of the Chern characters of the individual bundles. Using the fact that $K = \overline{T^{(1,0)}\Sigma} = T^{(0,1)}\Sigma$ one can rewrite this as follows:

$$\begin{aligned}
\mathrm{ch}(K^{1/2}\otimes\Phi^*(T^{(1,0)}X)) &= \mathrm{ch}(K^{1/2})\mathrm{ch}(\Phi^*(T^{(1,0)}X)) = \sqrt{\mathrm{ch}(K)}\Phi^*(\mathrm{ch}(T^{(1,0)}X)) \\
&= \left(1-\frac{1}{2}\,c_1(T^{(1,0)}\Sigma)\right)\left(d+\Phi^*(c_1(T^{(1,0)}X))\right) \qquad (1.20)\\
&= d+\Phi^*(c_1(T^{(1,0)}X)) - \frac{d}{2}\,c_1(T^{(1,0)}\Sigma)\,, \qquad (1.21)
\end{aligned}$$

where d is the complex dimension of the worldsheet. For simplicity, $T^{(1,0)}$ will be denoted by T and $T^{(0,1)}$ by $\overline{T}$, in the following. Using the relation $\mathrm{td}(T\Sigma) = 1 + \frac{1}{2}\, c_1(T\Sigma)$ for the Todd class and multiplying it all together, keeping only the two-forms, one gets

$$\ell_+ - \ell_- = \int_\Sigma \Phi^*(c_1(TX))\,. \tag{1.22}$$

Therefore, a correlation function must be of the form

$$\langle (\psi_+)^{\ell_+} (\overline{\psi}_-)^{\ell_+} (\psi_-)^{\ell_-} (\overline{\psi}_+)^{\ell_-} \rangle\,. \tag{1.23}$$

such that the difference is given by (1.22). If $c_1(TX) \neq 0$, this means that an operator with non-zero R_A charge has a vev (vacuum expectation value), which means that the symmetry is spontaneously broken, thus exhibiting an anomaly in the symmetry. The condition for this anomaly to vanish is $c_1(TX) = 0$: the target space is a Calabi-Yau 3-fold X.

To summarize:

- The R_V-charge is always preserved for any Kähler target space.
- The R_A-charge is preserved if and only if the target space is Calabi-Yau.

Additionally, some closing remarks on the worldsheet perspective of string theory on a CY manifold are given. There are scalar parameters controlling form and size of a CY manifold that are commonly called the *moduli of a CY*. These will be discussed in detail in the next section. Let it at this point be said though, that the CY's associated to some scalar moduli are not smooth. It was perceived more than twenty years ago, that the perturbative SCFT description breaks down at singular points (singularities will be discussed in chapter 3). The resolution of some of these singularities goes through the appearance of new massless degrees of freedom, which can generally be associated to branes. The description of the theory including the new degrees of freedom requires a different CY threefold: this is called a topology changing transition, which appears to be something dynamical and smooth within the physics of string theory on CY threefolds. Such non-perturbative conifold transitions interconnect different CY threefolds with completely different topologies. More radically, in [12, 13], it was even argued that all CY threefolds realized as complete intersections in products of projective spaces are connected through conifold transitions. The most daring idea is that all type II string theory compactifications on a CY 3-fold are related by perturbative and non-perturbative 'transitions', that is to say, this family of theories then is just a collection of momentary depictions of a dynamical whole: *type II string theory compactified on a Calabi-Yau 3-fold*. The reader who wishes to read more about this can take the lecture notes of Brian Greene, [14], as a starting point.

1.3 From 10D to 4d $\mathcal{N} = 2$ supergravity theories

As discussed previously, the type II superstring theories are believed to be described effectively by type II supergravity theories at low energies. Of particular relevance is the

compactification of these supergravities down to four dimensions. This may be seen as a counterpart to the discussion presented in the previous chapter on the worldsheet perspective of string theory. Here, the low energy spacetime perspective of compactifying string theory on a CY 3-fold is discussed. The presentation will be exclusively on the IIA and IIB $\mathcal{N} = 2, d = 4$ supergravity theories. A total space of the form $M_4 \times X$ will be chosen as a background, where M_4 denotes $4d$ Minkowski space, and X denotes a CY 3-fold. The starting points are the two $D = 10$ supergravities.

The bosonic massless field content of the non-chiral $\mathcal{N} = 2$, $D = 10$ IIA, and the chiral $\mathcal{N} = 2$, $D = 10$ IIB supergravities is summarized in the following table, indicating the fields' string theoretical origin.

	NS-NS sector		**R-R sector**	
IIA	metric (graviton)	G_{MN}	RR 1-form	$C^{(1)}$
10D	Kalb-Ramond 2-form	$B^{(2)}$	RR 3-form	$C^{(3)}$
supergravity	dilaton	Φ		
IIB	metric (graviton)	G_{MN}	RR 0-form	$C^{(0)}$
10D	Kalb-Ramond 2-form	$B^{(2)}$	RR 2-form	$C^{(2)}$
supergravity	dilaton	Φ	RR 4-form	$C^{(4)}$

A real irreducible (Majorana-Weyl) spinor in ten dimensions has 16 components, [15], and $\mathcal{N} = 2$ thus means 32 supercharges. The scalar Φ called the dilaton can be seen as dynamically determining the string coupling $g_s = e^{\Phi}$. There are various approaches as to how one can find these two supergravities involving massless fields. One could start with the maximal $D = 11$ supergravity believed to be a low energy limit of M-theory and do a dimensional reduction. Alternatively, they can be found by starting with the field content listed above, and as these supergravities are maximal, supersymmetry fully constrains the action to the form of which the bosonic part is given below.

Choose type IIA supergravity first. Apart from the bosonic field content, there are the fermionic fields: two spin $\frac{3}{2}$ *opposite* chirality gravitinos $\psi_\mu^\pm$ and two spin $\frac{1}{2}$ *opposite* chirality dilatinos $\lambda^\pm$. The action for the bosonic fields has a part for the dynamics of the fields arising from the NS-NS sector,

$$S^{10D,\text{NSNS}}_{\text{IIA,bosonic}} = \frac{1}{2\kappa_{10}^2}\int d^{10}x\sqrt{-G}e^{-2\Phi}(R + 4(\partial_M\Phi\partial^M\Phi) - \frac{1}{12}H_{MNP}H^{MNP}), \tag{1.24}$$

one for the dynamics of the fields from the RR-sector,

$$S^{10D,\text{RR}}_{\text{IIA,bosonic}} = -\frac{1}{4\kappa_{10}^2}\int d^{10}x\sqrt{-G}(|F^{(2)}|^2 + |\tilde{F}^{(4)}|^2), \tag{1.25}$$

using $\tilde{F}^{(4)} = F^{(4)} - C^{(1)} \wedge H^{(3)}$, and finally a (topological) Chern-Simons term,

$$S^{10D,\text{CS}}_{\text{IIA,bosonic}} = -\frac{1}{4\kappa_{10}^2}\int B^{(2)} \wedge F^{(4)} \wedge F^{(4)}, \tag{1.26}$$

yielding the bosonic action $S^{10D}_{\text{IIA,bosonic}} = S^{10D,\text{NSNS}}_{\text{IIA,bosonic}} + S^{10D,\text{RR}}_{\text{IIA,bosonic}} + S^{10D,\text{CS}}_{\text{IIA,bosonic}}$. The action is written in string frame, and the relation between Newton's constant, gravitational coupling constant and string length reads $16\pi G_{10} = 2\kappa_{10}^2 = 2\kappa^2 g_S^2 = (2\pi)^7 l_S^8 g_S^2$. G denotes the determinant of the 10D metric, Φ is the dilaton, $H^{(3)} = dB^{(2)}$ is the field strength belonging to the NS-sector two-form and $F^{(2)} = dC^{(1)}$ and $F^{(4)} = dC^{(3)}$ are the corresponding field strengths originating from the RR-sector of the theory. Note that the action can be transformed to the Einstein frame by a Weyl rescaling of the metric ($G_{\text{string}} = e^{-\frac{\Phi}{2}} G_{\text{Einstein}}$), in which the term for the metric will have the familiar form from the Einstein-Hilbert action.

Similarly, the bosonic part of the action for IIB string theory splits up into a term from the NS-NS sector, which is exactly the same as for type IIA,

$$S^{10D,\text{NSNS}}_{\text{IIB,bosonic}} = \frac{1}{2\kappa_{10}^2}\int d^{10}x\sqrt{-G}e^{-2\Phi}(R + 4(\partial_M\Phi\partial^M\Phi) - \frac{1}{12}H_{MNP}H^{MNP}), \tag{1.27}$$

one for the RR-sector,

$$S^{10D,\text{RR}}_{\text{IIB,bosonic}} = -\frac{1}{4\kappa_{10}^2}\int d^{10}x\sqrt{-G}(|F^{(1)}|^2 + |\tilde{F}^{(3)}|^2 + \frac{1}{2}|\tilde{F}^{(5)}|^2), \tag{1.28}$$

using $\tilde{F}^{(3)} = F^{(3)} - C^{(0)} \wedge H^{(3)}$ as well as $\tilde{F}^{(5)} = F^{(5)} - \frac{1}{2}C^{(2)} \wedge H^{(3)} + \frac{1}{2}B^{(2)} \wedge F^{(3)}$, and finally a Chern-Simons term,

$$S^{10D,\text{CS}}_{\text{IIB,bosonic}} = -\frac{1}{4\kappa_{10}^2}\int C^{(4)} \wedge H^{(3)} \wedge F^{(3)}, \tag{1.29}$$

yielding the bosonic action $S^{10D}_{\text{IIB,bosonic}} = S^{10D,\text{NSNS}}_{\text{IIB,bosonic}} + S^{10D,\text{RR}}_{\text{IIB,bosonic}} + S^{10D,\text{CS}}_{\text{IIB,bosonic}}$, where the action is again written out in string frame. There was a little (standard) cheating involved, though. The action on its own is not sufficient [2], one needs to impose one additional constraint,

$$\star\tilde{F}^{(5)} = \tilde{F}^{(5)}, \tag{1.30}$$

the self-duality of the five-form field strength $\tilde{F}^{(5)}$, as this does not follow from the action.

1.3.1 Compactification to four dimensions

Compactification in supergravity means performing a dimensional reduction, and the idea of dimensional reduction refers to effectively describing a higher dimensional theory in terms of a lower dimensional one. The first ideas on this appear to go back to Gunnar Nordström back in 1914 [16–18], but in general such theories became known as Kaluza-Klein theories, referring to their attempts to unify general relativity and electromagnetism in five dimensions, [19, 20].

[2] The action could be reformulated such that one can avoid having to impose an extra constraint, but only at the cost of considerable technical complication.

Kaluza-Klein truncation

The basic intuition can be gained from the easiest example, namely reduction on a circle S^1 of length $L = 2\pi R$. Imagine starting with a 10D theory consisting of massless fields and considering for example a massless scalar field Φ. In 10D, the equation of motion reads

$$\Box_{10}\Phi = 0. \tag{1.31}$$

One now chooses to write the 10D Minkowski spacetime as a product $\mathcal{M}_{1,9} = \mathcal{M}_{1,8} \times S^1$, and label the coordinates x_μ, $\mu = 0, ..., 8$ on $\mathcal{M}_{1,8}$ and y on S^1. This means that the d'Alembertian decomposes, $\Box_{10} = \Box_9 + \partial_y^2$. If one expands the scalar field in Fourier modes,

$$\Phi(x, y) = \sum_n \phi_n(x) e^{\frac{iny}{L}},$$

one sees that (1.31) decomposes into equations for the modes of the form

$$\Box_9\phi_n - \frac{n^2}{L^2}\phi_n = 0. \tag{1.32}$$

From a 9D point of view, each mode ϕ_n is again a scalar field, with mass $\frac{|n|}{L}$. This means that the size of the circle determines how massive these scalar fields are, and it is clear, that by choosing L very small, the modes will become extremely massive. If one chooses L to be of a certain length, the scalar fields will have masses of the corresponding order of magnitude. One would like to keep only the massless fields, in this case ϕ_0, and this is justifiable if the other modes are heavy enough, which is of course the case if the circle is small enough. The modes ϕ_n are called massive Kaluza-Klein modes and do not play any role at an energy scale much lower than the compactification scale.

If one is allowed to throw away the massive modes, the lower dimensional theory can be truncated down to the massless modes: this yields a consistent Kaluza-Klein truncation. In principle one has to check for all the fields whether the equations of motion allow neglecting of all the massive modes. For CY compactifications, this is an unsettled issue. Using special geometry and the cohomology of a CY, one can determine the massless modes for such a compactification, but no proof has been found as to whether the massive modes decouple from the massless ones. Unlike the case of the circle, where the Fourier modes are orthogonal, this decoupling is already non-trivial for a reduction on a three-sphere. These long-standing problems will not be addressed in this thesis.

It is clear that these explanations generalize to other types of fields. For example, a 10D metric G_{MN} will reduce to various types of fields: splitting up 10D indices according to $M = (\mu, y)$ and as a KK-ansatz taking G to be independent of y, one will obtain a metric in 9D, $g_{\mu\nu} = G_{\mu\nu}$, a vector field $A_\mu = G_{\mu z} = G_{z\mu}$ and a scalar $\phi = G_{zz}$. A similar reduction applies to all 10D n-form gauge fields.

When reducing over several dimensions, the d'Alembertian will split according to $\Box_D = \Box_d + \Box_{D-d}$ and it is clear that one will want to expand the forms into eigenstates of $\Box_{D-d}$ and the harmonic forms belonging to this operator will lead to the massless modes in

the reduced theory. In the case of the scalar field this harmonic 0-form was '$e^0 = 1$' belonging to ∂_y^2. On Riemannian manifolds, harmonic forms are determined by the cohomology. It is thus intuitively clear that the cohomology of the compact manifold determines the massless field content of the dimensionally reduced theory. A part of these aspects for the case of main interest, namely choosing the compact manifold to be a Calabi-Yau, will be discussed in 1.3.2. In the next section, type II supergravity theories will be analyzed a bit more closely for the case of a CY compactification. The reader not familiar with such spaces is at this point referred to the appendix, part A.1, providing him with various possible definitions and all the important key facts, which will be a firm basis for the rest of this chapter. He will find further sections, dwelling within Algebraic Geometry, allowing understanding of the actual construction of Calabi-Yau spaces within this powerful and beautiful mathematical framework. At this point, the first section of the appendix should be sufficient, the reader is advised to go back to the algebraic sections later.

Compactification of type II supergravity on a Calabi-Yau threefold

Although there seems to be little freedom for string theory / M-theory living in 10 / 11 dimensions, there is a humongous amount of choices upon compactification for the six compact dimensional space, that reduces to a theory in the four dimensions that one knows well. A few steps away from reality, but very interesting, is to let oneself be guided by requiring at least some unbroken supersymmetry in four dimensions, but not too much supersymmetry as this is at present unattractive when seeking to make contact with phenomenology. Compactification of a type II supergravity theory on a CY breaks $\frac{3}{4}$ of the original supersymmetry, leaving 8 out of the original 32 supercharges conserved, yielding $\mathcal{N} = 2$ supergravity in four dimensions. According to the preceding discussion, the massless wave equation $\Box_{10}\,\omega = 0$ in ten dimensions will split up according to

$$\Box_{10} = \Box_4 + \Box_{\mathrm{CY}}, \tag{1.33}$$

from which one sees that harmonic forms ω on the CY X satisfying $\Box_{\mathrm{CY}}\,\omega = 0$ determine the massless field content in four-dimensional compactifications. According to Hodge's famous theorem, there is exactly one harmonic form in every cohomology class, and thus, the CY's Hodge diamond determines the number of massless bosonic fields, and hence also of the massless (super) multiplets. These multiplets shall now be described. In 4d, fermionic charges belong to a spinor representation of $SO(1,3)$, and in the minimal supersymmetric case, supercharges have 4 real components. Writing the 4d Majorana spinor Q containing the supercharges with Weyl spinors $Q = \begin{pmatrix} Q_\alpha \\ Q_{\dot\alpha} \end{pmatrix}$, the $N = 2$ supersymmetry algebra is thus of the form

$$\{Q^i_\alpha, \bar{Q}^j_{\dot\beta}\} = \gamma^\mu_{\alpha\dot\beta} P_\mu \delta^{ij}, \tag{1.34}$$

(and $\{Q^i_\alpha, Q^j_\beta\} = 0, \{\bar{Q}^i_{\dot\alpha}, \bar{Q}^j_{\dot\beta}\} = 0$), where $i, j = 1, 2$, P_μ is the momentum operator and γ^μ is a 4d gamma matrix. The algebra allows three kinds of basic representations (note that tensor multiplets can be dualized into hypermultiplets). The massless field content

of a type II supergravity theory can be arranged into these three possible kinds of $\mathcal{N}=2$ multiplets:

- **Gravity multiplet:** a spin 2 graviton, two spin $\frac{3}{2}$ gravitini and a spin 1 graviphoton,
- **Vector multiplets:** each of which contains a spin 1 photon, two spin $\frac{1}{2}$ fermions and two real spin 0 scalars,
- **Hypermultiplets:** each of which contains two spin $\frac{1}{2}$ hyperfermions and four spin 0 hyperscalars.

On general grounds, check e.g. [21, 22], an $\mathcal{N}=2, d=4$ action, coupled to N_V abelian vector multiplets and N_H abelian hypermultiplets, can be determined to be of the general form (only listing the bosonic part):

$$\begin{aligned} S &= \frac{1}{16\pi G_4}\int d^4x\sqrt{-g}\big(R - g_{I\bar{J}}(\phi)\partial_\mu\phi^I\partial^\mu\bar{\phi}^{\bar{I}} - h_{uv}(q)\partial_\mu q^u\partial^\mu q^v \\ &+ \frac{1}{4}(\mathrm{Im}\mathcal{N}_{IJ})(\phi)\mathcal{F}^I_{\mu\nu}\mathcal{F}^{\mu\nu\,J} + \frac{1}{8}(\mathrm{Re}\mathcal{N}_{IJ})(\phi)\epsilon^{\mu\nu\rho\sigma}\mathcal{F}^I_{\mu\nu}\mathcal{F}^J_{\rho\sigma}\big), \end{aligned} \tag{1.35}$$

with a 4d metric g, N_V complex scalars ϕ^I, spanning a special Kähler manifold (as will be discussed), vector field strengths $\mathcal{F}^I$ and $4N_H$ real scalars q^u, spanning a quaternionic manifold. G_4 denotes the 4d Newton constant, $g_{I\bar{J}}$ denotes the metric on the target space of the involved scalar fields ϕ, h_{uv} the metric on the target space of the scalars q^u, and $\mathcal{N}$ is a complex symmetric matrix, determining the kinetic terms for the vectors. These structures will be discussed in more detail, below. The dimensional KK-reductions (and truncations) of type IIA and type IIB supergravities from ten dimensions indeed fit into this form, [23, 24]. According to this line of arguments, one can interpret such 4d type II supergravities as originating from 10D supergravity and string theory.

Type IIA supergravity in four dimensions

In the following, the bosonic massless field content of type IIA supergravity in 4d will be explained. The 10D origin of each field will be motivated by giving the 10D index structure and fields they originate from as massless modes: this will be indicated by an arrow pointing from the 10D field to the 4d field. Choose Greek indices $\mu = 0, 1, 2, 3$ for the non-compact 4d spacetime, and Latin indices $i, \bar{j}$ for the complex Calabi-Yau 3-fold. For example, $G_{\mu\nu} \to g_{\mu\nu}$, means that the 4d metric is inherited from the 10D metric components with indices in the four non-compact spacetime directions. The gravity and the universal hypermultiplet (universal because it always exists) are the same for every compactification, the number of additional multiplets depends on the specific Calabi-Yau manifold.

1. In the gravity multiplet, one obtains the (spin 2) 4d metric $G_{\mu\nu} \to g_{\mu\nu}$ and the (spin 1) graviphoton $C^{(1)}_\mu \to C_\mu$.

2. One obtains $h^{(1,1)}$ vector multiplets, one for every harmonic $(1,1)$-form on the CY 3-fold[3]. In each of them, one finds a (spin 1) vector $C^{(3)}_{\mu i\bar{j}} \to C^A_\mu$ $(A = 1, ..., h^{(1,1)})$ and two scalars, $B^{(2)}_{i\bar{j}} \to B^A$ and $G_{i\bar{j}} \to J^A$. Combined, $\phi^A = B^A + iJ^A$, they form the complexified Kähler moduli of the Calabi-Yau 3-fold.

3. Apart from the universal hypermultiplet, one obtains $h^{(2,1)}$ additional hypermultiplets, each containing four scalars, $G_{ij} \to a^I, G_{\bar{i}\bar{j}} \to b^I, C^{(3)}_{ij\bar{k}} \to c^I_1, C^{(3)}_{\bar{i}\bar{j}k} \to c^I_2$, where $I = 1, ..., h^{(2,1)}$. The a^I and b^I form the complex structure moduli z^I of the CY.

4. The universal hypermultiplet contains four scalars. One finds the dilaton $\Phi \to \phi$, and an axion $B^{(2)}_{\mu\nu} \to b_{\mu\nu} \Rightarrow a$, where the inherited two-form has been dualized into a scalar [4]. The two other scalars are obtained from the RR 3-form, specifically $C^{(3)}_{ijk} \to c_3$ and $C^{(3)}_{\bar{i}\bar{j}\bar{k}} \to c_4$, and reflect the existence of one harmonic $(3,0)$- and one $(0,3)$-form on the CY.

This is summarized as follows:

type of multiplet	**number**	**bosons**
1. gravity multiplet	1	$g_{\mu\nu}, C_\mu$
2. vector multiplets	$h_{1,1}$	C^A_μ, B^A, J^A
3. hypermultiplets	$h_{2,1}$	a^I, b^I, c^I_1, c^I_2
4. IIA universal hypermultiplet	1	ϕ, a, c_3, c_4

Type IIB supergravity in four dimensions

The massless field content of type IIB supergravity in 4d is organized as follows:

1. In the gravity multiplet, one obtains the (spin 2) 4d metric $G_{\mu\nu} \to g_{\mu\nu}$ and the (spin 1) graviphoton $C^{(4)}_{\mu ijk} \to C_\mu$.

2. Apart from the universal hypermultiplet, one now obtains $h^{(1,1)}$ additional hypermultiplets, each containing four scalars, $G_{i\bar{j}} \to J^I, B_{i\bar{j}} \to B^I, C^{(2)}_{i\bar{j}} \to c^I_1, C^{(4)}_{\mu\nu i\bar{j}} \to c^I_2$, where $I = 1, ..., h^{(1,1)}$. The $t^I = B^I + iJ^i$ form the complexified Kähler moduli of the CY.

3. This time one obtains $h^{(2,1)}$ vector multiplets, one for every harmonic $(2,1)$-form on the CY. In each of them, one finds a (spin 1) vector $C^{(4)}_{\mu i j\bar{k}} \to C^A_\mu$ $(A = 1, ..., h^{(2,1)})$ and two scalars, $G_{ij} \to a^A$ and $G_{\bar{i}\bar{j}} \to b^A$. Combined, $z^A = a^A + ib^A$, they form the complex structure moduli of the Calabi-Yau 3-fold.

[3]The Hodge diamond of a Calabi-Yau and the used notation is explained in the appendix, part A.1.

[4]Note that the field strength of a two form is Hodge dual to the field strength of a scalar in four dimensions: $db = \star da$.

4. In the universal hypermultiplet one finds the dilaton $\Phi \to \phi$, and an axion $B^{(2)}_{\mu\nu} \to b_{\mu\nu} \Rightarrow a$, where the inherited two-form has been dualized into a scalar. The two other scalars are obtained from the RR 2-form and 4-form, specifically $C^{(2)}_{\mu\nu} \to c_{\mu\nu} \Rightarrow c_3$ and $C^{(4)}_{\mu\nu ij} \to \tilde{c}_{\mu\nu} \Rightarrow c_4$.

This is summarized in the following table:

type of multiplet	**number**	**bosons**
1. gravity multiplet	1	$g_{\mu\nu}$, C_μ
2. hypermultiplets	$h_{1,1}$	B^I, J^I, c_1^I, c_2^I
3. vector multiplets	$h_{2,1}$	C_μ^A, a^A, b^A
4. IIB universal hypermultiplet	1	ϕ, a, c_3, c_4

The moduli spaces of CY manifolds: spacetime point of view

Both in the spectrum of IIA and of IIB supergravity on a CY manifold one came across some scalar fields which were given the name moduli of the CY, and this should be explained in some more detail. Giving the Hodge numbers of a Calabi-Yau space does not determine it completely. In fact, it can undergo two types of deformations parametrized by what are known as the Kähler moduli and the complex structure moduli. One can imagine that one has actually selected a whole family of Calabi-Yau manifolds, continuously related through these deformations of moduli, but one normally views this family as one Calabi-Yau manifold with a moduli space [5]. The meaning of these deformations shall now be discussed. Starting from a CY with a Ricci-flat metric $R_{i\bar{j}}(g) = 0$, one can deform the metric $g \to g + \delta g$, demanding that the new metric should again be Ricci-flat, $R_{i\bar{j}}(g + \delta g)$. One can consider deformations with pure indices (with respect to the complex structure),

$$\delta g_{ij} dz^i dz^j + \delta g_{\bar{i}\bar{j}} d\bar{z}^{\bar{i}} d\bar{z}^{\bar{j}}, \tag{1.36}$$

and deformations with mixed indices,

$$\delta g_{i\bar{j}} dz^i d\bar{z}^{\bar{j}} + \delta g_{\bar{i}j} d\bar{z}^{\bar{i}} dz^j. \tag{1.37}$$

It turns out that in order to result in a Ricci-flat metric the latter type of deformations (1.37) are required to be harmonic two-forms $\delta g_{i\bar{j}} dz^i \wedge d\bar{z}^{\bar{j}}$, which naturally associates them with elements in $H^{(1,1)}(X, \mathbb{Z})$. They do not change the index structure of the metric, but as can be pictured intuitively, they change the volume of the CY. In fact, they change the Kähler class J to a new element in $H^{(1,1)}(X, \mathbb{Z})$ [6]. In fact, one can also deform the $b_{i\bar{j}}$-components of the other vector-/ hyper- multiplet scalars accordingly, and one is naturally led to consider complexified Kähler deformations: $(\delta b_{i\bar{j}} + i\delta g_{i\bar{j}}) dz^i \wedge d\bar{z}\bar{j} = (B^A + iJ^A) D_A$,

[5] Apart from deformations, there may also be topologically distinct CY manifolds with the same Hodge numbers.

[6] Thus, they change volumes $\int_{C^n} J^{(n)}$ ($J^{(n)}$ stands for an outer product of the Kähler form, the integral yields the Kähler volume of a cycle) of various n-cycles C^n of the CY.

using the basis D_A for the even degree cohomology defined in the appendix. These are the deformations of the complexified Kähler structure.

Alternatively, and this will lead to the complex structure moduli, the deformations of type (1.36) change the index structure of the metric. In order to still get a Ricci-flat Kähler metric, one needs to amend this by changing the complex structure. This means that one is deforming the unique $(3,0)$-form Ω. Note that this form is harmonic ($\partial\Omega = 0$ and $\bar{\partial}\Omega = 0$) and thus defines a cohomology class in $H^{(3,0)}(X,\mathbb{Z})$. As nicely discussed in [25], the requirement that the new form Ω is again closed, imposes that the deformation is by a $(2,1)$-form, $\omega^{(2,1)}$, and it turns out that this form is also required to be harmonic. This can roughly be seen by writing the variation of coordinates as $dz_i \to dz_i + \mu_i^{\bar{j}} d\bar{z}_j$ (one often calls these forms 'μ' Beltrami differentials), and then writing out the holomorphic variation of $\Omega = f(z) dz_1 \wedge dz_2 \wedge dz_3$ out to first order. One observes that this variation is of type $H^{(3,0)}(X,\mathbb{Z}) \oplus H^{(2,1)}(X,\mathbb{Z})$, and checks that the new holomorphic 3-form is again closed. These deformations are thus naturally associated with elements in $H^{(2,1)}(X,\mathbb{Z})$.

To summarize: the moduli space of a CY 3-fold X splits into a product of the following two pieces, classified by cohomology groups.

$H^{(1,1)}(X)$	Kähler deformations
$H^{(2,1)}(X)$	complex structure deformations

Additionally, it turns out that the Kähler moduli space as well as the complex structure moduli space are both Kähler manifolds of their own, [26]. The Kähler potential $K_{\mathcal{K}}$ of the Kähler moduli space $\mathcal{M}_K$ is found to be

$$K_{\mathcal{K}} = \int_X J \wedge J \wedge J, \tag{1.38}$$

and the Kähler potential $K_{\mathcal{C}}$ of the complex structure moduli $\mathcal{M}_C$ space can be calculated as

$$K_{\mathcal{C}} = -\ln(i \int_X \Omega \wedge \bar{\Omega}), \tag{1.39}$$

using the Kähler form J and the holomorphic $(3,0)$-form Ω. An even more refined mathematical structure will be discussed in the next subsection. This section shall be closed with a few remarks about – in fact simpler – compactifications, retaining more supersymmetry in the 4d theory, as they connect to some of the author's research and will be used in chapter 5. It has been said that a Calabi-Yau compactification breaks $\frac{3}{4}$ of the supersymmetry, leaving behind an $\mathcal{N} = 2$ supergravity theory in 4d. One can also compactify on a six-torus T^6, breaking no supersymmetry, thus keeping 32 supercharges in 4d. As irreducible spinors in 4d are Majorana spinors with 4 components this leads to a $\mathcal{N} = 8, d = 4$ supergravity theory. In [5], we analyzed a class of multi-centered black holes in this setup, and this compactification is discussed in 5.2. Apart from that, one could also choose to compactify on a CY 2-fold times a two-torus, $K3 \times T^2$, breaking one half of the supersymmetry, leaving 16 conserved supercharges. This leads to an $\mathcal{N} = 4, d = 4$ supergravity theory. For an extremely insightful discussion of $K3$ CY-twofolds and their moduli spaces, the reader is referred to [27].

1.3.2 Special geometry of Calabi-Yau compactifications

It was already mentioned that the Kähler as well as the complex structure moduli spaces turned out to be Kähler manifolds, their Kähler potentials taking a simple form, (1.38, 1.39). However, the structure of these spaces is even more restricted. In general, for an $\mathcal{N} = 2, d = 4$ supergravity theory, the target spaces $\mathcal{M}_V$ for the scalars X^A (where $A = 0, 1, ..., h^{(1,1)}$ for type IIA and $A = 0, 1, ..., h^{(2,1)}$ for type IIB) arising in vector multiplets $X^A : \mathcal{M}^{(1,3)} \to \mathcal{M}_V$ obey a very restricted geometry, called special Kähler geometry, or simply '*special geometry*'. Note that the moduli consist of one extra scalar compared to the previous discussion. This extra scalar field X^0, which is unphysical, arises naturally when constructing $\mathcal{N} = 2, d = 4$ actions using superconformal tensor calculus and is convenient to present the mathematical structure from a coordinate independent viewpoint.

On the other hand, the target spaces $\mathcal{M}_H$ for the scalars arising in hypermultiplets $\phi : \mathcal{M}^{(1,3)} \to \mathcal{M}_H$ are also of a restricted type of geometry, called a quaternionic Kähler manifold (which itself is not Kähler). As the interest in this thesis lies in BPS black holes, the hypermultiplets are not of much further interest. They do not couple to the supergravity multiplet or to vector multiplets, and beyond this fact, quaternionic scalars can be set to any constant value for the black hole solutions, which will be considered. In particular, quaternionic scalars are not influenced by the attractor equations (see section 2.1.3) and their value is arbitrary, even at the event horizon. The point of interest here is that the vector multiplet scalars target in a special Kähler manifold. Some properties of special geometry will now be reviewed. For a thorough discussion of special geometry, the reader is referred to [25, 28–31] and for specific mathematical interest [32, 33]. Physically, special geometry governs the couplings of the vector multiplets as well as the metric of the scalar manifold. It will be presented from a somewhat abstract point of view first, as this will allow to stress the symmetry in structure between the situations arising from type IIA and IIB supergravities in a moment, also offering the chance to highlight the essential differences, contrasting the analogies.

A special Kähler manifold is nicely described using the machinery associated to a principal bundle $P(\mathcal{M}_V, \mathrm{Sp}(2N_V + 2))$ with structure group $\mathrm{Sp}(2N_V + 2)$ above the base space, which will, suggestively, already at this point be denoted as $\mathcal{M}_V$. Note that this is a bundle over the moduli space of a CY. Also picture that a CY 3-fold (with the corresponding Kähler/complex structure) is associated to each point $z \in \mathcal{M}_V$, namely the one with the corresponding Kähler/complex structure. A special Kähler manifold allows a nowhere vanishing holomorphic section Ω,

$$\Omega(z) = (X^A(z), F_A(z)), \tag{1.40}$$

of an associated vector bundle $P \times_\rho V$ corresponding to a vector representation ρ of $\mathrm{Sp}(2N_V + 2)$. The coordinates on the (vector space) fibers V are split up into X^A on the one hand, which can be seen as homogeneous coordinates on $\mathcal{M}_V$ (they are the scalars arising from compactification), and on the other hand the F_A coordinates. Actually, Ω is only defined projectively and one can consider a rescaling, $\Omega(z) \to e^{f(z)}\Omega(z)$, using a holomorphic function $f(z)$. One thus really specifies a section Ω of the product bundle

$(P\times_\rho V)\otimes\mathcal{H}$, where $\mathcal{H}$ is a line bundle over $\mathcal{M}_V$, whose first Chern class equals the Kähler form on $\mathcal{M}_V$. So, to be precise,

$$\Omega\in\Gamma(\mathcal{M}_V,(P\times_\rho V)\otimes\mathcal{H}), \tag{1.41}$$

where Γ denotes the space of sections. At each point z, Ω is an element of the fibre $(V\otimes H)_z\cong V\otimes H$. Such a choice of holomorphic section will be interpreted nicely for type II supergravity theories, shortly. For explicit calculations, it is appealing to choose local, so called *special coordinates* on $\mathcal{M}_V$, which are affine coordinates,

$$z^A=\frac{X^A}{X^0}. \tag{1.42}$$

Having chosen such a section (1.40), the Kähler potential and thus also the metric on the base space $\mathcal{M}_V$ are determined. The fibres V are endowed with a symplectic product, $\langle,,.\rangle: V\times V\to\mathbb{Z}$, yielding

$$\langle\Gamma_1,\Gamma_2\rangle=X_1^AF_A^2-X_2^AF_A^1, \tag{1.43}$$

for $\Gamma_{1,2}\in V$ expressed in coordinates as $\Gamma_i=(X_i^A,F_A^i)$. This allows writing the Kähler potential as

$$K=-\ln\left(i\langle\bar\Omega,\Omega\rangle\right)=-\ln\left(i(\bar X^AF_A-X^A\bar F_A)\right), \tag{1.44}$$

which is the great virtue of special geometry. Note that under the rescalings $\Omega\to e^{f(z)}\Omega$, mentioned above, the Kähler potential shifts by a Kähler transformation,

$$K\to K-f(z)-\bar f(\bar z), \tag{1.45}$$

thus leaving the metric invariant. In order to give one of various clean definitions of special Kähler geometry, one should in principle add the condition

$$\langle\mathcal{D}_A\Omega,\mathcal{D}_B\Omega\rangle=0, \tag{1.46}$$

which ensures that the matrix $\mathcal{N}_{AB}$, (1.48), to be defined below, is symmetric, using the covariant derivative

$$\mathcal{D}_A=\partial_A+\partial_AK, \tag{1.47}$$

which satisfies the desired property $D_A(e^f\Omega)=e^fD_A\Omega$.

Apart from these statements about the target space of the scalars, the coupling of the vector multiplet vectors C_μ^A $(A=1,...,N_V)$, together with the graviphoton C_μ, as well as their magnetic duals, alltogether yielding $2N_V+2$ vector fields, is also fully determined once a choice of holomorphic section (1.40) has been made. These vectors live in a section of a $\mathrm{Sp}(2N_V+2,\mathbb{Z})$-vector bundle *above spacetime*, and accordingly, these transformations mixing the graviphoton C_μ with the other N_V vectors C_μ^A as well as their magnetic duals, leave the action invariant, as was discussed first in [34]. The matrix $\mathcal{N}_{IJ}$ determines the kinetic terms of the vectors appearing in a $\mathcal{N}=2, d=4$ action, see formula (1.35), reads

$$\mathcal{N}_{AB}=\overline{H(F)}_{AB}+2i\frac{\mathrm{Im}(H(F))_{AB}z^B\,\mathrm{Im}(H(F))_{KL}z^L}{\mathrm{Im}(H(F))_{AB}z^Az^B} \tag{1.48}$$

using the Hessian $H(F)_{AB} = \partial_A \partial_B F$ of the prepotential F, which will be discussed below, and where $\partial_A = \frac{\partial}{\partial z^A}$ is written in affine coordinates (1.42).

According to what was stated before, for a type IIA compactification, the vector multiplet scalars target in the moduli space of Kähler deformations, $\mathcal{M}_V = \mathcal{M}_K$, whereas for a type IIB compactification the scalars target in the complex structure moduli space $\mathcal{M}_V = \mathcal{M}_C$. The structure of special geometry will now be inspected separately for the IIA and the IIB case in more detail.

Special geometry of the IIA Kähler moduli space

For type IIA supergravity compactified on a CY 3-fold, one has $N_V = h^{(1,1)}$ vector multiplets containing one scalar field each. One can again group them together with one more auxiliary scalar field X^0. They define homogeneous coordinates on the projective manifold $\mathcal{M}_V = \mathcal{M}_K$, where the last equation states that the target space for the scalars is the Kähler moduli space of the CY.

The $\mathrm{Sp}(2h^{(1,1)}+2)$-vector bundle V can now be specified. It has fibers $H^{2*}(X,\mathbb{Z})$ (even degree cohomology of the CY X), as defined in the appendix, (A.2). An even degree form Γ is expressed with the basis introduced in the appendix, $\Gamma = \Gamma^0 + \Gamma^A D_A + \Gamma_A \tilde{D}^A + \Gamma_0\, \omega$. The symplectic product on the fibers between two even degree cohomology forms is, up to some signs, defined as the integral over X of their wedge product, as follows. Using the map

$$\begin{aligned} \star: \quad & H^{2*}(X,\mathbb{Z}) \to H^{2*}(X,\mathbb{Z}), \\ & \Gamma = (\Gamma^0, \Gamma^A, \Gamma_A, \Gamma_0) \to \Gamma^* = (\Gamma^0, -\Gamma^A, \Gamma_A, -\Gamma_0), \end{aligned} \tag{1.49}$$

the intersection product reads

$$\langle \Gamma_1, \Gamma_2 \rangle = \int_X \Gamma_1 \wedge \Gamma_2^*, \tag{1.50}$$

where it is naturally understood that only the pairings yielding a six-form are considered to contribute to the integral.

A choice of holomorphic section as in (1.40) becomes a beautiful geometric statement: it means choosing a Kähler class. Put differently, it assigns volumes to the various cycle classes of the CY homology. Using the complexified Kähler form $\mathcal{J}_K = X^A D_A$, these volumes, which are by definition the periods of the complexified Kähler form, read

$$X^0 = \int_{D^0} 1, \tag{1.51}$$

$$X^A = \int_{D^A} \mathcal{J}_K, \tag{1.52}$$

$$F_A = \int_{\tilde{D}_A} \mathcal{J}_K \wedge \mathcal{J}_K, \tag{1.53}$$

$$F_0 = \int_X \mathcal{J}_K \wedge \mathcal{J}_K \wedge \mathcal{J}_K. \tag{1.54}$$

Note that the integrals only depend on homology classes of the cycles over which one integrates. Hence, the integration domains are written with the homology basis elements defined in the appendix, (A.5). The section $\Omega(z)$ is thus now just the period vector $\Omega = X^A D_A - F_A \tilde{D}^A$ [7] (literally the section in coordinates), where $A = 0, ..., h^{(1,1)}$.

Everything was now expressed in homogeneous coordinates, but this is not always convenient. One can switch to special coordinates on $\mathcal{M}_K$,

$$t^A = \frac{X^A}{X^0}, \qquad \text{IIA complexified Kähler deformation moduli} \tag{1.55}$$

which will be from now on called the Kähler moduli. Note that they are given by the complexified Kähler form $t = t^A D_A = B + iJ$, a $(1,1)$-form. The holomorphic section can now be written as

$$\Omega = -e^t = -e^{t^A D_A} = -(1 + t + \frac{1}{2} t \wedge t + \frac{1}{6} t \wedge t \wedge t), \tag{1.56}$$

where $A = 1, ..., h^{(1,1)}$, now. According to the geometric interpretation just given, it will also be referred to as the holomorphic period vector. The Kähler potential of the Kähler moduli space can be written out as

$$\begin{aligned} K &= -\ln\left(i\langle\Omega, \bar{\Omega}\rangle\right) = -\ln\left(i\int_X \Omega \wedge \bar{\Omega}^*\right), \\ &= -\ln\left(i\int_X e^t \wedge e^{-\bar{t}}\right) = -\ln\left(\frac{4}{3}\int_X (J \wedge J \wedge J)\right), \end{aligned} \tag{1.57}$$

noting that the operation star acts as $e^t \to e^{-t}$. This shows that the Kähler potential depends logarithmically on the volume of X. This period vector shall from now on be referred to as the holomorphic period vector, $\Omega_{\text{hol}} = -e^t$. For later reference, also the normalized period vector is introduced,

$$\Omega = e^{\frac{K}{2}} \Omega_{\text{hol}} = -e^{\frac{K}{2}} e^t, \tag{1.58}$$

which of course satisfies $i\langle\Omega, \Omega\rangle = 1$.

As shall be discussed more closely for the IIB case below, one can introduce a prepotential

$$F(X) = \frac{1}{2} X^A F_A, \tag{1.59}$$

which is homogeneous of degree two in the coordinates X^A, from which one can easily obtain the Kähler potential and thus the metric as $g_{A\bar{B}} = \partial_A \partial_{\bar{B}} K$. The dual periods can now be written as a derivative of the prepotential, $\partial_A F(X) = F_A$. For the type IIA supergravity compactification without any corrections, the prepotential reads

$$F(X) = \frac{D_{ABC}}{6} \frac{X^A X^B X^C}{X^0}. \tag{1.60}$$

[7] To check the signs appearing in Ω, compare with (A.6).

From the string theoretical point of view, the prepotential $F(X)$ is exact at tree level, it does not receive any string loop corrections. This is not hard to understand, if one goes back and considers in which multiplets the different scalars sit in an $\mathcal{N} = 2, d = 4$ compactification on a CY threefold. The scalars corresponding to periods of the 2-cycles, X^A, sit in a vector multiplet, whereas the dilaton sits in the universal hypermultiplet. As the dilaton determines the string coupling, which governs the string loop expansion, and there are no couplings between vector and hyper multiplets, it is clear that the prepotential will not receive any string loop corrections. However, it can and does receive perturbative corrections in $\alpha^{'}$, but this is not the complete story. For the prepotential arising in the IIA compactification, there is another type of corrections arising. This is also not hard to understand intuitively. The periods of the Kähler form, by definition measuring volumes of two-cycles, can receive instanton corrections by strings wrapping (holomorphic) curves. These are worldsheet instanton corrections, which depend on α' in a non-polynomial way. From supergravity considerations, it is clear that the form of the perturbative corrections in $\alpha^{'}$ is very restricted. In the classical supergravity description of the theory, the $\mathrm{Sp}(2h^{(1,1)} + 2, \mathbb{R})$-symmetry allows a shift in the B-field. This is known as the *Peccei-Quinn symmetry*, and it constrains the form of the perturbative corrections to the prepotential: the additional term can only be of the form $iC(X^0)^2$, with C a constant. In fact, this constant has been determined using mirror symmetry. The constant takes on the value $\frac{\zeta(3)\chi(X)}{2(2\pi)^3}$ (see [35]) with ζ being the Riemann-Zeta function and $\chi(X)$ the Euler characteristic of the CY X. More specifically, a direct relation has been established between the prepotential and the topological free energy of the A-model topological string theory (3.41). The prepotential including corrections thus takes the form

$$F(X) = \frac{D_{ABC}}{6}\frac{X^A X^B X^C}{X^0} + i\frac{\zeta(3)\chi(X)}{2(2\pi)^3}(X^0)^2 + F_{\text{nonpert}}, \tag{1.61}$$

where the last term F_{nonpert} arises from the worldsheet instantons mentioned before, and breaks the $\mathrm{Sp}(2h^{(1,1)} + 2, \mathbb{R})$-symmetry down to $\mathrm{Sp}(2h^{(1,1)} + 2, \mathbb{Z})$, a nice illustration of the discretization of symmetries realized in the low-energy supergravity descriptions string theory imposes. As will be discussed in chapter 3, the non-perturbative corrections are directly encoded in the Gromov-Witten expansion of the topological free energy.

Special geometry of the IIB complex structure moduli space

In this case one has $N_V = h^{(2,1)}$ vector multiplets, and the scalars in $\mathcal{M}_C$ parametrize the complex structure of the Calabi-Yau metric. The $\mathrm{Sp}(2h^{(2,1)} + 2)$-vector bundle has fibers $H^3(X, \mathbb{Z})$ (the third cohomology of the the CY X): this is known as a Hodge bundle. The name 'Hodge' bundle explains itself from the fact, that a choice of section of the bundle can be seen as fixing a choice of the complex structure of a CY, thus fixing index structure (what one calls holomorphic and anti-holomorphic) and therefore 'Hodge' structure of a CY. The symplectic intersection product defined on the fibers of the Hodge bundle is in this case as defined in the appendix, (A.6).

Again, a choice of holomorphic section (1.40) [8] has a beautiful geometric interpretation. It is given in terms of periods of the holomorphic $(3,0)$-form of the Calabi-Yau, using the basis of 3-cycles (A.7), given in the appendix A.1,

$$X^0 = \int_{A^0} \Omega, \tag{1.62}$$

$$X^I = \int_{A^I} \Omega, \tag{1.63}$$

$$F_I = \int_{B_I} \Omega, \tag{1.64}$$

$$F_0 = \int_{B_0} \Omega. \tag{1.65}$$

where $I = 1, ..., h^{(2,1)}$. The 'A-periods' X^I of the holomorphic 3-form Ω (note the analogy with (1.51)) yield coordinates on $\mathcal{M}_C$, and, as will be discussed, the 'B-periods' F_I are functions of the A-periods, $F_I = F_I(X)$. Again, one can also introduce affine or so-called 'special coordinates',

$$z^I = \frac{X^I}{X^0}, \qquad \text{IIB complex structure deformation moduli} \tag{1.66}$$

which shall from now on be called complex structure moduli of X.

Picking a holomorphic section for type IIB, as was done by fixing the periods, means fixing the holomorphic $(3,0)$-form (up to a rescaling). One can express the three-form as $\Omega = X^A\alpha_A - F_A\beta^A$, and the Kähler potential K of the complex structure moduli space reads

$$K = -\ln(i(\int_X \Omega \wedge \bar{\Omega})). \tag{1.67}$$

Now one can vary the complex structure moduli of X. This means moving in the complex structure moduli space, and this will generally transform the holomorphic $(3,0)$-form into a linear combination of a $(3,0)$-and a $(2,1)$-form. A general variation reads

$$\partial_I\Omega = K_I\Omega + \chi_I{}^J\alpha_J \tag{1.68}$$

where K_I is a function of the coordinates on $\mathcal{M}_C$, and $\chi_I{}^J\alpha_J$ is a $(2,1)$-form. Clearly, (1.68) implies $\langle\partial_I\Omega, \Omega\rangle = 0$, and it immediately follows that

$$F_I = X^J\partial_I F_J. \tag{1.69}$$

One can rewrite F_I as $F_I = \frac{1}{2}\partial_I(X^J F_J)$ and introduce the prepotential

$$F(X) = \frac{1}{2}X^I F_I, \tag{1.70}$$

[8] Note that the same symbol Ω is used for the holomorphic section of the vector bundle as for the holomorphic $(3,0)$-form on the Calabi-Yau X. As this seems the most common notation in the literature, it will be used here too, hoping that in the light of this remark, it will not cause any confusion to the reader.

which is homogeneous of degree two in the coordinates X^I. Again, the dual periods are obtained as a derivative, $\partial_I F(X) = F_I$.

The prepotential $F(X)$ for type IIB is exact. It cannot receive worldsheet instanton corrections, as one is now dealing with three-cycles, and there are no E2-branes in type IIB string theory. As mentioned above, the prepotential of the Kähler moduli space does receive corrections. However there is a symmetry, called *mirror symmetry* (which will be discussed in more detail in section 3.4), relating a type IIA compactifiation on a CY X to a IIB compactification on a so called mirror CY Y. As the physics of these two models are equivalent, mirror symmetry can be utilized to calculate quantities which receive an infinite series of corrections on the IIA side, by switching to the IIB side, where these quantities are determined by classical geometry. Again the prepotential is directly related to the free energy of topological string theory, but this time to the B-model.

1.4 BPS spectrum of type II string theory

This section is a short presentation of the BPS spectrum of type II string theories, a subspectrum of states conserving part of the supersymmetry. This short discussion only contains standard material included in many textbooks and reviews. Should the reader be familiar with D-branes, BPS states in general and also BPS supergravity solutions in particular, she/he can directly move on to chapter two. D-branes in type II theories will be picked out and construed as generalizations of charged particles in electromagnetism. This is followed by the relevant formulae for D-brane actions. The second part of this subsection is a discussion about the counterpart to the D-brane description of BPS states, consisting of solitonic solutions to supergravity: the *p-brane* solutions.

1.4.1 D-Branes in type II string theory

As mentioned earlier on, D-branes were originally defined as open string boundary conditions,

$$\begin{aligned} n^a \partial_a X^\mu &= 0 \qquad \mu = 0, ..., p\,, \\ X^i &= c^i \qquad i = p+1, ..., 9\,, \end{aligned}$$

where the c^i are constants, and n^a is a normal vector to the surface $X^i = c^i$ in 10D spacetime. A D-brane is thus an extended object, with p+1 worldvolume dimensions. The discovery by Polchinski in 1995, [8], that the extended classical objects on which open strings can end, called D-branes, multipresent in the weak string coupling description of string theory, are actually charged sources for closed strings in the RR sector, was certainly one of the milestones in the young history of string theory. In order to explain this a bit, it is worth going back to Maxwell-theory and discussing the concept of charge once more.

Electric and magnetic charges in electromagnetism

In a favourite notation, the Maxwell equations in the presence of charge and currents read

$$dF = *J_m, \tag{1.71}$$
$$d*F = *J_e, \tag{1.72}$$

where J_m is a magnetic four-current, and J_e is an electric four-current. A particle is said to carry a charge and act as a source for an electromagnetic gauge field A. This is described by an interaction of the form $S = e\int A$, whereas the charge of the particle can be calculated using Gauss' law, using the field strength $dA = F$. Electric (e) and magnetic (g) charge can be defined in terms of the field strength, as

$$e = \int_{S^2} *F,$$
$$g = \int_{S^2} F,$$

where the S^2 surrounds the sources. Note that F is a two-form field strength, and Hodge duality will send this to a $(d-2)$-form field strength, which is of course also a two-form for $d = 4$.

Charged Dp-branes

This concept of charge generalizes to higher dimensional objects. Just like a charged particle (1-dimensional worldline) couples to a one-form gauge field, a charged $(p+1)$-dimensional object, namely a Dp-brane is said to couple to a $(p+1)$-form, a circumstance which is accompanied by an interaction of the form

$$S = \mu_p \int C^{(p+1)}, \tag{1.73}$$

where integrand and integrator (not written explicitly) are given as the product of the value of the $(p+1)$-form gauge field $C^{(p+1)}$ with the induced volume element on the D-brane hypersurface in 10D spacetime, and μ_p is the charge of the p-brane (it can be either electrical or magnetical). As was stated previously, such $(p+1)$-form gauge fields arise from the RR-sector of type II string theories, and 'Dp-branes' are precisely the kind of objects charged with respect to these gauge fields $C^{(p+1)}$. This of course requires that the putative wavefunction of a D-brane transforms accordingly. One therefore speaks of the RR-charge of a D-brane.

In analogy to the charge in electromagnetism, a Dp-brane carries electric charge q_p (q stands for an electric charge, and the subscript indicates that it is the charge of a p-brane) measured by

$$q_p = \int_{S^{D-(p+2)}} *F_{p+2}, \tag{1.74}$$

where for string theory in $D = 10$, F_{p+2} is a $D-(p+2)$-form field strength and a D(p+2)-sphere is required to surround a Dp-brane. One can in complete analogy equally model magnetically charged branes, with magnetic charge p_p (p stands for a magnetic charge and the subscript again indicates the dimensionality of the brane) measured by

$$p_{6-p} = \int_{S^{p+2}} F_{p+2}, \tag{1.75}$$

where a S^{p+2} is required to surround a (6-p)-brane: the magnetic dual of Dp-brane is a D(6-p)-brane.

D-branes in IIA string theory

As discussed before, the low-energy spectrum contains a RR 1-form $C^{(1)}$ and a RR 3-form. From dimensionality, it is clear that one expects a D0-brane and a D2-brane. Fitting into the general scheme given above, the (electric) D0-brane charge reads $q_0 = \int_{S^8} *dC^{(1)}$, and correspondingly one can also define a magnetic charge $p_6 = \int_{S^2} dC^{(1)}$. Out of dimensional reasons, the S^2 can surround a D6-brane, which means that the magnetic dual of a D0-brane is a D6-brane. Similarly, the D2-brane charge is defined as $q_2 = \int_{S^6} *dC^{(3)}$, and the magnetically dual charge reads $p_4 = \int_{S^4} dC^{(3)}$, and the magnetically dual of a D2-brane is a D4-brane. One can also include a D8-brane in type IIA string theory, coupling to a non-physical gauge field, but this is of no relevance in this thesis.

Of specific interest for this thesis are D-branes which can be wrapped on cycles in CY manifolds and yield point-like objects from a 4d point of view. One can then imagine the 4d particle – or, if one generates enough mass, a black hole – as a beautifully 'geometrized' particle, or black hole. The following table summarizes the branes of interest, indicating whether they will be referred to as 'electric' or 'magnetic':

Type IIA electric and magnetic BPS D-branes	
D0-branes	electric q_0
D2-branes	electric q_2
D4-branes	magnetic p_4
D6-branes	magnetic p_6

D-branes in IIB string theory

The low-energy spectrum contains a RR 0-form $C^{(0)}$, a RR 2-form $C^{(2)}$, and a RR 4-form $C^{(4)}$. Again, from dimensionality, it is clear that one expects a D(-1)-brane (this is an object localized in space *and* time, thus an instanton, also called a *D-instanton*), a D1-brane and a D3-brane. The magnetic dual of a D-instanton has a charge of the form $p_7 = \int_{S^1} dC^{(0)}$ and is a D7 brane. The D1-brane charge reads $q_1 = \int_{S^7} *dC^{(2)}$, the magnetically dual is a D5-brane carrying the charge $p_5 = \int_{S^3} dC^{(2)}$. Finally, there are D3-branes carrying charges of the form $q_3 = \int_{S^5} *dC^{(4)}$, and the magnetic duals also turns out to be D3-branes, carrying charges $p_3 = \int_{S^5} dC^{(4)}$.

In analogy to the IIA case, the branes of interest for this thesis are summarized in the following table:

Type IIB electric and magnetic BPS D-branes	
D1-branes	electric q_1
D3-branes	electric q_3
D3-branes	magnetic p_3
D5-branes	magnetic p_5

Preservation of supersymmetry and BPS states

The branes presented for type IIA and IIB string theory are stable. One could also consider other branes, but these would not carry a conserved charge and would decay. These processes are complicated and are under present investigation, in particular in the context of tachyon condensations in string field theory. Stability of a D-brane is reflected in the fact that the massless open string spectrum ending on such a D-brane does not contain a tachyonic mode. It is beyond the scope of this thesis to go any further into these matters.

Another important fact is that these D-branes break half of the supersymmetry of the vacuum. This means that a brane placed in the 10D background will leave 16 out of the original 32 supercharges of type II string theories conserved. For this reason, they are also called $\frac{1}{2}$-BPS states, a terminology which will receive further explanation when p-brane solutions of supergravity will be discussed. On the other hand, if one considers a compactification on a CY, one has already broken $\frac{3}{4}$ of the original supersymmetry, leaving eight remaining conserved supercharges. Again, placing a D-brane in this background, breaks $\frac{1}{2}$ of the remaining supersymmetry, leaving 4 supercharges conserved, and one speaks of a $\frac{1}{2}$-BPS state of the compactified theory. Finally, one can also combine various D-branes, but superimposing them generically just breaks all supersymmetry. As is discussed in detail in [9], one can however superimpose a Dp-brane and a D(p-4)-brane, successively breaking half of the remaining supersymmetry, twice. This leads to what is called a $\frac{1}{4}$-BPS state. For example, the combination of a D4 brane with a D0 brane yields a $\frac{1}{4}$-BPS state of type IIA string theory compactified on a CY threefold. In the same way, one can of course also construct $\frac{1}{8}$-BPS states.

The Dirac-Born-Infeld and the Chern-Simons action

One can describe the physics of D-branes at low energy by an effective action. The following discussion will be restricted to the bosonic parts of the action. As can be followed in many textbooks, it turns out that the actions for D-branes in type II string theories are described by two terms. The first one arises from the RR-sector of the theory, and is a generalization of the Born-Infeld action for non-linear electrodynamics. For a Dp-brane, it takes the form

$$S_p = -T_p \int d^{p+1}x\, e^{-\phi} \sqrt{\det(g + b + 2\pi\alpha' F)}, \tag{1.76}$$

where the integral is over the D-brane worldvolume, and where

- T_p is the Dp-brane tension,
- $g = \Xi^*(G), b = \Xi^*(B^{(2)}), \phi = \Xi^*(\Phi)$ are the pullbacks of the 10D spacetime metric, the antisymmetric NS-NS 2-form and the dilaton to the worldvolume of the D-brane, respectively, using the map $\Xi : H \to \mathbb{M}_{1,9}$ to denote the embedding of the (p+1)-dimensional Dp-brane hypersurface H in 10D spacetime,
- the 2-form F is the field strength of the $U(N)$ gauge field living on a stack of N Dp-branes.

It was already discussed that a Dp-brane couples to RR gauge fields, and the action corresponding to minimal coupling is of the form $S = \int_H d^{p+1}xC^{(p+1)}$. However, as it turns out, from demanding (chiral) anomaly cancellation on the intersection between two (or more) branes, the true topological coupling is more complicated: it has been found to be a Chern-Simons type action, [36], and reads

$$S = \frac{T_p}{2} \int_H C \wedge \mathrm{ch}(F) \wedge \sqrt{\frac{\hat{A}(TH)}{\hat{A}(NH)}}, \tag{1.77}$$

where

- T_p again denotes the tension of the Dp-brane,
- C is the total RR potential (a sum of the RR forms $C^{(i)}$ of different degree),
- $\mathrm{ch}(F)$ is the Chern character belonging to the vector bundle F, which can be written out using the field strength of the $U(N)$ gauge field, $\mathrm{ch}(F) = \mathrm{Tr}\left(\exp(\frac{F}{2\pi})\right)$,
- $\hat{A}(TH)$ is the well known A-roof genus of the tangent bundle to the brane worldvolume H, and $\hat{A}(NH)$ is the A-roof genus of the normal bundle. For example, for a tangent bundle TH, the A-roof genus is related to the Todd class by $\hat{A}(TH) = \sqrt{\mathrm{td}(T_{\mathbb{C}}H)}$.

1.4.2 p-brane solutions in supergravity

Supergravity theories, and type II supergravity theories in particular, support a type of classical solutions of specific interest. At this point I will have to jump ahead of myself for just one moment and use some simple black holes as thought material. I will go back and discuss black holes more systematically, in the next chapter. One of the proximate generalizations of the easiest black hole solution, which has been around the longest, namely the Schwarzschild black hole, is a black hole carrying charge, besides mass. It is called a Reissner-Nordström (RN) black hole, and the metric is given in equation (2.3). This solution, being interesting in itself, turns out also to be a solution of supersymmetric generalizations of general relativity: supergravity. In fact, one can imagine a 4d supergravity theory originating from type IIA or type IIB theory with the RN black hole as a solution. The solution is characterized by its mass M, and its charge Q, which allows one to distinguish between three cases.

- $M > Q$: In this case, the RN black hole turns out to break all the supersymmetry present in the vacuum, and the solution is called non-extremal. Futhermore, the black hole has two event horizons.

- $M = Q$: Such a solution is called the *extremal* RN black hole, and it turns out to preserve $\frac{1}{2}$ of the original supersymmetry, rendering it a $\frac{1}{2}$-BPS solution in supergravity, terminology-wise. The two event horizons existing in the previous case approach each other when the values of mass and charge approach each other, and the two horizons become identical when having reached the extremal case.

- $M < Q$: In this case, the two horizons disappear, the solution describes a naked singularity, which is excluded from the physical spectrum by the cosmic censorship principle.

The example of an extremal RN black hole in supergravity theories allows commenting on the non-perturbative aspect of such a solution and the (satisfied) BPS bound, which are general features of BPS p-brane solutions to supergravity.

- **Non-perturbative solitonic nature**
  A RN black hole solution (or any black hole solution for that matter) is a called a *non-perturbative* solution to the non-linear equations of motion arising from supergravity (or general relativity), as it is a non-trivial solution, which cannot be found from a linearized version of the equations of motion. It is very distinct from the vacuum, as it carries a non-zero (topological) conserved quantum number (or charge), which is zero for the vacuum (and states which are perturbatively related to the vacuum). Thinking of a putative quantum theory of which supergravity is a classical limit, such a black hole solution should have a mass inverse to some power of a coupling constant, as it cannot be found in the weak coupling limit (perturbatively). It is thus very massive, and any possible quantum effects due to exchange of such 'solutions' is bound to be a *non-perturbative* effect. It is also a static (or at least a stationary) solution to non-linear differential equations, localized in nature, and finite, which are attributes associated to a soliton. For this reason, they are also called solitonic objects. Namely, such a soliton is thought to interpolate between the vacuum at infinite distance of the black hole, and the (asymptotic) near-horizon geometry. For example, the ordinary 4d Schwarzschild black hole interpolates between the vacuum and $\mathrm{AdS}_2 \times S^2$.

- **The BPS bound**
  The so-called extremal mass-charge bound, $M = Q$, is an example of the more general BPS bound. Actually, the $\mathcal{N} = 2$ supersymmetry algebra given in (1.34) can be (and in the presence of a solution like the RN black hole *is*) supplemented by a central charge Z, yielding the relations

$$\{Q^i_\alpha, Q^j_\beta\} = \epsilon_{\alpha,\beta}\epsilon^{ij}Z, \tag{1.78}$$

$$\{\bar{Q}^i_{\dot\alpha}, \bar{Q}^j_{\dot\beta}\} = \epsilon_{\dot\alpha,\dot\beta}\epsilon^{ij}Z. \tag{1.79}$$

Switching to a new basis, $\tilde{Q}^{\pm}_{\alpha} = \frac{1}{\sqrt{2}}(Q^1_{\alpha} \pm \epsilon_{\alpha\beta}\bar{Q}^2_{\dot{\beta}})$, and taking the system to the rest frame, $P^{\mu}(M,0,0,0)$, one gets the relations

$$\begin{aligned} \{Q^+_{\alpha}, Q^{+\dagger}_{\dot{\beta}}\} &= \delta_{\alpha,\dot{\beta}}(M+Z), \\ \{Q^-_{\alpha}, Q^{-\dagger}_{\dot{\beta}}\} &= \delta_{\alpha,\dot{\beta}}(M-Z),, \end{aligned}$$

(all the other anticommutators vanish). Unitarity thus imposes the requirement $M \geq Z$, which is called the Bogomolny-Prasad-Sommerfeld (BPS) bound.

If the BPS bound is satisfied, $M = Z$, it is obvious that one of the two anticommutators vanishes trivially. This means that a solution like the extremal RN black hole solution automatically preserves half of the supersymmetry: it is a $\frac{1}{2}$-BPS state.

There is a rich variety of such solitonic solutions, generally called p-branes, supporting a BPS bound as a general feature. The trailblazing insight of Polchinski in 1995 was that these solitons can be associated to Dp-branes, the objects appearing as boundary states in open string perturbation theory (hence the name p-branes). Their RR charges are the conserved charges that act as sources for the various anti-symmetric gauge fields appearing in the supergravity actions. What is presented for D-branes, can also be adapted to NS-branes. The solution, which is a source for the three-form $H^{(3)}$ appearing in the NS sectors of both type IIA and IIB string theory, has to be a 1-brane, and is referred to as a NS1 brane. One can show that the corresponding dual field strength in this case is a seven-form, which means that there is a magnetically dual NS5-brane, which exists in type IIA and in type IIB string theory. The example of an NS1-solution to supergravity is called a *black string*, and serves to give some further intuition for the notion of extremality. Already in 1991, it was discovered, that there is a whole family of black string solutions, [37]. These solutions are called 'black' because the string is in general surrounded by an event horizon. This is not the case, if the value of the mass M of the string is minimal (and is given by the charge Q in appropriate units). In this case, the string is not excited and satisfied the BPS bound. An 'excited state' is not BPS, and this is also the intuition one can keep in mind for black holes. A non-BPS black hole is 'excited', but by radiating, it drives itself down to the BPS bound, leaving behind an extremal black hole.

Constructing general p-brane solutions

The following lines are some remarks on how one finds p-brane solutions to supergravity. This provides the reader with some intuition about the origin and the form of the black hole solutions which will appear in this thesis. The main idea is to make an 'ansatz' imposing the symmetry the solution is supposed to have. For the case of an electric p-brane solution (which of course, depending on the charge, can correspond to either one or a stack of D-branes in the complementary picture) will break the 10D Lorentz symmetry down to $SO(1,p) \times SO(9-p)$, where the latter is the rotation group for the space transverse to the brane. At the same time, such a solution will only have a non-zero dilaton, a metric and the appropriate RR gauge field. This allows the truncation of the type II 10D supergravity

action down to something of the schematic form

$$S = \frac{1}{16\pi G_N}\int d^{10}x\sqrt{-G_E}(R - \frac{1}{2}d\phi^2 - \frac{1}{2}e^{\frac{(3-p)\phi}{2}}\frac{1}{(p+2)!}(dC^{(p+1)})^2), \tag{1.80}$$

written in the Einstein frame. From this action, one can derive the corresponding equations of motion, which should be supplemented with a source term, though. This corresponds to the fact that one adds the Dp-brane action of the form $S = T_p(S_{\rm DBI} + S_{\rm CS})$, consisting of a Dirac-Born-Infeld, and of a Chern-Simons term, as one is adding a 'source brane'. The spherically symmetric p-brane 'ansatz' is of the form $ds^2 = e^{2A(r)}d\vec{x}^2 + e^{2B(r)}d\vec{y}^2$, where the $\vec{x}$ are the 'longitudinal' coordinates, and the $\vec{y}$ are the 'transverse' coordinates. In principle, one could now plug this 'ansatz' into the equations of motion resulting from the truncated action, but it is much simpler to impose the preservation of the remaining supersymmetry first, and to then solve the first order BPS equations.

Without going into these details, acknowledge that an analysis of the supersymmetry equations for the fermions (the BPS equations) yield solutions of the form $A(r) = \frac{7-p}{16}C, B(r) = \frac{-(p+1)}{16}C, \phi = \phi_0 + \frac{p-3}{4}(C - C_0)$, provided $e^{-C} \equiv H_p(r) = e^{-C_0} + \frac{Q_p}{r^{7-p}}$ (with Q_p a constant, which one can interpret as the charge of the Dp-brane) is a harmonic function of the transverse coordinates, yielding a general p-brane solution (written in the Einstein frame) of the form

$$\begin{aligned} ds^2 &= H_p^{\frac{p-7}{8}}d\vec{x}^2 + H_p^{\frac{p+1}{8}}d\vec{y}^2, \\ C^{(p+1)} &= 1 - \frac{1}{H_p}, \\ e^{2\phi} &= H_p^{\frac{3-p}{2}}. \end{aligned} \tag{1.81}$$

Note that as $e^{\frac{\phi}{2}} = H_p^{\frac{3-p}{8}}$, the metrics in the string frame are even simpler,

$$ds^2 = \frac{1}{\sqrt{H_p}}d\vec{x}^2 + \sqrt{H_p}d\vec{y}^2, \tag{1.82}$$

and the harmonic function for a p-brane reads, [38],

$$H_p = 1 + \frac{c_p g_S N_p l_S^{7-p}}{r^{7-p}}, \tag{1.83}$$

with $c_p = (2\sqrt{\pi})^{5-p}\Gamma(\frac{1}{2}(7-p))$. The reader will recognize the appearance of such harmonic functions in numerous black hole solutions in the remainder of this thesis.

In principle, superpositions of such solutions can be considered, which (under certain conditions, allowing the preservation of supersymmetry) yield multi-centered p-brane solutions. Additionally, one can also find magnetically dual p-brane solutions, but such a construction will not be sketched here. The reader who wishes to jump into the topic of p-brane solutions of supergravity, or is interested to study the Dp-brane / p-brane correspondence, can start and find orientation with [38–40].

The central charge associated to a Dp-brane / p-brane system

Throughout this thesis, Dp-branes will be wrapped on p-cycles of Calabi-Yau manifolds (or a torus) to yield point-like objects traveling through time, from a spacetime point of view. Typically, one will consider a $(D6, D4, D2, D0)$-brane system with charges (p^0, p^A, q_A, q_0) in type IIA string theory. Charge can arise by wrapping branes on a cycle, and this will in general also induce lower dimensional brane charge, e.g. induced from curvature. Using the basis of the Poincaré dual cohomology with respect to the cycle classes on which one wraps branes, such Dp-brane charge systems can be parametrized using polyforms $\Gamma \in H^{2*}(X, \mathbb{Z}) = H^0(X, \mathbb{Z}) \oplus H^2(X, \mathbb{Z}) \oplus H^4(X, \mathbb{Z}) \oplus H^6(X, \mathbb{Z})$ for type IIA. One associates a central charge to such a brane system, of the form

$$Z(\Gamma, t) = \langle \Gamma, \Omega(t) \rangle, \tag{1.84}$$

which shows dependence on either the Kähler or the complex structure moduli t.

The name central charge for this originates from the fact, that it is actually this quantity that appears as a central charge in the supersymmetry algebra, check equations (1.78). The example above can be written out to yield

$$\begin{aligned} Z(\Gamma, t) &= e^{\frac{K}{2}} \int_X \Gamma \wedge (-e^{-t^A D_A})^*, \\ &= e^{\frac{K}{2}} (\frac{p^0}{6} D_{ABC} t^A t^B t^C - \frac{p^A}{2} D_{ABC} t^B t^C + q_A t^A - q_0), \end{aligned} \tag{1.85}$$

where in the large volume limit $e^{\frac{K}{2}} \approx \frac{1}{\sqrt{\frac{4}{3} D_{ABC} \mathrm{Im}(t^A) \mathrm{Im}(t^B) \mathrm{Im}(t^C)}}$.

1.5 Chapter summary and outlook

In this chapter it is discussed how type II (10D) string theories fit into the bigger framework of strings and branes, and how compactifications thereof are of special interest, especially the compactification on a Calabi-Yau 3-fold, leaving $\mathcal{N} = 2$ supersymmetry in 4d. This process was highlighted somewhat from the worldsheet theory perspective, focussing on the part of the superconformal algebra, describing the worldsheet physics in the wound-up dimensions in the direction of the CY 3-fold. Some basic material on the classical supergravity descriptions of the zero mode spectrum of type II string theories was included, as well as on KK reduction and truncation of the spectrum, to obtain $\mathcal{N} = 2, d = 4$ supergravity theories in 4d, which are interpreted as originating from string theory. Next, special geometry of type II supergravity theories in 4d was discussed. The geometry of the target space of the vector multiplet scalars as well as the couplings of the corresponding vectors is subject to restrictive constraints, allowing the bundling of all information in one holomorphic section of a bundle, or, adapted to concrete application, to write down a function called the prepotential, from which a variety of entities of interest are directly

calculable. This was followed by a brief summary of some aspects of the BPS spectrum of type II string theories. The BPS spectrum was discussed briefly from the point of view of D-branes and RR-charge, and also from the supergravity perspective, giving rise to BPS p-brane solutions. Such BPS spectra of four-dimensional black holes originating from type II string theory compactified on a Calabi-Yau manifold have been studied intensively over the last decade. The BPS property of extremal solutions and the supersymmetry are absolutely crucial, as under the identification of Dp-branes and p-brane solutions in supergravity, it allows for the varying of the string coupling and taking the physical system into different, complementary description regimes. The discovered connection between this picture and the supergravity approximation of string theory has been and still is deepening. This link is also not far from leading to the central topic in this thesis. In [41], [42], G. Moore studied the attractor mechanism devised to describe BPS black hole solutions, and put forth a correspondence between spherically symmetric solutions to the black hole attractor equations and BPS states in string theory. However, this correspondence turned out not always to hold. The remedy, developed in [43], is to consider not only single attractor flows, but also 'split attractor flows', which are conjectured to be in one-to-one correspondence with multi-centered BPS solutions. This is the topic of the next chapter.

One point which was sidestepped in the discussion up until now, on which the author owes some explanation to the reader, is the question of validity of low energy descriptions of compactified type II string theories. The question of validity of the low energy supergravity description in 4d, for a KK reduction (and truncation) on a CY threefold is singled out, here. There are a number of requirements one needs to impose in order for this description to make any sense. These issues are important when describing black holes and also their low charge 'counterpart', point particles (the 'geometrized' so-called D-particles). They can be summarized as follows:

- **Suppress quantum gravity**
  To describe black holes using p-brane solutions to supergravity, the curvature at the event horizon needs to be weak, in order to suppress quantum gravitational effects. As the horizon scales with the square (or, as is at the core of [1], with the cube for multi-centered black hole) of the charges, this translates into a condition that one needs large D-brane charges. Note that the fuzzball program, which is discussed in section 5.1, might shed a different light on some of these remarks.

- **Large radius regime**
  The 4d Lagrangian should not receive dominant α' corrections. As these are controlled by the volume V_X of the CY threefold X, one wants to be in the so-called large radius regime, $V_X >> 1$. If one leaves the large radius regime, one knows that the worldsheet instanton corrections to the prepotential become important for a type IIA theory.

- **Not too large radius regime**
  On the other hand, one wants KK modes to be light, which means that the CY volume must not be too large. This condition is expressed in the formula $\frac{A\, g_S^2}{V_X} >> 1$,

using the event horizon of the hole, A. Together with the previous condition, this yields an 'intermediate regime' for the size of the CY.

At some point in the research performed by the author, these requirements are no longer met, and one has to come up with a mechanism to include corrections to the supergravity theory. In chapter 4 the main virtue which comes to rescue lies in the power of mirror symmetry.

This ends the first main chapter, having taken the reader from the basic foundation of string theory, to the context of BPS states in type II string theory compactifications, illuminated from the geometric D-brane picture on the one hand, and the complementary spacetime picture provided by supergravity on the other hand.

Chapter 2

Black holes in string theory and the split attractor flow conjecture

Techniques to study black holes in string theory stand central in this thesis. This chapter presents the reader with the relevant background material on black holes and some important techniques such as split attractor flow trees. Split flow trees (or single flows) can be seen as depictions of the values of scalar fields belonging to vector multiplets (these were discussed in the previous chapter) for a specific black hole solution of supergravity. The meaning of split flow trees however extends beyond supergravity, they can be used to classify BPS bound states in type II string theory.

The present chapter is organized as follows. In the first section, the reader is quickly guided from the original Schwarzschild black hole solution (in general relativity) to black holes carrying angular momentum and charge. Such black hole solutions can also be found to the classical low energy descriptions of type II string theories, the type II supergravities. A special class of solutions, BPS black holes, are of special interest, as the index used to estimate the number of states is often invariant under continuous changes of the coupling constant. For this reason, such systems can also be investigated in the zero string coupling regime. In the latter, complementary description, such black holes become BPS D-brane systems and can be studied using classical geometry. After taking the reader from the Schwarzschild black hole to BPS black holes, the attractor mechanism governing the latter is explained. To get the reader acquainted with the attractor mechanism, the latter shall be explained very pictorially. The attractor equations determine the geometry of the compact dimensions for a black hole solution. In particular, it determines this geometry at the event horizon, independently of the background in which the black hole is placed. More specifically, the vector multiplet scalars are driven to so-called attractor values. Hence the name attractor mechanism.

The second section is a brief presentation on multi-centered BPS black hole bound states in supergravity, discovered by Denef and collaborators.

The third section is the most important one of this chapter: the introduction of split attractor flow trees and the formulation of the split attractor flow conjecture. Just as a 'single flow', depicting the former attractor mechanism, describes the value of the scalars

characterizing form (in IIA string theory) or size (in IIB string theory) of the geometry of the extra dimensions for a single-centered black hole, a split flow does this for the extra dimensions for a multi-centered black hole. In its strongest form, the split attractor flow conjecture is a far-reaching claim, that split flow trees can be used as an existence and classification criterion for BPS states in the full type II string theories. This idea has been put to use and tested by the author and his collaborators in two broad research programmes on black holes in string theory, as will be presented in chapters 4 and 5.

The fourth section is devoted to the laws of black hole thermodynamics and black hole entropy. From the analogy between black hole mechanics and thermodynamics, one can conclude that the entropy of a black hole is proportional to the area of its event horizon. The area of the horizon of supergravity black hole solutions can be computed, and such a result is referred to as the macroscopic entropy prediction. By taking such a black hole system into the complementary D-brane regime, and by using various computational techniques, the entropy of the black hole can be reproduced and moreover, explained microscopically, at least in certain charge regimes. This may be seen as one of the biggest qualitative successes achieved in string theory. On a qualitative level, it is very tempting to compare this to the microscopic explanation delivered by statistical thermodynamics of macroscopic quantities (such as pressure) appearing in thermodynamics.

Specific attention is given to D4-D2-D0 black holes in type IIA string theory. Keeping the D4-charge fixed, and summing over various D2-D0 brane charges, one arrives at a mixed ensemble, from which one can construct a black hole partition function. This is important in connection to a conjecture relating the black hole partition function to topological string theory, which will be discussed in chapter 3. If one chooses a small D4-charge, one is left with a D-particle. The partition function is given by an object known from conformal field theory: the elliptic genus. Elliptic genera for specific Calabi-Yau study models were computed by the author and collaborators, and are presented in chapter 4. Finally, a relevant concept is introduced: the notion of polar states. These are (within such mixed ensembles) charges (of D-particles or black holes), which do not support single-centered BPS states, but are exclusively realized as bound states. Polar states are crucial in all the research presented later on.

Finally, this chapter is again rounded off with a short summary of the gathered key ingredients, placing them in the context of the thesis as a whole.

2.1 Black holes from D-branes and the attractor mechanism

This section leads from the Schwarzschild black hole to black holes with angular momentum and charge. It also covers basic material on supersymmetric black holes, and on how black holes are perceived from the viewpoint of string theory. From the latter point of view, one models black holes by wrapping branes around various cycles in the wound-up dimensions. For such a setup of a brane system, it is possible to write down a corresponding

supergravity solution. The last part of this section is devoted to the attractor mechanism, which governs the values of the Kähler moduli (IIA) or the complex structure moduli (IIB) of a solution, driving them to the attractor values at the horizon of the black hole solution. This part is crucial, as it will be generalized to the split attractor mechanism, governing the corresponding scalars in a multi-centered black hole solution. As announced previously, split attractor flow trees are at the 'core' of the research presented in this thesis.

2.1.1 From the Schwarzschild to supersymmetric black holes

In 1915 Karl Schwarzschild discovered a solution to Einstein's newly found equations of general relativity, which is interpreted as a simple model of a black hole. While making his discovery, Schwarzschild was serving in the armed forces in the First World War, where he tragically died. Put very simply, his solution is just some mass sitting in a point (a singularity), surrounded by the vacuum.

The Schwarzschild black hole

According to Einstein's equations, the geometry of spacetime, given by the Einstein tensor G, is determined by the matter distribution, described by the energy-momentum tensor T:

$$G = R - \frac{1}{2}\mathcal{R}g = 8\pi T, \tag{2.1}$$

where R denotes the Ricci tensor, g is the metric, and $\mathcal{R}$ denotes the scalar Ricci curvature. If there is no matter, $T = 0$, the Einstein equations are solved by flat Minkowski space. Schwarzschild found a static, spherically symmetric solution to the case, when matter is placed at the origin in spacetime. In local (Schwarzschild) coordinates, the Schwarzschild metric reads

$$ds^2 = -\left(1 - \frac{2GM}{r}\right)dt^2 + \left(1 - \frac{2GM}{r}\right)^{-1} dr^2 + r^2 d\Omega_{S^2}^2, \tag{2.2}$$

where the three space dimensions are covered by spherical coordinates. This was interpreted as a black hole with mass M. Note that the metric shows no time dependence (at least outside of the event horizon). Furthermore, as the mass is sent to zero, the Minkowski spacetime (vacuum) is recovered. The metric in these coordinates possesses two singularities. One lies at $r_H = 2GM$, and one at $r = 0$. The latter is the singularity, where the black hole resides. This is where all the mass M is concentrated. The former singularity however is only a coordinate singularity. As can be followed in standard textbooks, this is (in this case) revealed by calculating the coordinate invariants scalar $R^{\mu\nu\rho\sigma}R_{\mu\nu\rho\sigma} = \frac{48G^2M^2}{r^6}$, which clearly blows up as $r \to 0$. It does not blow up at $r_H = 2GM$. In different coordinates, such as Kruskal coordinates, this singularity does not appear. The sphere at $r = r_H$ is called the *event horizon* of the black hole.

Before concluding the very quick recapitulation of the Schwarzschild black hole, let it be said, that one can interpret it as interpolating between the near-horizon geometry

$AdS_2 \times S^2$ and a flat Minkowksi space $\mathcal{M}_{1,3}$, very far away from the singularity ($r >> r_H$): this is what is referred to as the 'solitonic' nature of a black hole.

Adding charge to a black hole and the notion of extremality

In Einstein-Maxwell theory [1], one can also consider spherically symmetric black holes with electric charge q and possibly magnetic charge p. The metric for such a solution reads

$$ds^2 = -\left(1 - \frac{2GM}{r} + \frac{G(p^2+q^2)}{r^2}\right) dt^2 + \left(1 - \frac{2GM}{r} + \frac{G(p^2+q^2)}{r^2}\right)^{-1} dr^2 + r^2 d\Omega^2_{S^2}, \tag{2.3}$$

and is called the *Reissner-Nordström* black hole. Note that when one sets $p = q = 0$, one recovers the Schwarzschild solution. Again, one can ask where the metric becomes singular. The condition reads

$$r_\pm = GM \pm \sqrt{G^2M^2 - G(p^2+q^2)}, \tag{2.4}$$

and one has to distinguish between three different cases.

- $GM^2 < p^2 + q^2$: In this case, there is obviously no real solution, and one has to conclude that there is no event horizon. The singularity at $r = 0$ (one can again check that it really is a singularity) is unshielded, and one calls such a singularity a *naked singularity*. Most physicists consider such singularities unphysical, and this is put down as a conjecture, called the cosmic censorship conjecture, which simply states that no naked singularities exist.

- $GM^2 > p^2 + q^2$: In this case one finds two solutions, and one concludes that there is an inner and an outer event horizon. This gives rise to some weird observations, such as, that an observer should, in principle be able to cross the outer event horizon, is driven to the inner horizon, but after crossing the latter can choose to steer back out of the black hole. He would however exit into a different universe. Presumably, such observations are not describing anything realistic, but are peculiarities associated with such 'perfect' toy models like a Reissner-Nordström black hole.

- $GM^2 = p^2 + q^2$: This bound is reached, when 'the mass equals the charge' of the black hole. It is then called an *extremal* black hole. The two horizons from the previous, also referred to as the non-extremal case, combine into one single horizon at $r = GM$. Throughout this thesis, extremal black holes will be considered.

Adding angular momentum to a black hole and extremality revisited

Another possibility is to consider rotating black holes. Such a black hole was constructed

[1] The reader not familiar with Einstein-Maxwell theory can imagine it to be the combination of general relativity and classical electromagnetism, schematically described by a Lagrangian of the form $L = \sqrt{-g}R + \frac{1}{4}F^2$.

by Kerr in 1963. One can also combine charge and angular momentum, a black hole referred to as the Kerr-Newman black hole:

$$ds^2 = -\frac{\Delta}{\rho^2}(dt - a\sin^2\theta\, d\phi)^2 + \frac{\rho^2}{\Delta}dr^2 + \rho^2 d\theta^2 + \frac{\sin^2\theta}{\rho^2}\left((r^2+a^2)d\phi - dt\right)^2, \qquad (2.5)$$

using $\Delta = r^2 - 2GMr + a^2 + G(p^2+q^2)$ and $\rho^2 = r^2 + a^2\cos^2\theta$, and where the coordinates are referred to as Boyer-Lindquist coordinates and are related to Cartesian coordinates by

$$\begin{aligned} x &= \sqrt{r^2+a^2}\sin\theta\cos\phi, \\ y &= \sqrt{r^2+a^2}\sin\theta\sin\phi, \\ z &= r\cos\theta. \end{aligned}$$

Such a solution is no longer static, but it is still stationary. The interpretation is that of a charged black hole which is rotating at constant angular velocity. An asymptotic expansion in the radius r allows identification of an angular momentum as $J = aM$. Again, similar observations as for the Reissner-Nordström black hole are possible, also signaling in particular a lower mass bound $GM^2 > p^2+q^2+\frac{a^2}{G}$, corresponding to an extremal (rotating) black hole.

An interesting observation which followed from studying all of these named black holes, is that, spherically symmetric, stationary black holes are characterized by just three parameters: M, J and $Q = (p,q)$. In words: mass, angular momentum and charge. This fact is often emblematized by saying that black holes have no hair. This is of course only a statement about the classical solutions such as those presented here, and no longer applies, when considering possible quantum aspects of black holes.

Supersymmetric, extremal black holes in supergravity

Such black holes, possibly carrying charge and angular momentum are also solutions to supergravity. More generally, as was already mentioned in part 1.4.2, p-brane solutions (or superpositions of p-branes) to supergravity are used to model black holes. As was also discussed, the central charge Z of the brane system also appears as the central charge in the $\mathcal{N} = 2$ supersymmetry algebra. It was shown in [44] that every solution satisfied the BPS bound, $M \geq Z$. If the solution preserves some supersymmetry and is therefore a BPS state, it turns out that it saturates the bound. For example, the extremal Reissner-Nordström solution described above is a $\frac{1}{2}$ BPS solution to $\mathcal{N} = 2, d = 4$ supergravity. It thus conserves one half of the supersymmetry of the vacuum. Along the lines of the sketched D-brane/p-brane correspondence, one can access a complementary description of the same system, by driving the string coupling constant to zero, $g_S \to 0$. The special interest in BPS black holes results from the fact, that they are 'protected by supersymmetry' in the sense that Witten indices used to count/estimate the number of states with a specific charge remain invariant under variations of the coupling constant.

2.1.2 Supersymmetric black holes made from branes

The general picture from the viewpoint of string theory, is to model black holes by wrapping D-branes (various types of D-branes model different types of charges) around cycles in the extra dimensions. More specifically, one will wrap the Dp-branes around p-cycles, at one point in spacetime, such that one obtains a pointlike object traveling through time, from the spacetime point of view.

Inspired by these ideas, there is something like a general 'ansatz' to obtain BPS black hole solutions to supergravity, which is known as the *harmonic function rule*: one just superimposes the harmonic functions for different p-brane solutions. This is illustrated best by using a simple example which clarifies the general idea. Choose type IIB string theory compactified on $S^1 \times T^4$, for the moment. This breaks no supersymmetry, leaving 32 supercharges conserved in the 5d theory. According to what was stated earlier on, one can superimpose a Dp-brane with a D(p-4)-brane, leading to a $\frac{1}{4}$ BPS state: a D1-D5 system is chosen here. The following diagram illustrates around which dimensions one chooses to wrap a D1 brane and a D5 brane. A dot indicates that the brane is pointlike as concerns that dimension, a line indicates that the brane is extended in the corresponding dimension, and a $\sim$ denotes that it is smeared[2] in that direction.

	0	1	2	3	4	5	6	7	8	9
D5	–	·	·	·	·	–	–	–	–	–
D1	–	·	·	·	·	–	$\sim$	$\sim$	$\sim$	$\sim$
	t	$\vec{x}$				S^1	T^4			

Using the notation $\vec{x} = (x_1, x_2, x_3, x_4)$ for the non-compact space directions and x_5 for the circle S^1, the harmonic function rule yields

$$\begin{aligned} ds^2 &= \frac{1}{\sqrt{H_1 H_5}}(-dt^2 + dx_5^2) + \sqrt{H_1 H_5}\, d\vec{x}^2 + \sqrt{\frac{H_1}{H_5}}\, ds^2_{T^4}, \\ C^{(2)} &= 1 - \frac{1}{H_1} \qquad C^{(6)} = 1 - \frac{1}{H_5}, \\ e^{\phi} &= \sqrt{\frac{H_1}{H_5}}, \end{aligned} \tag{2.6}$$

written in the string frame, where H_1, H_5 are defined as suggested in the previous chapter. Note how there is a correspondence between 'coordinate dimensions' around which a brane is wrapped, and the powers of the harmonic functions appearing in front of specific parts of the metric. When adding a third type of charge, namely momentum P to the previous system, one obtains a three charge system in five dimensions: the famous D1-D5-P black hole. The reader can follow more details on these examples e.g. in [45].

[2]For a brane to be smeared in a direction means that its charge can be redistributed, but the brane does not explicitly extend in that direction.

2.1.3 The attractor mechanism for BPS black holes

BPS black holes in $\mathcal{N} = 2, d = 4$ supergravity theories are described not only by the metric, but also by the values of the gauge fields and of the scalars. As discussed before, scalars appear in vector multiplets and in hypermultiplets. The values of the hypermultiplet scalars can take on an arbitrary value throughout a solution and are therefore not of further interest. Something extremely enlightening however was revealed with the discovery that the vector multiplet scalars are governed by the so-called attractor mechanism. Namely, their values are highly constrained. After choosing a specific value at infinite distance ($r = \infty$) of the black hole (residing at $r = 0$), which will also just be referred to as choosing a 'background' from now on, their values are determined by the so-called BPS flow equations, presented below. In particular, their values at the event horizon are fixed at so-called 'attractor values', independently of the chosen background, thus depending only on the charges assigned to the black hole. This is worth being very clearly stated. Starting with a black hole solution (and corresponding solutions for the vectors and scalars), one can change the values of the scalars at infinity. As one follows the values of the scalars radially inwards, one will find that the attractor mechanism drives them to the same attractor values at the event horizon.

Often, in this context, $\tau = \frac{1}{r}$ is used as a radial coordinate. The vector multiplet scalars will be denoted as t^A in the following, and the background values (the value for the scalars chosen at $r = \infty, \tau = 0$) are denoted by t^A_∞. The attractor mechanism is illustrated in figure 2.1). The evolution of the values of the scalars as a function of the radius $t^A(\tau)$ can be called a flow, and is described by first order differential equations in τ. They are referred to as BPS 'attractor flow equations', or just 'attractor equations', for short.

Recall the form of a general metric for a static spherically symmetric BPS black hole,

$$ds^2 = -e^{2U(r)}dt^2 + e^{-2U(r)}d\vec{x}^2, \tag{2.7}$$

with a radial function $U(\tau)$, and where $\frac{1}{\tau} = r = \sqrt{\vec{x}^2}$. For black hole solutions in type II supergravity theories, the attractor mechanism was first described in 1995, [46], and recast as first order flow equations on moduli space in [47]:

$$\partial_\tau U = -e^U|Z|, \tag{2.8}$$

$$\partial_\tau t^A = -2e^U g^{A\bar{B}}\bar{\partial}_{\bar{B}}|Z|, \tag{2.9}$$

where t^A now stands either for the Kähler or the complex structure moduli, $g^{A\bar{B}}$ is the Kähler metric obtained from the Kähler potential on the Kähler or complex structure moduli space, and $Z = Z(\Gamma, t^A)$ is interpreted as the 'central charge' of the brane system Γ used to model the black hole, corresponding to t^A in moduli space. The central charge of the associated supergravity solution is retrieved as $Z(\Gamma, t^A_\infty)$, where the notation t^A_∞ indicates the values of the moduli one imposes at infinity $\tau = \frac{1}{r} \to 0$, also referred to, from now on, as the *background values* of the moduli. Note that the moduli as well as the function U entering the metric show a radial dependence, $(U = U(\tau), t^A = t^A(\tau))$. From (2.9) it follows directly that

$$\partial_\tau|Z| = -4e^U g^{A\bar{B}}\partial_A|Z|\bar{\partial}_{\bar{B}}|Z|, \tag{2.10}$$

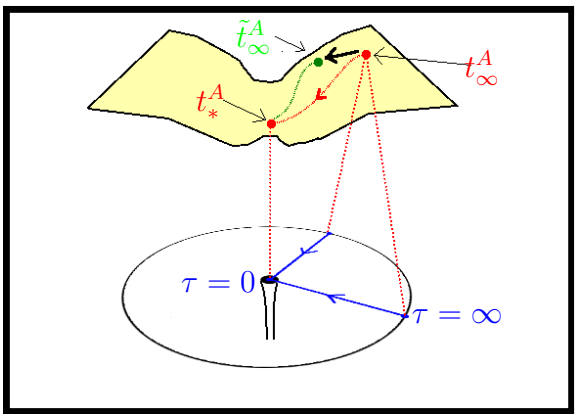

Figure 2.1: Schematic depiction of the BPS black hole **attractor mechanism** and a flow in moduli space/spacetime. The circle represents spacetime with a black hole sitting in the middle $(\tau = \infty, r = 0)$, the boundary of the circle represents spatial infinity, $(\tau = 0, r = \infty)$. The blue lines depict how one would approach the black hole from infinity, following an attractor flow. Two examples have been plotted, they could of course be chosen anywhere due to the spherical symmetry. The profile above indicates the corresponding geometry (in fact actually the Kähler or the complex structure moduli) of the extra dimensions, belonging to the Calabi-Yau manifold. Both background values t^A_∞ and $\tilde{t}^A_\infty$ given at infinity are driven to the same attractor point in moduli space, t^A_*. The flows in moduli space are depicted by the dotted red line for t^A_∞ and by the dotted green line for $\tilde{t}^A_\infty$. The independence of the attractor point (at the event horizon of the black hole) on the choice of background (the deformation from t^A_∞ to $\tilde{t}^A_\infty$ is indicated with a fat black arrow) is the powerful core feature of the attractor mechanism.

which implies $\partial_\tau |Z| \leq 0$: in other words, as one follows the flow radially inward, $|Z|$ converges to a minimum; the flow of $|Z|$ is a decreasing gradient flow.

An alternative form of these BPS attractor flow equations was derived in [43],

$$2\partial_\tau \left(e^{-U}\mathrm{Im}(e^{-i\alpha}\Omega)\right) = -\Gamma, \tag{2.11}$$

using $\alpha = \arg(Z)$. In fact, one can extract $2N_V + 2$ real equations from this, by taking the projections on to the basis for the corresponding cohomology, either $H^{2*}(X, \mathbb{Z})$ for the IIA case, or $H^3(X, \mathbb{Z})$ for the IIB case. However one component is redundant, as the intersection product of Γ with itself vanishes trivially, $\langle \Gamma, \Gamma \rangle = 0$, allowing elimination of one equation. This yields $2N_V + 1$ real equations determining the solutions of $2N_V + 1$ real variables $(U(\tau), \mathrm{Re}(t^A), \mathrm{Im}(t^A))$.

In the form (2.11), the BPS equations can be integrated easily, yielding

$$2e^{-U}\mathrm{Im}(e^{-i\alpha}\Omega) = -\Gamma\tau + 2\mathrm{Im}(e^{-i\alpha}\Omega)|_{\tau=0}, \tag{2.12}$$

and the attractor values of the moduli read

$$2\,\mathrm{Im}(\overline{Z(\Gamma, t_*(\Gamma))}\Omega) = -\Gamma. \tag{2.13}$$

In fact, using the implicit solution (2.12), it is convenient to define the right-hand side (up to a sign) as the harmonic function

$$H(r) = \frac{\Gamma}{r} - 2\mathrm{Im}(e^{-i\alpha}\Omega)\Big|_{r=\infty}. \tag{2.14}$$

One can interpret this harmonic function to express that one has placed a charge Γ at $r = 0$, and by setting the background moduli, one chooses the background $h = -2\mathrm{Im}(e^{-i\alpha}\Omega)\Big|_{r=\infty}$. Note that it is a cohomology valued function, $H = (H^0, H^A, H_A, H_0)$ with $2N_V + 2$ components. A complete explicit solution to the attractor equations (2.11) can be parametrized using a single function, called the entropy function, defined as

$$\Sigma(H(r)) = \frac{S(H(r))}{\pi} = e^{-2U(r)}. \tag{2.15}$$

Using this entropy function, the solution for a black hole, the scalar moduli and the gauge fields reads

$$\begin{aligned} ds^2 &= -\frac{1}{\Sigma}dt^2 + \Sigma\, d\vec{x}^2, \\ t^A &= \frac{H^A - i\partial_{H^A}\Sigma}{H^0 - i\partial_{H^0}\Sigma}, \\ A^0 &= -\partial_{H^0}\ln(\Sigma)dt - p^0\cos\theta\, d\phi, \\ A^A &= \partial_{H^A}\ln(\Sigma)dt - p^A\cos\theta\, d\phi. \end{aligned}$$

Another remark for future reference is at hand. Imagine that one is describing a BPS black hole modeled by a Calabi-Yau compactification of type II string theory. As will be explained in more detail in the next section, attractor equations are also meaningful when describing BPS states beyond the supergravity approximation. Although (2.12) is of course a solution to the attractor equations, knowledge of the explicit flows of the moduli $t^A(\tau)$ can in general not be obtained analytically. On one hand, when working near the large complex structure point in moduli space, this is feasible. On the other hand, one can work numerically, a method which has been exploited when performing major parts of the research treated in chapter 4. Given a certain charge, analysis of the attractor equations turned out to be very insightful. In 1998, Greg Moore distinguished three possible cases with regard to the possible 'end point' in moduli space, t^A, of a flow of $|Z|$, [41,42]. Namely, there is no guarantee that a flow continues until $\tau = \infty$.

1. **Attractor point t^A_***
   The flow ends at an attractor point and $Z(\Omega, t^A)$ takes on a minimal value, which will be denoted as $|Z|_* = Z(\Omega, t_*)$, where the moduli t^A take on their attractor values t^A_*. This means that there is a single-centered BPS solution subject to the corresponding attractor values for the scalars.

2. **Crash at a regular point t^A_0**
   The flow continues until the corresponding value $|Z|$ reaches zero, whereas the value

of the moduli signals a regular point in moduli space. This means that from a spacetime view on the flow, the flow stops at finite radius from the black hole. The flow terminates at a regular point in moduli space, it cannot be continued. As was explained in [48], this situation would imply that a massless particle exists at the locus where $|Z| = 0$, creating a singularity in moduli space, contradicting the supposed regularity of the point. This situation will be referred to as a *crash* of the flow at a regular point in moduli space. The conclusion is, that no single-centered BPS state with the charge Γ exist, More specifically, no spherically symmetric, static solution exists. One might ask oneself how it could be the case that this charge does not support a BPS solution. However, there is a way out, as will be discussed shortly.

3. **Crash at a singular point $t^A_{0,*}$**
   The flow can also continue until $|Z|$ reaches zero, but this time with a corresponding point in moduli space which is singular, or a boundary point of moduli space. In this case, the BPS equations might or might not have a solution. More information is needed to give a conclusive answer. There is e.g. a solution if the end point is a conifold point in moduli space, as will be discussed later on. In fact the latter type of solutions play a very prominent role in the research presented.

The reader interested in more detailed reviews on the attractor mechanism can start by consulting [41, 49, 50].

2.2 Multi-centered black holes

In $\mathcal{N} = 2, d = 4$ supergravity theories not all charges support single-centered BPS solutions. This alone is not surprising, as the BPS spectrum is only a subset of the full spectrum. According to the preceding discussions, one can model the BPS spectrum in the complementary D-brane picture. When searching for the corresponding BPS black hole solutions, this leads to a very surprising conclusion. The single-centered, spherically symmetric solutions do not account for the full BPS spectrum, [43], either. It turns out that the BPS states not supporting single-centered solutions are realized as multi-centered, stationary black hole bound states, carrying intrinsic angular momentum. By now, it has been established that BPS states of a given charge are often realized as multi-centered solutions in four-dimensional supergravity [43, 51, 52]. In general, such multi-centered solutions are genuine bound states of black holes, subject to specific equilibrium distances and not just superpositions of black holes, that are always mutually BPS (this will become clearer from explanations below). The latter are realizations of so-called mutually local charges, satisfying $\langle \Gamma_1, \Gamma_2 \rangle = 0$ and can just be superimposed without breaking any supersymmetry. Genuine multi-centered black hole bound states are important in this thesis. Therefore, to foster the reader's general understanding of multi-centered black holes, a short account of some of their properties is given in the following. A class of multi-centered black holes was constructed in the course of the research performed by the author and collaborators. This

can be found in section 5.2, where some more explanation about their construction can be found. A detailed instruction how to construct such solutions was developed in [52].

The metric of a stationary solution is of the general form

$$ds^2 = -e^{2U}(dt+\omega)^2 + e^{-2U}d\vec{x}^2, \tag{2.16}$$

where $\omega = \sum_{i=1}^{3}\omega_i dx_i$ is a one-form, describing the angular momentum of the solution. The BPS equations generalizing those for a single center (2.12) read, [43],

$$\begin{aligned} 2e^{-U}\mathrm{Im}(e^{-i\alpha}\Omega) &= -H, & (2.17)\\ *d\omega &= \langle dH, H\rangle. & (2.18) \end{aligned}$$

Note that, again, $H(\vec{x})$ is a form valued either in $H^{2*}(X,\mathbb{Z})$ or $H^3(X,\mathbb{Z})$, and $*$ denotes the ordinary Hodge star operators in three dimensions. For a multi-centered black hole with N centers corresponding to charges Γ_i at position $\vec{x}_i$, the harmonic function generalizes to

$$H(\vec{x}) = \sum_{i=1}^{N}\frac{\Gamma_i}{|\vec{x}-\vec{x}_i|} - 2\mathrm{Im}(e^{-i\alpha}\Omega)_{\tau=0}, \tag{2.19}$$

in asymptotically flat space. Just like for the single-centered case, it was shown in [52] that the whole solution is determined in terms of one entropy function,

$$S(H(\vec{x})) = \pi\cdot\Sigma(H(\vec{x})) = \pi\cdot e^{-2U(\vec{x})}. \tag{2.20}$$

whereas the moduli fields are given by

$$t^A = \frac{\frac{\partial S}{\partial q_A} + i\pi p^A}{\frac{\partial S}{\partial q_0} + i\pi p^0}. \tag{2.21}$$

Knowing the entropy function, one can for example also determine the electromagnetic field

$$\mathcal{A} = 2e^{U}\mathrm{Re}(e^{-i\alpha}\Omega)(dt+\omega) + \mathcal{A}_d, \tag{2.22}$$

with

$$d\mathcal{A}_d = -2*d(e^{-U}\mathrm{Im}(e^{-i\alpha}\Omega)) = *dH. \tag{2.23}$$

As discussed in [43], these multi-centered solutions have intrinsic angular momentum, in many ways analogous to the angular momentum stored in a monopole-electron system. It is given by

$$\vec{J} = \frac{1}{2}\sum_{i<j}\langle\Gamma_i,\Gamma_j\rangle\vec{x}_{ij}, \tag{2.24}$$

where $\vec{x}_{ij}$ is a unit vector pointing from $\vec{x}_j$ to $\vec{x}_i$. The positions of the centers are not arbitrary, as can be seen by the following constraint,

$$\sum_{j=1}^{N}\frac{\langle\Gamma_i,\Gamma_j\rangle}{|\vec{x}_i-\vec{x}_j|} = 2\mathrm{Im}(e^{-i\alpha}Z_i)|_{\tau=0}, \tag{2.25}$$

which is valid for every i, and can be easily derived from equation (2.17). It is insightful to examine this condition for a two-centered solution in more detail. It reads

$$|\vec{x}_1 - \vec{x}_2| = \frac{\langle \Gamma_1, \Gamma_2 \rangle}{2\mathrm{Im}(e^{-i\alpha} Z_1)}\Big|_{\tau=0} = \frac{\langle \Gamma_1, \Gamma_2 \rangle}{2} \frac{|Z_1 + Z_2|}{\mathrm{Im}(Z_1 \overline{Z}_2)}\Big|_{\tau=0}, \tag{2.26}$$

from which one can read off a necessary (but not sufficient) condition for the existence of a multi-centered solution,

$$\langle \Gamma_1, \Gamma_2 \rangle \cdot \mathrm{Im}(Z_1 \bar{Z}_2)_{\tau=0} > 0, \tag{2.27}$$

which can also be written as $\langle \Gamma_1, \Gamma_2 \rangle \cdot \sin(\alpha_1 - \alpha_2) > 0$, with the $\alpha_i = \arg(Z(\Gamma_i))|_{\tau=0}$ denoting the phases of the central charges. This shows that the background moduli are decisive in whether a multi-centered solution with centers corresponding to the charges Γ_1 and Γ_2 exists. Of course, one can vary the background values of the moduli, and when the sign of $\sin(\alpha_1 - \alpha_2)$ flips, the multi-centered solution leaves the spectrum (when starting with backgrounds such that the condition is fulfilled). When one is sufficiently close to the point where this flip occurs, one can approximately write the stability condition as

$$\langle \Gamma_1, \Gamma_2 \rangle \cdot (\alpha_1 - \alpha_2) > 0. \tag{2.28}$$

The locus where $\alpha_1 = \alpha_2$ is of special interest. The state 'marginally exists' for these backgrounds, and in fact, the locus in moduli space where this condition holds is called a *wall of marginal stability*. This will be explained in more detail, below. (2.28) is not a sufficient condition for the existence of a multi-centered solution, but it can be supplemented with two other conditions, which yields necessary and sufficient conditions for the existence of a multi-centered black hole solution, [1]:

- The condition $\sum_{j=1}^{N} \frac{\langle \Gamma_i, \Gamma_j \rangle}{|\vec{x}_i - \vec{x}_j|} = 2\mathrm{Im}(e^{-i\alpha} Z_i)|_{\tau=0}$,

- For IIA black holes made from D6-D4-D2-D0 branes, with charge $\Gamma = re^F(1 - \beta + n\omega)$, where F is worldvolume flux, $\beta \in H^2(X, \mathbb{Z})$ is D4 brane charge, and $n\omega \in H^6(X, \mathbb{Z})$ is $\overline{\mathrm{D0}}$ brane charge (check 3.3.3 below, for a detailed treatment of the charges used in this thesis). The entropy of the black hole can be written as $S = \frac{\pi}{3} r^2 \sqrt{\mathcal{D}}$, where $\sqrt{\mathcal{D}}$ is called the *discriminant function*, and reads

  $$\mathcal{D} = 8(\beta)^3 - 9n^2 \geq 0. \tag{2.29}$$

  Obviously, for the entropy to be real, and for the metric warp factor in (2.20) to be real, the discriminant has to be positive. In other words, $\mathcal{D} > 0$ has to lie in $\mathrm{dom}(S)$ for all $\vec{x} \in \mathbb{R}^3$. An analogous statement holds for type IIB black holes, [41, 42].

- The moduli fields t^A must remain within the physical moduli space throughout the solution: t^A must stay in the 'Kähler cone'. This is another way of saying that volumes of cycles should remain positive (except if they vanish).

Whereas the first condition is of course very easy to check, the second and third condition require knowledge of various fields throughout the solution, which renders these conditions very cumbersome for practical calculations. There is however a conjecture that there is a much simpler sufficient condition. This condition shows to be very powerful and is at the center of this thesis: the split attractor flow tree.

2.3 The split attractor flow conjecture

As emphasized before, the technique of split flow trees plays a central role in this thesis. Both 'single flows' – the attractor flow that was introduced earlier on – and split flow trees are assumed to be an existence criterion for BPS solutions in supergravity. In fact, as will be discussed shortly they are even conjectured to be an existence criterion for BPS states in the full string theory. They are graphical depictions of the flow of the Kähler moduli or the complex structure moduli belonging to a BPS solution of supergravity [3]. The single flow was already discussed, and can be seen as a subcase: the flow starts at the background value t_∞ at radial infinity and moves towards one attractor point t_* at the horizon of the black hole (recall figure (2.1)). Alternatively, for a multi-centered solution, the flow ends at several attractor points $(t_{1*}, ..., t_{m*})$, one for each center.

A split flow or split flow *tree* (the name 'tree' suggests the different 'branches') is built from several pieces, which are all 'partial' single flows by themselves. One follows the *incoming branch* [4] of a flow tree from radial infinity towards a putative attractor point, until one hits a *wall of marginal stability* for two constituents Γ_1 and Γ_2 such that $\Gamma = \Gamma_1 + \Gamma_2$. At this point, the flow splits into two branches. One can again follow a single flow for each of the two centers, starting at the split point, and flowing towards either an attractor point, or alternatively to another split point. For example, Γ_1 could again split into the constituents ${\Gamma_1}^a$ and ${\Gamma_1}^b$, and those could flow to their individual attractor points each, or a branch could split yet again. In this way, a split flow tree is built iteratively from single flows. Given their absolutely crucial role, it is necessary to discuss walls of marginal stability in more detail.

Walls of marginal stability

A wall of marginal stability between two charges Γ_1 and Γ_2 is defined as the hypersurface in moduli space where the phases of the two central charges align: $\arg(Z_1) = \arg(Z_2)$. The absolute value of a central charge measures the mass of the corresponding state (as it would be perceived should the corresponding modulus be chosen as a background value), whereas the phase indicates which $\mathcal{N} = 1$ supersymmetry of the original $\mathcal{N} = 2$ supersymmetry is preserved by the state. If the phases of two central charges align, the two states

[3] This is not completely true for a split flow tree, but it is a good first intuition. A depiction of the moduli would actually correspond to a fattened version of a split flow tree, as is discussed below.

[4] The term 'incoming branch' refers to the part of the flow tree connecting the background point and the first split point.

are mutually BPS (i.e. preserve the same supersymmetry) and the binding energy of the BPS bound state vanishes,

$$|Z_{1+2}| = |Z_1| + |Z_2|, \tag{2.30}$$

or equivalently,

$$\mathrm{Re}(\bar{Z}_1 Z_2) > 0, \qquad \mathrm{Im}(\bar{Z}_1 Z_2) = 0. \tag{2.31}$$

To render this more precise, the notion of a wall of *marginal* stability, as opposed to a wall of *threshold* stability, will be reserved for the case when the two charges are non-local: $\langle \Gamma_1, \Gamma_2 \rangle \neq 0$ [5]. If one reaches the wall from the side where $\langle \Gamma_1, \Gamma_2 \rangle (\arg(Z_1) - \arg(Z_2)) > 0$, the decay of $\Gamma \to \Gamma_1 + \Gamma_2$ is energetically favored. One then follows the flows of the constituents, which might decay again according to the same scheme, until every end branch flows towards an attractor point. Figure 2.2 illustrates a split flow tree with three endpoints corresponding to a solution with three centers.

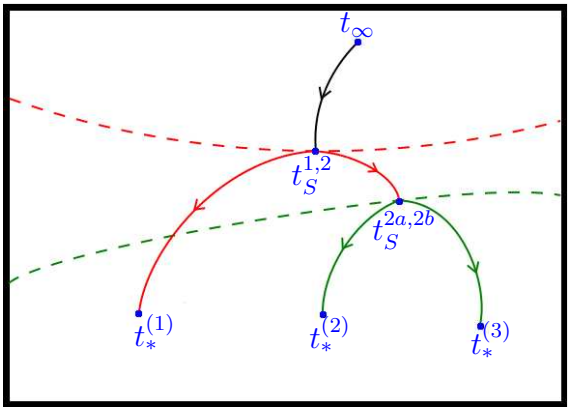

Figure 2.2: **Split flow tree for a three-centered solution**: One starts at the background point, t_∞, at the top, and follows the incoming branch (plotted in black) until one hits a wall of marginal stability (plotted in red) between Γ_1 and Γ_2. This is the first split point $t_S^{1,2}$, wherefrom single flows corresponding to the two centers continue (both branches are plotted in red). The first center reaches an attractor point, $t_*^{(1)}$, whereas the second branch again reaches a wall of marginal stability (plotted in green), at $t_S^{2a,2b}$. The two constituents $\Gamma_a^{(2)}$ and $\Gamma_b^{(2)}$ were denoted with $\Gamma^{(2)}{=}\Gamma_a^{(2)}{+}\Gamma_b^{(2)}$. Two branches plotted in green, corresponding to these two constituents, finally flow off to their attractor points, $t_*^{(2)}$ and $t_*^{(3)}$. All the relevant data belonging to this split flow tree are the background point, the two split points and the three end points, $(t_\infty, t_S^{1,2}, t_S^{2a,2b}, t_*^{(1)}, t_*^{(2)}, t_*^{(3)})$, all plotted in blue in this figure.

Now of course, a split flow tree does not have the same literal interpretation (like a single flow) as the set of points $t^A(r)$, a depiction of the Kähler moduli or the complex structure moduli in dependence of the radial coordinate. One can however imagine a fattened version of a split flow tree, including all the values $t^A(r, \theta, \phi)$. This is illustrated by figure 2.3.

[5] If the charges are 'local', $\langle \Gamma_1, \Gamma_2 \rangle = 0$, they are mutually BPS in a trivial way. More details can be found in the discussion on threshold walls.

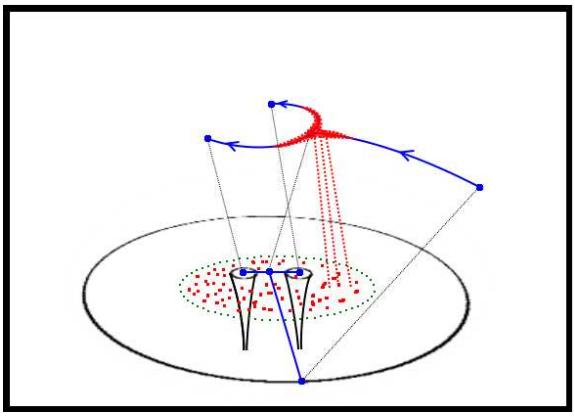

Figure 2.3: **The values of the moduli belonging to a multi-centered solution**: Spacetime is depicted below, the split flow drawn above takes place in the moduli space. The solution differs significantly from being spherically symmetric in some region. This region has been sketched as lying somewhere within the dotted green line. Should one map all the points to corresponding values of the moduli, one could get a fattened version of a split flow tree. The flow tree becomes thinner again, the further one gets away from the two centers. In other words, the black hole bound state starts resembling a spherically symmetric solution. Correspondingly, the nearer one gets to one of the centers, the more the geometry resembles that of a single black hole and spherical symmetry is approximately restored, so the 'pants' of the fattened flow tree become thinner again, as one approaches a center. Generally, it is clear, that the more the solution differs from a spherically symmetric case, the fatter the flow tree becomes.

Essentially, one can state the conjectured existence criterion for multi-centered BPS black holes in $\mathcal{N} = 2, d = 4$ supergravity as follows: a multi-centered BPS black hole solution (single-centered BPS solution) exists iff a split (single) flow tree exists.

Threshold walls

Apart from the walls of marginal stability, which separate regions in moduli space between which a BPS index can jump, there is a second type of wall that is also of importance in the research presented later on: walls of *threshold* stability. The distinction between these two kinds of walls was first discussed in [53], and was later explained in more detail in [54]. The threshold conditions are the same as for marginal stability,

$$\mathrm{Re}(\bar{Z}_1 Z_2) > 0, \qquad \mathrm{Im}(\bar{Z}_1 Z_2) = 0\,, \tag{2.32}$$

however this time, one is dealing with two mutually local charges, $\langle \Gamma_1, \Gamma_2 \rangle = 0$. As will become clear below, this has a microscopic picture to it. It means that there is no net force between the two branes, as there are either no tachyonic strings between the two branes that can condense to merge Γ_1 with Γ_2, or the interaction effects cancel out. Most importantly, a BPS index cannot jump when crossing the threshold stability wall with the background modulus. In the context of split flow trees, this means that a split flow can

change topology. It is convenient to illustrate this with the archetypical example.

Consider a three-centered solution, with one 'satellite' center, denoted γ, and two 'core' centers Γ_1 and Γ_2. The threshold wall is defined between the satellite γ and the total core $\Gamma = \Gamma_1 + \Gamma_2$. Thus, one would like to investigate a situation where the total core and the satellite are mutually local $\langle \Gamma, \gamma \rangle = 0$. One will find that the satellite center binds to one of the two 'core' centers, when choosing the background on one side of the wall, and binds to the other one, when one crosses the wall with the background moduli. Note that a core constituent and the satellite are in general not mutually local, $\langle \Gamma_i, \gamma \rangle \neq 0$, allowing a bound state to form. If one would place the background exactly on the threshold wall, one can picture that the forces between the satellite and either of the cores effectively cancel. The satellite can be placed at any distance from the total core, it is just 'relatively' BPS. This is completely analogous to what one would find, if the core Γ were realized as a single center. For the three-centered solution however, choosing the background on one side of the wall 'pushes' the satellite towards one of the cores.

Figure 2.4 illustrates this topology change associated to a threshold wall. Both kinds of walls appear throughout the studies on BPS states on various CY 3-folds in chapter 4.

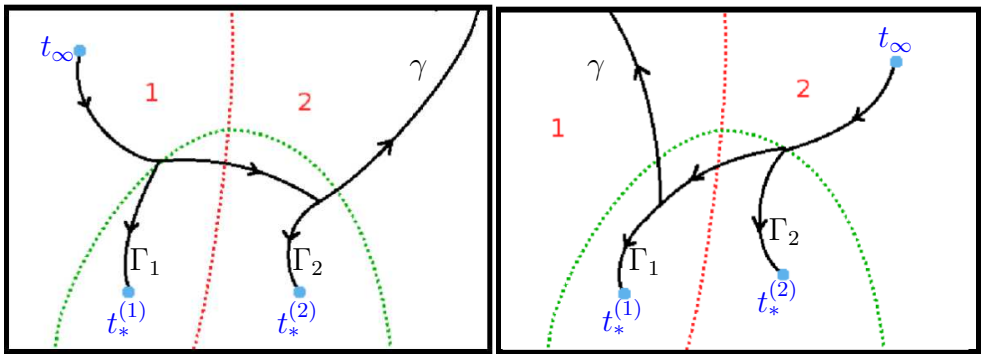

Figure 2.4: **Threshold walls and topology change of flow trees**: 1. On the left-hand side, the background t_∞ is chosen to lie to the left of the threshold wall (plotted in red); this background region is denoted by 1. The incoming branch reaches a wall of marginal stability (plotted in green) between Γ_1 and $\Gamma_2 + \gamma$ and splits. The satellite γ binds to the center Γ_2 with attractor point $t_*^{(2)}$ on the right-hand side of the wall. This bound state is realized as two centers, thus the flow splits once more (the wall of marginal stability for this split is not plotted in the figure). Typically, in the studies performed later on, the satellite will be realized as a $\overline{\text{D0}}$-brane, of which the attractor point lies at the LCS (large complex structure) point (the branch flows off to that limit in the picture). 2. On the right-hand side, the background is chosen to lie to the right of the threshold wall. This background is denoted as region 2. The split flow tree behaves analogously, but the satellite binds to Γ_1 with attractor point $t_*^{(1)}$.

The area code

In general, one finds several different split flow trees for a given total charge Γ, and maybe also a single flow. These all contribute to the total index of BPS states with this total

charge, which will be denoted by $\Omega(\Gamma)$. In general, this index of BPS states $\Omega(\Gamma)$ remains invariant under infinitesimal variations of the background moduli, t_∞, but it can jump when the moduli are driven through a wall of marginal stability. This is intuitively clear; a certain split might disappear from the spectrum, because the flow starts on the unstable side of the appropriate wall of marginal stability. Altenatively, a new type of split flow tree might enter the spectrum, as the new background lies on the stable side of the corresponding wall. If the spectrum changes, one speaks of having taken the background into a different *area*. The fact that there are different basins of attraction in moduli space has led to the name *area code* for the background. Hence, an index of BPS states should be denoted more precisely as $\Omega(\Gamma, t_\infty)$.

The split attractor flow conjecture

The split attractor flow conjecture from [1] states that:

- For a given background t_∞ in Kähler / complex structure moduli space, the existence of a split attractor flow tree starting at the background t_∞, with a given total charge Γ and endpoints corresponding to Γ_i, is equivalent to the existence of a multi-centered BPS solution in supergravity, with centers Γ_i.

- The number of split flow trees and hence the total number of states with a given charge Γ in a fixed background is finite, at least when charge quantization is imposed.

Now imagine one would like to know how many BPS states there are in the spectrum corresponding to the total charge Γ. According to the split flow tree conjecture, they are classified, and one just has to find the number of BPS states corresponding to each flow tree (this should be accomplished by calculating appropriate Witten indices). Figure 2.5 illustrates this.

One potential failure of the conjecture (in particular for classification of BPS states in supergravity) became clear fairly recently. Namely, it became apparent that there are multi-centered solutions which are not described by split flows, but might rather correspond to single flows, or not have an attractor description at all. This type of solutions have been called *scaling solutions*, [1], and are addressed in the next paragraph. Scaling solutions are multi-centered black holes with two (or more) centers lying so close together in spacetime, that their throats have melted together in the supergravity description. It is interesting to include them in the discussion and possible implications for the split attractor flow conjecture.

2.3.1 Scaling solutions

Scaling solutions owe their name to the special feature that the distance between their centers is not fixed, but rather a 'scaling' modulus. The appearance of scaling solutions can be understood easily using a concrete three-centered example. To make following

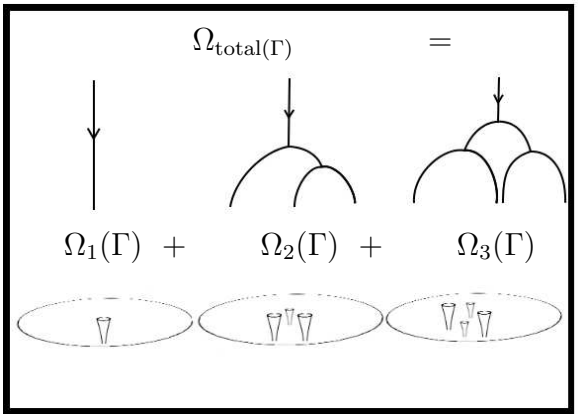

Figure 2.5: **Total number of BPS states** $\Omega(\Gamma)$: According to the split flow conjecture the BPS states in $\mathcal{N} = 2, d = 4$ supergravity of total charge Γ are classified by flow trees, and one can add up the number of states belonging to all existing flow trees. In the example in the figure, there is a single flow, a 3-centered split flow tree, and a 4-centered split flow tree, which means that this charge is realized as a single-centered black hole and two different types of multi-centered black holes.

equations transparent, the shorthand notation $\Gamma_{ij} = \langle \Gamma_i, \Gamma_j \rangle$ is introduced, as well as h to label the constants appearing in harmonic functions,

$$H(\vec{x}) = \sum_{i=1}^{N} \frac{\Gamma_i}{|\vec{x} - \vec{x}_i|} + h, \tag{2.33}$$

where $h = -2\text{Im}(e^{-i\alpha}\Omega)_{\tau=0}$. One can find a scaling solution to the integrability conditions (2.25), by treating $|\vec{x}_i - \vec{x}_j| = \lambda\Gamma_{ij}$ as independent variables and sending $\lambda \to 0$: this explains why these solutions are called 'scaling solutions'. The distances between the centers are not completely independent: in order for such a solution to exist, one must respect the triangle inequality $\Gamma_{21} + \Gamma_{13} \geq \Gamma_{32}$ (and cyclic permutations thereof). In the limit $\lambda = 0$ (or λ infinitesimally small), the locations of the centers in spacetime become identical, and the black hole solution becomes indistinguishable from a single-centered black hole for a distant observer, whereas for an observer remaining at finite distance from the centers, the solution stays multi-centered. The interpretation is, that the throats of the black holes have melted together and that the near observer has disappeared down the throat. This is illustrated in figure 2.6.

If a scaling solution exists, it will not decay upon variation of background moduli, and it thus seems that they cannot be described by split attractor flow trees, although they are multi-centered black hole solutions in supergravity. The fact that the constituent throats melt together renders them very similar to single-centered solutions in many respects. Due to the fact that such solutions can carry the same charges as a (large) black hole, they were interpreted as a 'deconstruction' of a D4-D0 black hole into zero-entropy constituents in [55]. This might also be a next step towards understanding the CFT dual of an asymtotically AdS_2 black hole, [56, 57], but this cannot be conclusively addressed at this time. It

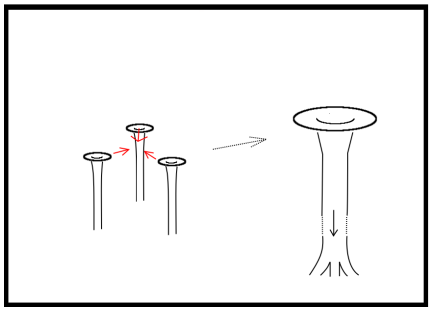

Figure 2.6: **Scaling solution**: As the positions of several black holes become identical, the throats belonging to the black holes melt together, eventually disappearing down the (infinitely long) throat of one big black hole. From the outside, it is indistinguishable from a single-centered black hole, for an observer placed somewhere down the throat it remains multi-centered.

is also not clear a priori how to count the number of states associated to a scaling solution using the methods put to work in this thesis.

The authors of [58] studied the quantization of the phase space of smooth supergravity solutions. In well understood situations (type IIB compactifications and the Strominger-Vafa (SV) black hole), it can be shown that the quantization of the phase space of smooth supergravity solutions (thus a restriction to the states carrying quantum numbers) is in one-to-one correspondence with the BPS microstates in the D-brane description. Microstates on the gravity side arise as wavefunctions, which localize on a unit of phase space. A classical solution can then be interpreted as the limit of this localized wavefunction. It can however be the case, that there are quantum states in the spectrum, which do not localize on such a unit of phase space, and it is questionable if these states have a reasonable classical description. On the other hand, the authors also argue, that 'nominally' classical solutions might occupy the same volume in quantized phase space (arise as limits of a state localized in the same volume), although they differ on a macroscopic scale in their gravitational description. This cannot be reasonable when taking into account Heisenberg's uncertainty principle, and thus 'classical solutions' of this kind might not be 'valid' geometries of the black hole. They might just be a peculiarity without physical significance, found in supergravity. This is exactly what the authors claim to be the case for scaling solutions. Thus, scaling solutions might not be valid classical limits of black hole microstates. Nevertheless, an index accounting for scaling solutions, based on the quantization of phase space was constructed in [58], and this might help when trying to match classical and quantum BPS states.

At present, the meaning of scaling solutions, in particular in relation to the split attractor flow conjecture is not completely clear. Scaling solutions might not be good classical limits of quantum microstates, or one might not understand them properly, yet. Maybe – being very careful not to make any overstatement – it is too much to hope for, that split attractor flow trees classify the full BPS spectrum. In any case, the split attractor flow tree conjecture is extremely accurate for a large number of BPS states in supergravity,

and also classifies BPS bound states outside of the regime of supergravity: this claim was successfully put to various non-trivial tests, and the results on this will be presented in chapter 4.

2.3.2 Microscopic D-brane picture

The meaning of split attractor flow trees outside the range of validity of the supergravity approximation to type II string theories is of interest in this thesis. Strictly speaking, it is the uncorrected supergravity action that entered the derivation of the split attractor flow equations from [43], [59]. Nevertheless, some ingredients of the derivation should be valid outside of the original regime. For example, arguments leading to stability or decay of a BPS state on one or the other side of a wall of marginal stability are still based on BPS mass and $\mathcal{N} = 1$ phase encoded in the central charge. As discussed in chapter 4, the central charge does receive quantum corrections that have to be taken into account, and, fortunately, can be taken into account. Using an appropriate measure of the charge of a D-brane system, $|\Gamma|$, the former (macroscopic) supergravity description of BPS states is valid at $g_S\,|\Gamma| >> 1$, whereas a microscopic D-brane description becomes valid at $g_S|\Gamma| << 1$.

Bound states and decay of bound states near a wall of marginal stability have some nice interpretations in the low energy description of the D-brane system. When the phases of the central charges of two D-branes are almost equal, light bosonic open strings stretch between the two branes. At low energy, the worldvolume $\mathcal{N} = 1, d = 4$ gauge theory describing several D-branes can be dimensionally reduced to one dimension, yielding supersymmetric quantum mechanics. The D-brane systems can be described as quivers [6], each D-brane 'center' is represented by one node. In the quiver quantum mechanics, light strings stretching between the D-branes become chiral multiplets, which are represented by arrows in the quiver picture and their masses can be seen as arising from a D-term potential. For the moment take for simplicity a system consisting of two D-branes. The symplectic intersection between the two charges,

$$\langle \Gamma_1, \Gamma_2 \rangle = n_+ - n_-, \tag{2.34}$$

now computes the difference of positively and negatively charged bifundamental fermionic zero modes. When one approaches a marginal stability wall in moduli space from the side where

$$\langle \Gamma_1, \Gamma_2 \rangle \cdot (\alpha_1 - \alpha_2) > 0, \tag{2.35}$$

where the α's are the respective phases, there will be tachyonic strings present between the two branes. Tachyon condensation on this side creates a bound state of total charge $\Gamma = \Gamma_1 + \Gamma_2$.

[6] Basically, quivers are graphic representations of the matter content of gauge theories, consisting of nodes (representing the branes) and arrows connecting the nodes (standing for the strings connecting the branes). Nodes come with a number, indicating which representation the gauge fields (arising from the strings ending on that brane) demand. More details can be found in [51].

Quite spectacularly, in [60], this setting was used to show how one can dynamically interpolate, by varying the string coupling constant, between the two complementary descriptions of a BPS bound state. If $g_S \to 0$, the supersymmetric ground state wave functions live in the Higgs branch of the quiver quantum mechanics, where all nodes are at the same position. This is the microscopic D-brane picture. As the string coupling is increased, these states are transformed into multi-centered molecules, BPS bound states. The supersymmetric ground state wave functions gain a life on the Coulomb branch of the theory, and the nodes acquire finite fixed distances from each other.

Flow tree data and the BPS spectrum of D-brane states

A correspondence between split flow trees and BPS states in string theory, valid outside of the large radius regime is supported by the quiver picture of bound states of D-branes. Branes can be imagined to get glued together through tachyon condensation, when following an inverse flow [60]. In a flow tree, background and attractor values of the Kähler modulus retain their meaning in the quiver picture. A smooth interpolation between the microscopic D-brane quiver picture and the supergravity picture of multi-centered solutions was given in [60]. The quiver picture has now been placed in the broad categorical framework as reviewed in [61].

In the D-brane description, the graphical representation of a flow tree associated to a charge and the constituents of the flow tree themselves somewhat lose their direct interpretation as the variation of the CY geometry along the radial coordinate of a BPS solution. However, microscopically one can think of splitting or gluing D-branes together through tachyon condensation when following a split flow tree in moduli space. Essentially, a split flow tree belonging to the total charge Γ and n constituents $(\Gamma_1, ..., \Gamma_n)$ can be reduced to a set of data

$$(t_\infty; t_{1,\text{split}}, ..., t_{n-1,\text{split}}; t_{1*}, ..., t_{n*}), \tag{2.36}$$

consisting of $2n$ points, a background value t_∞, a set of $n-1$ split points $t_{i,\text{split}}$ $(i = (1, .., n-1))$, and n attractor points, t_{j*} $(j = 1, ..., n+1)$, one for each center [7]. With this notation, a single flow would just be denoted $(t_\infty; t_*)$. The full correspondence between these sets of data (2.36) and BPS states in string theory is referred to as the *strong version of the split attractor flow conjecture*. As will be shown, the results presented in chapter 4 provide some very non-trivial tests of the strong version of the conjecture. However, in section 4.3, it is also argued that it needs emendation: certain indices corresponding to split flow trees have to be calculated with greater care, as the corresponding moduli spaces do not factorize, but rather have a non-trivial fibration structure.

[7] Note that this is based on the assumption that a charge always splits into two at a split point, however a more general situation is also possible where a charge splits into three or more constituents at a split point: this would require a slight generalization of the statements made.

2.4 Black hole entropy

The event horizon and the entropy of black holes already made their appearance in this chapter and will now be re-examined in more detail. Originally, these concepts arose from studying the macroscopic description of black holes as solutions to gravitational theories. Namely, they behave like thermodynamical objects with a temperature and an entropy. This entropy and therefore the amount of information carried by a black hole turns out to be proportional to the area of the event horizon.

The intriguing proposal, that the entropy is proportional to the area A of the event horizon, was first made by Bekenstein and further substantiated by Hawking, leading to

$$S = \frac{k_B A}{4 l_P^2}, \tag{2.37}$$

using the Boltzmann constant k_B and the Planck length l_P, which will be set to one from now on.

The laws of black hole mechanics

In fact, Carter, Hawking and Bardeen went on to suggest a stunning analogy between the laws of thermodynamics (TD) and of 'black hole mechanics' for stationary black holes carrying angular momentum and charge, [62]. These laws can be expressed as follows.

- **Zeroth law of black hole mechanics:**
  The event horizon has constant surface gravity κ for a stationary black hole. This is analogous to the zeroth law of TD stating that the temperature is constant throughout a body in thermal equilibrium.

- **First law of black hole mechanics:**
  The mass deformations dM of a black hole behave according to

  $$dM = \frac{\kappa}{8\pi} dA + \omega dJ + \Phi dQ, \tag{2.38}$$

  where dA is the change in surface area of the event horizon, ω is the angular velocity and dJ a change in angular momentum, Φ is the electrostatic potential and dQ is a change in the charge of the black hole. This shows some analogy with the thermodynamic law $dE = TdS - pdV + \mu dN$. The changes in mass of the black hole due to changes in angular momentum and charge can be seen as a sort of energy conservation, whereas the term proportional dA can be interpreted as analogous to the term dS in the first law of TD.

- **Second law of black hole mechanics:**
  The area of a black hole does not decrease over time: $dA \geq 0$. This matches the second law of TD, $dS \geq 0$.

- **Third law of black hole mechanics:**
  Finally, it is not possible to have a black hole with zero surface gravity, $\kappa = 0$. This is analogous to the third law of thermodynamics, stating that it is impossible to reach absolute zero temperature in a physical process.

Taking this analogy a step further, these laws suggest that the temperature of a black hole is proportional to the surface gravity, and the entropy of a black hole is proportional to its event horizon area. Furthermore, the famous semi-classical computation of Hawking, which will be discussed in chapter 5 (in the context of the problem of information loss in a black hole as well as possible resolutions to this problem), shows that a black hole should radiate at a temperature $T = \frac{\kappa}{2\pi}$, which allows to identify $S = \frac{A}{4}$.

It is clear that one would ideally like to have a microscopic explanation of such an entropy in terms of a degeneracy of possible microstates, allowing one to express the entropy in the form

$$S = k_B \cdot \ln(\Omega), \tag{2.39}$$

where Ω is the number of microstates of the black hole. Indeed, for some BPS black holes, some intriguing discoveries in this direction have been made, by relying on the invariance of indices to count the number of microstates under variation of the string coupling as well as concrete realizations of holography, allowing one to count microstates in an appropriate dual field theory.

2.4.1 A black hole made from a D4-D2-D0 brane system

Although the focus in this section will be on black holes made from a D4-D2-D0 brane system, some more general remarks will provide a useful background. A different type of black hole, in type IIB string theory, made from D1, D5 branes and momentum P is maybe the black hole for which microscopic entropy calculations are now best understood. The 5d D1-D5-P system for a type IIB compactification on $K3 \times S^1$ was also the first black hole for which a microscopic explanation for its entropy was given. This was done by Strominger and Vafa in 1996, [63]. Therefore, this system is sometimes also referred to as the SV (Strominger-Vafa) black hole. In a type IIA theory compactification on a CY 3-fold X, or an M-theory compactification on $X \times S^1$, a similar derivation was given by Maldacena, Strominger and Witten in 1997, [64]. This system is therefore sometimes referred to as the MSW system. The focus in the following will be on the IIA description of the MSW system, as this kind of setup is used most, later on in this thesis.

For the microscopic counting of the number of microstates of a D1-D5-P system in 5d from 1996, [63], it was central that the number of states of the black hole can (hopefully) be identified with a Witten index, which is independent of the string coupling. Strominger and Vafa analyzed a black hole made from N_5 D5-branes, N_1 D1-branes and N_P units of momentum, for a $K3 \times S^1$ compactification. They argue, for a regime where the radius of the S^1 is very large compared to the characteristic length in $K3$, that the low energy states are described by a 2d superconformal field theory on $S^1 \times \mathbb{R}$ with target

space $\mathrm{Sym}^{N_1N_5}(K3)$. This CFT has $(4,4)$ supersymmetry and left- and right-moving central charge $c_L = c_R = 6N_1N_5$. There is an index of BPS states, invariant under marginal deformations of this CFT, referred to as the $\mathcal{N} = (4,4)$ elliptic genus,check e.g. [65]. Specific results on the elliptic genus can be found in [66, 67]. Strominger and Vafa found $e^{2\pi\sqrt{N_1N_5N_P}}$, and the logarithm of this number of BPS states yields $S_{\text{micro}} = 2\pi\sqrt{N_1N_5N_P}$, which agrees with the macroscopic calculation.

The MSW system: a D4-D2-D0 / M5-M2-P black hole

Another intensively studied black hole system can be modeled either from a 5d point of view, using an M-theory compactification on $X \times S^1$, where X is a CY 3-fold and S^1 is the M-theory circle, or a type IIA 4d compactification on the same CY X. From a supergravity perspective, it is often possible to continuously interpolate between 4d and 5d configurations, a procedure which has become known under the name '4d-5d connection' [68, 69]. Starting from 4d solutions, this connection allows construction of 5d solutions through the performing of the so-called 'lift'. The former class of solutions is not completely general in 5d, as they always have at least one $U(1)$ isometry. On one hand, one can dimensionally reduce a 5d supergravity theory on a circle, without reference to a 10D supergravity or string theory origin. On the other hand, from a 10D point of view, the 4d or 5d descriptions are just valid in different regimes, between which can be interpolated by varying an appropriate circle. Later on in this thesis, a 4d solution will be lifted to 5d in a different setup, namely in IIB compactified on a six-torus T^6. The reader can find more details on that lift where it is actually performed, under 5.3.4. In the present case, one considers black holes with charges $(0, p^A, q_A, q_0)$ in the IIA picture, in other words, carrying no total D6-brane charge.

Using the notation for forms on CY manifolds introduced in the appendix, A.1, and modeling a CY manifold X by means of algebraic geometry, one wraps a D4 brane on some complex codimension one hypersurface $P \subset X$, which is Poincaré dual to a two form, and one can write the D4-brane charge as $p^A D_A$, where the D4 brane is wrapped on a hypersurface divisor (which one can think of as a formal sum of hypersurfaces adhering to the definition of a Weil divisor) in the homology class $\sum_A \mathrm{PD}(D_A)$, where $\mathrm{PD}(D_A)$ means the homology class of cycles Poincaré dual to the cohomology class D_A. On general ground, supersymmetry allows binding $(p-4)$-branes to p-branes, [9], one can thus bind a number of D0-branes to the D4-brane. In this thesis, the branes that bind to D4-branes are called anti-D0-branes, following the convention of [1]. In addition one can turn on $U(1)$-worldvolume flux, and when considering a stack of N branes for systems appearing in the discussions on the OSV conjecture, this flux will be restricted to diagonal fluxes lying in the subgroup $U(1)^N \subset U(N)$. The flux induces D2-brane charge,

$$q_A = D_A \cdot F, \tag{2.40}$$

using the notation $D_A \cdot D_B = \int_P D_A \cdot D_B$ as a product between two forms in $H^2(P, \mathbb{Z})$. There is one restriction imposed by supersymmetry: the fluxes have to be of type $(1,1)$, $F \in H^{(1,1)}(P, \mathbb{Z})$, [70]. Let $i_P : P \to X$ denote the embedding of P in X. It is clear that

the fluxes pulled-back from the CY X, $F = i_P^* \mathcal{F}$, from now on referred to as '*pullback-fluxes*', are automatically of this type, where $\mathcal{F}$ is a two-form on X (note that $h^{(2,0)}(X) = h^{(0,2)}(X) = 0$).

The total $\overline{\text{D0}}$-charge reads

$$q_0 = \frac{\chi(P)}{24} + \frac{1}{2}F^2 - N, \tag{2.41}$$

where

- $\frac{\chi(P)}{24} = \frac{P^3 + c_2 \cdot P}{24}$ is the (dissolved) curvature induced $\overline{\text{D0}}$-charge, which has been written out using the adjunction formula from algebraic geometry, discussed in the appendix, A.1,
- $\frac{1}{2}F^2$ is the flux-induced (dissolved) $\overline{\text{D0}}$-charge,
- N is the number of pointlike bound $\overline{\text{D0}}$-branes.

Upon lifting this configuration to 5d, one obtains M5-branes wrapped on $P \times S^1$. The fluxes and $\overline{\text{D0}}$-charges lift to fluxes inducing M2 brane charge as well as momentum $P = q_0$. From the 5d point of view, this system is a 'black string' wrapped and rotating around the S^1, with near horizon geometry $AdS_3 \times S^2$. A D6-brane gets mapped to Kaluza-Klein monopole (of higher origin). The resulting metric is often referred to as a Taub-NUT space. A black hole carrying total D6-charge has a different near horizon geometry (as in this case, the circle would pinch off where the black hole sits).

The entropy of the MSW black hole

According to earlier remarks, calculating the entropy through the area of the event horizon can be called a macroscopic calculation. Many such computations were performed around 1995, see e.g. [46, 71]. For the MSW system, in other words (from the IIA perspective) for a D4-D2-D0 black hole on a CY manifold carrying the charges $(0, p^A, q_A, q_0)$ it is in general quite difficult to write down the complete solution to the attractor equations. By taking a look at the general form of the metric (2.7) and the entropy function (2.20), one can easily see where the entropy function earned its name. From the form of the metric one sees that the area of the event horizon reads

$$A = 4\pi \cdot \lim_{r \to 0} \left(r^2 \Sigma(r) \right) = 4\pi \Sigma(\Gamma). \tag{2.42}$$

In other words, as $S = \frac{A}{4}$, the entropy function literally yields the entropy at the event horizon: $S = \pi \Sigma(\Gamma)$. The solution for the entropy function for Calabi-Yau black holes depends strongly on the form of the prepotential

$$F = \frac{D_{ABC}}{6} \frac{X^A X^B X^C}{X^0}, \tag{2.43}$$

using $D_{ABC} = \int_X D_A \wedge D_B \wedge D_C$. The general solution for the entropy function was found in [72]. Upon including also D6-brane charge p^0, for reasons which will become clear, a solution was not found to exist for all values of the charge p^0. The entropy function reads

$$\Sigma(H) = \sqrt{\frac{Q^3(H) - L^2(H)}{(H^0)^2}}, \tag{2.44}$$

using

$$\begin{aligned} L(H) &= H_0(H^0)^2 + \frac{1}{3}D_{ABC}H^AH^BH^C - H^AH_AH^0, \\ Q^3(H) &= (\frac{1}{3}D_{ABC}x^A(H)x^B(H)x^C(H))^2. \end{aligned}$$

The x^A are defined implicitly through the intersection numbers of a CY and have to be calculated on a case by case basis

$$D_{ABC}x^Ax^B = -2H_CH^0 + D_{ABC}H^AH^B.$$

Using the notation $p^3 := D_{ABC}p^Ap^Bp^C$ and defining the quantity $\hat{q}_0 = q_0 - \frac{1}{2}D^{AB}q_Aq_B$, which will play an important role further on in this thesis and shall be referred to as the 'reduced D0-brane charge', the equations for the attractor values of the moduli can then be written out as

$$t^A = D^{AB}q_B + ip^A\sqrt{\frac{-6\hat{q}_0}{p^3}}.$$

It is also useful for future reference, to introduce the notation $D_{AB} = D_{ABC}p^C$ and $D^{AB}D_{BC} = \delta^A{}_C$. Using (2.44), the entropy of the MSW black hole can be derived to be

$$S = 2\pi\sqrt{-\frac{p^3\hat{q}_0}{6}}. \tag{2.45}$$

The MSW CFT and the $\mathcal{N} = (0,4)$ modified elliptic genus

As indicated above, the other famous microscopic entropy is from 1997, where a computation analogous to the Strominger-Vafa computation was done for a 4d D4-D2-D0 black hole in IIA. In [64], the authors successfully reproduced (2.45). By growing the M-theory circle, the D4-D2-D0 configurations oxidize to M5-M2-KK-mode configurations. In the limit where the M-theory circle is large with respect to the CY threefold, the system is effectively described by a string. The corresponding (S)CFT on it is referred to as the MSW CFT. It has central charges

$$c_L = P^3 + c_2 \cdot P, \quad c_R = P^3 + \frac{1}{2}c_2 \cdot P, \tag{2.46}$$

where c_2 is the second Chern class of the CY X. The field content of this CFT can be very explicitly analyzed in a sigma model realization, [73], but this will not be discussed here.

For this theory, there is a supersymmetric index counting BPS states called the modified elliptic genus. It is defined as

$$Z(q,\bar{q},y) = \mathrm{Tr}\left(\frac{1}{2}F^2(-1)^F q^{L_0-\frac{c_L}{24}}\bar{q}^{\bar{L}_0-\frac{c_R}{24}}y^{J_0}\right), \tag{2.47}$$

and will be examined in more detail in the next section.

Again, growth estimates of BPS degeneracies performed in [64] rely on the famous Cardy formula, which restricts the regime of applicability. Namely (apart from the general restriction to zero D6-charge) the number of D0-branes N has to be very large. Check also [74], where the same system was analyzed in a IIA picture and where the same restriction was again imposed.

2.4.2 The modified elliptic genus

As explained in [75], the modified elliptic genus (2.47) is constrained to be a *weak Jacobi form* of weight $(-\frac{3}{2},\frac{1}{2})$ (the weight refers to transformations under the modular group). One can imagine such a weak Jacobi-form to be a vector containing modular forms as components: objects that transform under the modular group. As explained in [41, 42], one can associate a modular invariant theta function

$$\Theta_\Lambda = \sum_{F\in H^2(P,\mathbb{Z})} (-1)^{\frac{(f+\gamma)_{||}}{D}} e^{\frac{1}{2}\pi i\tau F_\perp^2+\frac{1}{2}\pi i\bar{\tau}F_{||}^2+2\pi i y^A q_A} \tag{2.48}$$

to the lattice of points Λ, representing all possible fluxes $F\in H^2(P,\mathbb{Z})$, that can be turned on on the D4-brane worldvolume. The notation $F_\perp$ and $F_{||}$ is used to distinguish between self-dual and anti-self-dual parts of the flux (with respect to the intersection form on $H^2(P,\mathbb{Z})$), $f_{||}+\gamma_{||}$ denotes the integer part of the flux in direction of the self-dual part of the flux lattice. This shall be explained a bit more closely.

The lattice of fluxes in $H^2(P,\mathbb{Z})$

One would like to turn on worldvolume flux on a D4 brane wrapped on a divisor $P\subset X$ of the CY X. These lie in $H^{(1,1)}(P,\mathbb{Z})$. This is not always exactly true. It might happen (and does for the examples explained in this thesis), that the divisor is a manifold that does not allow a spin structure. The examples do however support a spin-c structure. The same fact can also be seen as an anomaly from both a worldvolume perspective on the D-brane wrapped on the divisor, [76], and a string worldsheet [77] point of view (the latter has become known as the Freed-Witten anomaly). From a more mathematical point of view, one can express this as non-vanishing Stiefel-Witney classes, representing 'topological obstructions'. Discussing these viewpoints in detail is however beyond the scope of this thesis. Roughly, the fact that a manifold does not support a spin structure means that one cannot define transition functions for spinors, that close. One can compensate for this shortcoming by using a tensor product of the would-be spin bundle with a line bundle, the

latter chosen such that it has first Chern class $c_1(P)$. Of direct concern in this thesis is the fact that this is reflected by a half integer shift in the measured D-brane charges, or, in this case, flux values. The flux lattice is given by $\frac{c_1(P)}{2} + H^{(1,1)}(P,\mathbb{Z}) = \frac{P}{2} + H^{(1,1)}(P,\mathbb{Z})$. One can further decompose this flux lattice. The first type can be called pullback fluxes (i_P again denotes the embedding map $i_P : P \to X$),

$$L_X = i_P^*(H^2(X,\mathbb{Z})). \tag{2.49}$$

Clearly, $i_P^* D_A$ form a basis on L_X, with metric $D_{AB} = D_{ABC}\, p^C$. However, in general $\det(D_{AB}) \neq 1$, thus L_X is not unimodular, while $H^2(P,\mathbb{Z})$ has to be. L_X united with the orthogonal complement $L_X^\perp$ is not the full lattice, but only a sublattice of the possible fluxes. One defines the quotient of $H^2(P,\mathbb{Z})$ by $L_X \oplus L_X^\perp$, which yields a finite number of elements γ called gluing vectors (they glue together the full lattice of 'flux points'). Thus an element of the full lattice $F \in H^2(P,\mathbb{Z})$ can be decomposed as follows

$$F = \frac{P}{2} + f^{||} + f^\perp + \gamma, \tag{2.50}$$

where $f^{||} \in L_X$ and $f^\perp \in L_X^\perp$, and γ is given by gluing vectors in the flux lattice. When one splits up as $\gamma = \gamma^{||} + \gamma^\perp$ (even if these parts might in general not be integer forms corresponding to lattice points in L_X and $L_X^\perp$), one realizes that $\gamma^{||}$ and $\gamma^\perp$ have to be different from zero, at least when the divisor P is very ample [8] (this is the case for the examples used in this thesis). That $\gamma^{||} \neq 0$ is clear, because otherwise, $\gamma \in L_X^\perp$ in contradiction to the supposed splitting of the total flux. If on the other hand $\gamma^\perp = 0$, one can write $\gamma = r^A i_P{*} D_A$, where of course, if $\gamma \neq L_X$, r^A cannot be integer. For a very ample divisor P, the Lefshetz hyperplane theorem guarantees that the map $i_{P*} : H_2(P,\mathbb{Z}) \to H_2(X,\mathbb{Z})$ is surjective. Thus, one can choose a basis σ^A for $H_2(P,\mathbb{Z})$ such that the pushforwards of these basis elements, $i_{P*}(\sigma^A)$, also yield a basis for $H_2(X,\mathbb{Z})$, dual to the usual basis D_A for the cohomology of X. As γ is integral by definition (for any cycle σ^A), $\int_{\sigma^A} \gamma \in \mathbb{Z}$. However, this equals $\int_{\sigma^A} r^B i_P^*(D_B) = \int_{i_{P*}(\sigma^A)} r^B D_B = r^A$, and thus $r^A \in \mathbb{Z}$. This means that a gluing vector is always of the form $\gamma = \gamma^{||} + \gamma^\perp$.

Decomposition of the elliptic genus

The following statements are included to give the general picture. Justification can be found e.g. in [41, 42, 78]. The modular invariant theta function (2.48) associated to the flux lattice on the divisor can be decomposed as

$$\Theta_\Lambda(\tau,\bar\tau,y) = \sum_\gamma \Theta_{L_X^\perp+\gamma}(\tau)\Theta_{L_X+\gamma}(\tau,\bar\tau,y), \tag{2.51}$$

where γ runs through a finite set of gluing vectors. The theta functions $\Theta_{L_X+\gamma}$ will be abbreviated as Θ_γ, and can be written out, in the conventions used in this thesis, explicitly

[8] A divisor is very ample, when the associated line bundle allows enough sections to set up an embedding of its base variety into projective space.

as

$$\Theta_\gamma(\tau,\bar\tau,y)=\sum_{q_A=D_{AB}(\frac{1}{2}p^B+k^B)+\gamma_A}(-1)^{J^Aq_A}e^{2\pi i\tau\left(\frac{1}{2}(\frac{p^Ap^B}{D}-D^{AB})\right)q_Aq_B}e^{2\pi i\bar\tau\frac{(p^Aq_A)^2}{2D}}e^{2\pi iy^Aq_A}. \tag{2.52}$$

Using these latter functions (2.52), the modified elliptic genus can be decomposed as

$$Z(q,\bar q,z)=\sum_\gamma Z_\gamma(q)\,\Theta_\gamma(q,\bar q,z)\,, \tag{2.53}$$

where the $Z_\gamma(q)$ are meromorphic functions of the variable q. The dimensionality of the vector Z_γ is thus given by the number of independent elements γ of the discriminant group, the gluing vectors. Additionally, as discussed in [1, 41, 42, 78], it follows from modular invariance, that there is an identification

$$Z_\gamma=Z_\delta,\qquad \text{for}\quad \gamma=-\delta\mod L_X. \tag{2.54}$$

Roughly speaking, the modified elliptic genus behaves as a modular form with respect to q and as an elliptic function with respect to z. The Θ_γ form modular representations of weight $(\frac{1}{2}(h^{(1,1)}(X)-1),\frac{1}{2})$ Jacobi-forms (in the cases investigated in this thesis this means weight $(0,\frac{1}{2})$), and thus Z_γ is a Jacobi-form of weight $-\frac{3}{2}$.

One can add some D-brane charge interpretation to the terms appearing in the Z_γ's: Z_0 corresponds to a sum over states with no added D2-charge, and increasing D0-charge as the powers of q increase. Each coefficient in the q-expansion corresponds to the index of a state with fixed D0-charge. Similarly, the Z_γ's correspond to states with k units of added D2-charge [9]. Schematically, the first few terms of Z_γ will look as follows

$$Z_\gamma(q)=q^{-\alpha}(\#+\#\,q+\#\,q^2+\ldots)\,, \tag{2.55}$$

where $\hat q_0\equiv q_0-\frac{1}{2}D^{AB}q_Aq_B$, and α is the highest possible value of $\hat q_0$ for a given γ. In the analysis of chapter 4, only the $Z_\gamma(q)$ functions will be investigated explicitly, as they determine the full elliptic genus. A stringent mathematical property of weak Jacobi modular forms is the fact that they are entirely determined by their *polar part*, i.e. terms with negative powers of q. These terms correspond to charge configurations that satisfy $\hat q_0>0$, where the variables are defined in (4.10). Such configurations will be referred to as *polar states*.

To determine elliptic genera as in chapter 4, the method of generating modular representations was exploited. The basic idea is to write down a basis of modular forms in the correct modular representation. The number of basis elements should then correspond to the allowed number of polar states appearing in Z_γ, and the degeneracies of polar BPS

[9] The words 'no added' D2-charge were used, because there is some induced D-brane charge if the D4 is wrapped on a divisor lying in an uneven homology class, resulting from the shift in the flux lattice, to cancel anomalies, as discussed above.

states then determines the full modular vector. This method starts with so-called *seeding modular forms*, transforming in a particular m-dimensional modular representation of weight w. Successive differentiation of such forms yields forms with higher weights, and the basis elements collected in this way allow one to determine all the elliptic genera in this thesis. Details on this technique can be found in the appendix of [79].

2.4.3 A D4-D2-D0 black hole partition function

If one chooses the D4-brane to be wrapped on a divisor lying in a very large homology class, one can obtain enough mass to describe a system, which backreacts to yield a black hole in the gravitational description. In the following, some central ideas on the partition function of a black hole are gathered. This is worked out in detail in [1]. One would like to model a D4-D2-D0 black hole that arises from a mixed ensemble of D-brane charges. One would like to choose a (large) and fixed magnetic D4-brane charge p, and sum over all electric (D2-D0) charges. This is a mixed ensemble (microcanonical with respect to the magnetic charge, macrocanonical with respect to the electric charge).

One can write down a formal partition function

$$\mathcal{Z}_{\mathrm{BH}}(\phi;t)=\sum_{q}\Omega(p,q;t)e^{2\pi\phi^{\Lambda}q_{\Lambda}}, \tag{2.56}$$

where $\Omega(p,q;t)$ denotes the number of BPS states of total charge (p,q) (using a shorthand notation for magnetic and electric charges) at background values $t=t^A$ for the Kähler moduli. Note that this background dependence also leads to an overall background dependence of the black hole partition function. There is also a second dependence, namely on the variables ϕ^{Λ}, which are called electric potentials and are Legendre transformed variables of the electric charges q_{Λ}.

Writing out (2.56) as a sum over all possible fluxes and $\overline{\mathrm{D0}}$-charges, one gets

$$\mathcal{Z}_{\mathrm{BH}}(\phi^0,\phi^A;t)=\sum_{F,N}d(F,N)e^{2\pi\phi^0(\frac{\chi(P)}{24}+\frac{1}{2}F^2-N)+2\pi\phi\cdot F}, \tag{2.57}$$

where $d(F,N)$ is given by the second helicity supertrace, in a sector of fixed F,N, [1]. Up to a sign, this identifies this number with an Euler characteristic of the moduli space $\mathcal{M}_{F,N}$ of BPS configurations in the sector labeled by (F,N):

$$d(F,N)=(-1)^{\dim(\mathcal{M}_{F,N})}\chi(\mathcal{M}_{F,N}) \tag{2.58}$$

As discussed in detail in [1], a partition function of the form (2.57) is everywhere divergent, [1,80], but this can be remedied by introducing a Boltzmann weight $e^{-\beta H}$ with H denoting the BPS energy of the state. The partition function is then interpreted physically as the BPS partition function of a single D4-brane wrapping the divisor P and a Euclidean time circle of circumference β. This physical partition function can be investigated under S- and T-dualities. In fact, in [1], it is shown that this partition function is also a weak

Jacobi-form and after performing a 'TST' duality, the authors show that the whole partition function is determined by a finite part, namely the 'polar part'. Formally:

$$\mathcal{Z}_{\mathrm{D4}} = \sum_{A \in \mathbf{M}_{\mathrm{mod}}} A(\mathcal{Z}^{-}_{(-\frac{3}{2},\frac{1}{2})}), \tag{2.59}$$

where one sums over all images of $\mathcal{Z}^{-}_{(-\frac{3}{2},\frac{1}{2})}$ under the modular group. $\mathcal{Z}^{-}$ is called the *polar part* of the black hole partition function, and $(-\frac{3}{2},\frac{1}{2})$ signalizes the modular weight of this generalized weak Jacobi-form. From the preceding presentation, it should have become clear, that the D4-version from [1] of such a black hole partition function, is a generalization of the modified elliptic genus, presented above. It is an elliptic genus for a 'higher cohomology class divisor'.

2.4.4 Polar states

At this point, it is highly interesting to study D4-D2-D0 charge configurations in a mixed ensemble that are polar states from the supergravity point of view, and in particular with the split flow tree conjecture in mind. The holomorphic (the factor $e^{\frac{K}{2}}$ plays no role in the following argument) central charge for a D4-D2-D0 brane system $\Gamma = p^A D_A + q_A \tilde{D}^A + q_0 \omega$ in the large radius approximation reads

$$Z = \langle \Gamma, \Omega_{\mathrm{hol}} \rangle = -q_0 + q_A t^A - \frac{1}{2} D_{ABC} p^A t^B t^C. \tag{2.60}$$

Writing out the (complexified) Kähler moduli $t^A = B^A + iJ^A$, and changing the variable for the magnetic field $B^A \to \tilde{B}^A = B^A + D^{AB} q_B$, the holomorphic central charge reads

$$Z = -\hat{q}_0 - \frac{1}{2} D_{AB} (\tilde{B}^A + iJ^A)(\tilde{B}^B + iJ^B), \tag{2.61}$$

where $\hat{q}_0 = q_0 - \frac{1}{2} D^{AB} q_A q_B$. The quantity

$$\hat{q}_0 = q_0 - D^{AB} q_A q_B = q_0 - \frac{1}{2}(\frac{P}{2} + f^{||} + \gamma^{||})^2 = \frac{\chi(P)}{24} + \frac{1}{2}(f^{\perp} + \gamma^{\perp}) - N \tag{2.62}$$

is of crucial importance in this thesis, and will be referred to as the 'reduced D0 brane charge', and, as indicated, only depends on 'non-pullback' fluxes. One can now ask, in which charge regimes, the central charge will have a zero at a regular point in moduli space. Setting $Z = 0$, one obtains the two equations (real and imaginary part of Z both have to be zero)

$$\tilde{B} \cdot J = 0, \tag{2.63}$$

$$\frac{1}{2}(J^2 - \tilde{B}^2) = \hat{q}_0, \tag{2.64}$$

where the dot product is with reference to the metric D_{AB} on $H^2(P, \mathbb{Z})$. As $J = J^A D_A$ is a self-dual form (it is a pullback form), and $\tilde{B}$ is orthogonal to J by the first equation,

one knows that $\tilde{B} = \tilde{B}^A$ is anti-self dual: $J \in L_X = H^{(1,1)}_+(P,\mathbb{Z}), B \in L_X^\perp = H^{(1,1)}_-(P,\mathbb{Z})$. Thus, one obtains as a condition for a zero to exist, that

$$\hat{q}_0 > 0. \tag{2.65}$$

Put in words, the so called 'reduced D0-brane charge' has to be positive. This is the condition for polarity. In that case, one can e.g. see that the central charge vanishes at $\tilde{B} = 0, J = \sqrt{\frac{2\hat{q}_0}{P^3}}P$. Note that this analysis is based on the large radius approximation to the central charge.

2.5 Chapter summary and outlook

Generally speaking, this chapter gives a peak at a more holistic picture of black holes starting to crystallize from a string theoretical point of view. A main theme, at least for supersymmetric (BPS) black holes, is the moving back and forth between a supergravity and a D-brane perspective. The reader enjoying this sort of attempt to understand black holes from a broader point of view will find a further augmentation of these discussions on two fascinating conjectures about black holes: The first one is called the OSV conjecture, and can, at first glance, be stated as a conjecture on a wavefunction describing a black hole realized as a superposition of a mixed ensemble of D-brane charges. The second one is called the fuzzball conjecture and describes how microstates of a black hole are all given as smooth gravitational solutions coined fuzzballs. It is also in the context of these two conjectures, that split flow trees (and some other techniques) were put to use in the research presented in chapters 4 and 5.

More specifically, it was explained in this chapter, how black holes and especially the degeneracy of BPS states is approached from the supergravity and the D-brane perspective. Of central importance is the attractor mechanism for BPS black holes, governing the 'form/size' of the extra dimensions, driving the values of vector multiplet scalars to attractor points at the event horizon. Genuine multi-centered BPS black hole bound states, as discovered by Denef and collaborators, were presented after that. A manner of generalization of the attractor mechanism for multi-centered black holes was introduced, and the existence of a split attractor flow tree was proposed as an existence criterion for a multi-centered solution.

This idea was taken a step further in the presentation of the split attractor flow tree conjecture, according to which (in its strongest form) BPS states of type II string theory are classified by attractor flow trees, and this includes single-centered solutions corresponding to single flows. As the technique of split flow trees is at the core of this thesis, the non-expert reader might want to go back and take a look at figure 2.2. He will see in depiction of the scalar moduli space (for type IIA string theory, this is the Kähler moduli space of the Calabi-Yau 3-fold), how a flow starts at the background value of the scalar moduli and splits at a wall of marginal stability. A wall of marginal stability is defined as the locus, where two D-branes (the constituents after the split) are mutually supersymmetric.

This is a hypersurface in moduli space. The condition for a wall of marginal stability can be expressed as alignment of the phases of their central charges: $\arg(Z_1) = \arg(Z_2)$. This happens at the locus, where the following equation $|Z| \leq |Z_1| + |Z_2|$ reaches equality. Interpreting the central charge as a measure of the energy of a D-brane system, one can thus view the branes as marginally stable. Exactly at the wall of marginal stability, a split becomes energetically possible. Such splitting processes can occur repeatedly, and by an iterative procedure, one ends up with a split flow tree. The term 'tree' refers to the fact that one might find several 'end branches'. For each center of a BPS bound state, there will be one 'end branch' in the flow, ending at an attractor point.

It was discussed how the analogy of black hole mechanics and thermodynamics led to the idea that black hole entropy is proportional to the area of the event horizon of a black hole: $S = \frac{A}{4}$. An important goal for string theorists, which has been achieved for some supersymmetric (BPS) black holes, is to explain the entropy with a number of microstates: $S = k_B \cdot \ln(\Omega)$. For a type IIA string theory compactification on a Calabi-Yau 3-fold, a black hole (or just a particle in 4d) can be modeled by wrapping a D4 brane on a hyperplane of the Calabi-Yau, yielding a point-like object from the 4d point of view. Keeping the D4-brane charge fixed and considering various values for the D2- and D0-brane charges, one arrives at a mixed ensemble of states. Degeneracies are counted by a supersymmetric (BPS) index, called the elliptic genus. At large charge, this elliptic genus generalizes to an object which one can just call a black hole partition function. An elliptic genus (or a black hole partition function) is a generalized vector valued modular form. The central mathematical property of interest is, that they are completely determined by a finite set of degeneracies, much in the way a pole can entirely determine a complex function. The set of charges determining the full index are called polar states. In terms of D4-D2-D0 brane charges, the condition for a state to be polar reads

$$\hat{q}_0 > 0, \tag{2.66}$$

where $\hat{q}_0$ is called the reduced D0-brane charge. This quantity is just the D0-brane charge minus a small contribution, determined by the D4-worldvolume flux-induced D2-brane charge. Namely, one subtracts the contribution $\frac{1}{2}F_{||}^2$ arising from those fluxes, that do not encode any actual information on the degeneracy of the states and were referred to as pure pullback fluxes.

The degeneracies of these polar states determine the degeneracy of the full elliptic genus or the full black hole partition function. From a gravitational spacetime point of view, polar states (at least in a first approximation) do not support single-centered solutions. They are thus realized as bound states, and this can be used to obtain factorizations (at least approximately) of the degeneracies of these polar states. This will be addressed in detail in the following chapter. In the research presented in chapter 4, numerous polar states will be examined explicitly, and exact results will be obtained. The existence of polar states is established using split flow trees, and they are enumerated with techniques introduced in the following chapter. Also in chapter 5, split flow trees will be used as an existence criterion for a class of 4d multi-centered solutions, which are mapped to 5d black hole

microstates. The latter form fuzzball geometries for a black ring, thus relating 4d split flow trees to fuzzballs.

Chapter 3

Topological strings, split states and mirror symmetry

A beautiful connection between the six-dimensional topological string theories, which can be pictured to govern the topological subspectrum of states on the compact Calabi-Yau manifold, and black hole microstates has emerged over the last years. This chapter addresses this connection between black holes and topological strings, and more broadly, between microstates of an object modeled by wrapping D-branes around cycles in Calabi-Yau manifols. In 2004, Ooguri, Strominger and Vafa conjectured that the partition function of a black hole corresponding to a mixed ensemble of D-brane charges is related to the absolute value squared of the topological string partition function, $\mathcal{Z}_{\text{blackhole}} = |\mathcal{Z}_{\text{top}}|^2$. This statement has become known as the OSV-conjecture. It has been thoroughly investigated, clarified and refined by Denef and Moore, in [1], using split flow trees and the Donaldson-Thomas version of the topological string partition function.

Some basics of topological string theory are introduced briefly at the beginning of this chapter. The focus will be on the aspects relevant for later. Although, such claims are still in a conjectural phase, there is strong evidence that the partition function of topological string theory can be stated in different forms, harboring various physical interpretations. Namely, the original form sums over terms including topological invariants counting 'topological strings'. Resummations however can lead to a form where the terms contain topological invariants counting BPS bound states. One of these sums is the Donaldson-Thomas (DT) partition function. $\mathcal{Z}_{\text{top}} \equiv \mathcal{Z}_{\text{DT}} = \sum_{\beta,n} N_{\text{DT}}(\beta, n) u^n v^\beta$. The DT invariants $N_{\text{DT}}(\beta, n)$ count the number of BPS states of a D6-D2-D0 BPS state, with the D6 wrapping the CY 3-fold, the D2 brane wrapped on a cycle in homology class β and D0-brane charge n, at least when taking some subtleties into account. In [1], it was shown how a full black hole partition function is determined by the polar part (see section 2.4), consisting of polar states only, giving rise to a $D6-\overline{D6}$-realization of $|\mathcal{Z}_{\text{top}}|^2$. DT invariants will also be used to enumerate D6-D2-D0 states in chapter 4. Much of the research presented in that chapter uses techniques developed by Denef and Moore, but the analysis takes place at low D-brane charge. Thus, the research is really on a D-particle partition function and its enumeration.

Finally, the last part of this chapter discusses the topic of mirror symmetry, relating a IIA string theory compactification on a Calabi-Yau X to a type IIB compactification on the mirror Calabi-Yau Y, which is in general closely related to topological string theory, and plays a central role in the research in chapter 4. Given the massive scope of mirror symmetry, the author will present only the specific example for the quintic CY 3-fold. The generalization to the other CY's used in this thesis is straightforward.

The reader interested in jumping to the most important points in this chapter, is suggested to continue with section 3.3, directly, as the two following sections introduce the full context properly, but are not essential for gaining a basic understanding of this thesis.

3.1 Worldsheet instantons from topological string theory

To approach topological string theory in the first instance with insight, it is convenient to take a look at some features of topological field theory, as the key aspect of 'twisting' can be explained in this simpler setting. After all, topological string theory arises from coupling such a theory to gravity. There is a central idea called the 'topological twist', which goes back to Witten, and was invented to be able to make use of the power of localization, which allows the performing of quantum mechanically exact calculations by reducing (localizing) complicated path integrals to simpler ones. The latter is also the trait which attributes topological string theory with a certain simplicity as opposed to ordinary string theory. It is worth going back to the worldsheet non-linear sigma models, as introduced in chapter 1.

3.1.1 Twisting worldsheet sigma models

One would like to treat the globally supersymmetric worldsheet sigma model using Euclidean path integrals, with an arbitrary Riemann surface (with an arbitrary metric) as a worldsheet, and one thus wants supersymmetry parameters ϵ that are well-defined and covariantly constant throughout the whole worldsheet, not just a spacelike slice. This means, that the epsilons need to be covariantly constant sections of $K^{1/2}$ and $\overline{K^{1/2}}$. If these bundles are not trivial, they will only admit sections with at least one vanishing point. One can show that should an object that is covariantly constant everywhere have a vanishing point, then it has to be zero everywhere. Hence, it will in general not be possible to use the supersymmetry techniques for ordinary non-linear sigma-models, unless changes are made to the theory. The trick is to replace the spinor fields by fields that are sections of trivial bundles. This modification is Witten's *topological twist*.

When one defines the $\mathcal{N} = (2, 2)$ model (1.3), one first determines what kind of fields the theory should have (by superspace methods, for instance), and then one writes a Lagrangian such that it is Lorentz invariant (rotation invariant in the Euclidean case). Oppositely, one could look at the terms in the Lorentz invariant Lagrangian for the fermions,

$$L \sim +\overline{\psi_+}\, D_{\bar{z}}\, \psi_+ + \overline{\psi_-}\, D_z \psi_- \,, \tag{3.1}$$

and reverse-engineer what the transformation properties of the ψ's should be. Clearly, the derivative $D_{\bar{z}}$ transforms as a dual anti-holomorphic vector, i.e. as a section of $\overline{K}$, $z \mapsto e^{i\,\alpha}\, z$, $D_{\bar{z}} \mapsto e^{-i\,\alpha}\, D_{\bar{z}}$. Thus, in order to have a Lorentz invariant term in the Lagrangian, it is clear that the product of the two ψ's must transform oppositely to $D_{\bar{z}}$

$$\begin{aligned} D_{\bar{z}} &\mapsto e^{-i\,\alpha}\, D_{\bar{z}}, \\ \psi_+\, \overline{\psi}_+ &\mapsto e^{+i\,\alpha} \psi_+\, \overline{\psi}_+\,, \end{aligned} \tag{3.2}$$

i.e. their product must be a section of K. The first obvious choice was of course to take them each to be a section of $K^{1/2}$. However, as was argued before, this bundle may be non-trivial. The other two inequivalent choices [1] are the following: One can take ψ_+ to be a section of the trivial line bundle $\mathbb{I}$, (i.e. a scalar), and $\overline{\psi}_+$ to be a section of K (i.e. a holomorphic one-form). This is called the $(+)$ twist. One can also do the opposite, i.e. let ψ_+ be a section of K and $\overline{\psi}_+$ a section of the trivial bundle. This is obviously called the $(-)$ twist. To summarize

$$(\psi_+, \overline{\psi}_+) \in \Big(\Gamma(K^{1/2}), \Gamma(K^{1/2})\Big) \to \begin{cases} \Big(\Gamma(\mathbb{I}), \Gamma(K)\Big) & (+) \text{ twist} \\ \Big(\Gamma(K), \Gamma(\mathbb{I})\Big) & (-) \text{ twist}\,. \end{cases} \tag{3.3}$$

Similarly, one can define the $(\pm)$ twists for the other two spinors as follows:

$$(\psi_-, \overline{\psi}_-) \in \Big(\Gamma(\overline{K^{1/2}}), \overline{\Gamma(K^{1/2})}\Big) \to \begin{cases} \Big(\Gamma(\mathbb{I}), \Gamma(\overline{K})\Big) & (+) \text{ twist} \\ \Big(\Gamma(\overline{K}), \Gamma(\mathbb{I})\Big) & (-) \text{ twist}\,. \end{cases} \tag{3.4}$$

Up to the inversion of the worldsheet complex structure, i.e. switching the definitions of z and $\bar{z}$, there are only two inequivalent choices one can make for the whole model:

- The 'A-model': Taking the $(-)$ twist for ψ_+ and the $(+)$ twist for ψ_-.
- The 'B-model': Taking the $(-)$ twist for both ψ_+ and ψ_-.

To define the supersymmetry transformation rules for these new models, one must take into account that expressions like $\delta\phi \sim \epsilon\psi$ and $\delta\psi \sim \epsilon\partial\phi$ will only make sense if one also redefines the Lorentz properties of the ϵ's. The important result of these twisted models, is that half of the supersymmetry parameters have now become scalars (even though they are still Grassmann valued). It is always possible to define globally constant non-zero scalars. Now, one can use the full power of supersymmetry, without any obstructions of the non-trivial worldsheet topology.

There is another approach for defining the twists, which nicely generalizes to topological strings, namely using the algebra of symmetry generators. One can restate the A and B

[1] up to a redefinition of the complex structure, $z \to \bar{z}$.

twists by saying that the Lorentz transformation properties of the new fields should be related to the old transformation properties as follows:

$$\begin{aligned} M_A &= M_{\text{old}} - F_V \quad \text{for the A} - \text{model}\,, \qquad (3.5)\\ M_B &= M_{\text{old}} - F_A \quad \text{for the B} - \text{model}\,. \qquad (3.6) \end{aligned}$$

Defining $Q_A = \bar{Q}_+ + Q_-$ and $Q_B = \bar{Q}_+ + \bar{Q}_-$, one can check (using (1.8)) that $[M_A, Q_A] = 0$ and $[M_B, Q_B] = 0$, making Q_A (Q_B) a scalar under the new Lorentz group for the A-twist (B-twist). This means that one can define the A- and B- Lorentz group on arbitrary curved worldsheets.

3.1.2 Localizing to holomorphic maps: the A-model topological field theory

Now that the spinors are actually no longer spinors, it is convenient to introduce a notation that makes their transformation behavior more obvious.

$$\begin{aligned} \psi_+^i &\mapsto \psi_z^i\,, \quad \psi_+^{\bar{i}} \mapsto \chi^{\bar{i}} \\ \psi_-^i &\mapsto \chi^i\,, \quad \psi_-^{\bar{i}} \mapsto \psi_{\bar{z}}^{\bar{i}}\,. \end{aligned} \qquad (3.7)$$

The A-model action now reads

$$S_A = 2t \int_\Sigma (g_{i\bar{j}} \partial_z \phi^i \partial_{\bar{z}} \phi^{\bar{j}} + g_{i\bar{j}} \partial_{\bar{z}} \phi^i \partial_z \phi^{\bar{j}} + i g_{\bar{i}j} \psi_z^i D_{\bar{z}} \chi^{\bar{j}} + i g_{i\bar{j}} \psi_{\bar{z}}^{\bar{j}} D_z \chi^i + \frac{1}{2} R_{i\bar{j}k\bar{l}} \psi_z^i \psi_{\bar{z}}^{\bar{j}} \chi^k \chi^{\bar{l}})\,, \quad (3.8)$$

where the coupling constant t was introduced up front. Looking at the old supersymmetry transformations, one can check that α_- and $\tilde{\alpha}_+$ are now scalars, and α_+ and $\tilde{\alpha}_-$ are sections of the canonical and anti-canonical line bundle, respectively. One can now have a globally supersymmetric system, by throwing away the two latter, and keeping the scalar SUSY parameters. Denoting these parameters as α and $\tilde{\alpha}$, the supersymmetry transformations act on the fields as

$$\begin{aligned} \delta\phi^i &= i\,\alpha\chi \\ \delta\phi^{\bar{i}} &= i\tilde{\alpha}\,\chi^{\bar{i}} \\ \delta\psi_z^{\bar{i}} &= -\alpha\,\partial_z\phi^{\bar{i}} - i\,\tilde{\alpha}\,\chi^{\bar{k}}\,\Gamma^{\bar{i}}_{\bar{k}\bar{m}}\,\psi_z^{\bar{m}} \qquad (3.9)\\ \delta\psi_{\bar{z}}^i &= -\tilde{\alpha}\,\partial_{\bar{z}}\phi^i - i\,\alpha\,\chi^k\,\Gamma^i_{km}\,\psi_{\bar{z}}^m \\ \delta\chi^i &= \delta\chi^{\bar{i}} = 0\,. \end{aligned}$$

One can simplify this model by taking $\alpha = \tilde{\alpha}$, corresponding to defining an operator, which one calls the A-SUSY operator Q_A, as $Q_A = \bar{Q}_+ + Q_-$. Using this new operator, one can now express the action (3.8) as

$$S_A = i\,t \int_\Sigma \{Q_A, V\} + t \int_\Sigma \Phi^*(K)\,, \qquad (3.10)$$

where $V = g_{i\bar{j}}(\psi^i_z \partial_{\bar{z}} \bar{\phi}^j + \partial_z \phi^i \psi^{\bar{z}}_{\bar{j}})$, and K is the Kähler form of the target space. Hence, one can almost express the Lagrangian as Q_A-exact, which would by definition make the theory topological. The failure of this action to be a purely Q_A-exact action, is an integral over the worldsheet of the pullback of the spacetime Kähler form (to the worldsheet), i.e. the second term. However, this term depends only on the homology class of the image $\Phi(\Sigma)$ of the worldsheet under the embedding map. This means that one can split up the path integral into different sectors according to this homology class and factor this Kähler term out, as follows:

$$Z = \sum_{\beta \in H_2(X,\mathbb{Z})} e^{-t\, K\cdot\beta} \int_{[\Phi(\Sigma)]\in\beta} \mathcal{D}[\Phi]\mathcal{D}[\chi]\mathcal{D}[\psi] e^{-i\, t \int \{Q_A, V\}}\,. \tag{3.11}$$

It can be shown, that this theory is independent of the complex structures of Σ and X, and depends only on the Kähler class of the target space through the $\exp(-t\, K\cdot\beta)$. Otherwise, the model is *half topological* in the sense that it is independent of half of the moduli of the worldsheet and target space metrics. This path integral localizes to the minima of the action. For the bosonic part of the path integral, these are configurations satisfying

$$\partial_{\bar{z}} \phi^i = \partial_z \phi^{\bar{i}} = 0\,, \tag{3.12}$$

i.e. the holomorphic maps $\Phi : \Sigma \mapsto X$.

Anomalies

One can repeat an analysis of the zero modes analogous to the one done for the untwisted model. The number ℓ_χ of χ zero modes equals that of $\overline{\chi}$ zero modes (by simple complex conjugation of the zero mode equation), and similarly the number ℓ_ψ of $\overline{\psi}_z$ zero modes equals that of $\psi_{\bar{z}}$ zero modes. Therefore, there will be no R_V anomaly. There will be an R_A anomaly if $\ell_\chi \neq \ell_\psi$. The χ zero modes are elements of $H^0(\Phi^*(TX))$. From the Riemann-Roch theorem one obtains

$$\int_\Sigma \mathrm{ch}(\Phi^*(TX))\,\mathrm{td}(T\Sigma) = \dim H^0(\Phi^*(TX)) - \dim H^1(\Phi^*(TX))\,. \tag{3.13}$$

By Serre duality, one can write $H^1(\Phi^*(TX)) = H^0(K\otimes\Phi^*(\overline{TX}))^*$. This can be recognized as the dual to the space of ψ zero modes. Hence, the Riemann-Roch theorem yields the difference needed,

$$\begin{aligned} \ell_\chi - \ell_\psi &= 2\int_\Sigma (d + \Phi^* c_1(TX))\,(1 + \frac{1}{2}\, c_1(T\Sigma)) \\ &= 2\int_\Sigma \Phi^* c_1(TX) + d\,(1-g) \equiv 2\,k\,, \end{aligned} \tag{3.14}$$

where d is the complex dimension of the target space, and $\int_\Sigma c_1(T\Sigma) = \chi(\Sigma) = 2-2\,g$. The factor of two comes from the fact that the Riemann-Roch theorem computes complex dimensions. This result shows that a non-vanishing correlator must have $2\,k$ more insertions

of χ operators than of ψ operators. These must come in equal numbers of holomorphic and anti-holomorphic versions of the operators.

Observables

Physical observables in a topological field theory must be defined by correlators of operators that are closed under the Q_A operation and must be topological themselves, in the sense that the worldsheet and target metrics must not be involved in their construction. One can thus not use the ψ's, since they contain a worldsheet Lorentz index that needs to be contracted with the metric. Local operators are therefore of the form

$$\mathcal{O}(x) = C_{i_1 \dots i_p \bar{j}_1 \dots \bar{j}_q}(\phi(x)) \chi^{i_1 \cdots} \chi^{i_p} \chi^{\bar{j}_1 \cdots} \chi^{\bar{j}_q} \,, \tag{3.15}$$

where C is a function of the ϕ's, and is antisymmetric in its indices due to the fact that it is contracted with Grassmann variables. Here, x is the worldsheet position of the operator insertion. By using the transformation rules in (3.10), one easily sees that the variation of such an operator is the following:

$$\{Q_A, \mathcal{O}(x)\} \simeq \frac{\partial C_{i_1 \dots i_p \bar{j}_1 \dots \bar{j}_q}(\phi(x))}{\partial \phi^{\bar{k}}} \chi^{\bar{k}} \chi^{i_1 \cdots} \chi^{i_p} \chi^{\bar{j}_1 \cdots} \chi^{\bar{j}_q} + \frac{\partial C_{i_1 \dots i_p \bar{j}_1 \dots \bar{j}_q}(\phi(x))}{\partial \phi^{k}} \chi^{k} \chi^{i_1 \cdots} \chi^{i_p} \chi^{\bar{j}_1 \cdots} \chi^{\bar{j}_q} \,. \tag{3.16}$$

In other words, if one views $C(\phi(x))$ as a (p, q) form on X, then

$$\{Q_A, \mathcal{O}_C\} \simeq \mathcal{O}_{dC} \,, \tag{3.17}$$

where dC is the de Rham exterior derivative on C. One can identify (by a group isomorphism) the Q_A cohomology of physical operators with the de Rham cohomology of X, by viewing the χ^i as holomorphic differentials $d\phi^i$ and the $\chi^{\bar{i}}$ as the anti-holomorphic ones $d\phi^{\bar{i}}$:

$$H(Q_A) = H_{dR}(X) \,. \tag{3.18}$$

The result in the previous subsection prescribes that a correlator is only non-vanishing if one inserts a certain number of χ's and ψ's, whereby the difference in the numbers is given by

$$2\,k = 2 \int_\Sigma \Phi^* c_1(TX) + 2\,d\,(1-g) \,. \tag{3.19}$$

The theorem only gives a difference, it does not tell one how many ψ's are needed. The following will be restricted to the 'generic' case, when $\dim H^1(\Phi^*(TX)) = 0$. This is the case, if one makes no ψ-insertions, and those were excluded earlier on. The reader interested in a more general treatment will find a carefully chosen list of references at the end of section 3.2. One is studying correlators of the form

$$\langle \mathcal{O}_1 \dots \mathcal{O}_n \rangle = \int \mathcal{D}[\Phi] \mathcal{D}[\chi] \mathcal{D}[\psi]\, e^{-S}\, \mathcal{O}_1 \dots \mathcal{O}_n \tag{3.20}$$

(n-point functions) with $\mathcal{O}_i \in H^{(p_i,q_i)}(X)$. The analysis of anomalies presents a set of selection rules for non-trivial correlators, which thus contain the interesting information encoded by the model. The vector anomaly cancellation rule gave $\sum_{i=1}^n p_i = \sum_{i=1}^n q_i$, and this, combined with the axial anomaly cancellation, means $k = \sum_{i=1}^n p_i = \sum_{i=1}^n q_i$ with k given by the Riemann-Roch calculation.

Holomorphic maps from genus zero and genus one worldsheets

As this is a TFT, it is important to stress that one is working with a *fixed* genus g worldsheet Σ_g. More precisely, one is actually considering a Riemann surface with n punctures at positions $x_i \in \Sigma_g$, where one inserted the operators $\mathcal{O}_i$. From (3.10), one sees that one can rewrite correlators (3.20) as

$$\sum_{\beta \in H_2(X,\mathbb{Z})} e^{-tK\cdot\beta} \int_{[\Phi(\Sigma)]\in\beta} \mathcal{D}[\Phi]\mathcal{D}[\chi]\mathcal{D}[\psi]\, \mathcal{O}_1 ... \mathcal{O}_n\, e^{-i\,t\int\{Q_A,V\}}\,. \tag{3.21}$$

According to what was said above, the path integrals will localize on holomorphic maps. The basic idea now will be to 'pull the path-integral back' on to the space of all such holomorphic maps. Therefore, define a moduli space of holomorphic maps from the fixed genus g Riemann surface (the worldsheet) Σ_g into curve class β, $\mathcal{M}_{\Sigma_g}(X,\beta)$,

$$\mathcal{M}_{\Sigma_g}(X,\beta) := \{\phi : \Sigma_g \to X \quad \big| \quad \phi_*[\Sigma_g] = \beta \in H_2(X,\mathbb{Z}) \quad \text{and} \quad \bar\partial\phi = 0\}. \tag{3.22}$$

Note that a point in this moduli space is a holomorphic map, ϕ. In order to evaluate observables, one would like to construct a measure of integration on this space. A measure is given by the tangent directions. The basic idea is to deform the image of a point ϕ (this is a curve in X) and then study the pull-back of this. By doing this, one reaches a new map in moduli space, which should again be holomorphic. This means, that from the Calabi-Yau point of view, one has moved in a direction lying in $T^{(1,0)}X$. Recall that $\chi \in \phi^*(T^{(1,0)}(X))$. The link between the χ's and the tangent directions sought is clear from this, but it can be made more concrete. Taking a supersymmetry variation of the original map (the bosonic worldsheet scalar), one gets something proportional to χ: $\delta\phi^i \propto \chi^i$. If one requires this deformation to be holomorphic, one gets the zero mode equation $\bar\partial\chi^i = 0$. The reader can read this up in detail in [81]. Therefore, one can conclude that the χ-zero mode directions can be identified with directions in $T\mathcal{M}_{\Sigma_g}(X,\beta)$, providing the desired volume measure on $\mathcal{M}_{\Sigma_g}$.

For each operator $\mathcal{O}_i$ one can now define an evaluation map on this moduli space of maps, ev_i, $(i = 1, ..., n)$,

$$\mathrm{ev}_i : \mathcal{M}_{\Sigma_g}(X,\mathbb{Z}) \to X, \quad \phi \to \phi(x_i). \tag{3.23}$$

In other words, an evaluation map ev_i sends every map ϕ (a point in $\mathcal{M}_{\Sigma_g}(X,\mathbb{Z})$ to its value $\phi(x_i)$ at the point of the insertion of the associated operator $\mathcal{O}_i$. This allows one to write the operator $\mathcal{O}_i$ as a pullback uner the evaluation map of a form on the CY $\omega_i \in H^*(X)$: $\mathcal{O}_i(x_i) = \mathrm{ev}_i^*(\omega_i)$.

One can now write a correlator (3.21) as a path-integral on the moduli space of holomorphic maps

$$\langle \mathcal{O}_1 ... \mathcal{O}_n \rangle = \sum_{\beta \in H_2(X,\mathbb{Z})} e^{-t\,K\beta} \int_{\mathcal{M}_{\Sigma_{g,n}}(X,\beta)} \mathrm{ev}_1^*(\omega_1) ... \mathrm{ev}_n^*(\omega_n). \tag{3.24}$$

The expression $\int_{\mathcal{M}_{\Sigma_{g,n}}(X,\beta)} \mathrm{ev}_1^*(\omega_1) ... \mathrm{ev}_n^*(\omega_n)$ evaluates to the number of holomorphic maps $N_{g,n}^{\beta}$ from the genus g Riemann surface with n punctures, $\Sigma_{g,n}$, into curve class β in the CY target space. In short,

$$\langle \mathcal{O}_1 ... \mathcal{O}_n \rangle = \sum_{\beta \in H_2(X,\mathbb{Z})} e^{-t\,K\beta} N_{g,n}^{\beta}. \tag{3.25}$$

Since the theory considered is cohomological, differentiating the path integral with respect to the Kähler parameter t yields zero[2]. Hence, one can safely take the $t \to \infty$ limit. In this limit, the dominant contributions come from the maps whose image belongs to the trivial class $\beta = 0$. In other words, maps for which the image of the worldsheet is homologous to a point. For these maps, one finds $\mathcal{M}_{\Sigma_g}(X, 0) \simeq X$ and $\mathrm{ev}_i = \mathrm{id}_i$. That means that one gets an integral over the target space CY. For the A-model TFT with a CY 3-fold as a target space, one can easily read off, that the selection rules require the insertion of a $(3, 3)$ total form degree. One thus obtains an integral of the CY volume form. At genus one, no insertion is needed to find a non-zero result, and one is left with the partition function (3.11). At higher genus, there are no insertions possible: higher correlators are zero.

One could analyze the B-model, much in the same way as the A-model in this section, but for the sake of brevity this will not be presented in this thesis.

3.1.3 A-model topological string theory and Gromov-Witten invariants

For the A-model TFT on a fixed genus g Riemann surface Σ_g, one found selection rules for the correlators, by analyzing the potential for anomalous R-symmetries. The sum of the holomorphic degrees of any operator insertions as well as the sum of the anti-holomorphic degrees must be equal to an expression depending on the (complex) target space dimension, the first Chern class and the genus of the worldsheet:

$$\begin{aligned} \sum_k \deg_{p_k} \mathcal{O}_k^{(p_k,q_k)} &= \int \phi^*(c_1(\mathcal{M})) + d(1-g), \\ \sum_k \deg_{q_k} \mathcal{O}_k^{(p_k,q_k)} &= \int \phi^*(c_1(\mathcal{M})) + d(1-g). \end{aligned} \tag{3.26}$$

[2]Only the cohomological part is t-independent. The part that is factored out certainly depends on it.

This meant that one only found non-vanishing correlators when using a TFT with a genus zero and a genus one worldsheet and a target space CY 3-fold. The basic reason for this was that the degree of the insertion (as seen as an element of the target space de Rham cohomology $H^*(X)$) corresponds to the axial charge of the worldsheet operator, hence one cannot make any 'negative' insertions. However, one will be able to make negative insertions, when allowing a path-integral over the worldsheet metric field. One thus couples the (twisted) topological sigma model to gravity and arrives at topological string theory, which is a 2d conformal field theory.

One can develop some more intuition behind why there were no holomorphic maps from punctured Riemann surfaces of genus $g \geq 2$ to the CY 3-fold X. When considering a TFT, one works with a fixed genus g Riemann surface, and, more importantly, also with a fixed complex structure class. It is not hard to imagine, that given a fixed complex structure class, the conditions for mapping n points on the puncture Riemann surface to n points on X simply overdetermine a holomorphic map. By varying the complex structure class however, one might be able to 'catch' the conditions for the mapping of these n points. Let this serve as a motivation to include a path-integral over all possible metrics on Σ_g.

When integrating over all possible metrics on a genus g Riemann surface, one is confronted with a problem of 'overcounting metrics' known from ordinary string theory. Schematically, one deals with a partition function of the form

$$Z = \sum_{\Sigma_g} \int \mathcal{D}[g_{\Sigma_g}] \int \mathcal{D}[\phi]\mathcal{D}[\chi]\mathcal{D}[\psi]\, e^{-\int_{\Sigma_g} L[g,\phi,\xi,\psi]}, \tag{3.27}$$

written out as a sum over genus g contributions and a path-integral over all metrics on a specific worldsheet Σ_g. Again, the contributions will localize on holomorphic map contributions. The integral over all metrics is interpreted as a sum over all genus g Riemann surfaces with all possible metrics. As the theory exhibits conformal gauge symmetry, one has to fix a conformal gauge on each Riemann surface, also requiring the introduction of ghost and anti-ghost fields, according to the Fadeev-Popov procedure. The procedure for topological string theory is very similar to the bosonic string, a different gauge has to be chosen for each complex structure class. The volume of the conformal group is then factored out, and one is left with an integral over the moduli space of complex structures $\mathcal{M}_g$ on every genus g Riemann surface. In fact, one can also use BRST quantization for the topological string. This procedure will not be included in this thesis, however the reader familiar with the bosonic string may use his knowledge on the latter quantization to serve his intuition. The reader interested in a treatment of these matters is referred to [82].

Integrating over the moduli space of complex structures

At each genus, one fixes a conformal gauge and is left to integrate over a representative metric in each complex structure class. This can be translated into an integral over the moduli space of complex structures. In order to find a measure on the moduli space

of complex structures $\mathcal{M}_g$, one will, just like one did for the moduli space of holomorphic maps, search for the tangent directions. For the following argument, any specific genus g surface Σ_g can be chosen.

Recall that an almost complex structure (in this case on a Riemann surface) is an endomorphism $J \in \mathrm{End}(T\Sigma_g)$ (i.e. $J \in T\Sigma_g \otimes T^*\Sigma_g$, or — put differently – J is a $(1,1)$-tensor) squaring to minus the identity, $J^2 = -\mathbf{1}$. Defining projections for vector fields onto their holomorphic and anti-holomorphic parts (with respect to the almost complex structure J) according to

$$P = \mathbf{1} - \frac{iJ}{2},$$
$$\bar{P} = \mathbf{1} + \frac{iJ}{2},$$

one can nicely formulate the condition for J to be a complex structure. For two vector fields X, Y on Σ_g, (using the Lie bracket for vector fields) the (integrability) condition reads

$$\bar{P}[PX, PY] = 0.$$

This can be shown to be equivalent to the vanishing of the Nijenhuis tensor

$$N[X,Y] = [JX, JY] - J[X, JY] - J[JX, Y] - [X, Y] = 0. \tag{3.28}$$

One can now consider an infinitesimal deformation of the complex structure, $J \to J + \epsilon$. In coordinates $(z, \bar{z})$ on Σ_g, the map $J : T\Sigma_g \to T\Sigma_g$ reads

$$J = \begin{pmatrix} i & 0 \\ 0 & -i \end{pmatrix}. \tag{3.29}$$

For an infinitesimal deformation, the equation $(J+\epsilon)^2 = -\mathbf{1}$ yields

$$\epsilon = \begin{pmatrix} 0 & \epsilon_1 \\ \epsilon_2 & 0 \end{pmatrix}. \tag{3.30}$$

The requirement that the Nijenhuis tensor vanishes for $J+\epsilon$ (for an infinitesimal variation) leads to the restrictions $\bar{\partial}\epsilon_1 = 0$ and $\partial\epsilon_2 = 0$. In other words, ϵ_1 is a $(0,1)$ form with values in $T^{(1,0)}\Sigma_g$; it only has off-diagonal components, so to be valued in the holomorphic tangent bundle, it has to be of type $(0,1)$. This means $\epsilon_1 \in \Lambda^{(0,1)}(T^{(1,0)}\Sigma_g)$, and, accordingly $\epsilon_2 \in \Lambda^{(1,0)}(T^{(0,1)}\Sigma_g)$. These tangent bundle valued forms are known as 'Beltrami differentials' in the literature, and they appear in the same way when studying bosonic string theory. They can be denoted as

$$\mu = \mu^{z}{}_{\bar{z}}(z)\partial_z d\bar{z},$$
$$\bar{\mu} = \mu^{\bar{z}}{}_{z}(\bar{z})\partial_{\bar{z}} dz. \tag{3.31}$$

As $\bar{\partial}\epsilon_1 = 0$ and $\partial\epsilon_2 = 0$, one learns from this, that deformations of the complex structure are classified by $H^{(0,1)}(\Sigma_g, T_{\mathrm{hol}}\Sigma_g)$ and $H^{(1,0)}(\Sigma_g, T_{\text{anti-hol}}\Sigma_g)$. The dimensions of these spaces is

of course the same, so in order to calculate the dimension of the moduli space, one can restrict to the holomorphic one. One can write $H^{(0,1)}(T^{(1,0)}\Sigma_g) = H^1_{\bar\partial}(T^{(1,0)}\Sigma_g) = H^1(T\Sigma_g)$, where the first equality is mere notation and the second equality follows from the Čech-Dolbeault isomorphism. To summarize, this means that the tangent space to the moduli space of complex structures reads $T\mathcal{M}_g = H^1(T\Sigma_g)$.

This allows the calculation of the dimension of this moduli space. From the Riemann-Roch formula one obtains

$$\begin{aligned}\chi(\Sigma_g, T\Sigma_g) &= \dim H^0(T\Sigma_g) - \dim H^1(T\Sigma_g),\\ &= \int_{\Sigma_g} \mathrm{ch}(T\Sigma_g)\,\mathrm{td}(T\Sigma_g),\\ &= \int_{\Sigma_g} (\dim_{\mathbb{C}} T\Sigma_g + c_1(T\Sigma_g))(1 + \frac{c_1(T\Sigma_g)}{2}),\\ &= \frac{3}{2}\int_{\Sigma_g} c_1(\Sigma_g) = \frac{3}{2}\chi(\Sigma_g) = 3(1-g).\end{aligned} \tag{3.32}$$

Generically (this turns out to be true for genus $g \geq 2$), $\dim H^0(T\Sigma_g) = 0$, thus $\dim(\mathcal{M}_g) = 3(g-1)$. This in fact singles out a three complex dimensional Calabi-Yau target space as the case where TST calculates non-trivial information (numbers of holomorphic maps) at every genus.

For completeness, a few comments on the two non-generic cases: the sphere $\Sigma_0 = S^2$ and the torus $\Sigma_1 = T^2$. For a sphere, $\dim H^0(T\Sigma_0) = 3$, which means that $\dim(\mathcal{M}_0) = 0$ (and not 3). For a torus, $\dim H^0(T\Sigma_1) = 1$, which means that $\dim(\mathcal{M}_1) = 1$.

The Beltrami differentials thus generically yield a basis for the tangent space $T\mathcal{M}_f$ to the moduli space of complex structures. A measure on moduli space is thus provided by the dual one forms, which one can denote by dm_i and $dm_{\bar\jmath}$. Additionally, at each genus, operators are included in order to cancel axial charge anomalies, as inevitably encountered when wanting to define non-vanishing correlators for topological field theories at genus $g \geq 2$. The next step is to construct such operators. Namely, this allows one to obtain a partition function at every genus. One has no Beltrami differentials at one's availability for the sphere, one for the torus, and $3(1-g)$ for genus $g \geq 2$. The crucial point is that each of these Beltrami differentials can be contracted with an operator of axial ghost number minus one – a fact again familiar from the quantization of the bosonic string. Such an operator with axial ghost number minus one is in fact provided by the worldsheet partner of the energy-momentum tensor,

$$T = \{Q, G\}. \tag{3.33}$$

As the energy-momentum tensor is traceless, one can write

$$G = \begin{pmatrix} G_{zz} & 0 \\ 0 & G_{\bar z\bar z} \end{pmatrix}. \tag{3.34}$$

This allows one to form

$$\beta_i = \int d^2z\, G_{zz}(\mu_i)_{\bar{z}}{}^z,$$
$$\beta_{\bar{j}} = \int d^2z\, G_{\bar{z}\bar{z}}(\mu_{\bar{j}})_z{}^{\bar{z}}, \tag{3.35}$$

for $i, \bar{j} = 1, ..., 3g-3$, and these expressions provide the operators for each genus, with the desired axial charge. Note that the product of all the constructed expressions has axial charge $6(1-g)$.

Topological free energy of the A-model

This allows the stating of a formal definition of the free energy of the topological string

$$F_g = \int_{\mathcal{M}_g} \prod_{i,\bar{j}=1}^{3g-3} dm_i dm_{\bar{j}} \langle \beta_i\, \beta_{\bar{j}} \rangle, \tag{3.36}$$

related to the topological string partition function as $\mathcal{Z}_{\rm top} = e^{F_{\rm top}}$. Introducing a topological string coupling constant λ, one can write the topological string free energy as a perturbative power series

$$F_{\rm top} = \sum_g \lambda^{2g-2} F_g. \tag{3.37}$$

The interpretation of what is calculated can be taken over from the discussion on topological field theory, directly, but the spectrum is of course a lot richer. The computations localize on holomorphic maps, and the number of such holomorphic maps at each genus, into a specific homology class $\beta \in H_2(X, \mathbb{Z})$ are topological invariants, called Gromov-Witten invariants.

Gromov-Witten invariants N_g^β count maps ϕ from a given worldsheet Σ_g of genus g to a curve $\phi(\Sigma_g) \subset X$ in the (integral) spacetime homology class β. They have been conjectured to be rational, most generally, and form an example of a set of topological invariants associated to the Calabi-Yau X and computed by the A-model. Using Gromov-Witten (GW) invariants, the topological free energy of the A-model can be written as

$$F_{GW}(\lambda, q) = \sum_{g \geq 0} \sum_{\beta \in H_2^+(X)} \lambda^{2g-2} N_g^\beta q^\beta, \tag{3.38}$$

acquiring contributions from every worldsheet genus in analogy to ordinary string theory, and one sums over 'positive' elements of the second cohomology $H^2_+(X)$ (cycles with a positive coefficient). This can be interpreted as a sum over worldsheet instantons with amplitudes

$$q^\beta := e^{2\pi i \beta_A t^A}. \tag{3.39}$$

Contributions from genus g Riemann surfaces embedded in the CY X are weighted by their complex spacetime image area $e^A = q$, and multiplied with the appropriate number of maps.

Splitting the 'Gromov-Witten expansion of the topological string free energy' into the contributions arising from each genus,

$$F_{GW} = \frac{1}{\lambda^2} F_0 + F_1 + \sum_{g \geq 2} \lambda^{2g-2} F_g, \tag{3.40}$$

and splitting the contributions at each genus g into the contributions arising from different curve classes.

$$F_g = F_g^{\beta=0} + F_g^{\beta=1} + \sum_{\beta \geq 2} F_g^{\beta},$$

it is illustrative to see how things already discussed in this thesis fit. The constant map contributions – the ones where the whole genus g Riemann surface is mapped to a point in the CY – are dominant when studying a CY at large volume.

The genus zero constant map term and thus the Gromov-Witten invariant N_0^0 reads $F_0^{\beta=0} = \frac{D_{ABC}}{6} t^A t^B t^C$, where $D_{ABC} = \int_X J_A J_B J_C$, and t^A denote the (complexified) Kähler moduli of the Calabi-Yau X. At genus one, the constant map term is found to be $F_1^{\beta=0} = \int \frac{c_{2A} J}{24} t^A$, using $c_{2A} = \int_X J_A \cdot c_2(X)$. All other terms arise from worldsheet instantons and are thus non-perturbative in α'. To accentuate this, one can write

$$F_{\text{top}} = \ln(\mathcal{Z}_{\text{top}}) = \frac{1}{6\lambda^2} D_{ABC} t^A t^B t^C - \frac{1}{24} c_{2A} t^A + F_{\text{non-pert}}. \tag{3.41}$$

A comparison of (3.41) with the prepotential (1.61) of the CY X is striking: topological string theory computes the prepotential including quantum corrections. The first two terms appearing in (3.41) are the classical terms, which are perturbative in α'. The rest of the series is non-perturbative in the worldsheet (it arises from worldsheet instantons) as is indicated by the subscript. Such a perturbative expansion (in the topological string coupling) becomes the more accurate to calculate a prepotential, the closer one gets to the large radius limit of a Calabi-Yau compactification.

3.2 The Donaldson-Thomas partition function: D6-D2-D0 states

Clearly, the expansion of the topological free energy is perturbative in the topological string coupling. The complete topological free energy F_{top} is not known. This is archetypical for the situation in modern quantum field theories, but this is a particularly nice example, as one does not seem to be that far away from understanding the non-perturbatively complete free energy. In fact, it seems that one knows three different asymptotic series, approximating F_{top}. All three series are divergent everywhere, but two resummations, one of which will

be discussed in this section, do render parts of the Gromov-Witten series finite. Knowledge of the exact free energy is sometimes referred to as knowing the non-perturbative completion of the topological string. The three asymptotic series approximating the topological string free energy compute different sets of topological invariants associated to a Calabi-Yau manifold with interesting physical interpretations, each. The first set were the Gromov-Witten invariants counting worldsheet instantons. The second series is known as the Gopakumar-Vafa form, which is not of any further relevance in this thesis. The third form shall be presented now, and is known as the Donaldson-Thomas form of the topological string partition function.

This leads to the discussion of the Donaldson-Thomas invariants and the associated expansion of the topological free energy. Again, the identification with the topological free energy is conjectural at this stage, but a lot of evidence has been found in recent years. Donaldson-Thomas invariants were originally discovered in the context of pure algebraic geometry, and were conjectured to be related to the Gromov-Witten invariants in [83, 84], through $F_{\mathrm{GW}} = F_{\mathrm{DT}}$. Mathematically, they can be rigorously formulated as invariants counting ideal sheaves, however they will be treated from a physical point of view in this thesis. A more recent connection also with the Gopakumar-Vafa resummation of the topological free energy can be well illustrated using the the discoveries from [85].

Heuristic definition of Donaldson-Thomas invariants

Donaldson-Thomas invariants associated to a CY X can be understood in (at least) two complementary ways: As objects counting curves and points, which correspond to D2 and $\overline{\mathrm{D0}}$-branes on the D6 (or $\overline{\mathrm{D6}}$) wrapped on X, or as the Witten indices of the worldvolume gauge theory on the latter. More precisely, the invariant $N_{\mathrm{DT}}(\beta, n)$ computes the Witten index of a system with a D2 brane wrapping a curve of homology class β, and a collection of $\overline{\mathrm{D0}}$'s, such that the total D0 charge equals n. Although the U(1) flux on the D6 interacts with these lower branes, it does not alter the Witten index. In mathematical terms, the DT invariants compute the dimensions of the moduli spaces of the ideal sheaves corresponding to curves and points on the Calabi-Yau. They are indeed conjectured [83, 84] to contain equivalent information to the Gopakumar-Vafa invariants [86, 87], which count the states of M2 branes with momentum, where the M2's are wrapped on holomorphic curves. These ideal sheaves, just as ordinary Born-Infeld flux, will induce lower brane charges. Alternatively, one can think of these sheaves literally as lower dimensional brane charges. Depending on whether one is using an ideal sheaf or a dual ideal sheaf, the induced D2 charge will be dual to some curve class $\mp\beta$ (i.e. it is a $\overline{\mathrm{D2}}$ or a D2), where $\beta \in H^4(X, \mathbb{Z})$, and the D0 charge will be dual to $n\,\omega$, where

$$n = -\tfrac{1}{2}\,\chi(C_\beta) + N\,, \tag{3.42}$$

whereby $\chi(C_\beta)$ is the ordinary Euler number of the curve in the homology class β, N is the number of point-like $\overline{\mathrm{D0}}$'s, and ω is the volume-form of the CY.

The other way to view these invariants, is by treating the worldvolume gauge theory on the D6-brane as follows. It is known, that the Born-Infeld theory on a D6-brane is simply the reduction of $\mathcal{N} = 1$, $d = 10$ SYM on $\mathbb{R}^{4,1} \times X_{CY}$ down to X_{CY}. This yields a maximally supersymmetric ($\mathcal{N} = 2$) $d = 6$ SYM theory on the Calabi-Yau. However, because a (proper) Calabi-Yau manifold only admits one covariantly constant spinor, the theory is automatically topologically twisted. Nekrasov et al. [88] devised a trick to compute the path integral of this Euclidean 6d topological theory. By introducing a non-commutative deformation, this gauge theory now supports 'small' instantons with vanishing first Chern class, but non-vanishing second Chern character, which cannot exist in an ordinary Abelian gauge theory. The size of these instantons is a modulus, just like that of non-Abelian instantons in 4d. One can then show that the path integral of the non-commutative theory localizes on instantons of zero 'thickness', i.e. on instantons localized on holomorphic curves and points. The Donaldson-Thomas partition function is conjectured to be the Witten index of this theory [88]. One also expects this partition function to remain unchanged after turning the non-commutative deformation off. Keeping this in mind, one can view the GW-DT 'correspondence' as an open-closed duality, relating a theory of closed strings, given by the GW interpretation, to a theory of open strings on a D-brane, described by a worldvolume gauge theory at low-energy, leading to the DT interpretation of the topological string.

One can write the DT partition function $\mathcal{Z}_{\mathrm{DT}} = e^{F_{\mathrm{DT}}}$ as a generating function:

$$\mathcal{Z}_{DT}(u, v) = \sum_{\beta,n} N_{\mathrm{DT}}(\beta, n) u^n v^\beta =: \mathcal{Z}_{DT}^{\beta=0} \cdot \mathcal{Z}_{DT}^{'}. \tag{3.43}$$

Making the identification of variables $u = e^{\pm i\lambda}$ and $v = e^{2\pi i t}$, it is conjectured to be related to the GV form by

$$\begin{aligned} \mathcal{Z}_{DT}^{\beta=0} &= (\mathcal{Z}_{GV}^{\beta=0})^2, \\ \mathcal{Z}_{DT}^{'}(u, v) &= \mathcal{Z}_{GV}^{'}(-u, v). \end{aligned} \tag{3.44}$$

The MacMahon form of the GV partition function is already very suggestive of a D-brane world-volume gauge theory interpretation, and one can for instance read off the $\beta = 0$ part to be

$$\mathcal{Z}_{DT}^{\beta=0} = \sum_n N_{DT}(0, n) u^n = \prod_{k=1}^{\infty} (1 - (-e^{\pm i\lambda k}))^{-k\chi(X)}. \tag{3.45}$$

This should count D6-D0 states, and this function can indeed be retrieved by counting D0 particles in a D6 background. Similarly, it can be shown how to reproduce the form of $\mathcal{Z}_{DT}^{'}$ by counting D6-D2-D0 BPS states, check [1] and [80]. There is a strong connection between 4d BPS black hole degeneracies and the Donaldson-Thomas form of the topological string partition function. This is discussed in the next section.

3.3 Split brane states, flow trees and topological invariants

After a decline in the original interest in topological string theory, it saw a big revival in 2004, when a truly stunning conjecture by Ooguri, Strominger and Vafa (OSV) entered the stage, [89]. The OSV conjecture relates a BPS black hole partition function in type II string theory in 4d to the topological string partition function, $\mathcal{Z}_{\rm BH} \sim |\mathcal{Z}_{\rm top}|^2$. Between 1998 and 2001, a series of papers appeared, [90–97], which refined the predictions of black hole entropy by investigating the BPS black holes and the attractor mechanism including higher derivative corrections to the action. These corrections to black hole entropy were the main inspiration for the OSV conjecture, making a far-reaching conjecture about the correspondence between entropies as calculated in supergravity and microscopic statistical entropies. The black hole partition function is (formally) understood to arise from a mixed ensemble that is now concretely chosen to be in a type IIA setup, with magnetic and electric (p, q) charges. While the magnetic charge p is kept fixed, it arises as a sum over all electric charges of the form

$$\mathcal{Z}_{\rm BH}(\phi, t_\infty) = \sum_q \Omega(p, q; t_\infty)\, e^{2\pi\phi^\Lambda q_\Lambda}, \tag{3.46}$$

where ϕ^Λ denote electric potentials (Legendre transforms of the electric charges) and $\Omega(p, q; t_\infty)$ is an index enumerating the number of BPS states with charge (p, q) and Kähler background moduli t_∞.

3.3.1 The OSV conjecture: $\mathcal{Z}_{\rm blackhole} \sim |\mathcal{Z}_{\rm top}|^2$

The OSV conjecture can be stated in the two forms

$$\Omega(p, q; t_\infty) \sim \int d\phi\, e^{-2\pi\phi^\Lambda q_\Lambda} |\mathcal{Z}_{\rm top}|^2, \tag{3.47}$$

$$\mathcal{Z}_{\rm BH}(\phi, t_\infty) \sim |\mathcal{Z}_{\rm top}(g_{\rm top}, t)|^2, \tag{3.48}$$

where the topological string coupling and the Kähler moduli appearing in the topological string partition function depend on the values of the electric potential and the magnetic charges through

$$g_{\rm top} = \frac{4\pi i}{X^0} = \frac{4\pi}{2I^0{}_\Lambda \phi^\Lambda + i p^0}, \qquad t^A = \frac{2I^A{}_\Lambda \phi^\Lambda + i p^A}{2I^0{}_\Lambda \phi^\Lambda + i p^0}, \tag{3.49}$$

and $I^{\Lambda_1}{}_{\Lambda_2}$ denotes the symplectic intersection form between magnetic and electric charges introduced earlier on.

Many studies have been performed on the OSV conjecture since 2004. A large number of them focused on non-compact (local) CY manifolds, a number of studies have also been performed model independently, [98–101], and there are specific studies on compact CY

manifolds, [80, 102] and specifically on $K3 \times T^2$ or T^6 in [103]. Of specific interest for this thesis however is the very detailed study performed in [1], using split flow trees. This paper was the main inspiration for many of the studies presented in this thesis.

The OSV conjecture as originally formulated leaves many open questions. Among these is the issue, that $\mathcal{Z}_{\rm top}$ is only known through the asymptotic approximations, discussed above. This means that the OSV conjecture as it stands now can only hold approximately. Additionally, the regime of validity was not clear. Furthermore, the studies in [1,80,102,103] detected an extra measure factor $\mu = \frac{e^{-K}}{g_{\rm top}^2}$ in the formula for BPS indices $\Omega(p,q;t_\infty) \sim \int d\phi\, \mu\, e^{-2\pi\phi^\Lambda q_\Lambda} |\mathcal{Z}_{\rm top}|^2$.

3.3.2 Split states, flow trees and index factorization

In [1] by Denef and Moore, factorization of the integrand in

$$\Omega(p,q;t_\infty) \sim \int d\phi\, \mu\, e^{-2\pi\phi^\Lambda q_\Lambda} |\mathcal{Z}_{\rm top}|^2$$

results from the fact that all D4 indices can be expressed in terms of a finite number of polar indices, which do not form single centered black holes, but can be described by D6-$\overline{D6}$ bound states. The factorized indices for such polar states, developed in [1], are explained in part 3.3.3. In a suitable limit, these D6(-D4-D2-D0) BPS states are counted by Donaldson-Thomas invariants. If there were a perfect one-to-one map between all polar states and all possible pairs of single D6 and single $\overline{D6}$ states in which they are counted by DT invariants, this would lead to a complete proof of the OSV conjecture. However, not all polar states turned out to be realized as single D6-$\overline{D6}$ bound states. This realization only holds for sufficiently polar states. Using $(\hat{q}_0)_{\rm max}$ to denote the reduced D0-brane charge of the most polar state, one can introduce

$$\eta = \frac{(\hat{q}_0)_{\rm max} - \hat{q}_0}{(\hat{q}_0)_{\rm max}} \tag{3.50}$$

to label 'how polar' a state is. Obviously, $\eta = 0$ for the most polar state, polar states satisfy $0 \leq \eta \leq 1$, and for non polar states $\eta > 1$. One of the findings in [1] is, that an approximate factorization can be proved, when dropping all polar states with $\eta > \eta^*$, and much of [1] was devoted to finding out how large η^* can be taken.

Originally, the OSV conjecture was intended to hold at weak topological string coupling. The derivation of [1] however gives an approximate and refined OSV formula, holding at strong topological string coupling. The derivation relies on the two following conjectures.

- *The split attractor flow conjecture:* details on this conjecture were presented in section 2.3. It is well founded, although, according to the discussion in the previous chapter, there might be shortcomings in connection with scaling solutions. This conjecture is also at the 'core' of this thesis, and will be put to non-trivial tests in the research presented in the next chapter.

- *The extreme polar state conjecture:* this conjecture states that all polar states with $\eta < \eta^*$ can be realized as single D6-$\overline{\text{D6}}$ pairs with the constituent charges close to the constituents of the most polar state, a pure fluxed D6 and a pure $\overline{\text{D6}}$.

Assuming the former two conjectures hold true, and dropping polar states with $\eta > \eta^*$, they arrive at an approximate, refined OSV formula

$$\Omega(p,q;t=i\infty) = \int d\phi\, \mu e^{-2\pi q_\Lambda \phi^\Lambda} |\mathcal{Z}^\epsilon_{\text{top}}|^2 e^{\delta\mathcal{F}} \tag{3.51}$$

using an appropriate cutoff $\mathcal{Z}^\epsilon_{\text{top}}$ of the divergent Donaldson-Thomas partition function, and the substitutions

$$g_{\text{top}} = \frac{2\pi}{\phi^0}, \quad t^A = \frac{1}{\phi^0}(\phi^A + i\frac{P^A}{2}). \tag{3.52}$$

Note that the background in (3.51) was chosen to be $t = i\infty$. For further details on the cutoff of the DT partition function and a detailed error analysis, the reader is referred to the original reference. The next paragraph summarizes some important formulae developed in [1], which will be important in the following chapters.

3.3.3 Factorized wall-crossing indices for polar states

The conventions for the total charge vectors for D6 and $\overline{\text{D6}}$-branes used in this thesis come about as follows. The general formula for the induced charges on a D-brane (due to the WZ term in the Born-Infeld action) wrapped on a (sub)-manifold W is the following:

$$S^{\text{Dbrane}}_{W,C} = 2\pi \int_W C \wedge e^{-B} \operatorname{Tr} e^F \sqrt{\frac{\widehat{A}(TW)}{\widehat{A}(NW)}}, \tag{3.53}$$

where $\widehat{A}$ is the A-roof characteristic class, TW the tangent bundle of the brane, and NW its normal bundle.

In the case that will be of interest in this thesis, that of a D6-brane carrying U(1)-flux with field-strength F_1, a $\overline{\text{D2}}$ of class $-\beta_1$ and N_1 $\overline{\text{D0}}$'s, the above formula yields the following polyform:

$$\Gamma_{D6} = e^{F_1}\left(1 - \beta_1 - (\tfrac{1}{2}\chi(C_{\beta_1}) + N_1)\,\omega\right)\left(1 + \frac{c_2(X)}{24}\right), \tag{3.54}$$

where $\beta \in H^4(X,\mathbb{Z})$, and $c_2(X)$ is the second Chern class of the tangent bundle of the CY threefold X. Similarly, a $\overline{\text{D6}}$ with flux F_2 will bind to a D2 of class β_2 and N_2 $\overline{\text{D0}}$'s to give the following total charge vector:

$$\Gamma_{\overline{\text{D6}}} = -e^{F_2}\left(1 - \beta_2 + (\tfrac{1}{2}\chi(C_{\beta_2}) + N_2)\,\omega\right)\left(1 + \frac{c_2(X)}{24}\right), \tag{3.55}$$

The modification with respect to the general formula is the addition of D2 and D0 charge in the form of sheaves, which can be thought of as generalizations of bundles (U(1) fluxes).

Notice that the D6 will bind with a $\overline{\text{D2}}$, the $\overline{\text{D6}}$ with a D2, but both will bind to $\overline{\text{D0}}$'s.

In the research presented in the next chapter, the goal was to enumerate numbers of D4-D2-D0 BPS states using the D6 / $\overline{\text{D6}}$ tachyon condensation picture and split flow trees. To derive the results presented in section 4.2, the index for D4-D2-D0 BPS states of total charge Γ from [1] will be used,

$$\Omega(\Gamma) = \sum_{\Gamma \to \Gamma_1 + \Gamma_2} (-1)^{|\langle \Gamma_1, \Gamma_2 \rangle| - 1} |\langle \Gamma_1, \Gamma_2 \rangle| \, \Omega(\Gamma_1) \, \Omega(\Gamma_2), \tag{3.56}$$

with the sum running over all possible first splits $\Gamma \to \Gamma_1 + \Gamma_2$, belonging to a full split flow tree, and $\langle \Gamma_1, \Gamma_2 \rangle$ is the symplectic intersection of the two charges, as defined previously. The microscopic logic behind this formula is that all degrees of freedom in a D6/$\overline{\text{D6}}$ can be factorized as the degrees of freedom on the gauge theories of the D6 and $\overline{\text{D6}}$ plus the degrees of freedom of the tachyon field, that are counted by the intersection product. As shall be presented, this formula will need some refinement in general, when seeking exact results. To evaluate the number of states for the two building blocks after the first split, Donaldson-Thomas invariants for specific CY's will be used, which may naively just be interpreted as counting the number of D6-D4-D2-D0 BPS states. A split will contribute a term to the index of the D4 system as follows:

$$\Delta\Omega(\Gamma_{D4}) = (-1)^{|\langle \Gamma_{D6}, \Gamma_{\overline{\text{D6}}} \rangle| - 1} \, |\langle \Gamma_{D6}, \Gamma_{\overline{\text{D6}}} \rangle| \, N_{\text{DT}}(\beta_1, n_1) \, N_{\text{DT}}(\beta_2, n_2) \, , \tag{3.57}$$

where

$$n_i = \tfrac{1}{2} \, \chi(C_{\beta_i}) + N_i \, . \qquad (i = 1, 2) \tag{3.58}$$

The full index for the D4 will then be constructed by adding up all possible contributions of this form. In the studies presented later on however, this does require care, as it is not always trivial whether one is enumerating the D6-D2-D0 BPS states in the background where indeed N_{DT} yields the correct number of states.

3.4 Mirror symmetry for Calabi-Yau manifolds

This section presents a symmetry closely linked to topological strings, and important for the research presented in the next chapter. Whereas for IIA compactifications, the prepotential of a CY 3-fold X, and thus the topological free energy are determined by quantum geometry, they are determined classically for the IIB side. Mirror symmetry relates IIA string theory on X to IIB string theory on a mirror CY Y. Therefore it is clear that mirror symmetry is relevant to understanding the relationship between black hole entropy and topological strings. Mirror symmetry is one of the essential tools used in the research presented in chapter 4, which is essentially an enumeration of D-particle BPS states (a low-charge 'cousin' of a BPS black hole) by using split flows to establish existence of split states, and enumerating the centers using invariants computed by the topological string.

To be more precise, one should state that mirror symmetry is not generally proven, but it has more of the status of a conjecture, that has however been put to numerous tests and has received substantial evidence. From a purely mathematical point of view, it associates to every Calabi-Yau X a so-called mirror Calabi-Yau Y with a 'mirror Hodge diamond', $H^{(3-p,q)}(X) = H^{(p,q)}(Y)$. This means in particular that $h^{(1,1)}(X) = h^{(2,1)}(Y)$, and vice versa. From the viewpoint of physics one can go further and state mirror symmetry as the equivalence of a type IIA string theory compactified on X, and a type IIB string theory compactified on the mirror Y. This is a highly non-trivial observation, given the fact that from a classical point of view on geometry, X and Y are very different. One illustration of this is the difference in sign of their Euler characteristics $\chi(X) = -\chi(Y)$.

Mirror symmetry maps the Kähler moduli space of X to the complex structure moduli space of Y and vice versa. In the light of the preceding discussion on these moduli spaces, the reader will certainly be struck by such revolutionary ties between two very different setups: mirror symmetry relates classical geometry (on the complex structure side) to quantum geometry (on the Kähler side). More specifically, the prepotential of the Kähler moduli space F is an object which in general receives an infinite sum of quantum corrections, and it can be calculated from the mirror classical geometry. Translated to topological strings, this statement means that the classical periods of the mirror CY Y contain information about holomorphic curves of X, and also, according to the different interpretations of topological strings, about BPS states on CY 3-folds.

Mirror symmetry exemplified: the quintic threefold

Mirror symmetry will now be discussed by using a simple example: an algebraic Calabi-Yau variety, the quintic threefold. This makes sense as a substantial amount of research performed by the author was carried out using the quintic. The statements made for the quintic become more involved for other Calabi-Yau's, but the mechanism is the same, essentially. In particular, the other CY's used in this thesis are also one-modulus CY's embedded in weighted projective spaces, and the generalizations to these cases should become quite obvious. Most of the following material follows the famous paper of Candelas, de la Ossa, Green and Parkes from 1990, [104].

The quintic X

This paragraph begins by stating some basic features of the quintic. The reader can find a more general treatment in the appendix, section A.1. The quintic X is an algebraic variety. It is defined as the zero locus of a quintic polynomial in $C\mathbb{P}^4$. The ambient space $C\mathbb{P}^4$ can be covered with homogeneous coordinates $(x_1 : x_2 : x_3 : x_4 : x_5)$, and one can write a quintic polynomial as

$$p_X = a_1 x_1^5 + a_2 x_2^5 + a_3 x_3^5 + a_4 x_4^5 + a_5 x_5^5 + q^{(5)}(x) = 0, \tag{3.59}$$

with $q^{(5)}$ a general degree five polynomial involving monomials mixed in the coordinates x_i. The quintic has one Kähler modulus and 101 complex structure moduli. The one-form

on $C\mathbb{P}^4$, generating the second cohomology and Poincaré dual to a hyperplane (in this case the quintic), descends to the single generator of $H^{(1,1)}(X)$ [3]. Both the form on X and on the ambient space will be denoted by H. The cohomology class H on X will also be referred to as the hyperplane class. To study low charge D-brane BPS states, one will wrap a D4 brane on a cycle (or a formal sum of cycles) in the Poincaré dual 4-cycle PD$[H]$. These are divisors described by a linear equation such as $x_1 = 0$. Of course, one could also consider higher classes such as H^n. A corresponding divisor would then be given by a degree n polynomial.

According to the adjunction formula (note that $H^4 = 0$),

$$c(X) = \frac{c(C\mathbb{P}^4)}{c(\mathcal{O}(5))} = \frac{(1+H)^5}{1+5H} = 1 + 10H^2 - 40H^3, \tag{3.60}$$

where $\mathcal{O}(5)$ is the normal bundle N_X of X. Of course, by using the adjunction formula one can see that in order to obtain a CY ($c_1(X) = 0$), one has to choose a quintic polynomial to describe an appropriate hypersurface in $C\mathbb{P}^4$, as $c(C\mathbb{P}^4) = c(X)c(\mathcal{O}(5))$. Using the intersection number $\int_X H^3 = 5$ (check A.1), one obtains the Euler character by integrating over the top Chern class

$$\chi(X) = \int_X c_3(X) = -40 \int_X H^3 = -200, \tag{3.61}$$

and from the Hodge diamond of a CY, (A.1), one can see that $2(h^{(1,1)} - 2h^{(2,1)}) = -200$, which is consistent with earlier statements.

The mirror quintic Y

One way to represent the mirror quintic is again as a hypersurface within $C\mathbb{P}^4$, given as a quotient of the set described by the zero locus of the following quintic polynomial:

$$p_Y = a_1 x_1^5 + a_2 x_2^5 + a_3 x_3^5 + a_4 x_4^5 + a_5 x_5^5 - 5\psi x_1 x_2 x_3 x_4 x_5 = 0. \tag{3.62}$$

As mentioned earlier, Kähler and complex structure moduli are exchanged, and correspondingly $h^{(1,1)}(Y) = 101$ and $h^{(2,1)}(Y) = 1$. Note that the quintic equation is in this case in principle determined up to six parameters, $(a_1, ..., a_5, \psi)$, but a coordinate transformation, an element in $P\mathrm{GL}(5, \mathbb{C})$ will set the a_i to one, if one wishes to do so. There is thus only one parameter ψ in (3.62), which can be interpreted as the complex structure modulus of Y. Such a quintic is preserved under certain rescalings. Namely, one can consider the operation $x_i \to \lambda^{k_i} x_i$, where e.g. $\lambda = e^{\frac{2\pi i}{5}}$ is a fifth root of unity and $\sum_i k_i = 0 \pmod 5$. For the corresponding group G, operating on the locus where Y resides, using the notation $g = (k_1, k_2, k_3, k_4, k_5)$, where g acts as $x_i \to \lambda^{k_i} x_i$, it is clear that one can e.g. choose the

[3] This is not generally true, but it generically works for CY's with a low number of Kähler moduli.

following generators

$$\begin{aligned} g_1 &\doteq (1,0,0,0,4), \\ g_2 &\doteq (0,1,0,0,4), \\ g_3 &\doteq (0,0,1,0,4), \\ g_4 &\doteq (0,0,0,1,4). \end{aligned}$$

At first sight, one might be tempted to conclude that this group is $(\mathbb{Z}_5)^4$, but one must not forget the projective rescaling of $C\mathbb{P}^4$. The successive action of all these generators $\prod_i g_i$ introduces an overall phase in front of all the x_i's, leaving the possibility to be undone by a rescaling of the homogeneous coordinates, so three generators suffice. The group is therefore $G = (\mathbb{Z}_5)^3$, and the correct statement is to define the mirror quintic as the quotient of the zero locus of (3.62) by $(\mathbb{Z}_5)^3$.

This group has fixed points, which means that this is not precise, yet. In fact one should blow up the resulting singularites, each of which will then contribute to the Euler number of Y, which can be calculated to be $+200$ (this is $-\chi(X)$). This results in a generically smooth space, but this is not important in the present context. Furthermore, this is not the only possbility to present the mirror quintic. It can also be embedded as a degree 256 hypersurface in $WC\mathbb{P}^4_{41,48,51,52,64}$ or as a degree 320 hypersurface in $WC\mathbb{P}^4_{51,60,64,65,80}$, [26], having the advantage that one does not have to take a quotient, but it leads to a bit more complicated numerics.

In fact, ψ is not quite a good variable for the complex structure modulus, because transformations $\psi \to \lambda\psi$ with λ again denoting a fifth root of unity, are equivalent to a coordinate transformation of the form $x_i \to \frac{1}{\lambda}x_i$ (for any one i). Thus, only ψ^5 is an unambiguous coordinate on the complex structure moduli space.

The Picard-Fuchs equations

The essential strength of mirror symmetry is, that it allows one to map difficult problems in quantum geometry, typically encountered in IIA string theory compactifications, to problems of classical geometry, typically in IIB compactifications. In the latter case, the periods of the holomorphic three-form are exact and determine the prepotential. These periods are solutions to a set of differential equations, called the *Picard-Fuchs equations*. A brief derivation will be given for the quintic, and this will be supplemented with a general formula for a certain class of hypersurfaces in weighted projective spaces.

Define the $(4,0)$ form Θ on $C\mathbb{P}^4$ by $\Theta = \frac{1}{p}\sum_{i=i}(-1)^i dx_1 \wedge dx_2 \wedge ...x^i... \wedge dx_5$ (the form dx_i has been replaced by x_i). One considers $\frac{1}{p}$ as a prefactor with a quintic polynomial p, which renders the form well defined on $C\mathbb{P}^4$, except at the locus where it becomes singular, namely on the quintic Y. Now, one chooses $p = p_Y$ (a polynomial that vanishes on Y). One can then explicitly write down a holomorphic $(3,0)$-form on Y, by choosing a closed path γ around $p_Y = 0$ in $C\mathbb{P}^4$, and defining

$$\Omega = \int_\gamma \Theta. \tag{3.63}$$

To understand this, consider p_Y as a coordinate normal to the directions lying along the quintic Y, in the neighborhood of $p_Y = 0$. Choose affine coordinates, say, by setting $x_5 = 1$, and replace one coordinate, e.g. x_4 by p_Y. One can rewrite dx_4 as $\frac{\partial x_4}{\partial P} dP$ and integrate out to obtain

$$\Omega = \frac{x_5 dx_1 \wedge dx_2 \wedge dx_3}{\frac{\partial P}{\partial x_4}}.$$

Using a basis A_i for $H_3(X, \mathbb{Z})$, one can write the periods as

$$\Omega_i = \int_{A_i} \int_{\gamma} \Theta. \tag{3.64}$$

Next, the Picard-Fuchs equations for the quintic are stated, followed by a little derivation, which the reader not interested in any technicalities may skip.

Picard-Fuchs equations: quintic

$$\left((z\frac{d}{dz})^4 - 5^5 z \prod_{k=1}^{4} (z\frac{d}{dz} + \frac{k}{5}) \right) \omega_i = 0 \tag{3.65}$$

'Proof':

1. From (3.64) and regarding the form of a general mirror quintic polynomial (3.62), $\partial_\lambda \left(\Omega_i(\lambda a_1, \lambda a_2, \lambda a_3, \lambda a_4, \lambda a_5, \lambda\psi)\right) = -\frac{1}{\lambda^2}\Omega_i(a_1, a_2, a_3, a_4, a_5, \psi)$ follows immediately. Writing out this condition, one obtains the equation $(\sum_i a_i \frac{\partial}{\partial a_i} + \psi\frac{\partial}{\partial\psi} + \lambda)\Omega_i = 0$.

2. Similarly, one obtains $\partial_\lambda \Omega_i(a_1, ..., \lambda a_j, ..., \frac{a_5}{\lambda}, \psi) = 0$, for some $j \neq 5$, leading to $\left(a_j \frac{\partial}{\partial a_j} - a_5 \frac{\partial}{\partial a_5}\right) \Omega_i = 0$. As one can write out this equation for all values $j = 1, 2, 3, 4$, one concludes that $\Omega_i = \Omega_i(a_1 a_2 a_3 a_4 a_5)$.

3. Combining the two previous steps, one can conclude that $\Omega_i = \Omega_i(\frac{a_1 a_2 a_3 a_4 a_5}{\psi^6})$. To relate to the literature, one can rewrite this for convenience as $\Omega_i = \frac{1}{5\psi}\omega_i(\frac{a_1 a_2 a_3 a_4 a_5}{(5\psi)^5})$, and set $z := \frac{a_1 a_2 a_3 a_4 a_5}{(5\psi)^5}$.

4. Successive differentiations lead to $\prod_{i=1}^{5} \frac{\partial}{\partial a_i}\Omega_i = \frac{\partial^5 \Omega_i}{\partial p^5} \prod_{i=1}^{5} \frac{\partial p}{\partial a_i} = \frac{\partial^5 \Omega_i}{\partial p^5}(x_1 x_2 x_3 x_4 x_5)^5$, which is equal to $-\frac{1}{5}\frac{\partial^5}{\partial\psi^5}\Omega_i = -(\frac{1}{5})^5 \frac{\partial^5 \Omega_i}{\partial p^5}(\frac{\partial p}{\partial\psi})^5 = -(\frac{1}{5})^5 \frac{\partial^5 \Omega_i}{\partial p^5}(-5x_1 x_2 x_3 x_4 x_5)^5$ $= \frac{\partial^5 \Omega_i}{\partial p^5}(x_1 x_2 x_3 x_4 x_5)^5$. Adapting to the notation introduced in the previous step, and replacing ∂_{a_i} by $\frac{1}{a_i} z \frac{d}{dz}$, this equality results in the equation $\left(\frac{1}{a_1 a_2 a_3 a_4 a_5}(z\frac{d}{dz})^5 + (\frac{1}{5}\frac{\partial}{\partial_\psi})^5\right) \Omega_i = 0$.

5. From $\frac{1}{5}\partial_\psi \frac{1}{(5\psi)^N} f(z) = -\frac{1}{(5\psi)^{N+1}}(5z\frac{d}{dz} + N)f(z)$ it easily follows that $\left(\frac{1}{5}\partial_\psi\right)^5 \frac{1}{5\psi} f(z) = -\frac{1}{5\psi^6}(5z\frac{z}{dz} + 5)(5z\frac{z}{dz} + 4)(5z\frac{z}{dz} + 3)(5z\frac{z}{dz} + 2)(5z\frac{z}{dz} + 1))f(z)$. Applying this to the

previous equation one obtains $\left((z\frac{d}{dz})^5 - 5^5 z(z\frac{d}{dz}+1)\prod_{k=1}^{4}(z\frac{d}{dz}+\frac{k}{5})\right)\omega_i = 0$. Note that $z(z\frac{d}{dz}+1)f(z) = (z\frac{z}{dz})zf(z)$, which allows to factor out the differential operator $z\frac{d}{dz}$, leading to the PF equations $\left((z\frac{d}{dz})^4 - 5^5 z\prod_{k=1}^{4}(z\frac{d}{dz}+\frac{k}{5})\right)\omega_i = 0$.

It is not hard to imagine, seen how scaling arguments associated to the quintic embedded in $C\mathbb{P}^4$ entered this little derivation of the Picard Fuchs (PF) equations and that this will generalize to something similiar with specific dependence on the scaling parameters for a general hypersurface in a weighted projective space. For later reference, the general PF equations for weighted projective spaces are stated:

$$\left(z\frac{d}{dz}\prod_{i=1,\ldots,q}(z\frac{z}{dz}+\beta_i) - z\prod_{j=1,\ldots,p}(z\frac{d}{dz}+\alpha_j)\right)\omega_i = 0, \tag{3.66}$$

where the β_i and α_j are model-dependent constants. For the quintic, $\alpha_j = \frac{j}{5}$ $(j = 1, 2, 3, 4)$ and $\beta_i = 1$ $(i = 1, 2, 3)$, which recovers the PC equations for the quintic given above, when rescaling the coordinate z to $z \to 5^5 z$. The PF equations are generalized hypergeometric equations, for which the solutions are given in terms of generalized hypergeometric functions, called Meijer-G-functions.

Singularities in moduli space and D-branes wrapping vanishing cycles

There are three special points in moduli space, which are of importance for the physics of D-branes and black holes in CY compactifications. For convenience, set the parameters $a_i = 1$ in (3.62):

$$x_1^5 + ... + x_5^5 = 5\psi x_1 x_2 x_3 x_4 x_5. \tag{3.67}$$

- **The Gepner point,** $\psi = 0$
  Setting $\psi = 0$, one immediately observes, that the group G, leaving the CY equation (3.62) invariant, is enlarged from $(\mathbb{Z}_5)^3$ to $(\mathbb{Z}_5)^4$, as one can still do the rescalings, but the condition $\sum_i k_i = 0$ (mod 5) is no longer a restriction. This point in moduli space is referred to as the *Gepner point* and is thus a $\mathbb{Z}_5$ orbifold singularity.

- **The conifold point,** $\psi = 1$
  The hypersurface (in this case the mirror quintic) Y becomes singular when $p_Y = 0$ and $\vec{\nabla}_x p_Y = 0$, where the latter means $\partial_{x_i} p_Y = 0, \forall i$. In addition to (3.4) this leads to $x_i^5 = \psi x_1 ... x_5, \forall i$. One finds that this condition can be fulfilled when $\psi = e^{\frac{2\pi i n}{5}}, n \in \mathbb{Z}$. These are (the copies of the) *conifold point* in moduli space. Namely, the CY associated to this modulus contains a singularity at a point, where $|x_i| = |x_j|, \forall i, j$. Using the projective rescaling and the group $\mathbb{Z}_5^3$ this point can be represented as $(1 : 1 : 1 : 1 : 1)$ in homogeneous coordinates, and a coordinate transformation and expansion near this point indeed shows that this point is a conifold singularity. This means that the CY is of the form $z_1 z_2 - z_3 z_4 = 0$ in the vicinity of this point (mapped to 0 in these coordinates).

- **The large complex structure point, $\psi = \infty$**
  Finally, one can also satisfy the conditions for a singularity in the CY, for $\psi \to \infty$. In this case, one finds, that the CY is of the form $x_1x_2x_3x_4 = 0$ in affine coordinates. In this case, the CY contains a union of singular surfaces as a sublocus. The point $\psi = \infty$ is referred to as the (large complex structure) *LCS point*, and is mapped on to the point known as the large volume limit under mirror symmetry.

The reason why singularities are interesting for this thesis, is that certain cycles in the CY shrink in their vicinity and eventually vanish. Certain D-branes can become massless at those points in moduli space, when they wrap a vanishing cycle. The corresponding point in moduli space is also the attractor point for that brane system, and the vanishing cycles are also called saturated cycles. For example, one can follow the behavior of 3-cycles as one varies the complex structure modulus of the mirror quintic (or some other Calabi-Yau Y). A specific cycle will shrink to zero at the conifold point, and a certain D3-brane will wrap a vanishing cycle and become massless. From the viewpoint of mathematics, the cycles on which a D3-brane has an attractor point, are called Lagrangian 3-cycles, and have been intensively studied by Joyce, [105]. Note that the singularities of the complex structure moduli space were discussed here, but there are corresponding analogs in the Kähler moduli space. Thus, one will also find vanishing cycles upon varying the Kähler moduli of a CY, and a D6-brane becomes massless at the conifold point. These facts will be reflected in the attractor points found in the research, presented in the following chapter.

3.5 Chapter summary and outlook

In this chapter, the stage was set for the research presented in the next chapter. Topological string theory was introduced, and different interpretations of topological data computed by topological strings were discussed. The reader interested in gaining a deeper understanding of topological string theory is referred to [106–109]. A review with special focus towards the OSV conjecture and black holes is provided by [110]. There is also the book called 'Mirror Symmetry' [11], which provides the reader with a very detailed account of TST.

Building upon the basics of TST discussed, the OSV conjecture was introduced, relating the partition function of a BPS black hole modeled as a mixed ensemble (with respect to the D-brane charges) of states to the partition function of topological string theory. How Frederik Denef and Greg Moore studied and refined the OSV conjecture in a IIA picture was then presented, using split flow trees to establish existence of polar states in the black hole partition function, and enumerating them by using Donaldson-Thomas invariants.

The research to be presented in chapter 4 inspects mixed ensembles of low-charge BPS states. Again, existence of polar states (and some non-polar states) is performed using split flow trees and the centers of split states are enumerated using Donaldson-Thomas invariants. It is important for the reader to remember that a Donaldson-Thomas invariant $N_{\mathrm{DT}}(\beta, n)$ counts the number of D6-D2-D0 BPS bound states of a D6 wrapping the CY, with the D2-brane wrapped on a cycle of homology class $\beta \in H_2(X, \mathbb{Z})$ and with n D0-branes added.

In this low-charge setting, higher order corrections to the action become important, and central charges of brane systems have to be calculated by exploiting mirror symmetry. In the last part of this chapter, the topic of mirror symmetry has been introduced, by presenting a specific example, namely the quintic 3-fold which was extensively studied in this Ph.D. In principle, the research presented in the next chapter is closely connected to an OSV-like statement for D-particles. The question is of course again, in what regime such a conjecture is valid, and how exact it is. The topological string partition function will be used to enumerate D6 (and lower dimensional brane charge) systems, or, in the mirror picture, to count D3-brane systems. Schematically, these relations can be expressed as

$$\mathcal{Z}_{D_{\text{particle}}} \sim |\mathcal{Z}_{\text{top}}|^2 \approx |\mathcal{Z}_{\text{DT}}|^2 \approx |\mathcal{Z}_{D6}|^2 = |\mathcal{Z}_{D3}|^2. \tag{3.68}$$

A conjecture $\mathcal{Z}_{D_{\text{particle}}} \sim |\mathcal{Z}_{\text{top}}|^2$ is of course a toy model in which to examine more details on the OSV conjecture. This is one of the motivations for the research presented in the following chapter. The research should just be viewed as a step in this program. To end this outlook, some brief comments on the different conjectured and approximated identities are added:

- $\mathcal{Z}_{D_{\text{particle}}} \sim |\mathcal{Z}_{\text{top}}|^2$: This step is the OSV-like statement for a D-particle.
- $|\mathcal{Z}_{\text{top}}|^2 \approx |\mathcal{Z}_{\text{DT}}|^2$: The topological string partition function is not known, in this case the Donaldson-Thomas asymptotic expansion is used.
- $|\mathcal{Z}_{\text{DT}}|^2 \approx |\mathcal{Z}_{D6}|^2$: Donaldson-Thomas invariants count D6-D4-D2-D0 BPS states, the closer relationship has been clarified in [1] and has been commented on, in this chapter.
- $|\mathcal{Z}_{D6}|^2 = |\mathcal{Z}_{D3}|^2$: Finally, this is where mirror symmetry comes into play, and in fact, one examines the mirror D3-brane systems, as one can calculate the exact central charges. Alternatively, one could of course also just view this as a method and not directly interpret this as an enumeration in type IIB.

The goal of the research presented in the next chapter is to describe all polar (and some non-polar) D4-D2-D0 configurations as bound states of D6-D2-D0 and $\overline{\text{D6}}$-D2-D0 with U(1) fluxes on them, whereby the D4 charge is induced by the latter fluxes. This will allow to factorize the indices of D4 systems as products of D6 and $\overline{\text{D6}}$ indices. BPS indices of the D6 and $\overline{\text{D6}}$ systems are enumerated by Donaldson-Thomas invariants. The rough scheme discussed above is followed up in the next chapter, resulting in various elliptic genera for specific CY 3-fold study models, obtained from a new perspective. The research can also be viewed as a highly non-trivial test of the split flow tree conjecture.

Chapter 4

Elliptic genera from split flows and Donaldson-Thomas partitions

In this chapter research results are presented on BPS degeneracies of D-particles on Calabi-Yau manifolds. Several elliptic genera are obtained, and various non-trivial checks on the methods used are performed. It is shown however, that in order to obtain exact results on BPS degeneracies more generally, previous techniques have to be refined. In particular, a more refined index is suggested for bound states, and is succesfully put to the test. The studies discussed in this chapter can be seen as a highly non-trivial test of the split attractor flow conjecture. Additionally, as was mentioned at the end of the previous chapter, this work can be seen to consist of low-charge counterpart studies to the more involved OSV setup of [1]. Some of the main results discussed in the following stem from a collaboration with Andrés Collinucci and are published in [3], others have been obtained in a collaboration with Walter Van Herck, and have been published in [4].

The D-particles considered in this chapter are modeled with mixed ensembles of (D4-D2-D0)-branes wrapped on an algebraic CY 3-fold. For various examples, including different choices for the Calabi-Yau 3-fold, exact elliptic genera (the partition functions for these D-particles) are obtained, through exact knowledge of the degeneracy of all polar states. This is accomplished by using split attractor flow trees and the index factorization formulae from [1]. Polar states are realized as bound states, with D6- and $\overline{\text{D6}}$-systems as constituents. These are enumerated using Donaldson-Thomas invariants, provided by topological string theory. Using these techniques allows exact results to be obtained, even though various charges exhibit quite complicated area codes for the split flow trees. In this sense, the results found are strong evidence for (a strong version of) the split attractor flow conjecture, discussed extensively, in chapter 2.

Additionally, several non-polar states, which are also realized as bound states, are analyzed using the same techniques. As the degeneracy of these states is fixed by modularity, this can be seen as a non-trivial check on the techniques used. It is found, that to obtain exact results in general, the index associated to a split flow tree has to be calculated with greater care. Namely, the index of a bound state does not factorize in general, but this can be taken care of. As a consequence, the separation of the states of a center into

generic states (which behave the way one naively expects) and special states (which are 'perceived' differently within the bound states) is possible. This translates into a splitting up of Donaldson-Thomas invariants (counting the BPS states associated to such a constituent center) into what has been named Donaldson-Thomas partitions, consisting of a part counting generic, and of a part counting special states. Although the full meaning of these partitions is not yet clear, they do exhibit highly interesting features. Should the refined index for bound states computed in this chapter turn out to be correct, this refines the wall-crossing index of Denef and Moore, [1], and could be interpreted as the correct physical picture associated to the general wall-crossing formula of Kontsevich and Soibelman, [2] [1].

The setup in this chapter will always be a single D4 brane wrapped on a hyperplane class divisor $P = H$ of a one-modulus CY 3-fold. While this charge is kept fixed, one then considers different possible fluxes $F \in H^2(X, \mathbb{Z})$ and $\overline{D0}$-branes. In order to determine the full partition function, according to the explanations in chapter 2, it is sufficient to restrict attention to polar states, but some interesting non-polar states will be discussed in detail as well. As one is working at low charge, instanton corrections to the central charges of the brane systems under consideration become important.

In the first section of this chapter, how mirror symmetry can be used to obtain fully corrected central charges is discussed. Following this, polar states and some non-polar states on the quintic are analyzed, resulting in a first encounter of Donaldson-Thomas partitions. The results are compared to other derivations of the index of such an ensemble. An exact agreement with the results in [99], and the enumeration of a non-polar state is improved to yield the exact result. This is followed by similar enumerations for a series of other models, again accompanied by a comparison to previous results. Exact results are obtained by utilizing the method stated here and thus the ideas put forth earlier are confirmed. The refinement of the prescription to enumerate states does however lead to a slight modification in the prediction of the elliptic genus for one model. Various non-polar states are analyzed, and an exact confirmation of the suggested method is found. This chapter is concluded with a summary of the obtained results and some comments on future research directions.

4.1 Mirror symmetry and instanton corrected central charges

For configurations with low D-brane charges, the attractor flow equations drive the horizon size of solutions to very small sizes in string scale units. This automatically leads far outside the supergravity regime, requiring higher curvature corrections. However, as will be confirmed shortly, the main tool of analysis, namely split attractor flow tree techniques, will retain its meaningfulness as predicted by the strong split attractor flow tree conjecture. As the attractor equations will typically drive the cycles and the CY itself to stringy sizes,

[1] The author would like to thank Markus Reineke for pointing this out.

the central charges of brane systems receive important worldsheet instanton corrections as a consequence, and these need to be taken into account. In type IIA string theory this would be an impossible task. Luckily, mirror symmetry solves the problem as the central charges are exactly determined classically by the periods of the holomorphic three-form in type IIB string theory on the mirror CY manifold. Note that the mass of a BPS saturated brane wrapping an even cycle corresponds exactly to the notion of quantum volume of that cycle from [111]. The general scheme is to identify an integral basis of three-cycles, calculate the periods of these cycles, find the explicit mirror map and in this way define the quantum volume of any even dimensional cycle of the mirror.

As discussed in section 3.4, the periods of the mirror are determined as Meijer G-functions. Thus, it is not possible to write down analytic formulae for central charges, and certainly not possible to work with split attractor flow trees analytically. This hurdle is overcome in the following by means of numerical approximations with Mathematica[2]. Basically, the periods are evaluated to create a lattice, from which the function can be approximated by interpolation. Split flow trees and single flows are then established numerically. More details on the applied technique can be found in [51]. The mirror symmetry induced monomial-divisor map is used, to convert Kähler to complex structure modulus, and map $(D6, D4, D2, D0)$ brane systems Γ_A into their $(D3, D3, D3, D3)$ brane mirrors Γ_B, $L : H^{2*}(X, \mathbb{Z}) \to H^3(Y, \mathbb{Z})$, and then analyze the attractor flows of the exact central charges in complex structure moduli space (or more precisely in the five-fold cover w-plane). In the IIB picture, black holes are made of D3-branes wrapped along special Lagrangian three-cycles of the internal Calabi-Yau manifold, whereby these D3's (and their corresponding three-cycles) can split up into intersecting D3's, by moving in the complex structure moduli space of the CY across some 'line of marginal stability'.

The techniques explained in the following are adapted from [111]. For concreteness and simplicity, again the quintic shall be treated explicitly, but the reader can easily repeat these steps for the other models used, given the former reference.

The mirror map L can be found from a comparison of the IIA and IIB periods of the quintic near the LCS point: (check [51] for more explanations)

$$L = \begin{pmatrix} -1 & 0 & 0 & 0 \\ 0 & 1 & 0 & 0 \\ \frac{25}{12} & \frac{11}{2} & 1 & 0 \\ 0 & -\frac{25}{12} & 0 & -1 \end{pmatrix}. \tag{4.1}$$

It relates the even cycles of real dimension $2j$ on the CY X_A to the three-cycles γ_i of the mirror CY manifold X_B. The periods $\Pi_i = \int_{\gamma_i} \Omega$, of the holomorphic three-form on the γ_i have leading logarithmic behavior $\log^j(z)$ near $z = 0$ (LCS point), using the coordinate $z = \psi^{-5}$. As stated before, these periods are solutions to the generalized hypergeometric equation, known as the Picard-Fuchs equation,

$$\Big[z\,\partial_z \prod_{i=1\ldots q} (z\,\partial_z + \beta_i - 1) - z \prod_{j=1\ldots p} (z\,\partial_z + \alpha_j)\Big] u = 0, \tag{4.2}$$

[2]Special thanks to Frederik Denef for sharing his Mathematica code with the author [51].

where the α_j and the β_i are model dependent constants, which in the case of the quintic are $\alpha_j = \frac{j}{5}, \beta_i = 1,\ j = 1, ..., 4, i = 1, 2, 3$ [3]. For the quintic, the Meijer-functions (G-functions) $U_j(z)$ can be expressed as

$$U_j(z) = \frac{1}{(2\pi i)^j} \oint \frac{\Gamma(-s)^{j+1} \prod_{i=1}^{4} \Gamma(s+\alpha_i)((-1)^{j+1}z)^s}{\Gamma(s+1)^{3-j}} ds. \tag{4.3}$$

This particular basis of periods is related to three branching points (LCS point, conifold point and Gepner point) which are connected by appropriately chosen branch cuts. This was important when establishing flow trees, as flow tree branches often cross such branch cuts in moduli space, and this needs to be taken into account when building more complicated flow trees. Associated to these branch cuts are three types of monodromies, which can be expressed as matrices acting on the periods. The monodromy $T(0)$ around the LCS point $(z = 0, \psi = \infty)$ and the monodromy $T(\infty)$ around the Gepner point $(z = \infty, \psi = 0)$ act on the period vector $\mathbf{U}(z) = (U_j(z))_{j=1...4}$ as follows,

$$\begin{aligned} \mathbf{U}(e^{2\pi i}z) &= T(0)\,\mathbf{U}(z), \qquad |z| << 1 \\ \mathbf{U}(e^{2\pi i}z) &= T(\infty)\,\mathbf{U}(z), \qquad |z| >> 1. \end{aligned} \tag{4.4}$$

The third monodromy matrix of course follows directly from the other two, as a monodromy can always be seen either as 'around one of the branching points' or, equivalently as a monodromy 'around the two other branching points' in the appropriate directions. For the monodromy around the conifold point one has

$$\begin{aligned} T(1) &= T(\infty)T(0)^{-1} \qquad \mathrm{Im}(z) < 0, \\ T(1) &= T(0)^{-1}T(\infty) \qquad \mathrm{Im}(z) > 0. \end{aligned} \tag{4.5}$$

Adhering to the conventions in [51], a period basis can be defined by the vector $\mathbf{\Pi} = L\mathbf{U}$, where L is the following matrix:

$$L = \frac{8\,i\,\pi^2}{125} \begin{pmatrix} 0 & 5 & 0 & 5 \\ 0 & 1 & -5 & 0 \\ 0 & -1 & 0 & 0 \\ 1 & 0 & 0 & 0 \end{pmatrix}. \tag{4.6}$$

Knowing the exact periods one can calculate the Kähler potential

$$e^{-K} = i \int_Y \Omega_B \wedge \overline{\Omega_B} = i\,\mathbf{\Pi}^\dagger(z) \cdot I^{-1} \cdot \mathbf{\Pi}(z)\,, \tag{4.7}$$

where Ω_B is the holomorphic $(3,0)$-form of type a IIB CY compactification Ω_B, and I is the symplectic intersection matrix given by

$$I = \begin{pmatrix} 0 & 0 & 0 & -1 \\ 0 & 0 & 1 & 0 \\ 0 & -1 & 0 & 0 \\ 1 & 0 & 0 & 0 \end{pmatrix}. \tag{4.8}$$

[3] The values for the α_i need to be replaced with $(\frac{1}{6}, \frac{1}{3}, \frac{2}{3}, \frac{5}{6})$, $(\frac{1}{8}, \frac{3}{8}, \frac{5}{8}, \frac{7}{8})$ and $(\frac{1}{10}, \frac{3}{10}, \frac{7}{10}, \frac{9}{10})$ for the sextic, the octic, and the decantic, used in this chapter, respectively.

The fully quantum corrected central charges of a IIB charge vector $\mathbf{q} = (p^0, p, q, q_0)$ can now be computed as follows:

$$Z(\Gamma) = e^{K/2}\, \mathbf{q} \cdot \mathbf{\Pi}\,. \tag{4.9}$$

4.2 Enumeration of D4-D2-D0 BPS states on the quintic

It is time to present split flow trees and BPS indices for a type IIA string theory compactification on the quintic. The results offer strong evidence that the split attractor flow conjecture holds accurately for the BPS states under investigation, suggesting a 'strong' correspondence between flow tree data and BPS solutions of the worldsheet instanton corrected theory. It becomes clear however, that one has to take care of some subtleties in order to establish a correspondence for all charge systems considered. The results will also be compared to the calculations of the modified elliptic genus performed by means of geometric and CFT-inspired techniques, as well as the use of modular invariance, performed by Gaiotto, Strominger and Yin, [99].

Using the notation for the charge vectors (3.54,3.55), a charge polyform on the quintic reads

$$\Gamma = p^0 + pH + \frac{q}{5}H^2 + \frac{q_0}{5}H^3. \tag{4.10}$$

As stressed under 2.4.4, whether a charge is polar or non-polar has decisive implications for the existence of attractor flows, at least in the large volume regime. If the central charge $Z(\Gamma, t)$ vanishes on a regular point in the moduli space, then no single-centered solution exists. In the large radius approximation, the central charge of system with $(D4, D2, D0)$ charge (p, q, q_0) reads $Z = \langle \Omega, \Gamma \rangle = -\frac{5p}{2}t^2 + qt - q_0$. Under a shift of the B-field, $B \to B - \frac{1}{5}q$, this becomes $Z = -\frac{5p}{2}t^2 - \hat{q}_0$. For this shift in the B-field not to affect the BPS spectrum one has of course to assume that the background Kähler modulus does not cross a wall of marginal stability. Writing the Kähler modulus as $t = B + iJ$ and setting $Z = 0$ leads to $B \cdot J = 0$ and $\frac{1}{2}(J^2 - B^2) = \hat{q}_0$, from which one can deduce that one needs $\hat{q}_0 > 0$ to have a solution[4]. Thus, it turns out that in the large radius approximation, $\hat{q}_0 > 0$ is the condition for a single flow to crash at a regular point in moduli space, whereas for $\hat{q}_0 < 0$ the flow will terminate at a regular attractor point. As will be discussed shortly, this is no longer true when working in the regime where the central charge receives dominant instanton corrections.

Clearly, there is no algorithm to find all attractor flows for the charge systems under investigation. However, a certain set of rules was followed when gathering all attractor flows contributing to an index. One might say very loosely that one chose the most convenient and least complicated topological background sector in moduli space, but one may elaborate more on that. First of all, one searches for a value of the background complexified Kähler modulus where no single flow exists for a given system. One then looks for splits

[4]Recall that J is in the self-dual part of $H^2(P, \mathbb{Z})$.

into a single D6-brane (potentially with U(1) flux, D2 ($\overline{\text{D2}}$) and $\overline{\text{D0}}$-branes) and a single $\overline{\text{D6}}$ (again potentially carrying lower-dimensional brane charge) and restricts attention to D2's (or $\overline{\text{D2}}$'s) wrapped on holomorphic curves of up to degree three, either rational or elliptic. A next criterion was to select a topological sector of the background where there is no single flow, but only split flows are possible. All the splits discussed in this chapter are splits into single D6/$\overline{\text{D6}}$ pairs. However, the author and his collaborators also searched for splits into higher rank stacks, whenever it seemed intuitively reasonable to expect these, but did not find any.

As mentioned before, the centers were enumerated using DT invariants. Note that when using a DT-invariant to count a number of D6-D2-D0 states, one must be careful not to overcount the states involved in a flow tree. Such issues are discussed in more detail on a case by case basis in what follows and in the appendix.

For convenience, some DT invariants for the quintic are stated in the following table, including all the ones used to derive the results.

Donaldson-Thomas invariants: quintic				
	$\mathbf{n=0}$	$\mathbf{n=1}$	$\mathbf{n=2}$	$\mathbf{n=3}$
$\beta=\mathbf{0}$	1	200	19'500	1'234'000
$\beta=\mathbf{1}$	0	2875	569'250	54'921'125
$\beta=\mathbf{2}$	0	609'250	124'762'875	12'448'246'500
$\beta=\mathbf{3}$	609'250	439'056'375	76'438'831'000	7'158'676'736'750

By the conjectured identity between the generating functional for GV invariants and DT invariants [85], one can easily obtain these from [112], [113], where the GV invariants for the quintic were calculated up to high order.

4.2.1 Polar states: $\hat{q}_0 > 0$

All polar states are analyzed, moving from more polar to less polar. The following table, 4.2.1, summarizes the polar charge systems with one $p=1$ magnetic D4-brane wrapped on a hyperplane class divisor of the quintic. Charges systems are labeled by their deviation in D2-brane charge Δq and D0-brane charge Δq_0 as measured from the most polar state with charge vector

$$\Gamma = H + \frac{1}{2}H^2 + \frac{7}{12}H^3, \tag{4.11}$$

which means D2-brane charge $q=\frac{5}{2}$ and D0-brane charge $q_0=\frac{35}{12}$. Thus, $\hat{q}_0 = q_0 - \frac{1}{10}q^2 = \frac{55}{24}$. In the 'charge shift' notation it is denoted as $\Delta q = 0, \Delta q_0 = 0$.

Polar brane systems				
D2/D0 shifts			Total charge	Reduced D0 brane charge $\hat{q}_0$
1.	$\mathbf{\Delta q = 0}$	$\mathbf{\Delta q_0 = 0}$	$H+\frac{1}{2}H^2+\frac{7}{12}H^3$	$55/24 \approx 2.29$
2.	$\mathbf{\Delta q = 0}$	$\mathbf{\Delta q_0 = -1}$	$H+\frac{1}{2}H^2+\frac{23}{60}H^3$	$31/24 \approx 1.29$
3.	$\mathbf{\Delta q = 1}$	$\mathbf{\Delta q_0 = -1}$	$H+\frac{7}{10}H^2+\frac{23}{60}H^3$	$83/120 \approx 0.69$
4.	$\mathbf{\Delta q = -1}$	$\mathbf{\Delta q_0 = -2}$	$H+\frac{3}{10}H^2+\frac{11}{60}H^3$	$83/120 \approx 0.69$
5.	$\mathbf{\Delta q = 0}$	$\mathbf{\Delta q_0 = -2}$	$H+\frac{1}{2}H^2+\frac{11}{60}H^3$	$7/24 \approx 0.29$

In the following, small pictograms will be used to denote flow trees. Indices corresponding to a flow tree will be calculated right after the first split point, at the wall of marginal stability, as in [1]. The various branches of a pictogram will be denoted by the corresponding brane charge, where D6- or D4-branes are denoted with a subscript indicating possible worldvolume flux and bound (anti-) D2- or D0-branes. When stating a flux dual to a curve on a D4-brane or stating the type of curve on which one wraps a (anti-) D2-brane, the curves of degree d will be denoted by C_d when they are rational (i.e. genus zero), otherwise the genus will be stated explicitly.

1. $\mathbf{\Delta q = 0, \Delta q_0 = 0}$:
   The first state to be analyzed is the most polar state: a pure D4-brane ($\hat{q}_0 \approx 2.29$). One needs to turn on a half-integer flux for anomaly cancellation as the hyperplane class divisor does not support a spin structure, [76], [77]. This pure fluxed D4-brane has charge $\Gamma = H + \frac{H^2}{2} + (\frac{\chi(P)}{24} + \frac{1}{2}F^2)\,\omega = H + \frac{1}{2}H^2 + \frac{7}{12}H^3$ where $\omega \in H^6(X, \mathbb{Z})$ denotes the volume form on X. One finds a split flow tree with two endpoints, corresponding to charges

$$\begin{aligned} \Gamma_1 &= 1 + H + \frac{H^2}{2} + \frac{c_2(X)}{24} + \frac{H^3}{6} + \frac{c_2(X)\cdot H}{24}, \\ \Gamma_2 &= -1 - \frac{c_2(X)}{24}. \end{aligned}$$

   It looks and is enumerated as follows:

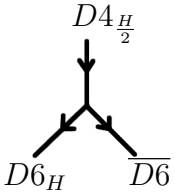

$= \quad 5.$

   The first center is a D6-brane with one unit of worldvolume flux turned on, the second center is a pure $\overline{\text{D6}}$. Note that the correction from the second Chern class of the quintic $c_2(X)$ on D2- and D0-brane charges has been taken into account for both centers. As discussed in [51], the attractor points for these centers lie on copies of the conifold singularity. They might be viewed as some 'microscopic building blocks' of an empty hole. The BPS index reads

$$\Omega = (-1)^{|\langle\Gamma_1,\Gamma_2\rangle|-1}|\langle\Gamma_1,\Gamma_2\rangle| N_{\text{DT}}(0,0)\cdot N_{\text{DT}}(0,0) = (-1)^4\cdot 5\cdot 1\cdot 1 = 5. \qquad (4.12)$$

2. $\mathbf{\Delta q = 0, \Delta q_0 = -1}$:
   The next polar state is obtained by binding one $\overline{\text{D0}}$-brane $N = 1$ to the D4-brane. This system has total charge $\Gamma = H + \frac{H^2}{2} + (\frac{\chi(P)}{24} + \frac{1}{2}F^2 - N)\,\omega = H + \frac{H^2}{2} + \frac{23}{60}H^3$. One finds a split flow tree with three endpoints corresponding to a D6-brane with one unit of worldvolume flux, a pure $\overline{\text{D6}}$ and an $\overline{\text{D0}}$. Depending on the background

value of the Kähler modulus, the $\overline{\text{D0}}$-brane is on the side of the D6 or of the $\overline{\text{D6}}$. There is a threshold wall for the $\overline{\text{D0}}$ running through the fundamental wedge. One finds what one expects: the $\overline{\text{D0}}$ binds to the D6 on one side of the TH wall and it binds to the $\overline{\text{D6}}$ on the other side of the wall. One possibility is the flow tree:

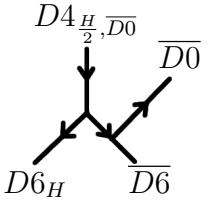

$= \quad -800,$

leading to the BPS index

$$\Omega = (-1)^{|\langle\Gamma_1,\Gamma_2\rangle|-1}|\langle\Gamma_1,\Gamma_2\rangle|N_{\text{DT}}(0,1)\cdot N_{\text{DT}}(0,0) = (-1)^3\cdot 4\cdot 200\cdot 1 = -800.$$

Note, that in calculating this index one has now in some sense approximated the degeneracy (index) by treating the whole flow tree as though it corresponded to a two-centered solution (instead of a three-centered one). The physical justification for this, which is based on the supergravity picture (which is a priori not valid at low charge), is that, during the first split, the $\overline{\text{D6}}$ (or the D6-brane, depending on the side of the threshold wall) with a bound $\overline{\text{D0}}$ behaves approximately as a single particle in spacetime, since the distance between the $\overline{\text{D6}}$ and the $\overline{\text{D0}}$ is negligible compared to the distance between the D6 and the $\overline{\text{D6}}$. Of course, this does not immediately imply how one would go about computing the exact index for a three-centered solution. In this case here, the DT invariant correctly counts the number of BPS states. It can and will happen, though, that one has to work harder to get the correct index for a whole flow tree. In that case a more detailed area code analysis becomes relevant.

3. $\mathbf{\Delta q = 1, \Delta q_0 = -1}$:
The next state ($\hat{q}_0 \approx 0.69$) is obtained in the D4-picture by turning on a flux dual to a degree one rational curve. This leads to the total charge $\Gamma = H + \frac{7}{10}H^2 + (\frac{\chi(P)}{24} + \frac{1}{2}F^2)\omega = H + \frac{7}{10}H^2 + \frac{23}{60}H^3$. One finds a split flow tree ending with a D6 with one unit of worldvolume flux and a $\overline{\text{D6}}$ with a sheaf corresponding to a D2-brane wrapped on a degree one rational curve. The holomorphic Euler character for this curve is $n_2 = \chi_h(C_1) = 1$, so one sets $(\beta_2, n_2) = (1,1)$. The split flow tree looks like

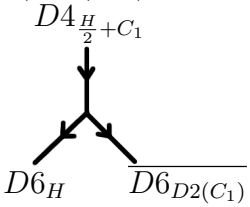

$= \quad 8'625,$

which leads to the BPS index

$$\Omega = (-1)^{|\langle\Gamma_1,\Gamma_2\rangle|-1}|\langle\Gamma_1,\Gamma_2\rangle|N_{\text{DT}}(0,0)\cdot N_{\text{DT}}(1,1) = (-1)^2\cdot 3\cdot 1\cdot 2'875 = 8'625.$$

4. $\mathbf{\Delta q = -1, \Delta q_0 = -2}$:
Similarly there is the state ($\hat{q}_0 \approx 0.69$) with total charge $\Gamma = H + \frac{3}{10}H^2 + (\frac{\chi(P)}{24} + \frac{1}{2}F^2)\omega = H + \frac{3}{10}H^2 + \frac{11}{60}H^3$. One finds the split flow tree with a D6 with one unit of worldvolume flux and a sheaf corresponding to an $\overline{\text{D2}}$ wrapped on a degree one rational curve on one side, and an $\overline{\text{D6}}$ on the other side, as centers. One therefore sets $(\beta_1, n_1) = (1, -1)$. The split flow tree looks like

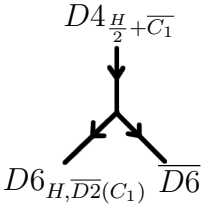

$= \quad 8'625,$

and one obtains the BPS index

$$\Omega = (-1)^{|\langle\Gamma_1,\Gamma_2\rangle|-1}|\langle\Gamma_1,\Gamma_2\rangle| N_{\text{DT}}(1,1) \cdot N_{\text{DT}}(0,0) = (-1)^2 \cdot 3 \cdot 1 \cdot 2'875 = 8'625.$$

5. $\mathbf{\Delta q = 0, \Delta q_0 = -2}$:
Next, one can bind two $N = 2$ $\overline{\text{D0}}$'s to the D4. This yields a total charge $\Gamma = H + \frac{H^2}{2} + (\frac{\chi(P)}{24} + \frac{1}{2}F^2 - N)\omega = H + \frac{H^2}{2} + \frac{11}{60}H^3$. One finds one split flow tree of the schematic form

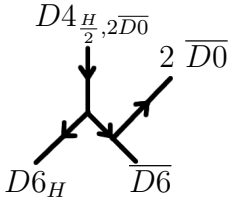

$= 58'500,$

and one is led to the BPS index

$$\Omega = (-1)^{|\langle\Gamma_1,\Gamma_2\rangle|-1}|\langle\Gamma_1,\Gamma_2\rangle| N_{\text{DT}}(0,2) \cdot N_{\text{DT}}(0,0) = (-1)^2 \cdot 3 \cdot 19'500 \cdot 1 = 58'500.$$

One can check that all the results for the polar states exactly match the corresponding numbers from the elliptic genus obtained in [99], by analyzing the degrees of freedom associated to a charge lifted to M-theory in the MSW CFT.

4.2.2 Non-polar states: $\hat{q}_0 < 0$

Here is a summary of the non-polar charges that will be considered.

Non-polar brane systems				
D2/D0 shifts			Total charge	Reduced D0 brane charge $\hat{q}_0$
6.	$\mathbf{\Delta q = 2}$	$\mathbf{\Delta q_0 = -1}$	$H + \frac{9}{10}H^2 + \frac{23}{60}H^3$	$-13/120 \approx -0.11$
7.	$\mathbf{\Delta q = 1}$	$\mathbf{\Delta q_0 = -2}$	$H + \frac{7}{10}H^2 + \frac{11}{60}H^3$	$-37/120 \approx -0.31$
8.	$\mathbf{\Delta q = 0}$	$\mathbf{\Delta q_0 = -3}$	$H + \frac{1}{2}H^2 + \frac{-1}{60}H^3$	$17/24 \approx -0.71$
9.	$\mathbf{\Delta q = 2}$	$\mathbf{\Delta q_0 = -2}$	$H + \frac{9}{10}H^2 + \frac{11}{60}H^3$	$83/120 \approx -1.11$

6. $\mathbf{\Delta q = 2, \Delta q_0 = -1}$:
The first non-polar state ($\hat{q}_0 \approx -0.11$) can be obtained in the D4-picture by turning on flux dual to a degree two rational curve. This system has charge $\Gamma = H + \frac{9}{10}H^2 + (\frac{\chi(P)}{24} + \frac{1}{2}F^2)\omega = H + \frac{9}{10}H^2 + \frac{23}{60}H^3$. One finds the split flow tree

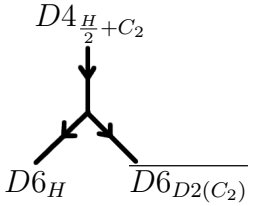

$= \quad -1'218'500,$

which leads to the index

$$\Omega = (-1)^{|\langle\Gamma_1,\Gamma_2\rangle|-1}|\langle\Gamma_1,\Gamma_2\rangle| N_{\mathrm{DT}}(0,0)\cdot N_{\mathrm{DT}}(2,1) = (-1)^1\cdot 2\cdot 1\cdot 609'250 = -1'218'500.$$

7. $\mathbf{\Delta q = 1, \Delta q_0 = -2}$:
The next state ($\hat{q}_0 \approx -0.31$) can be viewed as a D4-brane with worldvolume flux dual to a degree one rational curve as well as ($N = 1$) one $\overline{\mathrm{D0}}$, corresponding to the total charge $\Gamma = H + \frac{7}{10}H^2 + (\frac{\chi(P)}{24} + \frac{1}{2}F^2 - N)\omega = H + \frac{7}{10}H^2 + \frac{11}{60}H^3$. This system is the first with a non-trivial area code. The correct index receives different contributions in different background regimes. The reader interested in the details of the area code is referred to the appendix B. Tuning the background to the simplest case, two split flow trees contribute. First, there is the split into a D6-brane with one unit of worldvolume flux, a pure $\overline{\mathrm{D6}}$ and a D2-D0 halo particle. The halo is on the anti-D6 side after the first split. Second, there is the split into the D6-brane with one unit of worldvolume flux, a $\overline{\mathrm{D6}}$ with sheaf corresponding to a D2 on a degree one rational curve and one $\overline{\mathrm{D0}}$, where the $\overline{\mathrm{D0}}$ is on the $\overline{\mathrm{D6}}$ side after the first split. This schematically corresponds to

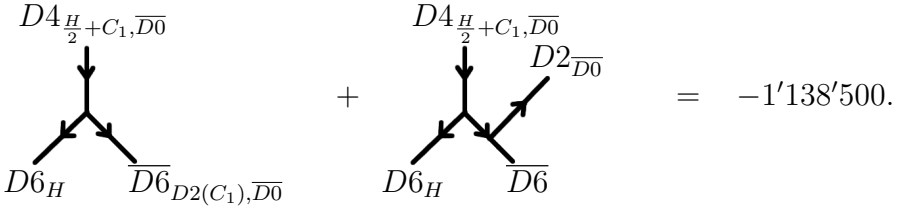

$= \quad -1'138'500.$

These two flow trees sum up according to the following:

$$\Omega = (-1)^{|\langle\Gamma_1,\Gamma_2\rangle|-1}|\langle\Gamma_1,\Gamma_2\rangle| N_{\mathrm{DT}}(0,0)\cdot N_{\mathrm{DT}}(1,2) = (-1)^1\cdot 2\cdot 1\cdot 569'250 = -1'138'500.$$

8. $\mathbf{\Delta q = 0, \Delta q_0 = -3}$:
One then considers a state ($\hat{q}_0 \approx -0.71$) which can be seen as a D4-brane with three $\overline{\mathrm{D0}}$'s ($N = 3$). The total charge is $\Gamma = H + \frac{1}{2}H^2 + (\frac{\chi(P)}{24} + \frac{1}{2}F^2 - N)\omega = H + \frac{1}{2}H^2 - \frac{1}{60}H^3$. One finds two contributions to the total index. The first split flow tree is

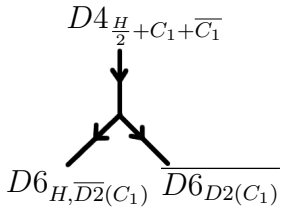

$= \quad 8'265'625,$

and contributes by

$$\Omega_A = (-1)^{|\langle\Gamma_1,\Gamma_2\rangle|-1}|\langle\Gamma_1,\Gamma_2\rangle| N_{\mathrm{DT}}(1,1)\cdot N_{\mathrm{DT}}(1,1) = (-1)^0\cdot 1\cdot 2'875\cdot 2'875 = 8'265'625.$$

The second type of split flow tree is one with three centers, a D6-brane with one unit of worldvolume flux, a pure $\overline{\mathrm{D6}}$ and three $\overline{\mathrm{D0}}$'s. Again, a threshold wall interpolates between areas where the $\overline{\mathrm{D0}}$'s are on the D6 side after the first split, or on the $\overline{\mathrm{D6}}$ side, respectively. The flow tree looks like

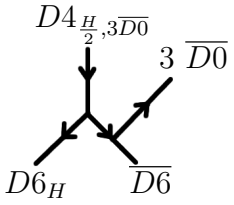

$= \quad -2'468'000,$

and contributes

$$\begin{aligned}\Omega_B &= (-1)^{|\langle\Gamma_1,\Gamma_2\rangle|-1}|\langle\Gamma_1,\Gamma_2\rangle| N_{\mathrm{DT}}(0,3)\cdot N_{\mathrm{DT}}(0,0)\\ &= (-1)^1\cdot 2\cdot 1'234'000\cdot 1 = -2'468'000.\end{aligned}$$

Altogether this leads to

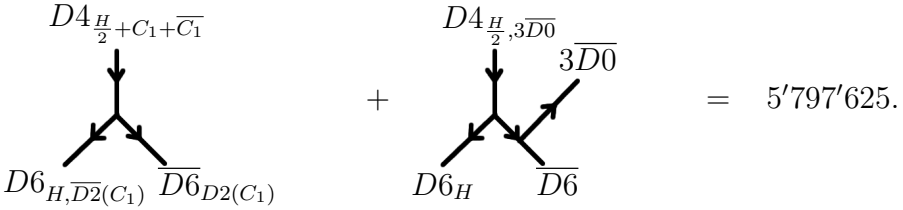

$= \quad 5'797'625.$

9. $\mathbf{\Delta q = 2, \Delta q_0 = -2}$:
The last state ($\hat{q}_0 \approx -1.11$) considered has the most complicated area code. In the D4 picture, one obtains it by turning on flux dual to a degree two rational curve as well as binding one anti-D0-brane ($N = 1$). The total charge reads $\Gamma = H + \frac{9}{10}H^2 + (\frac{\chi(P)}{24} + \frac{1}{2}F^2 - N)\omega = H + \frac{9}{10}H^2 + \frac{11}{60}H^3$. Again, the reader can find a detailed discussion in the appendix B. Choosing a convenient background, one finds three split flow trees.
The first two contribute as follows:

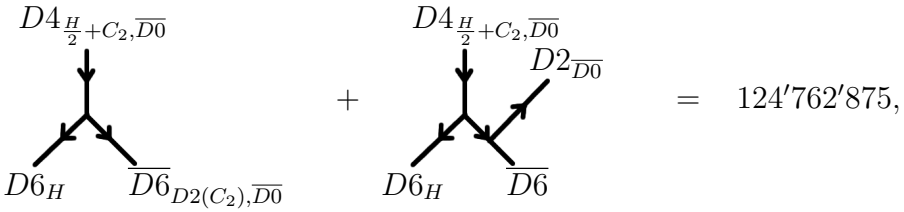

which is calculated according to

$$\begin{aligned}\Omega_B &= (-1)^{|\langle\Gamma_1,\Gamma_2\rangle|-1}|\langle\Gamma_1,\Gamma_2\rangle|N_{\rm DT}(0,0)\cdot N_{\rm DT}(2,2)\\ &= (-1)^0\cdot 1\cdot 1\cdot 124'762'875 = 124'762'875.\end{aligned}$$

Note that the subscript of the index will become clear in the appendix, where the area code for this charge system is discussed in detail. The next contribution arises from a split flow tree with a D6 with two units of flux and additional sheaf corresponding to a $\overline{\rm D2}$ wrapped on a degree three rational curve $(\beta_1, n_1) = (3, 1)$ as well as a $\overline{\rm D6}$ with one unit of worldvolume flux. This flow tree looks like

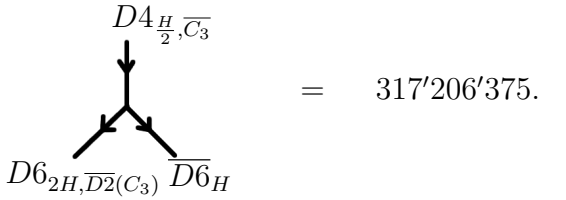

One might at first have thought that this flow tree would yield the index

$$\Omega_C = (-1)^{|\langle\Gamma_1,\Gamma_2\rangle|-1}|\langle\Gamma_1,\Gamma_2\rangle|N_{\rm DT}(0,0)\cdot N_{\rm DT}(3,1) = 439'056'375\,,$$

but closer inspection shows that one would overcount the number of BPS states corresponding to this flow tree. Namely, one would also enumerate the number of BPS states corresponding to the case, when the D6-brane would have a $\overline{\rm D2}$ on an elliptic degree three curve, ${C_3}^{g=1}$, and an extra $\overline{\rm D0}$. However, one does not find this type of split flow tree. A simple trick allows the substraction of the right number of states from $439'056'375$: Imagine that this type of split existed. In that case one might also find a threshold wall for the $\overline{\rm D0}$. If one would take the background into a region, where the $\overline{\rm D0}$ flips side after the first split, one would then enumerate this split as follows:

$$\Omega_{C2} = (-1)^0\cdot 1\cdot N_{\rm DT}(0,1)\cdot N_{\rm DT}(3,0) = 200\cdot 609'250 = 121'850'000.$$

Again, the subscript '$C2$' of the index will become clear in the appendix, where the area code is discussed in detail. As the index cannot jump at a threshold wall, this is presumably also the index that one has to substract. One then obtains

$$\Omega_{C1} = \Omega_C - \Omega_{C2} = 439'056'375 - 121'850'000 = 317'206'375.$$

This can also be graphically depicted by

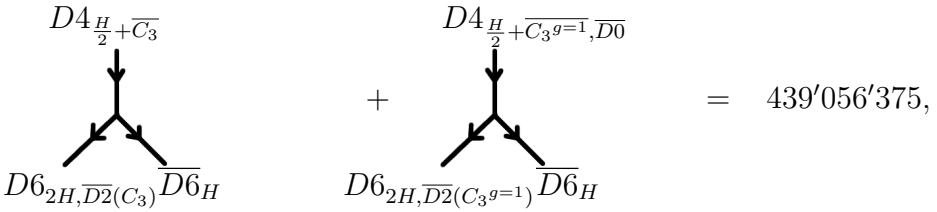

and

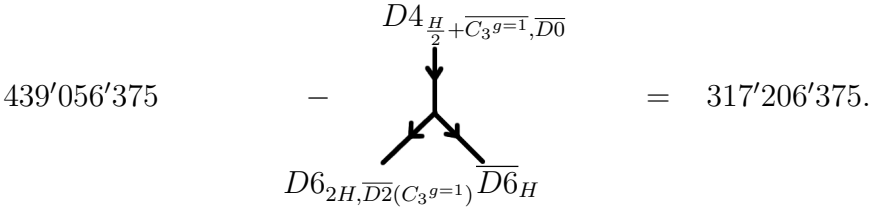

Finally, one can sum up to obtain the total BPS index:

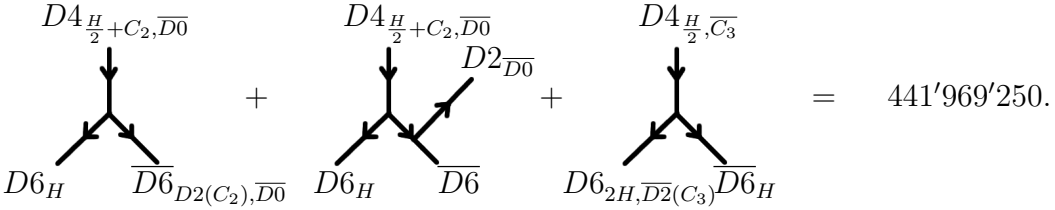

Before continuing to analyze and extend the results, one should consider one more important remark. Overviewing all polar and non-polar states and their split flow trees obtained numerically, and taking into account that a BPS index cannot possibly jump when crossing a wall of threshold stability[5] , one may safely conclude that there is indeed a background region where all indices are valid simultaneously, making the enumeration valid as a whole.

4.2.3 Non polar states without any single flows

In the large radius regime the notion of a polar state automatically coincided with a state that does not support a single attractor flow. On the other hand, for a non-polar state, one was able to write down an attractor point for a single flow. As mentioned previously and as now observed, this property is altered when using instanton corrected central charges, exhibiting an interesting difference with the large radius regime. As discussed, three of the non-polar states do not allow for any single-centered attractor flows[6]. This might have been expected, as the criterion in [1] for the existence of a crash in the flow was based on the central charge, which gets strong instanton corrections in the regime one is working in. The criterion for having a crash in the single flow is therefore no longer $\hat{q}_0 > 0$. Put differently, non-polarity no longer guarantees the existence of single-centered solutions.

[5]As explained earlier in this thesis, unlike a wall of marginal stability, a wall of threshold stability means that there are no tachyon fields between the would-be products of a decay process. Therefore, the decay is *kinematically* impossible.

[6]Note that also the fourth non-polar state does not allow single flows in certain background regimes.

4.2.4 Comparison to the elliptic genus

A partition function for a D4-D2-D0 black hole or a D-particle was discussed in chapter 2. It is appropriate, to restate once more, how to obtain the elliptic genus from the viewpoint exploited in this thesis. It is sufficient to enumerate degeneracies of all polar states. One proceeds as follows.

1. Find all the non-pullback fluxes, corresponding to the gluing vectors, in the flux lattice $H^2(P,\mathbb{Z})$ on the divisor. For each gluing vector, add various numbers of anti-D0-branes, and in this way classify all polar states.

2. For each of these polar states, find all the split flow trees with corresponding indices, and add them up to yield the total index.

3. Write down a basis of modular forms of the right weight and dimension, using the techniques explained in [79]. Finally, determine the full elliptic genus, by using the polar state indices to fix a specific vector, written out in the basis constructed.

In the following, the gluing vectors for the quintic are briefly re-examined and supplemented with some additional intuition. States will be labeled by their gluing vector, and by the reduced D0-brane charge, as $[\gamma, \hat{q}_0]$.

Gluing vectors and fluxes dual to curves

- $\gamma = 0$
  From the D4-picture of mixed ensemble on the quintic, one can easily classify the states. Turning on no flux (apart from the mandatory $\frac{H}{2}$ for anomaly cancellation), one obtains three equivalence states to consider. These are $[0, \frac{55}{24}]$, $[0, \frac{31}{24}]$ and $[0, \frac{7}{24}]$. Of course, this means 'no gluing vector' in the flux lattice.

- $\gamma = C_1$
  The next obvious step might be to turn on a flux in a cohomology class dual to a degree one rational curve, which will sloppily be written as $F = C_1$. The reduced D0-brane charge reads $\hat{q}_0 = \frac{\chi(P)}{24} + \frac{1}{2}F_\perp^2$. As mentioned in [99], for a curve which one embeds algebraically, the adjunction formula allows the calculation of $C\cdot C + C\cdot H = 2g-2$, and generically, a degree one curve will intersect the hyperplane once, $C_1 \cdot H = 1$. Using this, one gets $C_1 \cdot C_1 = -3$, and thus $\frac{1}{2}F^2 = \frac{1}{2}(\frac{H}{2}+C_1)^2 = -\frac{3}{8} = \frac{1}{2}F_{||}^2 + \frac{1}{2}F_\perp^2$. Note that one can fix the part pointing in direction of L_X using the D2-charge, $q = F\cdot H = \frac{7}{2}$, thus $f_{||} + \gamma_{||} = \frac{H}{5}$. One thus gets the equation for the non-pullback flux
  $$\frac{1}{2}F_\perp^2 = \frac{1}{2}(f_\perp + \gamma_\perp)^2 = -\frac{8}{5}. \tag{4.13}$$
  For this gluing vector, $[C_1, \frac{83}{120}]$ is the only class of states.

- $\gamma = C_2$
  In analogy to the discussion on the degree one curve, one can turn on a flux dual to a degree two rational curve. However, this automatically means that one gets a non-polar state: $\hat{q}_0 = -\frac{37}{24}$.

One might go on and consider fluxes dual to curves of higher degree, but the elliptic genus of the quintic is a modular vector of dimension five, (2.53). This means that there are five different values for γ (including zero), but as can be followed e.g. in [1, 41, 42, 78], $Z_\gamma = Z_\delta$ or $\gamma = -\delta \mod L_X$ eliminates two). This is reflected by the fact that Z_3 and Z_4 in (2.53) are determined, once one knows Z_γ ($\gamma = 0, 1, 2$). One therefore expects, that one can restrict oneself to working with fluxes dual to curves up to degree two, and this is sufficient to account for all the degeneracies to determine the full elliptic genus, and therefore account for all the degeneracies of the D-particle analyzed.

Quintic elliptic genus

For the quintic, the theta function (2.52) is determined to be

$$\Theta_\gamma(\bar{q}, z) = \sum_n (-1)^{n+|\gamma_{||}|}\, \bar{q}^{\frac{5}{2}(n+\frac{|\gamma_{||}|}{5}+\frac{1}{2})^2}\, z^{5\,n+|\gamma_{||}|+\frac{5}{2}}\,, \tag{4.14}$$

where, according to the preceding discussion, the sum over the variable γ corresponds physically to a sum over possible $U(1)$ fluxes on the worldvolume of the D4-brane that cannot be written as the pullback of some two-form on the ambient space. In the above formula, the notation $|\gamma_{||}| = \gamma_{||} \cdot H$ has been used. For a flux dual to a degree one curve, e.g. $|\gamma_{||}| = \frac{H}{5} \cdot H = \frac{1}{5}\int_P H^2 = \frac{1}{5}\int_X H^3 = 1$, for a flux dual to a degree two curve, similarly $|\gamma_{||}| = 2$. If $|\gamma_{||}|$ reaches five, then the flux can be represented as the pullback $\imath_*(H)$ of the hyperplane class on the CY space. Hence, the sum terminates at four, and the elliptic genus is of the form

$$Z_0(q)\Theta_0(\bar{q}, z) + ... + Z_4(q)\Theta_4(\bar{q}, z). \tag{4.15}$$

One can now restrict attention to the functions $Z_\gamma(q)$.

Four numbers determine the full elliptic genus for the quintic through

$$\begin{aligned}
Z_0(q) &= q^{-\frac{55}{24}}(5 - 800q + 58'500q^2 + 5'817'125q^3 + 75'474'060'100q^4 + ...),\\
Z_1(q) &= Z_4(q) = q^{-\frac{83}{120}}(8'625 - 1'138'500q + 3'777'474'000q^2 + 3'102'750'380'125q^3 + ...),\\
Z_1(q) &= Z_3(q) = q^{\frac{13}{120}}(-1'218'500 + 441'969'250q + 953'712'511'250q^2 ...).
\end{aligned}$$

All the other numbers can thus be viewed as non-trivial consistency checks, and of course as highly intricate tests of the split attractor flow conjecture.

The following table summarizes the results for BPS indices obtained using split flow trees and DT invariants to this point, and compares them with the predictions from the modular form (for non-polar states, obtained from the knowledge of the polar states) as well as their results obtained by performing a geometric counting for the D4-D2-D0 moduli

space, and then improved by analyzing the degeneracies of the $(0,4)$-MSW-CFT dual states from [99]. The latter is just denoted with the short term 'CFT results' in the following table.

Reduced D0 charge $\hat{q}_0$	Modular form prediction	CFT results	**Split flows and DT**
2.29	+5	+5	+5
1.29	-800	-800	-800
0.69	+8'625	-8'625	+8'625
0.69	+8'625	-8'625	+8'625
0.29	+58'500	+58'500	+58'500
−0.11	-1'218'500	-1'218'500	-1'218'500
−0.31	-1'138'500	+1'138'500	-1'138'500
−0.71	+5'817'125	+5'797'625	+5'797'625
−1.11	+441'969'250	+441'969'250	+441'969'250

It is intriguing to see that our results match the numbers from [99], but do correct some signs. At the same time our and their result differs from the exact prediction from the modular form on one of the states. The next section is devoted to a resolution of this puzzle.

4.3 Flow tree index refinement: non-trivially fibered moduli spaces

The results obtained in the last section are almost fully satisfying. The $\Delta q = 0, \Delta q_0 = -3$ state is the only case where the result expected from modularity was not directly reproduced. The index yields $+5'797'625$, whereas the expected value would be $+5'817'125$. Interestingly enough, this is off by $19'500$, which exactly equals $N_{\mathrm{DT}}(0,2)$ for the quintic. Luckily, careful consideration of the geometry from the D4 perspective does shed some light on this discrepancy. In [79], Gaiotto and Yin calculated this index by refining the geometric counting of the D4-moduli space. They found that the index for this state had two contributions: a D4-brane with three $\overline{\mathrm{D0}}$'s bound to it, and a D4-brane with two degree one rational curves on it. This is analogous to the author and his collaborator's findings. We had a case with a D6/$\overline{\mathrm{D6}}$ split with three $\overline{\mathrm{D0}}$'s bound to one of these two branes, and a case where there is one degree one rational curve on each of the two constituent branes. For the contribution arising from a D4 with three $\overline{\mathrm{D0}}$'s, careful consideration is taken of the fact that the three $\overline{\mathrm{D0}}$'s can be aligned, which enhances the moduli space of the D4-brane. This raises one very interesting question. Does this special *collinear locus* of the three $\overline{\mathrm{D0}}$-branes leave a footprint on the structure of the split flow trees? In other words, does something special happen in the supergravity picture when these branes align?

Based on a supergravity analysis (ignoring validity of the description for the moment), one might expect a scaling solution for this brane system. A possible (although not specifically motivated) speculation is, that the states with collinear $\overline{\mathrm{D0}}$-branes could be quantum

states, that are described as scaling solutions, after taking a classical limit (see subsection 2.3.1). As explained in subsection 2.3.1, these are are multi-centered supergravity solutions that are parametrically connected to single-centered solutions. In other words, the distance between the centers is no longer fixed by the BPS condition, but becomes a modulus. They might correspond to a single flow, but it is also possible, that they do not have an attractor description at all. In any case, we were not able to find any single-centered solutions, or single flows for that matter, corresponding to the $(0, -3)$-state. This may be due to finiteness in the numerical precision of our approach, as every single-centered flow seems to want to go straight through the Gepner point in the CY moduli space. The author and his collaborators do not believe that scaling solutions (or 'quantum partners' of these) lie at the heart of the problem encountered here. A different calculation will reveal the exact way to compute the number of BPS states for the charge system of interest, and it seems unlikely to the author, that there is room in the quantum BPS spectrum for states, that would serve as candidates to become scaling solutions, after taking a classical limit. This will be commented on further in the discussion of this chapter, 4.6.

In the language used in the approach advocated in this thesis, the moduli space of the D4-brane translates into the degrees of freedom of the tachyonic strings stretching between the D6 and the $\overline{\text{D6}}$. The actual number of tachyonic degrees of freedom is computed by the DSZ intersection product. The index factorization scheme does not 'see' this possibility for the three $\overline{\text{D0}}$'s to align. Let this be made more precise.

Suppose one just had a D6 with flux $F_1 = H$, and a $\overline{\text{D6}}$ flux $F_2 = 0$. Then the DSZ intersection product gives 5. This DSZ product is actually computing an index via the Riemann-Roch theorem

$$\int_X \mathrm{ch}(F_2^*)\,\mathrm{ch}(F_1)\,\mathrm{Td}(X) = \int_X \mathrm{ch}(H)\,\mathrm{Td}(X)\,. \tag{4.16}$$

The tachyon field between the two branes is a section of $F_2^* \otimes F_1$, and this index is just counting the basis elements in the space of sections of this bundle. In this case, the general form of the tachyon will be a polynomial of degree one:

$$T = a_1\,x_1 + \ldots + a_5\,x_5\,. \tag{4.17}$$

Hence, one can see where the '5' comes from. After tachyon condensation, a D4-brane will emanate at the locus $T = 0$[7].

Suppose now, that one also turned on an ideal sheaf on the D6, localized at a point p on X. If one computes the DSZ product, which now becomes a Grothendieck-Riemann-Roch type of index, it will actually compute the number of sections of the bundle one had before, tensored with the ideal sheaf. In other words, the index computes the number of independent sections of the bundle $F_2^* \times F_1$ that vanish on the point p. Geometrically, this means that the D4 brane resulting from the condensation will be at the locus $T = 0$, and that this hypersurface will actually pass through p. In this case, the DSZ index gives

[7]From the point of view of the D4 divisor, the moduli space is a projectivization of the moduli space of sections of the tachyon bundle.

4. This reflects the fact that the tachyon field loses one degree of freedom due to the restriction of having to vanish on p.

If one now puts an ideal sheaf localized on three generic points on X, then this will impose three linear constraints on the tachyon field. The index in this case gives 2. However, if these three points happen to be collinear, then the three linear constraints on T are not linearly independent. The DSZ index, analogously to any index, relies on the 'genericity' of the choice of the three points. It only computes a 'virtual' or 'expected' 'dimension' of the tachyon moduli space. In the collinear case, however, the true 'dimension' is 3. That is, the system with three collinear $\overline{\text{D0}}$'s behaves as a system with only two $\overline{\text{D0}}$'s.

When one computes the index in the straightforward fashion, one is not properly taking this special *collinear locus* in moduli space into account. Note that this collinear locus is *not* a singularity of the moduli space. It has nothing to do with having coincident points, which the Donaldson-Thomas invariants automatically take into account.

We therefore proposed a refinement of the prescription

$$Z(A+B) = (-1)^{\langle A,\, B\rangle - 1} |\langle A,\, B\rangle|\, N_{\text{DT}}(A)\, N_{\text{DT}}(B)\,, \tag{4.18}$$

where A and B are D6 and $\overline{\text{D6}}$ states, respectively. In general, the A and B configurations have moduli spaces, $\mathcal{M}_A$, $\mathcal{M}_B$, corresponding to the displacements of the $\overline{\text{D0}}$'s on them, plus the moduli of the Riemann surfaces on which the D2's are wrapped. Alternatively, these are the moduli spaces of the ideal sheaves on the D6 and $\overline{\text{D6}}$. These spaces have Euler characteristics given by the Donaldson-Thomas invariants. The other component of the configuration is the tachyon field T connecting A and B. It has its own moduli space $\mathcal{M}_T$, whose Euler number is computed by means of the DSZ intersection number $|\langle A,\, B\rangle|$, which is nothing other than an Atiyah-Singer topological index. Naively, the full moduli space should be a product

$$\mathcal{M}_{total} = \mathcal{M}_A \times \mathcal{M}_B \times \mathcal{M}_T\,. \tag{4.19}$$

However, in general, the total space will be a non-trivial fibration of $\mathcal{M}_T$ over the other two factors, with the fiber dimension jumping at special loci. This is also explained from the D4-brane point of view in [1]. In the $(0,-3)$ case, the tachyon moduli space is typically a $\mathbb{CP}^1$, and the index is -2. However, whenever the three $\overline{\text{D0}}$'s align, the system behaves effectively like a two-particle state. In this case, the $\mathcal{M}_T$ gets enhanced to a $\mathbb{CP}^2$, and the index should really be $+3$. One can therefore propose to heuristically define what one might refer to as *DT-densities* $\mathcal{N}_{\text{DT}}$ such that w.l.o.g.

$$\int_{\mathcal{M}_A} dz^i\, \mathcal{N}_{\text{DT}}(A,z) = N_{\text{DT}}(A)\,, \tag{4.20}$$

where the z^i are coordinates of the moduli space. Actually, the virtual dimension of these moduli spaces is zero [114], so this integral can be written as a sum:

$$\sum_i \mathcal{N}_{\text{DT}}(A,i) = N_{\text{DT}}(A)\,, \tag{4.21}$$

where the index i labels a sector in the moduli space of the sheaves. One can also give $\mathcal{N}_{\rm DT}(A,i)$ the name of a 'DT partition'. The 'densities' can be thought of as the DT analogs of the top Chern class or the Euler class of a tangent bundle, which integrates over a manifold to give an Euler number. The proper procedure to compute the BPS index is provided by the following refined index:

$$\begin{aligned} Z(\mathcal{M}_{total}) &= \int_{\mathcal{M}_A\times\mathcal{M}_B} dz^i\, dz'^j (-1)^{\langle A,\,B\rangle(z,z')-1} |\langle A,\,B\rangle(z,z')|\, \mathcal{N}_{\rm DT}(A,z')\, \mathcal{N}_{\rm DT}(B,z') \\ &= \sum_{i,i'} (-1)^{\langle A,\,B\rangle_{i,i'}-1} |\langle A,\,B\rangle_{i,i'}|\, \mathcal{N}_{\rm DT}(A,i)\, \mathcal{N}_{\rm DT}(B,i')\,, \end{aligned} \tag{4.22}$$

where $\langle A,\,B\rangle_{i,i'}$ is a function of the moduli.

In the $(0,-3)$ state, the moduli space of the D6 is trivial, and the moduli space $\mathcal{M}_B$ of the $\overline{\rm D6}$ must be divided into two parts, $\mathcal{M}_{B_1}$ and $\mathcal{M}_{B_2}$, where the first part corresponds to the generic configuration of three particles, and the second part corresponds to the subspace where the three particles are aligned, effectively behaving like two particles. Accordingly, one can divide the states consisting of a $\overline{\rm D6}$ and three $\overline{\rm D0}$s into generic states and special states, yielding the *Donaldson-Thomas partitions* [8] for the quintic:

$$\begin{aligned} \mathcal{N}^{(g)}_{\rm DT}(0,3) &= 1'253'500, \\ \mathcal{N}^{(s)}_{\rm DT}(0,3) &= -19'500. \end{aligned} \tag{4.23}$$

This generic states are associated to a tachyon index -2, whereas the special, effective two-particle states are associated to a tachyon index -3. The Witten index for the supersymmetric quantum mechanics of a three particle state on X has the form

$$\chi(X)^3 + \text{corrections for coincidence loci} = -1'234'000\,, \tag{4.24}$$

where $\chi(X) = -200$. The case of a two-particle state has

$$\chi(X)^2 + \text{corrections} = +19'500\,. \tag{4.25}$$

Hence, the two have a relative sign difference. The total refined index Z' (excluding the contribution from the curves) is then given by

$$Z'(0,3) = N_{\rm DT}(0,0) \times \int_{\mathcal{M}_{(0,-3)}} (-1)^{\langle (0,0),\,B\rangle-1} |\langle (0,0),\,B\rangle|\, \mathcal{N}_{DT}(0,3) \tag{4.26}$$

$$= \int_{\mathcal{M}_{B_1}} \mathcal{N}_{DT}(0,3)\, (-1)^{\langle (0,0),\,B_1\rangle-1} |\langle (0,0),\,B_1\rangle| \tag{4.27}$$

$$+ \int_{\mathcal{M}_{B_2}} \mathcal{N}_{DT}(0,3)\, (-1)^{\langle (0,0),\,B_2\rangle-1} |\langle (0,0),\,B_2\rangle| \tag{4.28}$$

$$= -2\,(1'234'000 + 19'500) + -3\,(-19'500) = -2'448'500\,. \tag{4.29}$$

One must therefore equate one flow tree anew:

[8] The partitions are thus 'integrations of the densities' on the generic / special part of moduli space.

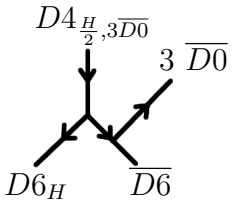

$$= \quad -2'448'500.$$

This means

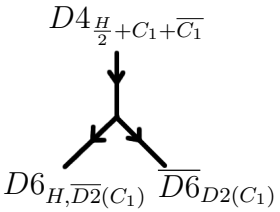

$+$

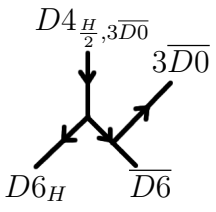

$$= \quad 5'817'125,$$

agreeing with the modular prediction! Note that this disagrees with the result in [79]. Whereas the authors of that paper conclude the same index for the D4-picture version of the state with three $\overline{\text{D0}}$'s, they obtain a different index for the state with the curves, because they applied a Pauli exclusion principle for these two curves. The fact that one did not encounter their problem here has a nice geometrical interpretation: one considered these two curves to lie on different branes (i.e. the D6 and $\overline{\text{D6}}$ as opposed to the D4), so in this case, the Pauli exclusion principle does not apply.

In connection with the split flow conjecture, one can add the following remarks. Every supergravity tree flow corresponds to a family of microscopic states of fixed charges. The moduli space of the latter need not be a product of the moduli spaces of the constituents times the moduli space of the tachyon field, but can be a non-trivial fibration of the latter over the former. Therefore, the index of such states need not be a product of three indices, but will instead be an integral of *index densities* over the moduli spaces of the constituent branes. If the tachyon index is a constant over these moduli spaces, then the integral factorizes, however, it will typically be a *locally constant* function with discontinuous jumps.

4.4 More elliptic genera from split flows and DT invariants

It will now be presented, how one can determine the elliptic genus for two other Calabi-Yau hypersurfaces in weighted projective spaces. Again, numerical algorithms are used to establish the existence of flow trees. The relevant data to obtain such a lattice of points, is available for a certain family of CY hypersurfaces in weighted projective spaces (into which the three present models fall), ready for use, in [111]. The exact functions cannot be written out analytically, so again a grid of points can be evaluated in order to then numerically interpolate the solutions to the Picard-Fuchs equations.

4.4.1 Polar states on the sextic hypersurface in $WC\mathbb{P}^4_{11112}$

In $WC\mathbb{P}^4_{11112}$, the adjunction formula shows that one can obtain a CY hypersurface, by choosing a degree six polynomial. This CY will be referred to as the 'sextic'. The total Chern class reads $c(X) = \frac{(1+H)^4(1+2H)}{1+6H} = 1 + 14H^2 - 68H^3$, and using $\int_X H^3 = \int_{WC\mathbb{P}^{11112}_4} H^4 = 3$, one gets $\chi(X) = -204$. As $\int_X H^3 = 3$, there are three possible classes of gluing vectors (these will correspond to no extra flux, to a flux dual to a degree one, and one dual to a degree two rational curve), the modular vector is in this case three-dimensional:

$$Z(q, \bar{q}, z) = \sum_{\gamma=0}^{2} Z_\gamma(q)\, \Theta_\gamma(\bar{q}, z)\,, \tag{4.30}$$

and, by the identification (2.54), one only needs to determine $Z_0(q)$ and $Z_1(q)$ for a complete knowledge of the elliptic genus on the sextic CY.

For convenience, all DT invariants for the sextic needed are listed in the following table.

Donaldson-Thomas invariants: sextic				
	$\mathbf{n=0}$	$\mathbf{n=1}$	$\mathbf{n=2}$	$\mathbf{n=3}$
$\beta=\mathbf{0}$	1	204	20'298	1'311'584
$\beta=\mathbf{1}$	0	7884	1'592'568	156'836'412
$\beta=\mathbf{2}$	7884	7'636'788	1'408'851'522	136'479'465'324
$\beta=\mathbf{3}$	169'502'712	443'151'185'260	5'487'789'706'776	440'554'251'409'968

1. $\mathbf{\Delta q = 0, \Delta q_0 = 0}$, $\quad [\mathbf{0}, \frac{\mathbf{45}}{\mathbf{24}}]$:
   The pure D4-brane again carries half a unit of flux to ensure anomaly cancellation, and has total charge $\Gamma = H + \frac{H^2}{2} + (\frac{\chi(P)}{24} + \frac{1}{2}F^2)\,\omega = H + \frac{1}{2}H^2 + \frac{3}{4}H^3 = (0, 1, \frac{3}{2}, \frac{9}{4})$, where the notation
   $$\Gamma = (p^0, p, q, q_0), \tag{4.31}$$
   has been introduced, which will be used from now on. This state has $[\gamma, \hat{q}_0] = [0, \frac{45}{24}]$. One finds a split flow tree with centers
   $$\begin{aligned} \Gamma_1 &= (1, 1, \frac{13}{4}, \frac{9}{4}), \\ \Gamma_2 &= (-1, 0, -\frac{7}{2}, 0), \end{aligned}$$
   of the form
   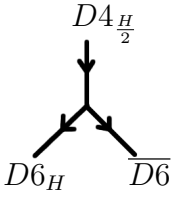

   $= \quad -4.$

This is of course completely analogous to what was found on the quintic. The BPS index for this state reads

$$\Omega = (-1)^{|\langle\Gamma_1,\Gamma_2\rangle|-1}|\langle\Gamma_1,\Gamma_2\rangle|N_{\rm DT}(0,0)\cdot N_{\rm DT}(0,0) = (-1)^3\cdot 4\cdot 1\cdot 1 = -4. \quad (4.32)$$

It is worth pointing out from various viewpoints, how one can understand that the number of BPS states is -4 for the sextic, while the number of most polar states was 5 on the quintic. First of all, in the D4-brane picture, one can easily see that the moduli space of a general hyperplane divisor $H \subset X$ is not a $C\mathbb{P}^4$ as for the quintic, but only a $C\mathbb{P}^3$, and the Euler character yields $\chi(C\mathbb{P}^3) = 4$. This is because the ambient space is a $WC\mathbb{P}^{11112}_4$, and hence the coordinate with weight 2 can of course not be used to define a hyperplane. In the D6-brane picture, the intersection number between Γ_1 and Γ_2 yields 4 (up to a sign), and this can be understood from the viewpoint that one cannot use this very same coordinate to write down a general polynomial describing a tachyon field connecting the two branes (compare with the discussion in the previous section).

2. $\mathbf{\Delta q = 0, \Delta q_0 = -1}$, $\quad [\mathbf{0}, \mathbf{\frac{21}{24}}]$:
Adding one $\overline{\rm D0}$, one gets the total charge $(0, 1, \frac{3}{2}, \frac{5}{4})$, with reduced D0-brane charge $\hat{q}_0 = \frac{21}{24}$. The flow tree is again analogous to what one finds for the quintic (the side of the $\overline{\rm D0}$ after the first split can be chosen, according to where one is with respect to the appropriate threshold wall). The charges of the centers after the first split read

$$\begin{aligned}\Gamma_1 &= (1, 1, \frac{13}{4}, \frac{9}{4}),\\ \Gamma_2 &= (-1, 0, -\frac{7}{4}, -1),\end{aligned}$$

and the flow tree looks like

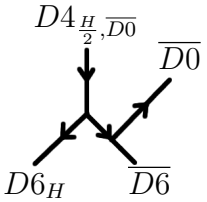

$= \quad 612,$

where of course

$$\Omega = (-1)^{|\langle\Gamma_1,\Gamma_2\rangle|-1}|\langle\Gamma_1,\Gamma_2\rangle|N_{\rm DT}(0,0)\cdot N_{\rm DT}(0,1) = (-1)^2\cdot 3\cdot 1\cdot 204 = 612. \quad (4.33)$$

3. $\mathbf{\Delta q = 1, \Delta q_0 = -1}$, $\quad [\gamma_{\mathbf{1}}, \mathbf{\frac{5}{24}}]$:
One can also consider a flux dual to a degree one rational curve, which includes a gluing vector that one denotes by γ_1. This leads to the total charge $(0, 1, \frac{5}{2}, \frac{5}{4})$, and to the reduced D0-brane charge $\hat{q}_0 = \frac{5}{24}$: thus, adding more $\overline{\rm D0}$ branes, one would already render the state non-polar. One finds the split flow tree with a pure fluxed

D6 on one side, and a $\overline{\text{D6}}$ with a D2 on a degree one rational curve, as one might have expected. The charges read

$$\begin{aligned}\Gamma_1 &= (1, 1, \frac{13}{4}, \frac{9}{4}),\\ \Gamma_2 &= (-1, 0, -\frac{3}{4}, -1),\end{aligned}$$

and the split flow tree is of the form

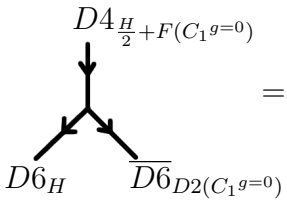

$$= \quad = -15'768.$$

The BPS index is calculated according to

$$\Omega = (-1)^{|\langle\Gamma_1,\Gamma_2\rangle|-1}|\langle\Gamma_1,\Gamma_2\rangle|N_{\text{DT}}(0,0)\cdot N_{\text{DT}}(1,1) = (-1)^1\cdot 2\cdot 1\cdot 7'884 = -15'768. \tag{4.34}$$

Using a basis for modular forms of weight $-\frac{3}{2}$ in a 3d representation, one can use these numbers to determine the modular form (4.30) with

$$Z_0(\tau) = q^{-\frac{45}{24}}(-4 + 612q - 40'392q^2 + 146'464'860q^3...), \tag{4.35}$$

$$Z_1(\tau) = Z_2(\tau) = q^{-\frac{29}{24}}(-15'768q + 7'621'020q^2 + ...). \tag{4.36}$$

This agrees with the findings of [79] (up to an overall sign), which does not come as a surprise, given the small number of polar states and the fact that their enumeration involves no subtleties. It is however very interesting to study some non-polar states for the sextic. This will be one of the topics of the next section, but beforehand, the polar states will be enumerated for another model.

4.4.2 Polar states on the octic hypersurface in $WC\mathbb{P}^4_{11114}$

For $WC\mathbb{P}^4_{11114}$, the adjunction formula shows that one can obtain a CY hypersurface, by choosing a degree eight polynomial. This CY will be referred to as the 'octic'. The total Chern class reads $c(X) = \frac{(1+H)^4(1+4H)}{1+8H} = 1 + 22H^2 - 148H^3$, and using $\int_X H^3 = \int_{WC\mathbb{P}^{11114}_4} H^4 = 2$, one gets $\chi(X) = -296$. As $\int_X H^3 = 2$, the elliptic genus is two-dimensional:

$$Z(q,\bar{q},z) = \sum_{\gamma=0}^{1} Z_\gamma(q)\,\Theta_\gamma(\bar{q},z)\,, \tag{4.37}$$

which means that one needs to determine Z_0 and Z_1. For convenience, the DT invariants of interest (for the octic) are listed in the following table.

Donaldson-Thomas invariants: octic				
	$\mathbf{n=0}$	$\mathbf{n=1}$	$\mathbf{n=2}$	$\mathbf{n=3}$
$\beta=\mathbf{0}$	1	296	43'068	4'104'336
$\beta=\mathbf{1}$	0	29'504	8'674'176	1'253'300'416
$\beta=\mathbf{2}$	564'332	204'456'696	45'540'821'914	6'127'608'486'208
$\beta=\mathbf{3}$	8'775'447'296	6'313'618'655'104	1'225'699'503'521'536	141'978'726'005'461'504

The following report on enumeration of polar states will be quite brief, given the analogy with the previously discussed cases.

1. $\mathbf{\Delta q=0, \Delta q_0=0}$, $\quad [\mathbf{0}, \frac{\mathbf{23}}{\mathbf{12}}]$:
The most polar state is the D4-brane carrying flux $\frac{H}{2}$ for anomaly cancellation, with total charge $(0,1,1,\frac{13}{6})$. The reduced D0-brane charge can be calculated to be $\hat{q}_0=\frac{23}{12}$, and the state can also be denoted by $[\gamma,\hat{q}_0]=[0,\frac{23}{12}]$. One finds a split flow tree with the centers

$$\begin{aligned}\Gamma_1 &= (1,1,1,\frac{13}{6}),\\ \Gamma_2 &= (-1,0,-\frac{11}{6},0),\end{aligned}$$

of the form

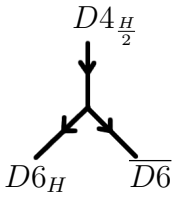

$= \quad -4,$

and the BPS index is calculated as

$$\Omega=(-1)^{|\langle\Gamma_1,\Gamma_2\rangle|-1}|\langle\Gamma_1,\Gamma_2\rangle|N_{\rm DT}(0,0)\cdot N_{\rm DT}(0,0)=(-1)^3\cdot 4\cdot 1\cdot 1=-4. \qquad (4.38)$$

Note that again the fact that the intersection number between Γ_1 and Γ_2 equals -4 corresponds with the fact that one cannot use one of the five coordinates to define a hyperplane, in the D4-picture (and the statement given for the sextic in the D6-picture can be repeated equally).

2. $\mathbf{\Delta q=0, \Delta q_0=-1}$, $\quad [\mathbf{0}, \frac{\mathbf{11}}{\mathbf{12}}]$:
Adding one $\overline{\rm D0}$ yields the total charge $(0,1,1,\frac{7}{6})$, with reduced D0-brane charge $\hat{q}_0=\frac{11}{12}$. The flow tree is again analogous to what was found for the quintic or the sextic (the side of the $\overline{\rm D0}$ after the first split can be chosen, according to the location of the chosen background modulus with respect to the appropriate threshold wall).

The charges of the centers after the first split read

$$\begin{aligned}\Gamma_1 &= (1,1,\frac{17}{6},\frac{13}{6}),\\ \Gamma_2 &= (-1,0,-\frac{11}{6},-1),\end{aligned}$$

and the flow tree is of the form

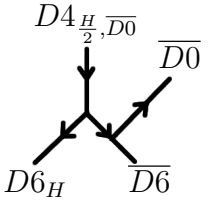

$= \quad 888,$

where of course

$$\Omega = (-1)^{|\langle\Gamma_1,\Gamma_2\rangle|-1}|\langle\Gamma_1,\Gamma_2\rangle|N_{\rm DT}(0,0)\cdot N_{\rm DT}(0,1) = (-1)^2\cdot 3\cdot 1\cdot 296 = 888. \quad (4.39)$$

3. $\mathbf{\Delta q = 1, \Delta q_0 = -1}$, $\quad [\boldsymbol{\gamma_1}, \frac{\mathbf{1}}{\mathbf{6}}]$:
One can now consider a flux dual to a degree one rational curve, also denoted as the gluing vector γ_1. This leads to the total charge $(0,1,2,\frac{7}{6})$, and to the reduced D0-brane charge $\hat{q}_0 = \frac{1}{6}$: thus, there is again only one polar state in this γ_1-class. One finds the split flow tree with a pure fluxed D6 on one side, and a $\overline{\rm D6}$ with a D2 on a degree one rational curve, as one might expect. The charges read

$$\begin{aligned}\Gamma_1 &= (1,1,\frac{17}{6},\frac{13}{6}),\\ \Gamma_2 &= (-1,0,-\frac{7}{6},-1),\end{aligned}$$

with the split flow tree

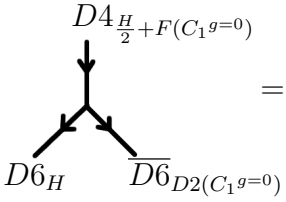

$= \quad -59'008.$

The BPS index is calculated according to

$$\Omega = (-1)^{|\langle\Gamma_1,\Gamma_2\rangle|-1}|\langle\Gamma_1,\Gamma_2\rangle|N_{\rm DT}(0,0)\cdot N_{\rm DT}(1,1) = (-1)^1\cdot 2\cdot 1\cdot 29'504 = -59'008. \quad (4.40)$$

Using the usual techniques, one can use these numbers to determine the modular form (4.37) with

$$Z_0(\tau) = q^{-\frac{23}{12}}(-4+888q-86'140q^2+131'940'136q^3...), \quad (4.41)$$

$$Z_1(\tau) = Z_2(\tau) = q^{-\frac{7}{6}}(-59'008q+8'615'168q^2+...). \quad (4.42)$$

This again agrees with the findings of [79] (up to an overall sign).

4.5 A refined BPS wall-crossing index and Donaldson-Thomas partitions

In this section, non-polar states for the sextic and the octic that demand the use of a refined prescription for the computation of the BPS index for bound states will be discussed. In section 4.3, a refined index was computed for a non-polar BPS state on the quintic 3-fold: the refined computation yielded an exact match with the result predicted from modularity. In subsection 4.5.4, it will also be shown that refinements can also alter the enumeration of polar states. In the cases treated in this section, the reason for the necessity for refined calculations is different, but again, exact agreement is found with the results predicted by modularity, for all tractable examples.

The reason, why refinement is necessary was explained in section 4.3, but it shall be summarized once more. The index for BPS bound states, presented in subsection 3.3.3 is based on the assumption, that the moduli space of a bound state factorizes into the tachyon moduli space, the moduli space of the D6-brane, and the moduli space of the $\overline{\text{D6}}$-brane:

$$\mathcal{M} = \mathcal{M}_{\text{T}} \times \mathcal{M}_{D6} \times \mathcal{M}_{\overline{\text{D6}}}. \tag{4.43}$$

To compute an index, one thus uses

$$\underbrace{(-1)^{|\langle\Gamma_1,\Gamma_2\rangle|}|\langle\Gamma_1,\Gamma_2\rangle|}_{\mathcal{M}_{\text{T}}} \quad \cdot \quad \underbrace{N_{\text{DT}}(\beta_1,n_1)}_{\mathcal{M}_{D6}} \quad \cdot \quad \underbrace{N_{\text{DT}}(\beta_2,n_2)}_{\mathcal{M}_{\overline{\text{D6}}}},$$

where $(-1)^{|\langle\Gamma_1,\Gamma_2\rangle|}|\langle\Gamma_1,\Gamma_2\rangle|$ and $\mathcal{I}_{\text{T}}$ (the index of the tachyon moduli space) agree up to a sign.

In general, this moduli space is non-trivially fibered, and thus the dimensionality of the fiber jumps. As a consequence, this index is not always accurate: it computes a virtual dimension, [106], which does not always equal the real dimension of the moduli space. The reason is basically, that tachyonic strings gluing together the bound state do not perceive all the constituent states 'generically'. For simplicity, the discussion will be restricted for now to the case that only one of the two constituents is not perceived generically, namely the $\overline{\text{D6}}$-consistuent. We will also focus on the case, where $\overline{\text{D0}}$-branes are not perceived generically by the tachyon fields, although it will be shown for an example, that an analogous phenomenon holds for special D2-states (and the curves on which these are wrapped). Generalizations of the presented scheme will become clear from examples later on in this section.

The moduli space of a BPS bound state splits up, and can be grouped into two pieces:

$$\mathcal{M} = \mathcal{M}_{\text{T}_g} \times \mathcal{M}_{D6} \times \mathcal{M}_{\overline{\text{D6}}_g} \qquad \oplus \qquad \mathcal{M}_{\text{T}_s} \times \mathcal{M}_{D6} \times \mathcal{M}_{\overline{\text{D6}}_s}. \tag{4.44}$$

The first part, with the subscripts 'g' stands for the part, where the tachyon fields perceive the constituent states 'generically', and hence the virtual dimension of $\mathcal{M}_{\text{T}}$ is actually the real dimension, and the part with the subscripts 's' stands for the part, where the tachyon

fields perceive the constituent states as 'special states' (in the present studies, the special states will always concern the $\overline{\text{D6}}$-system). This usually happens, because the tachyon fields do not perceive all $\overline{\text{D0}}$'s, that are bound to the $\overline{\text{D6}}$, which results in a *constraint loss* on the tachyon field T. For example, generically three $\overline{\text{D0}}$'s mean that the independent sections have to vanish at three points. If the tachyon is 'blind' to one of the three, this number is reduced to two, resulting in a jump in the dimension of the fiber of the moduli space of the bound state. Typically, the dimension of $\mathcal{M}_{\text{T}_s}$ will thus be greater by one, as opposed to $\mathcal{M}_{\text{T}_g}$.

In section 4.3, it was proposed to define Donaldson-Thomas densities (in analogy to a top Chern class), which integrate over moduli space to a Donaldson-Thomas invariant. This allows the definition of a product formula for the bound state index, on the level of index densities. One can also decide to integrate these densities on the various partitions of moduli space, with a constant dimension of the fiber of the tachyon moduli space: this leads to *Donaldson-Thomas partitions* (DT partitions). They separately enumerate generic and special D6-D2-D0 states, and a series of examples of such DT partitions will be calculated. Using these, one can write down, how refined indices come about:

$$\underbrace{(-1)^{|\langle\Gamma_1,\Gamma_2\rangle|}|\langle\Gamma_1,\Gamma_2\rangle|}_{\mathcal{M}_{\text{T}_g}} \cdot \underbrace{N_{\text{DT}}(\beta_1,n_1)}_{\mathcal{M}_{D6}} \cdot \underbrace{\mathcal{N}^{(g)}_{\text{DT}}(\beta_2,n_2)}_{\mathcal{M}_{\overline{\text{D6}}_g}}$$
$$+ \underbrace{(-1)^{|\langle\Gamma_1,\Gamma_2\rangle|}||\langle\Gamma_1,\Gamma_2\rangle|+1|}_{\mathcal{M}_{\text{T}_s}} \cdot \underbrace{N_{\text{DT}}(\beta_1,n_1)}_{\mathcal{M}_{D6}} \cdot \underbrace{\mathcal{N}^{(s)}_{\text{DT}}(\beta_2,n_2)}_{\mathcal{M}_{\overline{\text{D6}}_s}}.$$

Before giving explicit examples, a more detailed instruction will now be presented on how to separate the 'generic' from the 'special' states, thereby resulting in a calculation of Donaldson-Thomas partitions.

4.5.1 Algebraic techniques to deal with special constituent states

In the case of the quintic, $D4-3\overline{\text{D0}}$ states had to be treated more carefully, because the tachyon fields of a D6-($\overline{\text{D6}}$-3$\overline{\text{D0}}$)-bound states do not perceive three *collinear* $\overline{\text{D0}}$'s generically. Rather, they appear only as two particles. In terms of algebraic geometry, this is simple to express: the three constraints on the tachyon field are not independent (only two of them are independent). For the following examples, *constraint loss* occurs for two reasons, which shall be referred to as 'special loci', and as 'special tangent directions' (which are important when blowups are performed, required for dealing with coincident loci for two $\overline{\text{D0}}$'s). The special loci appear because the Calabi-Yau varieties are embedded in weighted projective spaces, which means that there is not a complete democracy amongst coordinates: If a $\overline{\text{D0}}$ sits at a position with non-zero coordinates of a higher weight only, it will not impose a constraint on the tachyon, as the higher weight coordinates cannot be included in the definition of the tachyon map.

1. **Constraint loss because of special loci**
   For simplicity, consider a CY embedded in $WC\mathbb{P}^4_{1111n}$ with $n>1$ using coordinates

$(x_1, ..., x_5)$, and a bound state of a D6-brane with flux $F = H$ (one unit of flux), and a $\overline{\text{D6}}$ without flux. In this case, H is a line bundle of which the coordinates x_i form sections. However, x_5 is forbidden as a section, as it has a higher weight. This means, that there are only four instead of five independent sections for the tachyon $T \in \Gamma(H)$ (F_2^* is the trivial bundle in this case). The most general tachyon field reads $T = a_1x_1 + ... + a_4x_4$. In general, placing a $\overline{\text{D0}}$ on the $\overline{\text{D6}}$ means imposing one constraint on the tachyon field. A good way to think about this, is by treating the $\overline{\text{D0}}$ on the $\overline{\text{D6}}$ with point particle quantum mechanics, (check [115]). If one puts the particle at $x_5 = 1$ (and all other coordinates zero) it will not impose a constraint on the tachyon. This might be of relevance and it might not: one still has to check whether this point actually lies on the Calabi-Yau. This will be the case for examples investigated in this section.

2. **Constraint loss because of special tangent directions**
An additional complication arises, as soon as one considers two (or more) $\overline{\text{D0}}$-particles: orbifold singularities arise, when particles meet. This is dealt with by performing a blowup, which imposes a distinction between the particles, that inhabit the same spot on the brane (and hence on the CY). One can intuitively picture this, as considering an infinitesimally short time period before they meet, and distinguishing the particles upon all the different tangent directions (which of course have to be tangent directions to the Calabi-Yau variety under consideration), from which the two particles can approach each other. Two particles lying on the same spot in the Calabi-Yau would originally only impose one constraint on the tachyon field, according to the previous discussion. After performing a blowup, an additional constraint arises, from the splitting through the tangent direction. This means, that the tachyon moduli space fiber does not jump (at least generically) for states, where particles lie at the same locus. The point is: it *can* jump, though. Namely, one (or several) tangent directions might be built from coordinates, that do not impose constraints. Thus, also after performing blowups, one still has to distinguish between generic and special states of particles, that lie at coincident loci.

Let the two situations when special states occur (in this case for $\overline{\text{D0}}'s$) be summarized once more:

- For non-coincident $\overline{\text{D0}}'s$, one needs to check whether the particles lie at 'special loci', where they do not impose a constraint on the tachyon fields. One could refer to these cases as the *special non-blowup loci*.

- For a bound state, there are cases, when various $\overline{\text{D0}}$'s are coincident: in this case one needs to perform blowups. These blown-up states have to be separated into generic and special states, according to whether the tangent direction (arising from the blowup) imposes a constraint on the tachyon fields or not. One might refer to these latter cases as the *special blowup loci*.

As will become clear from an example later on, analogous implications arise for bound D2-branes, depending on whether the curves (on which those branes are placed) impose 'enough' constraints on the tachyon fields (to make the bound state 'generic').

4.5.2 Special points and DT partitions $\mathcal{N}_{\mathbf{DT}}^{(g,s)}(0,2)$

In the following, a few interesting non-polar states on the sextic and the octic CY's for which the elliptic genera were predicted in the previous section, are examined. The refined caculations match the predictions from modularity.

The state $\mathbf{\Delta q = 0, \Delta q_0 = -2}$ on the sextic

For this charge system, one finds a split flow tree with centers

$$\begin{aligned}\Gamma_1 &= (1,1,\frac{13}{4},\frac{9}{4}),\\ \Gamma_2 &= (-1,0,-\frac{7}{4},-2),\end{aligned}$$

of the form

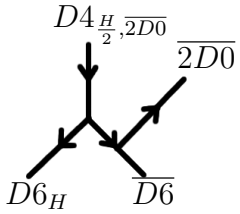

$$= \quad -2 \cdot 20'298 = -40'596,$$

and obviously, the index obtained naively Ω_{naive} differs from the exact index, which is given by $\Omega_{\text{exact}} = -40'392$. This can be put right, using the refined index, as the non-trivially fibered moduli space of this bound state dictates.

One can either argue from the D6-picture, or from a purely algebraic geometrical D4-perspective. Essentially the two arguments are identical. In the first picture, one places two $\overline{\text{D0}}$-branes on the D4, in the second case, one chooses two point-like sheaves to lie on the vanishing locus of the polynomial describing the tachyon.

As discussed before, for the most polar state, the most general tachyon map is of the form

$$T = a_1 x_1 + ... a_4 x_4 = 0, \tag{4.45}$$

choosing coordinates $(x_1, ..., x_4, x_5)$ on $WC\mathbb{P}^4_{11112}$ transforming with weights $(1,1,1,1,2)$. Setting two $\overline{\text{D0}}$-branes on the $\overline{\text{D6}}$ means that the map has to 'pass' through two points, so in general, the moduli space of the tachyon will be reduced to from $C\mathbb{P}^3$ to $C\mathbb{P}^1$, yielding $\chi(C\mathbb{P}^1) = 2$. This is where the intersection number 2 comes from. It will now be shown that the dimension of this fiber jumps (as was observed for a state on the quintic 3-fold, though it happens for a different reason. One might remark, that two $\overline{\text{D0}}$-particles behave

as one, on a specific 'special' locus. The scheme is to analyze the remaining moduli describing this tachyon, demanding that two points as well as the tangent directions at these points lie on the CY, as well as on the zero locus of the tachyon.

Finding special tangent directions arising from blowups

For the cases, when constraint loss on the tachyon matrix happens because of *special tangent directions*, in other words, for special blowup loci, one needs to be able to determine which tangent directions are special.

Generically, demanding two points to lie in the zero of (4.45), imposes two independent constraints, reducing the number of moduli by two. Denote the coordinates of the two points by $x_i^{P_1}$ and $x_i^{P_2}$. This is not that clear if the two points lie on top of each other $x_i^{P_1} = x_i^{P_2}$. However, this is generically resolved by the blowup procedure, rendering the tangent directions of the particles independent, again leading to two constraints. However, as one is working with a weighted projective space, the coordinate x_5 does not appear in (4.45). Different x_5-coordinates are not 'seen' by the tachyon. The points do however have to lie on the sextic, for which one can choose a representative given by a transverse polynomial, [116],

$$p_{\text{sextic}} = x_5^3 + p^{(6)}(x_1, x_2, x_3, x_4) = 0. \tag{4.46}$$

That means that the case $x_5^{P_1} = 1^{\frac{k}{3}} x_5^{P_2}$ for $k = 0, 1, 2$ with all other coordinates equal $x_i^{P_1} = x_i^{P_2}$ for $i = 1, 2, 3, 4$ is possibly of interest.

If the first four coordinates of the two points are identical, this amounts to imposing only one instead of two constraints on the tachyon field. After the usual blowup procedure (as explained above), the particles are however *distinguished by a tangent direction, which can be interpreted as the direction from which they 'approach' each other.*

Consider thus a tangent vector $X^i \partial_i$, and demand that it is indeed a direction tangent to the sextic CY;

$$\nabla_X p_{\text{sextic}} = 0, \tag{4.47}$$

but it also acts on (4.45)

$$\nabla_X T = X^1 a_1 + ... + X^4 a_4. \tag{4.48}$$

This equation is like a second constraint. The particles are in general distinguished after a blowup. This is also the reason why a coincident locus does not in general lead to a jump in the tachyon fiber above that locus. Namely, (4.48) does not lead to an extra constraint, iff

$$\text{rank} \begin{pmatrix} x_1 & x_2 & x_3 & x_4 \\ X^1 & X^2 & X^3 & X^4 \end{pmatrix} < 2, \tag{4.49}$$

which can happen if either $X^1 = ... = X^4 = 0$ or if $X^i = \lambda x_i$. It will be shown where this can happen in the present case. One can distinguish between

- $x_5 \neq 0$: This means one can choose affine coordinates with $x_5 = 1$. Thus, in these coordinates, one knows that $X^5 = 0$ for the tangent vector (and hence the case

$X^1 = ... = X^4 = 0$ is ruled out and only the case $X^i = \lambda x_i$ remains). The tangent vectors should remain in the CY, (4.47), which leads to $6\lambda p^{(6)} = 0$. Differentiating with respect to x_5 yields $p^{(6)} = 0$, which would imply $x_5 = 0$ upon plugging this into (4.46). If $x_5 \neq 0$, the two particles are distinguished after the blowup.

- $x_5 = 0$: In this case, fix (w.l.o.g.) $x_1 = 1$. This means $X^1 = 0$ for the tangent vector. To have only one instead of two 'constraint' equations for the tachyon, one thus needs $X^1 = ... = X^4 = 0$. This occurs when the tangent vector equals $X^5\partial_5$, which is possible at the locus $x_5 = 0$. Note that there is *one* tangent direction for which this occurs. This is where the fiber of the tachyon jumps and needs to be taken into account.

Calculating the refined index

Starting from the naive form for the index of this bound state,

$$\chi(\text{two particles}) \cdot \chi(\text{tachyon}) = \chi(X)^2 \cdot \chi(C\mathbb{P}^1) + \text{corrections}, \tag{4.50}$$

one can see nicely, how the refinement comes in. The refined index receives the following contributions (where $\chi(X) = -204$ denotes the Euler character of the sextic).

- $\frac{1}{2}(\chi(X)^2 - 3\chi(X) + 2\chi_0) \cdot \chi(C\mathbb{P}^1)$: this is the generic locus, where the two particles are separated, but the locus where the two particles are identical as well as the locus where $x_i^{P_1} = x_i^{P_2}$ for $i = 1, 2, 3, 4$ and $x_5^{P_1} = 1^{\frac{k}{3}} x_5^{P_2}$ for $k = 0, 1, 2$ have been substracted. Note that one has to be careful not to substract the locus where the first four coordinates are identical and $x_5 = 0$ more than once. This has been taken into account with the $+2\chi_0$ term. The Euler character χ_0 of the locus $x_5 = 0$ can be calculated from the adjunction formula and is found to be $\chi_0 = 108$.

- $(\chi - \chi_0) \cdot \chi(C\mathbb{P}^2) \cdot \chi(C\mathbb{P}^1)$: this accounts for the locus where the two $\overline{\text{D0}}$'s coincide, without the locus $x_5 = 0$. Note that the $\chi(C\mathbb{P}^2)$ results from the blowup of a codimension 3 locus.

- $2 \cdot \frac{1}{2}(\chi - \chi_0) \cdot \chi(C\mathbb{P}^2)$: this takes into account the loci where $x_5^{P_1} = 1^{\frac{k}{3}} x_5^{P_2}$ for $k = 1$ and $k = 2$ (hence the overall factor of two, as these loci both contribute equally). Note that the fiber of the tachyon has jumped, these two particles are seen as one.

- $\chi_0 \cdot (\chi(C\mathbb{P}^2) - 1) \cdot \chi(C\mathbb{P})^1$: here, the locus $x_5 = 0$ is dealt with. In principle one just has to do a blowup of a codimension 3 locus (hence a factor of $\chi(C\mathbb{P}^2)$. After the blowup, the tachyon in principle 'sees' two $\overline{\text{D0}}$'s. However, one needs to substract the one tangent direction found in the analysis above, because one loses one of the two constraints on the tachyon. This one tangent direction is taken into account on the next line.

- $\chi_0 \cdot 1 \cdot \chi(C\mathbb{P})^2$: for this one blowup direction (for which the 1 stands for as an index), the tachyon again sees only one particle.

Note that had one ignored the subtlety with the locus x_5, one would have retrieved the calculation where one finds a product of the tachyon index 2, and the Donaldson-Thomas invariant $N_{\rm DT}(0,2)$. Collecting all the pieces linked to the value 2 or 3 for the tachyon index (up to a sign), one can state the correct index in the form

$$\Omega_{\rm exact} = -2 \cdot (20'298 + 204) - 3 \cdot (-204) = -40'392. \tag{4.51}$$

This allows the stating of the *Donaldson-Thomas partitions* $\mathcal{N}_{DT}^{(g,s)}(0,2)$ *for the sextic*:

$$\mathcal{N}_{\rm DT}^{(g)}(0,2) = 20'504, \tag{4.52}$$

$$\mathcal{N}_{\rm DT}^{(s)}(0,2) = -204. \tag{4.53}$$

$\mathcal{N}_{\rm DT}^{(g)}(0,2)$ counts the generic D6-2$\overline{\rm D0}$ BPS states, for which the tachyon perceives two $\overline{\rm D0}$'s, and $\mathcal{N}_{\rm DT}^{(s)}(0,2)$ counts the special D6-2$\overline{\rm D0}$ BPS states, for which the tachyon perceives only one $\overline{\rm D0}$-brane. Note that there is a sign difference between these indices.

$$N_{\rm DT}(0,2) = \mathcal{N}_{\rm DT}^{(g)}(0,2) + \mathcal{N}_{\rm DT}^{(s)}(0,2). \tag{4.54}$$

On the octic, one finds a state that behaves similarly.

The state $\Delta q = 0, \Delta q_0 = -2$ on the octic

For this charge system, one finds a split flow tree with centers

$$\Gamma_1 = (1,1,1,\frac{13}{6}),$$

$$\Gamma_2 = (-1,0,-\frac{11}{6},-2),$$

of the form

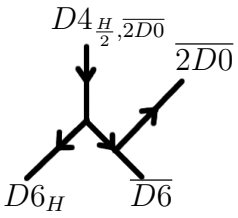

$$= \quad -2 \cdot 43'068 = -86'136.$$

For the octic, one can choose

$$p_{\rm octic} = x_5^2 + p^{(8)}(x_1,x_2,x_3,x_4) = 0 \tag{4.55}$$

as a transverse polynomial. This time, the cases where the particles have four equal coordinates, and where $x_5^{P_1} = 1^{\frac{k}{2}} x_5^{P_2}$, are possibly of interest. The analysis of the locus, where the tachyon field perceives the BPS state with two $\overline{\rm D0}$'s differently and where the fiber changes dimension is analogous to the sextic case, and the discussion will therefore be brief. One again starts by searching for the 'special tangent directions', by considering (4.49):

- $x_5 \neq 0$: This means one can choose affine coordinates with $x_5 = 1$. Again, one knows that $X^5 = 0$ for the tangent vector (and hence the case $X^1 = ... = X^4 = 0$ is ruled out and only the case $X^i = \lambda x_i$ remains). The tangent vectors should remain in the CY, which leads to $8\lambda p^{(8)} = 0$. $p^{(8)} = 0$ would imply $x_5 = 0$, contradicting the first assumption.

- $x_5 = 0$: In this case, fix (w.l.o.g.) $x_1 = 1$. This means $X^1 = 0$ for the tangent vector. To have only one instead of two 'constraint' equations for the tachyon, one thus needs $X^1 = ... = X^4 = 0$. This occurs when the tangent vector equals $X^5\partial_5$, which is possible at the locus $x_5 = 0$. Note that there is again *one* tangent direction for which this occurs. This is where the fiber of the tachyon jumps and needs to be taken into account.

Calculating the exact index

The index receives similar contributions to the case on the sextic, but the calculation is slightly simpler.

- $\frac{1}{2}(\chi(X)^2 - 2\chi(X) + \chi_0) \cdot \chi(C\mathbb{P}^1)$: this again is the generic locus, but as in this case $x_5^{P_1} = 1^{\frac{k}{2}} x_5^{P_2}$ for $k = 0, 1$ one substracts two instead of three loci with index $\chi(X)$. Instead of substracting the locus $x_5 = 0$ three times, one does this twice, and needs to compensate once. In this case, $\chi_0 = 304$.

- $(\chi - \chi_0) \cdot \chi(C\mathbb{P}^2) \cdot \chi(C\mathbb{P}^1)$: this accounts for the locus where the two $\overline{\text{D0}}$'s coincide, without the locus $x_5 = 0$. Note that the $\chi(C\mathbb{P}^2)$ results from the blowup of a codimension 3 locus.

- $\frac{1}{2}(\chi - \chi_0) \cdot \chi(C\mathbb{P}^2)$: this takes into account the locus where $x_5^{P_1} = -x_5^{P_2}$. This is again a locus where the tachyon index has jumped.

- $\chi_0 \cdot (\chi(C\mathbb{P}^2) - 1) \cdot \chi(C\mathbb{P})^1$: here, the locus $x_5 = 0$ is dealt with. In principle one just has to do a blowup (hence a factor of $\chi(C\mathbb{P}^2)$. After the blowup, the tachyon in principle 'sees' two $\overline{\text{D0}}$'s. Again, one needs to substract the one tangent direction one found in the analysis above, because one loses one of the two constraints on the tachyon. This tangent direction is taken into account on the next line.

- $\chi_0 \cdot 1 \cdot \chi(C\mathbb{P})^2$: for this one blowup direction, the tachyon again sees only one particle.

Collecting all the pieces linked to the value 2 or 3 for the tachyon index (up to a sign), one can state the correct index in the form

$$\Omega_{\text{exact}} = -2 \cdot 43'064 + 3 \cdot (-4) = -86'140. \tag{4.56}$$

This means, that the *Donaldson-Thomas partitions* $\mathcal{N}_{DT}^{(g,s)}(0,2)$ *for the octic* read:

$$\mathcal{N}_{\text{DT}}^{(g)}(0,2) = 43'064, \tag{4.57}$$

$$\mathcal{N}_{\text{DT}}^{(s)}(0,2) = -4. \tag{4.58}$$

Note that the sum of the partitions yields $N_{\text{DT}}(0,2)$.

4.5.3 Special curves and DT partitions $\mathcal{N}_{\mathbf{DT}}^{(g,s)}(1,2)$

Up until now, refinements were presented, which were necesary due to the fact, that the tachyon fields did not perceive $\overline{\mathrm{D0}}$'s generically. An example will be given now, where an analogous refinement is necessary because of the fact, that a D2/D0-state (with the D2 wrapped on a curve) is not perceived generically. A different way of expressing this is to state, that there are *special $D2/D0$ bound states*, or again put differently, one might refer to these states as *special curves* on CY manifolds.

The state $\mathbf{\Delta q = 1, \Delta q_0 = -2}$ on the octic

For this charge system, one finds a split flow tree with centers

$$\begin{aligned}\Gamma_1 &= (1,1,\frac{17}{6},\frac{13}{6}),\\ \Gamma_2 &= (-1,0,-\frac{7}{6},-2),\end{aligned}$$

of the form

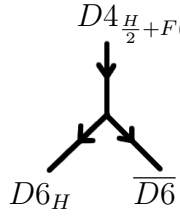

$$= \quad -8'674'176,$$

with an index naively calculated as

$$\Omega = (-1)^{|\langle\Gamma_1,\Gamma_2\rangle|-1}|\langle\Gamma_1,\Gamma_2\rangle|N_{\mathrm{DT}}(0,0)\cdot N_{\mathrm{DT}}(1,2) = (-1)^0\cdot 1\cdot 1\cdot 8'674'176 = 8'674'176. \quad (4.59)$$

This naive index needs refinement again. In this case, for simplicity, choose the Fermat–polynomial for the octic:

$$p_{\mathrm{octic}} = x_5^2 + x_1^8 + x_2^8 + x_3^8 + x_4^8 = 0 \quad (4.60)$$

A degree one rational curve on the octic can be represented as a degree one map from $C\mathbb{P}^1$ to the Calabi–Yau. Consider for example the map

$$(s,t) \to (s, \mathrm{i}s, t, \mathrm{i}t, 0). \quad (4.61)$$

This generically imposes two constraints on the tachyon field, reducing its moduli space to $C\mathbb{P}^1$. Adding an extra D–particle will then reduce this moduli space to $C\mathbb{P}^0$, unless something special happens:

- The particle ($\overline{\mathrm{D0}}$) lies on the curve, but nevertheless produces no extra constraint. It is easy to verify that this cannot possibly happen for this example.

- The particle lies on the curve, which means that a blowup needs to be performed, in the directions normal to the curve. Again, one might encounter special tangent directions, which do not impose an extra constraint on the tachyon. Following a similar procedure to the previous examples, one can indeed verify that this is the case for the direction $X^5\partial_5$. As $x_5 = 0$ lies on the curve (4.61), this direction is automatically also tangent to the octic.

Calculating the exact index

The various contributions to the exact index according to the refined prescription read:

- $N_{DT}(1,1)(\chi(X) - \chi_C)\chi(C\mathbb{P}^0)$, where $\chi_C = 2$ is the Euler characteristic of the curve. This term deals with the case, when the $\overline{\text{D0}}$ is placed at a locus different from the curve, thereby reducing the tachyon moduli space to $C\mathbb{P}^0$.

- $N_{DT}(1,1)\chi_C[\chi(C\mathbb{P}^1)-1]\chi(C\mathbb{P}^0)$, dealing with the case, when the $\overline{\text{D0}}$ is located on the curve, but the blowup tangent direction leads to an extra constraint on the tachyon.

- $N_{DT}(1,1)\chi_C \cdot 1 \cdot \chi(C\mathbb{P}^1)$, which deals with the case, when the $\overline{\text{D0}}$ lies on the curve, and a blowup is performed leading to a special tangent direction. This is an example of what was referred to as a special D2/D0 bound state, or alternatively just as a special curve. In this case, the tachyon field moduli space remains a $C\mathbb{P}^1$.

In total, this leads to the index

$$\Omega_{\text{exact}} = |1 \cdot (-8'733'184) + 2 \cdot (59'008)| = 8'615'168. \tag{4.62}$$

Spectacularly, by comparing this number to the prediction from modularity, (4.41), one also finds exact agreement for this case. One can thus state the *Donaldson-Thomas partitions* $\mathcal{N}_{DT}(1,2)$ *for the octic*:

$$\mathcal{N}^{(g)}_{\text{DT}}(1,2) = -8'733'184, \tag{4.63}$$
$$\mathcal{N}^{(s)}_{\text{DT}}(1,2) = 59'008. \tag{4.64}$$

Again, note that the sum of the partitions yields $N_{\text{DT}}(1,2)$.

To summarize, one can conclude that all results obtained in this section provide exact agreement with the predictions from modularity. This clearly is strong evidence, that the suggested procedure for computing refined bound state indices is indeed correct. These results also provide a non-trivial and successful test for the split attractor flow conjecture. In the next subsection, states on another CY-manifold will be be discussed, for which a non-polar state also requires calculation of a refined bound state index.

4.5.4 Refined predictions for elliptic genera

In this subsection, it will be shown how a refined index computation alters the prediction for an elliptic genus of a CY, realized as a degree ten hypersurface in $WC\mathbb{P}^4_{11125}$. One can choose coordinates $(x_1, ..., x_4, x_5)$, corresponding to the weights $(1, 1, 1, 2, 5)$. This CY will be referred to as the *decantic*, in the following. The total Chern class of this space reads $c(X) = \frac{(1+H)^4(1+2H)(1+5H)}{1+10H} = 1 + 34H^2 - 288H^3$, and using $\int_X H^3 = \int_{WC\mathbb{P}^{11125}_4} H^4 = 1$, one obtains $\chi(X) = -288$. Again, a D4-brane is wrapped on the hyperplane class divisor $P = H$. For the lattice of fluxes, one finds in this case, that the pullback $L_X = i_P^*(H^2(X, \mathbb{Z})$ and it's orthogonal complement, $L_X \oplus L_X^\perp$, are already unimodular, thus no gluing vectors exist, and the elliptic genus is a 'one-dimensional vector',

$$Z(q, \bar{q}, z) = Z_0(q)\, \Theta_0(\bar{q}, z)\,. \tag{4.65}$$

The list of DT invariants of interest is again stated for convenience.

Donaldson-Thomas invariants: decantic				
	$\mathbf{n=0}$	$\mathbf{n=1}$	$\mathbf{n=2}$	$\mathbf{n=3}$
$\beta = \mathbf{0}$	1	288	40'752	3'774'912
$\beta = \mathbf{1}$	1150	435'827	89'103'872	11'141'118'264
$\beta = \mathbf{2}$	-64'916'198	40'225'290'446	9'325'643'249'563	1'119'938'319'168'004

1. $\mathbf{\Delta q = 0, \Delta q_0 = 0}$, $\quad [\mathbf{0}, \frac{\mathbf{23}}{\mathbf{12}}]$:
   As usual, the most polar state is the D4-brane carrying flux $\frac{H}{2}$ for anomaly cancellation, with total charge $(0, 1, \frac{1}{2}, \frac{19}{12})$. The reduced D0-brane charge can be calulcated to be $\hat{q}_0 = \frac{35}{24}$, thus the state lies in the class $[0, \frac{35}{24}]$. One finds a split flow tree with centers

$$\begin{aligned} \Gamma_1 &= (1, 1, \frac{23}{12}, \frac{19}{12}), \\ \Gamma_2 &= (-1, 0, -\frac{17}{12}, 0), \end{aligned}$$

   with split flow tree

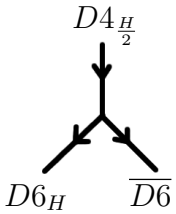

$= \quad 3,$

   where the BPS index is calculated according to

$$\Omega = (-1)^{|\langle\Gamma_1,\Gamma_2\rangle|-1}|\langle\Gamma_1, \Gamma_2\rangle| N_{\mathrm{DT}}(0,0) \cdot N_{\mathrm{DT}}(0,0) = (-1)^2 \cdot 3 \cdot 1 \cdot 1 = 3. \tag{4.66}$$

   As usual, the number 3 can be nicely understood along the lines of previous explanations. In $WC\mathbb{P}^4_{11125}$ one can only use three coordinates to define a hyperplane, and $\chi(C\mathbb{P}^2) = 3$, so the correspondence between divisor moduli in the D4-picture and tachyonic degrees between the D6 and the $\overline{\mathrm{D6}}$ again works out nicely.

2. $\mathbf{\Delta q = 0, \Delta q_0 = -1}$, $\quad [\mathbf{0}, \mathbf{\frac{11}{24}}]$:
Adding one $\overline{\text{D0}}$, one obtains the total charge $(0, 1, \frac{1}{2}, \frac{7}{12})$, with reduced D0-brane charge $\hat{q}_0 = \frac{11}{24}$. The flow tree is again analogous to the previous findings, the side of the $\overline{\text{D0}}$ after the first split governed by the appropriate threshold wall. The charges of the centers after the first split read

$$\begin{aligned} \Gamma_1 &= (1, 1, \frac{23}{12}, \frac{19}{12}), \\ \Gamma_2 &= (-1, 0, -\frac{17}{12}, -1), \end{aligned}$$

and the flow tree looks like

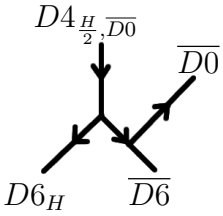

$= \quad -576,$

from which one is tempted to conclude

$$\Omega = (-1)^{|\langle\Gamma_1,\Gamma_2\rangle|-1}|\langle\Gamma_1,\Gamma_2\rangle| N_{\text{DT}}(0,0) \cdot N_{\text{DT}}(0,1) = (-1)^1 \cdot 2 \cdot 1 \cdot 288 = -576. \quad (4.67)$$

Using these two polar degeneracies, the elliptic genus would be determined by

$$Z_0(\tau) = q^{-\frac{35}{24}}(3 - 576q + 271'704q^2 + 206'401'533q^3 + 21'593'767'647q^4 ...), \quad (4.68)$$

which agrees with the findings in [79]. It will now be argued that this is not quite correct, and the (essential part of the) elliptic genus will be predicted to be

$$Z_0(\tau) = q^{-\frac{35}{24}}(3 - 575q + 271'955q^2 + 206'406'410q^3 + 21'593'817'025q^4 ...). \quad (4.69)$$

The reason for this lies in the fact that the index (4.67) is not correct, because the state $\Delta q = 0, \Delta q_0 = 1$ has a non-trivially fibered moduli space. This will allow the calculation of partitions of $N_{\text{DT}}(0, 1)$ for the decantic.

DT partitions $\mathcal{N}^{(g,s)}_{\mathbf{DT}}(0,1)$: generic and special D6-$\overline{\text{D0}}$ states

Note that the tachyon map for the most polar state is a section of the bundle H, and is of the general form

$$T = a_1 x_1 + ... a_3 x_3 = 0, \quad (4.70)$$

as the coordinates x_4 and x_5 are 'forbidden' (weight too high). This yields a moduli space with Euler character $\chi(C\mathbb{P}^2) = 3$, accounting for the degeneracy of the most polar state. If one adds a $\overline{\text{D0}}$-brane to the system, the tachyon map has to vanish on an additional point.

Inserting this in (4.70) generically eliminates one of the moduli, reducing to a tachyon moduli space with Euler character $\chi(C\mathbb{P}^2) = 3$. The problem is that one can place the $\overline{\text{D0}}$-brane at the locus $x_1 = x_2 = x_3 = 0$, which is indeed a point lying on the decantic X. Placing the $\overline{\text{D0}}$ on this point, means that this 'particle' will not imply a constraint on (4.70). The Euler character of this locus ($x_1 = x_2 = x_3$) χ_0 can easily be determined: $\chi_0 = 1$ (this is trivial, as the locus is just a point).

Thus, the correct index for the $\Delta q = 0, \Delta q_0 = -1$ system reads as follows:

$$\Omega = 2 \cdot (\chi(X) - \chi_0) + 3 \cdot \chi_0 = -575. \tag{4.71}$$

In other words, $N_{\text{DT}}(0,1)$ can be partitioned, into the DT-partitions

$$\mathcal{N}^g_{\text{DT}}(0,1) = |\chi(X) - \chi_0| = 289, \tag{4.72}$$
$$\mathcal{N}^s_{\text{DT}}(0,1) = |\chi_0| = 1. \tag{4.73}$$

Again, note that $N_{DT}(0,1) = |\mathcal{N}^g_{\text{DT}}(0,1)| + |\mathcal{N}^s_{\text{DT}}(0,1)|$. Recall that the superscript g stands for generic, and $\mathcal{N}^g_{\text{DT}}(0,1)$ counts the number of D6-$\overline{\text{D0}}$ states, which are perceived by the tachyon generically. The superscript s stands for special. Accordingly, $\text{N}^s_{\text{DT}}(0,1)$ counts the number of D6-$\overline{\text{D0}}$ states, where the $\overline{\text{D0}}$ sits at a special locus, where the tachyon matrix does not perceive the particle.

Of course, this also means, that the index for the split flow tree must be stated correctly as:

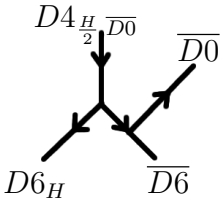

$= \quad -575.$

The elliptic genus (4.65) is thus determined by

$$Z_0(\tau) = q^{-\frac{35}{24}}(3 - 575q + 271'955q^2 + 206'406'410q^3 + 21'593'817'025q^4 ...). \tag{4.74}$$

It is interesting to note that the authors of [79], after having predicted a slightly deviating elliptic genus (as explained above), find $271'952$ as a prediction for the number of BPS states of the system, which is denoted (in the 'charge shift notation') as $\Delta q = 0, \Delta q_0 = -2$. This is only off by 3 of the modular result predicted, as opposed to the 248 from the result predicted by the 'naive elliptic genus' (4.68). This might be seen as an indicator, that the new prediction is indeed correct. Unfortunately, the present technique does not allow for checking this prediction, as a single flow exists for this state. It is thus not possible to confirm the next term in (4.74) with absolute certainty, but strong evidence for the computational scheme used here has been collected.

Still, it is nevertheless interesting from a computational point of view to predict Donaldson-Thomas partitions $\mathcal{N}^{(g,s)}(0,2)$ for the decantic.

The state $\Delta q = 0, \Delta q_0 = -2$ on the decantic

The total charge for this system reads $\Gamma = (0, 1, \frac{1}{2}, -\frac{5}{12})$, which implies $\hat{q}_0 = -\frac{13}{24}$: this is thus a non-polar state. One finds a split flow tree with the centers

$$\begin{aligned} \Gamma_1 &= (1, 1, \frac{23}{12}, \frac{19}{12}) \\ \Gamma_2 &= (-1, 0, -\frac{17}{12}, -2), \end{aligned}$$

and a flow tree of the form

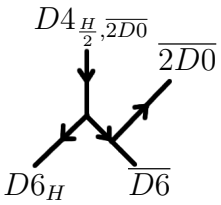

$= \quad = 40'752,$

which would naively yield an index

$$\Omega = (-1)^{|\langle\Gamma_1,\Gamma_2\rangle|-1}|\langle\Gamma_1,\Gamma_2\rangle| N_{\mathrm{DT}}(0,0) \cdot N_{\mathrm{DT}}(0,2) = (-1)^0 \cdot 1 \cdot 1 \cdot 40'752 = 40'752. \quad (4.75)$$

For the decantic, one can choose

$$p_{\mathrm{decantic}} = x_5^2 + x_4^5 + p^{(10)}(x_1, x_2, x_3) = 0 \quad (4.76)$$

as a transverse polynomial. Note that the moduli space for the tachyon was $C\mathbb{P}^2$ for the most polar state. Generically, this is reduced to $C\mathbb{P}^0$ when placing two $\overline{\mathrm{D0}}$'s, but there are a lot of subtleties involved. Namely, the cases when the $\overline{\mathrm{D0}}$'s have three equal coordinates x_1, x_2, x_3 and $x_4^{P_1} = 1^{\frac{j}{5}} x_4^{P_2}, x_5^{P_1} = 1^{\frac{k}{2}} x_5^{P_2}$ (with $j = 0, 1, 2, 3, 4$ and $k = 0, 1$) are of special interest. Additionally, the locus $x_1 = x_2 = x_3 = 0$ is special. Again, constraint loss will occur for some loci directly, but will also result from blowups, when placing the two $\overline{\mathrm{D0}}$'s on the same locus. Thus, one again has to analyze which tangent directions are special.

The condition for a constraint loss to occur after a blowup reads

$$\mathrm{rank} \begin{pmatrix} x_1 & x_2 & x_3 \\ X^1 & X^2 & X^3 \end{pmatrix} < 2, \quad (4.77)$$

which can happen either if $X^1 = ... = X^3 = 0$ or if $X^i = \lambda x_i$.

- $x_4 \neq 0$ or $x_5 \neq 0$: Assuming that not all coordinates x_1, x_2, x_3 vanish at the same time (this case will be dealt with separately), an analysis shows that for the cases that either (or both) of the coordinates x_4, x_5 do not vanish, one finds one tangent direction for which a constraint loss occurs. These subcases shall be discussed briefly:

  - $x_4 \neq 0, x_5 \neq 0$: In this case set $x_4 = 1$, thus $X^4 = 0$. One can easily check that $X^1 = X^2 = X^3 = 0$ is not possible as it would imply $X^5 = 0$. Thus, set $X^i = \lambda x_i$ $(i = 1, 2, 3)$, which leads to $\nabla_X p_{\text{decantic}} = 10\lambda p^{(10)} + 2X^5 x_5 = 0$. Combining this with (4.76) yields $x_5^2 + 1 = \frac{1}{5\lambda} X^5 x_5$. This completely fixes the tangent vector, thus there is one direction for which constraint loss occurs.
  - $x_4 \neq 0, x_5 = 0$: w.l.o.g. set $x_4 = 1$, thus $X^4 = 0$. Choosing $X^1 = X^2 = X^3$ yields $\nabla_X p_{\text{decantic}} = 2X^5 x_5 = 0$, thus one finds one special tangent direction.
  - $x_4 = 0, x_5 \neq 0$: w.l.o.g. set $x_5 = 1$, thus $X^5 = 0$. Choosing $X^1 = X^2 = X^3$ yields $\nabla_X p_{\text{decantic}} = 5X^4 x_4^5 = 0$, and one again finds one special tangent direction.

- $x_4 = x_5 = 0$: In this case, one can choose $x_1 = 1$, and thus $X^1 = 0$. So, a general tangent vector reads $X_2\partial_2 + ... + X^5\partial_5$. Setting $X^1 = X^2 = X^3 = 0$, and plugging this into $\nabla_X p_{\text{decantic}} = 0$ yields $5X^4 x_4 + 2X^5 x_5 = 0$, which can be satisfied. Thus, the tangent directions, for which there is a constraint loss, form a $C\mathbb{P}^1$.

- $x_1 = x_2 = x_3 = 0$: In this case, set $x_5 = 1$. Thus, (4.76) reads $x_4^5 + 1 = 0$. One might think that one has found five points on the CY, but taking the equivalence into account under the group action, one realizes, that this is only one point. In this case $X^4 = X^5 = 0$, and thus $X^1 = X^2 = X^3 = 0$ is not possible. Therefore, there is no (extra) constraint loss, when considering a blowup, when the two $\overline{\text{D0}}$'s coincide at this point on the decantic.

Calculating the exact index

Using the adjunction formula, one can calculate the Euler character associated to a number of loci of interest for the following calculation:

1. $x_4 = 0 : \chi_4 = 76$.
2. $x_5 = 0 : \chi_5 = 295$.
3. $x_4 = x_5 = 0 : \chi_{45} = -70$.
4. $x_1 = x_2 = x_3 = 0$: Recall that this is only one point. The Euler character is thus $\chi_0 = 1$.

A careful calculation reveals the following contributions:

- $\frac{1}{2}((\chi(X) - \chi_0)^2 - 10(\chi(X) - \chi_0 - \chi_4 - \chi_5 + \chi_{45}) - 2(\chi_4 - \chi_{45}) - 5(\chi_5 - \chi_{45})$ $-\chi_{45}) \cdot \chi(C\mathbb{P}^0)$: this is the generic locus. The case $x_1 = x_2 = x_3 = 0$ has been substracted from the beginning on, and additionally, also the cases when the coordinates x_1, x_2, x_3 of the two $\overline{\text{D0}}$'s are identical and $x_4^{P_1} = 1^{\frac{j}{5}} x_4^{P_2}, x_5^{P_1} = 1^{\frac{k}{2}} x_5^{P_2}$, $j = 0, 1, 2, 3, 4; k = 0, 1$ will be treated independently. These cases have been substracted, but for each possibility (j, k), the subloci where $x_4 = 0, x_5 = 0$ or both have been substracted and will be treated separately.

- $(\chi-\chi_0-\chi_{45})\cdot(\chi(C\mathbb{P}^2)-1)\cdot\chi(C\mathbb{P}^0)$: this is the most general case when the two $\overline{\text{D0}}$'s coincide. One has to treat various loci separately: the case, when the two particles lie on the point $x_1=x_2=x_3$ (this is substracted by the term $-\chi_0$), and also the cases when $x_4=x_5=0$ have been removed (the term $-\chi_{45}$). The factor $\chi(C\mathbb{P}^2)$ arises from the blowup of a codimension 3 locus. According to the analysis presented above, one does however need to substract one direction, for which there will be a constraint loss. In this case two constraints on the tachyon are imposed, reducing the moduli space to $C\mathbb{P}^0$.

- $(\chi-\chi_0-\chi_{45})\cdot 1\cdot\chi(C\mathbb{P}^1)$: This is the case analogous to the previous, but associated to the blowup direction yielding a constraint loss.

- $\chi_{45}\cdot(\chi(C\mathbb{P}^2)-\chi(C\mathbb{P}^1))\cdot\chi(C\mathbb{P}^0)$: When the two $\overline{\text{D0}}$'s coincide and $x_4=x_5=0$, a blowup is performed, but the previous analysis revealed two tangent directions associated to a constraint loss. That locus will be dealt with, next. In this case, two constraints are imposed on the tachyon, yielding a $\chi(C\mathbb{P}^0)$.

- $\chi_{45}\cdot\chi(C\mathbb{P}^1)\cdot\chi(C\mathbb{P}^1)$: This is the case, when the blowup is associated to a constraint loss, with the two $\overline{\text{D0}}$'s coincident on a locus with $x_4=x_5=0$.

- $\chi_0\cdot\chi(C\mathbb{P}^2)\chi(C\mathbb{P}^1)$: When the two $\overline{\text{D0}}$'s lie on the point $x_1=x_2=x_3=0$, there is only one constraint on the tachyon, arising from the tangent directions after the blowup. Recall that there is no constraint from placing a particle at this point: this subtlety appeared already when considering the state $D4-\overline{\text{D0}}$ on the decantic, previously.

- $(\chi-\chi_0)\cdot\chi_0\cdot\chi(C\mathbb{P}^1)$: This contribution arises, when one $\overline{\text{D0}}$ is placed on the locus $x_1=x_2=x_3=0$ (this $\overline{\text{D0}}$ will not impose a constraint on the tachyon), and the other one somewhere else.

- $\frac{1}{2}\cdot 9(\chi-\chi_0-\chi_4-\chi_5+\chi_{45})\cdot\chi(C\mathbb{P}^1)$: These are the cases, when the two $\overline{\text{D0}}$'s have identical coordinates x_1,x_2,x_3, but differ in at least one of the other coordinates, $x_4^{P_1}=1^{\frac{j}{5}}x_4^{P_2}, x_5^{P_1}=1^{\frac{k}{2}}x_5^{P_2}$. In these cases, there is only one constraint on the tachyon. The cases when $x_4=0$, $x_5=0$ (or both) will be treated separately, though.

- $1\cdot\frac{1}{2}(\chi_4-\chi_{45})\cdot\chi(C\mathbb{P}^1)$: This is as the previous case, but additionally $x_4=0$.

- $5\cdot\frac{1}{2}(\chi_5-\chi_{45})\cdot\chi(C\mathbb{P}^1)$: Again, the conditions as previously, but with $x_5=0$.

Collecting all the pieces linked to the value 0 or 1 for the tachyon index (up to a sign), one can state the correct index in the form

$$\Omega_{\text{exact}}=1\cdot(40'752+3'127)+2\cdot(-3'127)=37'625. \tag{4.78}$$

The *Donaldson-Thomas partitions* $\mathcal{N}_{DT}^{(1,2)}(0,2)$ *for the decantic* thus read

$$\mathcal{N}_{\text{DT}}^{(g)}(0,2) = 43'879, \tag{4.79}$$

$$\mathcal{N}_{\text{DT}}^{(s)}(0,2) = -3'127. \tag{4.80}$$

Again, note that the sum of the partitions yields $N_{\mathrm{DT}}(0,2)$.

Clearly, the number $37'625$ is still very far off from the modular prediction $271'955$, the missing states (at least the single-centered states) however cannot be enumerated at the moment. Namely, one finds a single flow for this charge system, so there is little hope of obtaining the correct index exclusively using the methods utilized in this thesis. It is left as a problem for future research to enumerate the number of BPS states corresponding to this single flow, and (possibly) find and enumerate other split flow trees.

4.6 Discussion

Results on the BPS spectrum of Calabi-Yau study models were presented in this chapter. The existence of states was examined using split attractor flow trees. D-particles modeled with mixed ensemble of D4-D2-D0 branes were considered, choosing minimal magnetic D4-brane charge $p = 1$, and varying over different electric D2-D0 charges. This meant that instanton corrections to the central charges became important for establishing (split) flows numerically. This was accomplished by using mirror symmetry and was explained in more detail in the first section. After establishing split flow trees, the number of states corresponding to such a split flow was computed using the methods developed by Denef and Moore, [1]. The number of states was enumerated as perceived on the wall of marginal stability, where the first split occurs. This number is then typically (although this is not always the case) a product of the number of states of the first center, a D6-brane (including lower dimensional brane charge), the number of states of the tachyonic modes gluing the two centers together, and the number of states of the second center, a $\overline{\mathrm{D6}}$-brane (including lower dimensional brane charge). The D6- and the $\overline{\mathrm{D6}}$-center are both enumerated using Donaldson-Thomas invariants.

The partition function of a D-particle of the type discussed goes under the name of an elliptic genus. Elliptic genera are generalized modular forms and are determined by a finite number of terms, when considering their expansion. Knowledge of this finite number of terms corresponding to polar states, allows one to determine the complete elliptic genus from modularity. All polar states were enumerated for the models considered. For three of the models, the method discussed yields exact results. For another model, (presumably) exact results were found, after taking into account a subtlety, which will be discussed shortly.

After enumerating all polar states, the complete elliptic genus is determined by modularity. The predictions on the number of BPS states for the first few non-polar states thus offers a very interesting ground for testing the methods used. Indeed, for many non-polar states, the exact results can be found. Given the fact, that some area codes were considerably complicated, this can be interpreted as strong evidence for a strong version of the split attractor flow conjecture, stating that split attractor flow trees provide an exact classification for all BPS states in type II string theory. For some states one finds a result however, which is close, but not exact. The reason for this as well as the solution have been found: the moduli space of a BPS bound state consisting of two branes (in this case

a D6- and a $\overline{\text{D6}}$-brane glued together by tachyonic fields) is not a direct product space, but a non-trivial fibration. By taking this into account correctly, a perfect matching could be found for all examples considered (at least for those, in which a result could be found without having to enumerate single flows, which was not possible at this point). This suggests, that the split attractor flow conjecture holds, when using refined indices to enumerate the number of corresponding states.

The fact that the refined computation works perfectly for all studied examples makes it seem very unlikely that this is coincidental. If the index can be correctly defined [9], it generalizes the BPS wall-crossing index of Denef and Moore from [1], and furthermore could be associated to the more precise physical picture of wall-crossing, consistent with the formula of Kontsevich and Soibelman, [2]. This point needs to be further investigated.

Additionally, the fact that the dimension of the moduli space belonging to the tachyon field of a bound state jumps, allows the splitting up of the states belonging to a center into 'generic' states, that are perceived as one generically expects, and 'special' states, that are perceived (by the tachyons) as though there were less brane charge present on that constituent. D6-D2-D0 states split up into these two sorts of states, and this also allows the partitioning of Donaldson-Thomas invariants. The two pieces are referred to as Donaldson-Thomas partitions $\mathcal{N}^{(g)}_{\text{DT}}$, $\mathcal{N}^{(s)}_{\text{DT}}$ (where the superscripts 'g/s' stand for 'generic/special') in this work. The partitions always sum up to yield the ordinary Donaldson-Thomas invariant: $\mathcal{N}^{(g)}_{\text{DT}}(i,j) + \mathcal{N}^{(s)}_{\text{DT}}(i,j) = N_{\text{DT}}(i,j)$.

Should the approach to model black holes and D-particles using mixed ensembles of D-branes turn out to be of crucial importance, the relevance of polar states cannot be overestimated. In an attempt to make the results accessible to a general public, this fact led the author to interpret the research context and results using a metaphor. Polar states are realized as a pair of branes, and the set of all polar states determines the complete partition function of a black hole or a D-particle. In the same spirit, a finite set of chromosomes, also appearing in pairs, determine the complete microbiological structure of an organism. Polar states are given the interpretation of chromosomes of black holes (and of D-particles). The D-particle on the other hand, can be seen as a 'simpler organism' than a black hole, and might be seen as a fruit fly in quantum gravity. In this interpretation, the author's research can be seen as an analysis of D-particle genomes. The reader will find more on this topic in the 'concluding discussion' and in the 'Dutch summary' (appendix D).

One more point was announced in this chapter, namely the question, whether the results obtained on BPS spectra of D-particles might shed any light on the mysterious nature of scaling solutions. For the following charge systems, one might naively expect a scaling solution in supergravity: $\Delta q = 0, \Delta q_0 = -3$ on the quintic, $\Delta q = 0, \Delta q_0 = -2$ on the sextic, $\Delta q = 0, \Delta q_0 = -2$ on the octic and $\Delta q = 0, \Delta q_0 = -1$ on the decantic. For the first three of the listed charge systems, the number of BPS states in the spectrum can be predicted by modularity, and the methods used in this thesis allow for exact results to be derived, based on the prescriptions for refined calculations presented in this chapter. One is led to believe, that one has indeed exhausted the BPS spectrum of the quantum theory, in

[9] The author would like to thank Frederik Denef and Markus Reineke for clarifications on this point.

the sense that one has classified and enumerated all BPS microstates of the corresponding D-particles, carrying the desired charge. At the same time, this means, that the split attractor flow conjecture worked perfectly. For none of the mentioned charge systems is there seemingly room for states, which would be described by scaling solutions, after taking a classical limit (compare with the explanations on this in subsection 2.3.1). This can be concluded from the fact, that an index (as suggested in [58]) for scaling solutions seems to yield results that strongly deviate from any numbers contributing to the total number of BPS states one would expect. It seems reasonable to suppose that the exact numbers for BPS states for the D-particles investigated can be interpreted as indicators that the interpretation of [58] on scaling solutions is indeed correct. It would be wrong however to make an overstatement, as these implications do remain quite speculative, and there are no properly legitimated methods to compute an 'index for scaling solutions', taking into account the regime of validity needed in this case. One should at this point remain open to other ideas, one of which might be the wild proposal that 'special states' could be quantum partners of scaling solutions. The author believes this to be rather unlikely, but further investigation on this exciting topic remains for the future.

In any case, to the reader, the importance of polar states and split flow trees will have become clear. They will also form the bridge to the next chapter, in which polar states in 4d will be inspected using split flow trees, and mapped to 5d fuzzball geometries. This relates one of the major research programs on black holes in string theory at this moment in time, namely the fuzzball program (this will be introduced briefly at the beginning of the next chapter), to the formalism and techniques used and developed further in this chapter.

The discussion of this chapter is concluded by indicating some future directions of research. A central goal certainly is, to investigate and state a proper mathematical definition of the refined index introduced in this chapter, and above all, test the consistency of this index with the wall-crossing formula of Kontsevich and Soibelman, [2]. Apart from this, it might be interesting to work out more study models like the ones used in this chapter explicitly, in order to perform further tests on the split flow tree conjecture, and also to find out, how Donaldson-Thomas partitions behave more generally. It would also be interesting to be able to enumerate single flows, and see if one could find a matching with the modular result for the state $\Delta q = 0, \Delta q_0 = -2$ on the decantic. Furthermore, it would be interesting to extend the type of computations presented to Calabi-Yau varieties embedded in toric varieties. In those cases, the refinements should appear frequently and play a prominent role. In general, what can be learned about the problems associated to the OSV-conjecture from the considerations presented in this chapter is an open question. In the light of the discovery of the Donaldson-Thomas partitions, it is especially interesting to find out more about the type of information they carry about bosonic vs. fermionic states. Finally, it is a goal to gain a rigorous understanding of the Donaldson-Thomas partitions introduced from the viewpoint of algebraic geometry.

Chapter 5

5d fuzzball geometries and 4d polar states

This chapter is based on research performed together with Joris Raeymaekers, Bert Vercnocke and Walter Van Herck, presented in [5]. The prominent role played by multi-centered black holes in four dimensions should be clear from the preceding chapters. In five dimensions, BPS objects are also not restricted to single-centered black holes. One also finds supersymmetric black rings and combinations of black holes and rings [117–119], often called black saturns. Furthermore, there are Kaluza-Klein monopole supertube solutions which carry the charges of a black hole or a black ring and are smooth and horizonless [120–123]. These solutions can be viewed as gravity duals to individual microstates in the CFT description of the black hole, which lead to the 'fuzzball' picture proposed by Mathur and his collaborators. According to their proposal, the naive picture of a singular black hole is actually only a coarse approximation to the microstructure, given by smooth gravitational 'fuzzball' microstates. More precisely, the fuzzball conjecture suggests that all black hole geometries in string theory are horizon-free (also states, which one might not be able to describe using supergravity). A 'naive' black hole solution as well as an event horizon should be interpreted as a result of an 'averaging procedure' with respect to all fuzzball geometries. Each single microstate on the gravitational side of the theory (as opposed to the holographically dual CFT description) does not have either a horizon or a singularity: it is completely 'smooth'.

In order to provide the reader with some background on the fuzzball proposal, some main features of this research program will be presented first, in 5.1, including some basic ideas on how the fuzzball proposal presumably resolves the black hole information paradox. This will be followed by a presentation of the research, establishing an interesting link between fuzzball geometries in 5d and multi-centered black holes in 4d. The 4d picture will be discussed first. The reader can find a short review on the construction of multi-centered solutions in the STU-model in the appendix, 5.2. Solutions carrying the charges (5.15) were constructed, and the author and his collaborators gave an explanation why these states are polar and confirmed their existence by establishing split flow trees (assuming the split attractor flow tree conjecture to hold). In the next subsection, 5.3, a transformation to a

U-dual type IIB duality frame is presented, and the lift of these solutions to 10 dimensions is discussed. The reduction formulae in the type IIB duality frame have been worked out and can be found under C. It is shown that the solutions in the type IIB frame represent supertubes embedded in Taub-NUT space, and the 5d limit is discussed. Finally, in subsection 5.4, the microscopic interpretation of these configurations is discussed, from a 4d and a 5d point of view. Some prospects for future research in this direction are given in subsection 5.5.

5.1 The black hole information paradox and the fuzzball conjecture

At the present time, the black hole information paradox is an important issue in theoretical physics, especially in the quest towards a better understanding of quantum gravity. This paradox has been around for more than thirty years, since the appearance of Stephen Hawking's analysis suggesting that black holes radiate. The fuzzball conjecture by Samir Mathur is a promising remedy for the problem of information loss in a black hole. In order to give a brief explanation on this, the black hole information paradox will be presented first, followed by the solution which the fuzzball program has to offer. The reader is referred to some recent and thorough reviews, such as [124–128] for more detail and completeness. This section should provide the reader with enough context to place the research performed by the author, linking polar states in 4d (in the IIA picture) and a specific class of fuzzball geometries in 5d (in the IIB picture).

5.1.1 The black hole information paradox

Essentially, the naive picture of a black hole, as appreciated through the theoretical framework of general relativity and also of supergravity theories, is that of a point-like singularity, surrounded by an event horizon. Already in 1975, Stephen Hawking performed his famous semi-classical calculation, examining quantum fields in a classical black hole background, [129]. He showed that black holes do not exist eternally, but actually slowly radiate (eventually losing all of their mass) – a phenomenon now known as the *Hawking effect*. Some basic ideas on this calculation and the resulting problem shall be sketched next. To be specific, recall the metric for the Schwarzschild black hole (setting $G_N = 1$),

$$ds^2 = -(1 - \frac{2M}{r})dt^2 + (1 - \frac{2M}{r})^{-1}dr^2 + r^2(d\theta^2 + \sin^2\theta d\phi^2). \tag{5.1}$$

As mentioned earlier on, the metric is written in Schwarzschild coordinates, which are good coordinates outside of the event horizon $r = 2M$. It might seem that this metric is globally time independent, and one could therefore take a globally time-independent spacelike slice. This is not correct however, as when one crosses the event horizon, time and space interchange their roles. Outside of the horizon ($r > 2M$), one can choose $t = t_0$ as a spacelike slicing, but inside the horizon ($r < 2M$), a spacelike slicing is of the form $r = r_0$.

Particle creation in curved spacetime

It is a basic, but very intriguing (inherently) quantum effect that a curved spacetime background will automatically lead to particle creation. Some thought material on this will now be borrowed from many of the reviews by Mathur himself. Imagine starting with a Lagrangian for a scalar field, $L = \frac{1}{2}\partial_\mu\phi\partial^\mu\phi$, expanding the field into Fourier modes, and then concentrating on only one of the modes with amplitude a. For simplicity assume dependence on only just one space dimension and on time, $\phi = \sum_{n=-\infty}^{n=\infty} e^{i(n+\frac{1}{2})x}a_n(t)$. The Lagrangian for the mode a_n turns out to be $L = \frac{1}{2}\dot{a_n}^2 - \frac{1}{2}\omega^2 a_n^2$, where one set $\omega = n + \frac{1}{2}$. This is nothing else but a harmonic oscillator. The field starts in the vacuum mode $|0\rangle$. Now, imagine that the space expands (as time evolves): this means that the frequencies belonging to the modes change. If the space expands very slowly, the field has time to react, and the vacuum 'evolves along with the stretching of the potential'. However, if the space expands too quickly, the mode 'will not have time to adapt' to the change in potential, and the state will not be in a vacuum mode anymore. This is illustrated in figure 5.1.

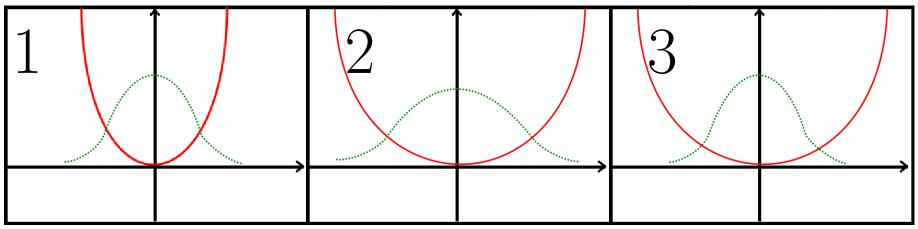

Figure 5.1: Stretching of space: change of particle frequency modes. **1. Left:** the ground state wave function in green corresponding to the potential of the harmonic oscillator in red. **2. Middle:** When space has expanded, the potential has been stretched, the ground state wave function experiences a stretching, too. **3. Right:** If space expands too quickly (imagine a strong curvature of spacetime), a mode has not had time to stretch according to the change of potential. This is essentially why particles are created in curved spacetime.

Rather, the ground state corresponding to the old ground state frequency ω will be a superposition of the new ground state (with frequency $\omega^{'}$) and multi-particle states,

$$|0\rangle_\omega = \sum_{i\in\mathbb{Z}_{2n}^+} c_i|i\rangle_{\omega'} = c_0|0\rangle_{\omega'} + c_2|2\rangle_{\omega'} + c_4|4\rangle_{\omega'} + ...^1\,, \tag{5.2}$$

where the c_i are some coefficients, depending of course on the amount of expansion of space considered.

[1]Note that in this specific little example for a mode of a harmonic oscillator only even particle states arise in the superposition as the overall wavefunction is even – this however has no relevance for the present concern.

Wave-packets stretching across the event horizon of a black hole

Now imagine a wave-packet stretching across the horizon of the Schwarzschild black hole. As time evolves, one can analyze what happens to such a wave-packet. The wave-packet will be stretched at different rates, according to the different amounts of curvature surpassed. Keeping the intuition in mind, gained by the brief discussion of mode evolution of the harmonic oscillator in curved spacetime, it is not hard to imagine that this leads to particle creation inside and outside the event horizon. This however leads to an entangled state of the states created inside the horizon, $|i_j\rangle$, and the ones outside the horizon, $|o_j\rangle$, [129].

The concept of entanglement can be explained easily using a system of two particles with spin. The entangled state $|\psi\rangle$ (the situation if one had for example created a particle-anti-particle pair) is of the form

$$|\psi\rangle = \frac{1}{\sqrt{2}}(|\uparrow\rangle_1 \otimes |\downarrow\rangle_2 + |\downarrow\rangle_1 \otimes |\uparrow\rangle_2) \tag{5.3}$$

where $|\uparrow\rangle_1$ denotes spin-up for particle one, etc. It is clear that if one measures spin up for particle one, one will automatically know that particle two has spin down and vice versa. An example of a state where the particle spins behave independently would be the tensor product of states:

$$|\psi\rangle = |\psi_1\rangle \otimes |\psi_2\rangle = \frac{1}{2}(|\uparrow\rangle_1 + |\downarrow\rangle_1) \otimes (|\uparrow\rangle_2 + |\downarrow\rangle_2). \tag{5.4}$$

When the whole black hole has radiated away completely, this leaves behind particles entangled with nothing, as the particles inside are destroyed, and only the ones outside survive. This means a violation of unitarity, as will now be explained.

Loss of unitarity, information loss in a black hole

Unitarity is one of the most sacred principles of quantum theory. In the Schrödinger picture, pure quantum states $|\psi\rangle_t$ are evolved into later-time pure states $|\psi\rangle_{t'}$ with the unitary time evolution operator, $U = \exp(\frac{i}{\hbar}H(t - t_0))$:

$$|\psi\rangle_{t'} = e^{\frac{i}{\hbar}H(t'-t)}|\psi\rangle_t. \tag{5.5}$$

A black hole that has been radiated away completely leaves behind a whole series of particles $|o\rangle_j$, entangled with nothing. This means that these particles are described by a *mixed state*. If a pure state evolves into a mixed state, unitarity of quantum theory is lost. Put differently, this mechanism leads to *information loss*. The information that entered the black hole has disappeared into nowhere. Nothing is left but particles in a mixed state.

Over the last decades, people have come up with several resolutions to this problem. Amongst these, the suggestion has been made that indeed unitarity is not a feature of quantum theory. Alternatively, researchers suggested that subtle quantum gravitational

effects can alter the form of the emitted radiation, encoding the information about the black hole. Sometimes researchers also claim that unitarity might well be violated, but that one might be able to resolve the information paradox in the dual CFT. Probably, a majority is however convinced that if unitarity really were violated, the dual quantum theory would not be consistent, and one would not be able to use any AdS/CFT dualities. In the following, a different resolution to the problem will be sketched, namely Mathur's fuzzball proposal.

The difference between a black hole and a piece of coal

It is convenient to introduce some more thought material widely used by Mathur. It is nice to compare the classical picture of a black hole and the Hawking radiation leaving the latter, to an ordinary piece of coal (one could of course for the sake of argument choose something different from a piece of coal) and the radiation leaving the coal, when the coal burns away. Why is there no information loss when one burns a piece of coal? The key point is that the quanta emitted from the coal interact with what is (or is about to be) left of the coal. A particle leaving the coal might well be entangled with the rest of the coal, but the following emission is not independent of the first emission. Imagine that the spin of all the particles in the coal are dependent on the spin of a particle leaving. This means that the following emitted quanta will carry some information about this. In contrast, a particle leaving a black hole is not influenced by any previous emission, as the particles were just created from the vacuum. The big difference is that the particles leaving the coal interacted with the 'rest material', the particles leaving a black hole did not – they were created from the vacuum. This is a result of the fact that the event horizon of a black hole (in the classical sense) is surrounded by the vacuum. The fuzzball proposal alters exactly this idea about black holes, rendering them more similar to a piece of coal.

5.1.2 The fuzzball conjecture: there are no black holes

As just mentioned, the central idea leading to the fuzzball picture is that a black hole is not formed by a singularity, surrounded by vacuum, eventually sheltered off from the outside by an event horizon, but rather, by matter/energy density spread out all across the spacetime region within the event horizon. This is illustrated in figure 5.2.

The 'classical idea' of a black hole involves the notion that there is no matter and no energy density located anywhere near the horizon. One can suggestively call such a horizon an 'information-free horizon'. As discussed previously, the reason that the radiation emmited does not carry any information about the black hole is that the quanta emitted do not interact with any quanta carried by the black hole. If the matter in microstates of the black hole spreads out to the event horizon, the situation is essentially different. Note that the idea that black holes are actually effective descriptions of underlying horizon-free objects is somewhat surprising, because it is in contradiction with the intuition that the curvature of spacetime near the event horizon of a black hole is small and thus one would expect no (or at least hardly any) effects of quantum gravity. A simple example will be

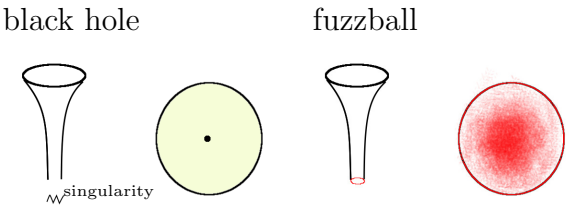

Figure 5.2: Naive black hole versus fuzzball picture. **Left: Black hole.** All the matter/energy of a black hole sits in a singularity of order of Planck length. Spacetime is curved to the extent that an infinite throat forms at the end of which there is a singularity, drawn as a edgy line. The matter located in a singularity is surrounded by vacuum (the pink region) all the way out to the event horizon. As the event horizon lies in the vacuum, it is called an 'information free horizon'. **Right: Fuzzball microstate.** The throat of a fuzzball microstate is not infinitely deep, but ends at a finite distance (this is indicated with a small red circle). The matter(drawn in red) is spread all across the spacetime region bounded by the event horizon. The horizon only appears as an 'effective' barrier. The distribution of the 'fuzzy' matter probably becomes denser (as indicated in the picture) towards the center of the region.

given next, to illustrate the relation of a 'naive' black hole metric to fuzzball microstate metrics.

Two-charge black hole and fuzzball geometries (NS1-P)

It is worth recapitulating a few thoughts on modeling of black holes in string theory. According to the conjectures on duality and chains of dualities in string theory, all theories are related by dualities and one can choose any one of them to model a black hole without losing any generality. The fuzzball proposal is normally approached using type IIB string theory. Here, type IIB string theory compactified to 5d is chosen, using $\mathbf{M}_{1,4} \times S^1 \times T^4$ as a background, where one S^1 with radius R has been singled out from the 5-torus. The coordinates on the 5d Minkowski space will be labeled as $(t, r = (\sum_{i=1}^{4} x_i^2)^{\frac{1}{2}})$, the coordinate on the S^1 will be called y, and the coordinates on T^4 will be called z_a $(a = 1, 2, 3, 4)$.

One might start by trying to model a black hole using only one kind of brane charge: for example with Q_1 units of fundamental string (NS1-brane) charge. A bound state of N_1 strings results in one big string, winding N_1 times around the circle S^1, thus exhibiting a total length of $2\pi N_1 R$. If one wants to describe one black hole and not several, one wants to locate all the charge in one point of spacetime. One finds however that this system does not yield a black hole, and one needs to add at least a second type of brane charge. One can choose to add Q_p units of momentum P to the string. One now wants to describe a multiwound string with traveling waves in the S_1 direction y. The metric, which one

obtains for this charge system using the methods explained in chapter 2, reads

$$ds^2 = \frac{1}{1+\frac{Q_1}{r^2}}(-dt^2+dy^2+\frac{Q_p}{r^2}(dt+dy)^2)+\sum_{i=1}^{4}dx_i^2+\sum_{a=1}^{4}dz_a^2.$$

In order to compare the singular black hole geometry, which one associates to this charge system, to the fuzzball microstates, it is convenient to introduce the coordinates $u = t+y, v = t-y$. The 'naive' proposal for the 10D-metric as well as the other non-zero fields for this system could read

$$\begin{aligned} ds^2 &= H(-dudv+Kdu^2)+\sum_{i=1}^{4}dx_i^2+\sum_{a=1}^{4}dz_a^2, \\ B_{uv} &= -\frac{1}{2}(H-1), \\ e^{2\phi} &= H. \end{aligned} \tag{5.6}$$

using $H^{-1} = 1+\frac{Q_1}{r^2}$ and $K = \frac{Q_p}{r^2}$. It is important to note that from a 5d point of view, all the mass is concentrated in a single point at $r = 0$. From the viewpoint of the fuzzball program, this is not the correct metric to describe a string with momentum.

The main intuition for why the correct metric is not of this form is that a string with momentum has a vibrational profile. This means that the state is not localized in a point, but has a small extension in spacetime (one might picture this as rendering the system 'fuzzy'). Solutions to this charge system have been found, suggested to be the real geometries belonging to such a NS1-P charge system. From the viewpoint of the fuzzball program, the metric (5.6) is not an accurate physical description of this 'black hole' in gravity, but it is just a (purely mathematical) solution to the supergravity equations *away from* $r = 0$. In the string frame, fuzzball solutions of the supergravity equations for the metric, the gauge field B as well as the dilaton profile read, [121, 130],

$$\begin{aligned} ds^2 &= H(-dudv+Kdv^2+2A_idx_idv)+\sum_{i=1}^{4}dx_i^2+\sum_{a=1}^{4}dz_a^2, \\ B_{uv} &= -\frac{1}{2}(H-1), \qquad B_{vi} = HA_i, \\ e^{2\phi} &= H, \end{aligned} \tag{5.7}$$

with

$$\begin{aligned} \frac{1}{H} &= 1+\frac{Q_1}{L_T}\int_0^{L_T}\frac{dv}{|\vec{x}^2-\vec{F}(v)|^2}, \\ K &= \frac{Q_1}{L_T}\int_0^{L_T}\frac{dv(\dot{F}(v))^2}{|\vec{x}^2-\vec{F}(v)|^2}, \\ A_i &= -\frac{Q_1}{L_T}\int_0^{L_T}\frac{dv\dot{F}_i(v)}{|\vec{x}^2-\vec{F}(v)|^2}. \end{aligned} \tag{5.8}$$

where $\vec{F} = F_i(t, y)$. The function $\vec{F}$ is called the profile function of a fuzzball and can be interpreted as describing the profile of the vibrating string. It is thus a function of time and the coordinate on S^1, $\vec{F} = \vec{F}(t, y)$. As is generically the case for fuzzball microstates that one can describe in supergravity, these geometries do not have a horizon, and they do not end in an infinite throat, but they cap off. Note the difference between (5.6) and (5.7): it arises from terms which are obtained as integrals over $\vec{F}$. One can interpret intuitively, that the movement of the string in the S^1 direction gives the object a little extension, and it is this geometrical backreaction which makes the fuzzball solutions deviate from the naive geometry. Another point of interest is the question as to what size these fuzzballs have in terms of spacetime extension. The entropy of the NS1-P black hole arises from distributing momentum across the string. The string does not carry any longitudinal vibrations. All the momentum is carried in transverse directions, and it is intuitively clear that this will lead to some 'fuzziness' from the 5d point of view. In fact, as the reader can follow in [125] (where he will also find further references), it turns out that the mass/energy is not spread across a region of Planck length l_p, but rather a region that scales with $\sqrt{N_1 N_p}$ – and this seems to be a generic feature of all solutions believed to be fuzzball microstates of the NS1-P black hole. In other words, the size of such a fuzzball has been estimated to be of order $\sqrt{N_1 N_P}$. Furthermore, when considering all constructed fuzzball geometries, the entropy of the black hole (originally 'guessed' by the macroscopic calculation of the area of the event horizon) could be reproduced: $S_{\text{fb}}^{NS1-P} \equiv \sqrt{N_1 N_p}$, [125]. In other words, an entropy, macroscopically known from the area of the event horizon, microscopically explained using holography, can also be explained by finding *enough* microstates in the gravitational theory.

Fractionation: how branes are partitioned enabling to squeeze information

This is a good moment to introduce another interesting thought important to the fuzzball program. The total momentum on the string is given by $P = \frac{N_P}{R} = N_P \cdot \frac{2\pi}{L}$. One unit of momentum evaluates to

$$\frac{2\pi}{L} = \frac{2\pi N_1}{N_1 L} = \frac{2\pi N_1}{L_{\text{string}}},$$

where $L_{\text{string}} = 2\pi N_1 R = N_1 \cdot L$ and L labels the length of the circle S^1. This means that adding one unit of momentum to the string looks like adding N_1 units of momentum to the multiwound string – one might call these units N_1 fractional momentum units. This phenomenon is a simple example of what has been called 'fractionation', [131]. Upon dualizing to other systems this also leads to other *fractional brane charges*. The splitting up of units of charge in a bound state can intuitively be pictured as leading to a large degeneracy through all the different ways of being partitioned. Mathur and collaborators argue that this is one of the central insights into black hole physics: modeling black hole physics requires the use of bound states of branes. Fractionation enables such a huge entropy in such a small region of spacetime. It is claimed to be the key principle behind the most dense form of packaging information. Just like crystals choose a dense form of organizing their atoms, one might say that black holes choose bound states of branes allowing fractionation,

which leads to entropy maximization. Mathur claims that this situation has analogies with the splitting up of simple elementary particles (branes) into quark constituents (fractional branes), and the understanding of QCD. Hence one of the central goals is to develop a good understanding of these fractional units of brane charge in order to gain a better understanding of black hole entropy. In the case of the NS1-P black hole, fractionation of momentum leads to a large degeneracy of possibilities when distributing momentum among different harmonics. Upon dualization to the D1-D5 black hole (this will be mentioned briefly, next), these fractional momentum modes map to fractional branes, which have fractional brane tension. Again, very intuitively, it is these fractional tensions which allow the microscopic quanta to extend over such large regions, thereby allowing the fuzzy matter in a black hole to extend all the way out to the event horizon, [132].

Dualization to fuzzball picture of D1-D5 black hole

This system can be dualized to the well known D1-D5 system, which appeared previously in this thesis. As all dualities have been performed on the extra dimensions, nothing changes with respect to the 4d observations. Thus one still has a black hole of the same extension. The naive metric becomes

$$ds^2 = \frac{1}{\sqrt{(1+\frac{Q_1}{r^2})(1+\frac{Q_5}{r^2})}}(-dt^2+dy^2) + \sqrt{(1+\frac{Q_1}{r^2})(1+\frac{Q_5}{r^2})}\sum_{i=1}^{4} dx_i^2 + \sqrt{\frac{1+\frac{Q_1}{r^2}}{1+\frac{Q_5}{r^2}}}\sum_{a=1}^{4} dz_a^2 \tag{5.9}$$

upon dualization, whereas the fuzzball geometries dualize to

$$\begin{aligned} ds^2 &= \sqrt{\frac{H}{1+K}}(-(dt-A_i dx^i)^2 + (dy+B_i dx^i)^2) + \sqrt{\frac{1+K}{H}}\sum_{i=1}^{4} dx_i^2 \\ &\quad + \sqrt{H(1+K)}\sum_{a=1}^{4} dz_a^2, \end{aligned}$$

$$\begin{aligned} \frac{1}{H} &= 1 + \frac{\mu Q_1}{L_T}\int_0^{\mu L_T} \frac{dv}{|\vec{x}^2 - \vec{F}(v)|^2}, \\ K &= \frac{\mu Q_1}{L_T}\int_0^{\mu L_T} \frac{dv(\mu^2 \dot{F}(v))^2}{|\vec{x}^2 - \mu\vec{F}(v)|^2}, \\ A_i &= -\frac{\mu Q_1}{L_T}\int_0^{L_T} \frac{dv\mu\dot{F}_i(v)}{|\vec{x}^2 - \mu\vec{F}(v)|^2}, \\ B_i &= -\star_4 dA, \end{aligned} \tag{5.10}$$

where $\star_4$ denotes the Hodge operator on the 4d non-compact space using the flat metric.

The fuzzball program

This allows to state the 'fuzzball program'. One starts by modeling a black hole in string theory, wrapping various (p, q)-branes around compact dimensions, generating mass in spacetime. One can then calculate the entropy by calculating the area of the event horizon belonging to the singular black hole geometry. One might also be able to microscopically explain this entropy using a holographically dual CFT. The goal of the fuzzball program is to then find all gravitational solutions, which should altogether account for this entropy. The fuzzball conjecture has received a lot of attention in the context of type IIB 4d and 5d compactifications on $T^6, K3 \times T^2$ or T^5. Extremal black holes have been studied intensively: for 2-charge systems (such as the NS1-P or the dual D1-D5 system) all fuzzball solutions have been found, for 3-charge (e.g. D1-D5-P) and 4-charge systems (e.g. D1-D5-P-KK) not all, but large numbers of fuzzball solutions have been found. In addition, there are also some papers where non-extremal fuzzball solutions have been constructed, check e.g. [133].

Before discussing the more specific aim of the research presented in this chapter, a few final remarks on fuzzballs in general shall be given. It is ironic and amusing to think, that if the fuzzball program is on the right track, black holes do not really exist. Fuzzballs do actually interact with the outside world, just like a piece of coal does. Fuzzballs only seemed to be black holes because of the long time scales inherent to their life cycles. In order to understand this, one can consider two different time scales. The first one is the time it takes a quantum to fall into the fuzzy hole and interact with the quanta forming the hole: one can call this the 'crossing time'. The second time scale can be denoted as the 'evaporation time'; this is the time needed for a black hole to evaporate. In order to solve the information paradox, quanta must have time to interact with the hole, before the latter disappears: otherwise, the whole idea of a black hole being similar to a piece of coal is meaningless, as this would be purely theoretical. For a Schwarzschild black hole it turns out, that roughly, $t_{\text{evap}} \cdot \frac{M}{m_p} = t_{\text{cross}}$, where M denotes the mass of the black hole, and thus $t_{\text{evap}} \gg t_{\text{cross}}$. Nevertheless, from the viewpoint of human life spans, it takes far too long for matter to interact and come out of a fuzzball for this to be of any relevance – this means that fuzzballs behave pretty much like one imagines a black hole to behave.

Another point which should be stated clearly is that the fuzzball conjecture does not imply that all the smooth gravitational microstates (smooth in the sense that the microstates do not contain a singularity) can be described as solutions to the supergravity limit of string theory. Some of them can, and in the case of the two-charge system it would seem that this works for all microstates. There might however (and probably will) also be 'quantum' microstates, that do not have a nice limit in supergravity, are stringy and quantum in nature, and characterized by string scale curvatures and large quantum fluctuations. In the light of these remarks, one can ask oneself the question, how a smooth, horizonless fuzzball geometry in supergravity could possibly be a microstate of a black hole. As discussed in [134], it seems correct not to interpret a smooth geometry as presented earlier on as an 'actual microstate' of the corresponding black hole. Rather, one might in-

terpret them as classical limits of quantum mechanical microstates localized in one unit of volume in the phase space of solutions. Only in taking the classical limit of this procedure, may one really think of fuzzball geometry as a microstate. Quantum microstates may also not localize in a unit volume of phase space and are not likely to have any sort of classical limit [2]. The important point is that they will typically have an interesting, non-trivial microstructure stretching all the way up to the horizon: this is the central message of the fuzzball conjecture.

Finally, as stressed in this section, according to the fuzzball conjecture, the matter of a black hole is not concentrated in a singularity of size of order of the Planck length l_P, or string length l_s. It is rather spread out as 'quantum fuzz', and the size of a black hole (actually of a fuzzball) increases with the amount of brane quanta included, according to some law of the form $N^\alpha l_P$. If the fuzzball proposal turns out to be the correct way to go, quantum gravity effects reach out to a length scale of the form $N^\alpha l_P$, rather than being confined to e.g. the Planck length l_P.

5.1.3 Relating polar states in 4d to fuzzball geometries in 5d

It will have become clear from previous chapters, that multi-centered black holes and especially polar states in four dimensions are of special interest. Having explained the interest in the fuzzball program, which is more closely linked to a 5d setup, it is not hard to imagine that one would like to make contact between these two frameworks. It seems that it is typical for fuzzball geometries for a D1-D5-P black hole to be given as KK-anti-KK monopole configurations, which seems very similar to the D6-anti-D6 deconstruction of black holes made from D4-branes. It is also a goal to gain a better understanding of OSV-like statements, polar states in 4d and the connection to such 'fuzzball deconstructions' of D1-D5(-P) black holes in 5d. It is well known that four- and five-dimensional BPS configurations are related, and it is often possible to continuously interpolate between 4d and 5d configurations using the '4d-5d connection', [68,69,135–138]. Given a general multi-centered solution in 4d, or more specifically, the metric (2.16) ds^2_{4d}, the moduli (2.21) t^A and the gauge field (2.22) A_{4d}, one can write down a solution to 5d supergravity:

$$\begin{aligned} ds^2_{5d} &= (2V)^{\frac{2}{3}}(d\psi + \mathcal{A}^0_{4d})^2 + \frac{1}{(2V)^{\frac{1}{3}}} ds^2_{4d}, \\ \mathcal{A}^A_{5d} &= \mathcal{A}^A_{4d} + \mathrm{Re}(t^A)(d\psi + \mathcal{A}^0_{4d}), \\ Y^A &= \frac{\mathrm{Im}(t^A)}{V^{\frac{1}{3}}}. \end{aligned} \tag{5.11}$$

where $V = \frac{D_{ABC}}{6} J^A J^B J^C$ denotes the volume of the CY X, and the scalars appearing in a 5d action have been labeled as Y^A. Five-dimensional configurations can often be embedded in Taub-NUT space in a supersymmetric manner. The spatial geometry of Taub-NUT

[2] Note that this was suggested to be the case for the scaling solutions, discussed earlier on – a crucial point in connection to the split attractor flow tree conjecture.

space interpolates between $\mathbb{R}^4$ near the origin and $\mathbb{R}^3 \times S^1$ at infinity. By varying the size of the S^1, one can then interpolate between effectively five- and four-dimensional configurations. Under this map, a point-like configuration at the center of Taub-NUT space becomes a 4d pointlike solution with added Kaluza-Klein monopole charge. A ring-like configuration at some distance from the center goes over into a two-centered solution where one center comes from the wrapped ring and the other contains Kaluza-Klein monopole charge. Angular momentum in 5d goes over into linear momentum along S^1 in four dimensions. The goal of the research presented in this chapter was to give an explicit mapping between supertube solutions arising in the fuzzball picture in five dimensions and multi-centered solutions in four dimensions under the 4d-5d connection, and to interpret the resulting configurations using split attractor flow trees.

We (the author and collaborators) worked in toroidally compactified type II string theory, and considered a symmetric class of 2-charge supertubes, which are described by a circular profile [120–123], as well as 3-charge solutions obtained from those under spectral flow [139–142]. Placing such supertubes in Taub-NUT space gives the solutions that were constructed in [143, 144]. Applying the 4d-5d connection, we showed that, in the standard type IIB duality frame, one obtains 4d solutions which are two-centered Kaluza-Klein monopole-antimonopole pairs carrying flux-induced D1- and D5-brane charge as well as momentum. These solutions can be described within an STU-model truncation of $N = 8$ supergravity and can be seen as simple examples of 'bubbled' solutions [145–153] (for a review, see ([154]). To make contact with the techniques developed for analyzing multi-centered configurations in Calabi-Yau compactifications, we transformed these configurations to a type IIA duality frame where all charges and dipole moments carried arise from a D6-D4-D2-D0 brane system. In this duality frame, the relevant configurations are two stacks of D6-branes and anti-D6 branes with worldvolume fluxes turned on. Those configurations fall into the class of 'polar' states in 4d for which no single-centered solution exists.

Before moving on to present our research in detail, a brief summary of our results is given. We considered 5d supertube solutions carrying D1 charge N_1, D5 charge N_5 and momentum P and which are the gravity duals of a class of symmetric states in the D1-D5 CFT with quantum numbers

$$\begin{aligned} &L_0 = N_1 N_5 \left(m^2 + \tfrac{m}{n} + 1/4\right) , && \bar{L}_0 = \tfrac{N_1 N_5}{4} , \\ &J^3 = -\tfrac{N_1 N_5}{2} \left(2m + \tfrac{1}{n}\right) , && \bar{J}^3 = -\tfrac{N_1 N_5}{2n} , \\ &P = L_0 - \bar{L}_0 = N_1 N_5 m \left(m + \tfrac{1}{n}\right) . \end{aligned} \tag{5.12}$$

These represent Ramond sector states that are in a right-moving ground state and form excited states on the left, in a twisted sector. The integer n labels the twist sector and should be a divisor of $N_1 N_5$. In a component string picture, n represents the length of the component strings. These states can be seen as obtained from Ramond ground states through a left-moving spectral flow transformation determined by the parameter m, which should be an integer. They exclusively carry momentum when m is nonzero.

After applying the 4d-5d connection to these configurations, we interpreted them in a U-dual type IIA frame where all the charges arise from D6-D4-D2-D0 branes. Only 4

$q_0:$	$D0$	$p^0:$	$D6(T_1 \times T_2 \times T_3)$
$q_1:$	$D2(T_1)$	$p^1:$	$D4(T_2 \times T_3)$
$q_2:$	$D2(T_2)$	$p^2:$	$D4(T_1 \times T_3)$
$q_3:$	$D2(T_3)$	$p^3:$	$D4(T_1 \times T_2)$

Table 5.1: Type IIA D-brane charges carried by the considered configurations. The submanifold wrapped by the brane is indicated in brackets.

electric charges q_I and magnetic charges p^I are turned on in these solutions. They arise from wrapping D-branes on the internal cycles given in table 5.1.

Under the 4d-5d connection, the 5d quantum numbers (5.12) map to the following 4d charges

$$\begin{array}{|c|ccccc|} \hline 5d: & N_1 & N_5 & J^3 & \bar{J}^3 & P \\ 4d: & p^2 & p^3 & -\frac{q_1}{2} & -J_z & -q_0 \\ \hline \end{array} \tag{5.13}$$

Writing charges as $\Gamma = (p^I, q_I)$, the 4d BPS state corresponding to (5.12) carries the charge

$$\Gamma_{\text{tot}} = \left(0, 1, N_1, N_5, \left(2m + \frac{1}{n}\right) N_1 N_5, 0, 0, -m\left(m + \frac{1}{n}\right) N_1 N_5\right) . \tag{5.14}$$

This is a polar charge, for which there is no single-centered solution. It is realized as a two-centered solution consisting of two stacks of D6 and anti-D6 branes with fluxes, which can be written as

$$\begin{aligned} \Gamma_1 &= -n e^{-\left(m+\frac{1}{n}\right) D_1 + m N_1 D_2 + m N_5 D_3} , \\ \Gamma_2 &= n e^{-m D_1 + \left(m+\frac{1}{n}\right) N_1 D_2 + (m+\frac{1}{n}) N_5 D_3} . \end{aligned} \tag{5.15}$$

The length of the component string n has become the number of D6 and anti-D6 branes in the 4d picture, while the spectral flow parameter m has become a flux parameter. The restrictions on these parameters from charge quantization match the quantization conditions in the CFT description.

5.2 A class of polar states in $N = 8$ supergravity

In this section, the construction of two-centered solutions of type IIA supergravity compactified on a torus T^6, built from D6 and anti-D6 branes with flux, is presented. Split attractor flow trees are established, suggesting the existence of these states. First, the truncation of the torus-compactification of IIA supergravity to an STU-model will be briefly reviewed.

5.2.1 STU-truncation of type IIA on T^6

In the low-energy limit type IIA string theory compactified on a six-torus reduces to $N = 8$ supergravity in four dimensions. In $N = 2$ language, the $N = 8$ gravity multiplet decom-

poses into the $N = 2$ gravity multiplet, 6 gravitini multiplets, 15 vector multiplets, and 10 hypermultiplets. For our purposes, it was sufficient to consider a consistent truncation to a sector where only gravity and 3 vector multiplets are excited. This sector is described by the well-known STU model [155, 156], consisting of $N = 2$ supergravity coupled to 3 vector multiplets with symmetric prepotential

$$F = \frac{D_{ABC}}{6}\frac{X^A X^B X^C}{X^0} = \frac{X^1 X^2 X^3}{X^0}\,,$$

where $D_{ABC} = |\epsilon_{ABC}|$. The bosonic part of the action is given by

$$\begin{aligned} S &= \frac{1}{16\pi G_4}\int d^4x\sqrt{-g}\Big[R - \frac{1}{2}\sum_{A=1}^{3}\frac{\partial_\mu z^A \partial^\mu \bar{z}^A}{(\mathrm{Im}z^A)^2} \\ &\quad + \frac{\beta^2}{2}\mathrm{Im}\mathcal{N}_{IJ}\mathcal{F}^I_{\mu\nu}\mathcal{F}^{J\,\mu\nu} + \frac{\beta^2}{4}\mathrm{Re}\mathcal{N}_{IJ}\epsilon^{\mu\nu\rho\sigma}\mathcal{F}^I_{\mu\nu}\mathcal{F}^J_{\rho\sigma}\Big]\,. \end{aligned} \tag{5.16}$$

with $z^A = X^A/X^0 \equiv a_A + ib_A$, $A = 1, 2, 3$, $I = 0, 1, 2, 3$ and $\epsilon^{0123} \equiv 1$. An arbitrary normalization constant β was left in front of the kinetic terms of the $U(1)$ fields for easy comparison with different conventions used in the literature. The matrix $\mathcal{N}$ is given by

$$\mathcal{N}_{IJ} = \bar{F}_{IJ} + 2\mathrm{i}\frac{\mathrm{Im}(F_{IK})X^K \mathrm{Im}(F_{JL})X^L}{\mathrm{Im}(F_{MN})X^M X^N}\,, \tag{5.17}$$

where $F_{IJ} = \frac{\partial}{\partial X^I}\frac{\partial}{\partial X^J}F$. The explicit form of $\mathcal{N}$ can be found in the appendix (C.10). In the conventions used here, the scalars b_A have to be positive in order to have the correct kinetic term for the $U(1)$ fields. For simplicity, the hypermultiplet moduli are chosen such that the six-torus is metrically a product of three 2-tori $T_1 \times T_2 \times T_3$[3]. The 10-dimensional origin of the fields in (5.16) is the following. The vector multiplet scalars $z^A = X^A/X^0, A = 1, 2, 3$ describe complexified Kähler deformations of the tori T_A:

$$B + iJ = z^A D_A\,, \tag{5.18}$$

where D_A are normalized volume forms on T_A satisfying $\int_{T_A} D_B = \delta^A_B$. The constants D_{ABC} entering in the prepotential are proportional to the intersection numbers: $D_{ABC} = \int D_A \wedge D_B \wedge D_C$. The four $U(1)$ field strengths $\mathcal{F}^I = d\mathcal{A}^I, I = 0, \ldots, 3$ arise from dimensional reduction of the RR sector. Charged BPS states can carry electric and magnetic charges under the four $U(1)$ fields. The magnetic charges are denoted by p^I and the electric charges by q_I, and a general charge vector Γ is written either by a row vector or an element of the even cohomology of T^6:

$$\Gamma = (p^0, p^A, q_A, q_0) = p^0 + p^A D_A + q_A D^A + q_0\omega_{\mathrm{vol}}\,, \tag{5.19}$$

[3]For later convenience, T_1 is chosen to be rectangular, and its two circles are denoted by S^4, S^5.

with $D^A = \frac{1}{2} D_{ABC} D_B \wedge D_C$ and $\omega_{\rm vol} = D_1 \wedge D_2 \wedge D_3$ and $A = 1, \ldots, 3$. Taking into account charge quantization, the components p^I, q_I should be integers or $\Gamma \in H^{\rm even}(T^6, \mathbb{Z})$. In analogy to the CY case treated in previous chapters, the symplectic inner product reads

$$\langle \Gamma, \tilde{\Gamma} \rangle = -p^0 \tilde{q}_0 + p^A \tilde{q}_A - q_A \tilde{p}^A + q_0 \tilde{p}^0 \,. \tag{5.20}$$

From a 10-dimensional point of view, the charged BPS states arise from D-branes wrapping internal cycles. The D-brane interpretation of the charges is given in table 5.1. Dimensionally reducing the D-brane Born-Infeld and Wess-Zumino action leads to point-particle source terms to be added to the bulk action [157] (5.16):

$$S_{\rm source} = \frac{\beta}{G_4} \int \left[-|Z(Q)| ds + \frac{\beta}{2} \langle Q, \mathcal{A} \rangle \right] \,. \tag{5.21}$$

Here, Q is a vector whose components have the dimension of length defined as

$$\int_{S^2} \mathcal{F}^I = 4\pi Q^I, \qquad \int_{S^2} \mathcal{G}_I = 4\pi Q_I, \tag{5.22}$$

where $\mathcal{G}_I = {\rm Im}\mathcal{N}_{IJ} \star \mathcal{F}^J + {\rm Re}\mathcal{N}_{IJ} \mathcal{F}^J$ and $\star$ denotes the Hodge dual. As the size of one of the internal directions will be taken to infinity, it will be useful to work in conventions for later convenience, where the coordinate volume of the internal cycles is not fixed. The components of Q are then given by[4]

$$Q^I = \frac{\sqrt{8}}{\beta} T^I V^I G_4 p^I \,, \qquad Q_I = \frac{\sqrt{8}}{\beta} T_I V_I G_4 q_I \,. \tag{5.23}$$

where T^I, T_I are the tensions of the branes in table 5.1 and the V^I, V_I are the coordinate volumes of the cycles they are wrapping. The quantity $Z(Q)$ in (5.21) is the central charge

$$Z = \langle Q, \Omega \rangle \,, \tag{5.24}$$

and Ω is the normalized period vector defined as

$$\Omega = \frac{\Omega_{\rm hol}}{\sqrt{8 b_1 b_2 b_3}} \,, \tag{5.25}$$

with $\Omega_{\rm hol} = -e^{z^A D_A}$. A stack of D-branes with worldvolume flux F turned on sources lower D-brane charges according to

$$\Gamma = {\rm Tr}\, e^F \,. \tag{5.26}$$

This particular embedding of the STU model in toroidally compactified type II string theory will be denoted as 'duality frame A' in what follows. Later, in section 5.3, an embedding of the STU model into a U-dual type IIB duality frame is considered, which will be called 'frame B'.

[4] To find agreement with [52], one should take the coordinate volume of all cycles equal to one in units of $2\pi\sqrt{\alpha'}$. In that case, the relation between Q and Γ is $Q = \frac{\sqrt{G_4}}{\beta} \Gamma$. Furthermore, $\beta = 1$ in [52].

5.2.2 Multi-centered BPS solutions

Now, the construction of general multi-centered BPS solutions in the STU model considered above will be reviewed, along the lines of Bates and Denef [52]. Such solutions can be constructed from the harmonic functions

$$H^I = h^I + \sum_s \frac{Q^I}{|\vec{x} - \vec{x}_s|}, \qquad H_I = h_I + \sum_s \frac{Q_I}{|\vec{x} - \vec{x}_s|}\,, \tag{5.27}$$

where the index s runs over the centers and x_s are the locations of the centers in $\mathbb{R}^3$. As explained in chapter 2, the metric and gauge fields are then completely determined from the knowledge of a single function $\Sigma(H)$ on $\mathbb{R}^3$:

$$\Sigma(H) = \sqrt{\frac{4\kappa_1\kappa_2\kappa_3 - L^2}{(H^0)^2}}\,, \tag{5.28}$$

with

$$\begin{aligned} \kappa_A &= 3D_{ABC}H^B H^C - H_A H^0\,, \\ L &= 2H^1H^2H^3 + H_0(H^0)^2 - H^A H_A H^0\,. \end{aligned} \tag{5.29}$$

If one replaces the harmonic functions H in $\Sigma(H)$ by the charge vector Γ, the result is proportional to the Bekenstein-Hawking entropy $S(\Gamma)$ of a black hole with charge vector Γ: $\Sigma(\Gamma) = S(\Gamma)/\pi$. The constants h in the harmonic functions are related to the asymptotic Kähler moduli as follows,

$$h = -\frac{2}{\beta}\mathrm{Im}\frac{\bar{Z}_{\rm hol}\Omega}{|Z_{\rm hol}|}\,\Big|_\infty\,, \tag{5.30}$$

where $Z_{\rm hol}$ is the holomorphic central charge

$$Z_{\rm hol} = \langle \Gamma_{\rm tot}, \Omega_{\rm hol}\rangle\,. \tag{5.31}$$

Of the 8 components of h, only 6 are independent, corresponding to the asymptotic values of the 6 moduli $a_A,\ b_A$. Indeed, from the expressions above it follows that the h satisfy two constraints

$$\begin{aligned} \Sigma(h) &= \frac{1}{\beta^2}\,, \\ \langle h, Q_{tot}\rangle &= 0\,. \end{aligned} \tag{5.32}$$

The metric of the multi-centered solution is given by

$$ds_4^2 = -\frac{1}{\beta^2\Sigma(H)}(dt+\omega)^2 + \beta^2\Sigma(H)d\vec{x}^2\,, \tag{5.33}$$

where ω is a 1-form on $\mathbb{R}^3$ that satisfies

$$\star_3 d\omega = \beta^2\langle dH, H\rangle = \beta^2\left(-H_0 dH^0 + H_A dH^A - H^A dH_A + H^0 dH_0\right)\,, \tag{5.34}$$

where the Hodge star $\star_3$ is to be taken with respect to the flat metric on $\mathbb{R}^3$. The integrability condition for the existence of ω leads to constraints on the positions of the centers:

$$\sum_t \frac{\langle Q_s, Q_t\rangle}{|x_s - x_t|} + \langle Q_s, h\rangle = 0\,. \tag{5.35}$$

An important condition for the existence of the supergravity solution is that, when the above conditions are imposed, the function $\Sigma(H)$ should be real everywhere. Multi-centered solutions whose charges are non-parallel also carry angular momentum given by

$$\vec{J} = \frac{1}{2}\sum_{s<t}\langle \Gamma_s, \Gamma_t\rangle \frac{\vec{x}_s - \vec{x}_t}{|\vec{x}_s - \vec{x}_t|}\,. \tag{5.36}$$

In the special case of only 2 centers, the constraint on the distance a between the centers simplifies to

$$a = \frac{\langle Q_1, Q_2\rangle}{\langle Q_2, h\rangle}\,, \tag{5.37}$$

while the angular momentum is

$$J_z = \frac{1}{2}\langle \Gamma_1, \Gamma_2\rangle\,, \tag{5.38}$$

where the z-axis has been chosen to run in the direction from the second to the first center. The solution for the scalar moduli reads

$$z^A = \frac{\frac{\partial \Sigma(H)}{\partial H_A} - iH^A}{\frac{\partial \Sigma(H)}{\partial H_0} + iH^0}\,. \tag{5.39}$$

More explicitly, splitting z^a into real and imaginary parts $z^A = a_A + ib_A,\ A = 1, 2, 3$ one finds

$$\begin{aligned} a_A &= -\frac{H^A}{H^0} + \frac{L}{2\kappa_A H^0}\,, \\ b_A &= \frac{\Sigma}{2\kappa_A}\,. \end{aligned} \tag{5.40}$$

The gauge fields read

$$\begin{aligned} \mathcal{A}^0 &= \frac{1}{\beta}\frac{\partial \ln \Sigma(H)}{\partial H_0}(dt + \omega) + \mathcal{A}^0_D\,, \\ \mathcal{A}^A &= -\frac{1}{\beta}\frac{\partial \ln \Sigma(H)}{\partial H_A}(dt + \omega) + \mathcal{A}^A_D\,, \end{aligned} \tag{5.41}$$

where the Dirac parts $\mathcal{A}^I_D$ have to satisfy

$$\star_3 d\mathcal{A}^I_D = dH^I\,. \tag{5.42}$$

This can be worked out to yield

$$\begin{aligned}\mathcal{A}^0 &= -\frac{1}{\beta}\frac{L}{\Sigma^2}(dt+\omega)+\mathcal{A}^0_D\,,\\ \mathcal{A}^A &= \frac{1}{\beta}\frac{6D_{ABC}\kappa_B\kappa_C-H^A L}{H^0\Sigma^2}(dt+\omega)+\mathcal{A}^A_D\,.\end{aligned} \tag{5.43}$$

These quantities can be rewritten as

$$\Sigma = \sqrt{-4H_0H^1H^2H^3-4H^0H_1H_2H_3+(H^IH_I)^2-2\sum_I(H_I)^2(H^I)^2}\,, \tag{5.44}$$

$$\begin{aligned}a_A &= \frac{H_0H^0+H_AH^A-\sum_{B\neq A}H_BH^B}{D_{ABC}H^BH^C-2H_AH^0}\,,\\ b_A &= \frac{\Sigma}{D_{ABC}H^BH^C-2H_AH^0}\,,\end{aligned} \tag{5.45}$$

$$\begin{aligned}\mathcal{A}^0 &= \frac{1}{\beta\Sigma^2}\left(H^0\left(H_IH^I-2H_0H^0\right)-\frac{1}{3}D_{ABC}H^AH^BH^C\right)(dt+\omega)+\mathcal{A}^0_D\,,\\ \mathcal{A}^A &= -\frac{1}{\beta\Sigma^2}\left(H^A\left(H_IH^I-2H^AH_A\right)-D_{ABC}H_BH_CH^0\right)(dt+\omega)+\mathcal{A}^A_D\,.\end{aligned} \tag{5.46}$$

One can also consider the effect of large gauge transformations of the B-field, under which the B-field shifts with a harmonic form. Gauge invariance requires that this is accompanied by a shift in the worldvolume flux, resulting in a transformation of the charge vector:

$$B\to B+S \qquad \Gamma\to e^S\Gamma\,. \tag{5.47}$$

In the 4d effective theory, the above transformation is induced by a symplectic transformation

$$X^A\to X^A+S^AX^0. \tag{5.48}$$

Taking charge quantization into account, S should be restricted to be an element of the integer cohomology. Large gauge transformations change the boundary conditions at infinity and, in the dual conformal field theory, have the effect of inducing a spectral flow [54, 101, 158].

5.2.3 Solutions for polar states

A particular set of 2-centered solutions will now be described, where the centers are stacks of D6 and anti-D6 branes with worldvolume fluxes turned on. It will also be shown that no single-centered solutions with the same total charge exist for these configurations. As can be traced in the previous chapters, they correspond to polar states and, according to the split attractor flow conjecture, their existence can be established from split attractor flow trees.

We considered two classes of polar states: the first class carries no D0-brane charge and has four net D4-D2 charges p^1, p^2, p^3, q_1. These are the configurations (5.15) with $m = 0$. By performing a spectral flow transformation of the form (5.47) one obtains a second class of solutions ($m \neq 0$ in (5.15)), which carry the above four charges as well as D0-brane charge q_0. In section 5.3, it will be shown that these two classes of configurations, after a U-duality transformation, give rise to smooth 'fuzzball' solutions placed in a Taub-NUT background. The solutions without D0-charge will map to fuzzball solutions with D1-charge and D5-charge in Taub-NUT space while the solutions carrying D0-charge will map to fuzzball solutions with D1-D5 charge and momentum P in Taub-NUT.

Configurations without D0-charge

The first class of solutions considered consists of a stack of n D6 branes and a stack of n anti-D6 branes. Each stack of branes has $U(n) = U(1) \times SU(n)$ gauge fields living on the worldvolume. Worldvolume fluxes are chosen to lie in the $U(1)$ part so that each stack carries lower-dimensional D-brane charges as well. Three numbers characterize the fluxes, which, for later convenience, are labeled N_K, N_1, N_5. The charges at the centers are

$$\begin{aligned} \Gamma_1 &= -n\, e^{-\frac{N_K}{n} D_1} = (-n, N_K, 0, 0, 0, 0, 0, 0)\ , \\ \Gamma_2 &= n\, e^{\frac{N_1}{n} D_2 + \frac{N_5}{n} D_3} = \left(n, 0, N_1, N_5, \frac{N_1 N_5}{n}, 0, 0, 0\right)\ . \end{aligned} \tag{5.49}$$

In the quantum theory, charge quantization restricts n, N_K, N_1, N_5 to be integers and n to be a divisor of $N_1 N_5$. These configurations carry 4 nonzero net charges p^1, p^2, p^3, q_1:

$$\Gamma_{\rm tot} = \left(0, N_K, N_1, N_5, \frac{N_1 N_5}{n}, 0, 0, 0\right)\ . \tag{5.50}$$

One can choose coordinates on $\mathbb{R}^3$ such that the first center Γ_1 is located at the origin and Γ_2 lies on the positive z-axis at $z = a$. The harmonic functions are

$$\begin{aligned} H^0 &= h^0 - \tfrac{Q_n}{r} + \tfrac{Q_n}{r_+}\,, & H_0 &= h_0\,, \\ H^1 &= h^1 + \tfrac{Q_K}{r}\,, & H_1 &= h_1 + \tfrac{Q_1 Q_5}{Q_n r_+}\,, \\ H^2 &= h^2 + \tfrac{Q_1}{r_+}\,, & H_2 &= h_2\,, \\ H^3 &= h^3 + \tfrac{Q_5}{r_+}\,, & H_3 &= h_3\,. \end{aligned} \tag{5.51}$$

r_+ was defined to be the radial distance to the second center:

$$r_+ \equiv \sqrt{r^2 + a^2 - 2ar\cos\theta}\,. \tag{5.52}$$

From now on, the normalization constant β in (5.16) will be chosen to be

$$\beta = \frac{1}{\sqrt{2}}. \tag{5.53}$$

Using (5.23), the normalizations in the harmonic functions are then given by

$$\begin{aligned} Q_n &= \tfrac{1}{2}\sqrt{\alpha'}gn & Q_K &= \tfrac{(2\pi)^2(\alpha')^{\frac{3}{2}}g}{2V_{T_1}}N_K \\ Q_1 &= \tfrac{(2\pi)^2(\alpha')^{\frac{3}{2}}g}{2V_{T_2}}N_1 & Q_5 &= \tfrac{(2\pi)^2(\alpha')^{\frac{3}{2}}g}{2V_{T_3}}N_5 \end{aligned} \tag{5.54}$$

where g is the 10D string coupling constant. One can simplify the form of the solution by picking convenient values for the asymptotic moduli and correspondingly the constants h. We chose six of the constants to be

$$h_0 = -1; \qquad h^1 = h^2 = h^3 = 1; \qquad h_2 = h_3 = 0\,. \tag{5.55}$$

The remaining constants h^0, h_1 are then fixed by the constraints (5.32):

$$h_1 = -h^0 = \frac{Q_1 Q_5}{Q_n Q_K}\,. \tag{5.56}$$

From (5.45) one can see that this choice of harmonic constants corresponds to turning on asymptotic B-field on T_1 but not on $T_2,\ T_3$. The constraint (5.37) on the distance between the centers reads

$$a = \frac{Q_K Q_1 Q_5}{Q_n^2 - Q_1 Q_5}\,. \tag{5.57}$$

The solution carries angular momentum given by (5.38):

$$J_z = \frac{N_K N_1 N_5}{2n}. \tag{5.58}$$

One can then find the explicit expressions for the metric, scalar fields and $U(1)$ fields from (5.33, 5.45, 5.46). For configurations where $H_2 = H_3 = 0$, the expression (5.44) for Σ simplifies to

$$\Sigma = \sqrt{-4H_0H^1H^2H^3 - (H_0H^0 - H_1H^1)^2}\,. \tag{5.59}$$

For the solution to the equations (5.34) and (5.42) for ω and the Dirac parts $\mathcal{A}^I_D$ one finds, using (5.57) and choosing convenient integration constants,

$$\begin{aligned} \omega &= \frac{Q_K Q_1 Q_5}{2aQ_n}\left(\frac{r+a}{r_+} - 1\right)(\cos\theta - 1)d\phi\,, \\ \mathcal{A}^0_D &= Q_n\left(-\cos\theta + \frac{r\cos\theta - a}{r_+}\right)d\phi\,, \\ \mathcal{A}^1_D &= Q_K\cos\theta d\phi\,, \\ \mathcal{A}^2_D &= Q_1\frac{r\cos\theta - a}{r_+}d\phi\,, \\ \mathcal{A}^3_D &= Q_5\frac{r\cos\theta - a}{r_+}d\phi\,. \end{aligned} \tag{5.60}$$

Spectral flow and adding D0-charge

One is interested in a second class of solutions obtained from the ones considered above by a spectral flow transformation of the form (5.47) $\Gamma \to e^S\Gamma$. One can choose S such that the new configuration carries nonzero p^1, p^2, p^3, q_1 charges as well as D0-charge q_0, while keeping q_2 and q_3 zero. There is a one-parameter family of spectral flows S which does the job and which will be labeled by a parameter m:

$$S = -mN_K D_1 + mN_1 D_2 + mN_5 D_3 \,. \tag{5.61}$$

When taking charge quantization into account, the parameter m could be fractional but such that m is a common multiple of $1/N_1, 1/N_5$ and $1/N_K$. The charges carried by the two centers are then the ones anticipated in (5.15):

$$\begin{aligned} \Gamma_1 &= -ne^{-\left(m+\frac{1}{n}\right)N_K D_1 + mN_1 D_2 + mN_5 D_3}\,, \\ \Gamma_2 &= ne^{-mN_K D_1 + \left(m+\frac{1}{n}\right)N_1 D_2 + (m+\frac{1}{n})N_5 D_3}\,, \end{aligned} \tag{5.62}$$

and the total charge of the solution is

$$\Gamma_{\rm tot} = \left(0, N_K, N_1, N_5, \left(2m + \frac{1}{n}\right) N_1 N_5, 0, 0, -m\left(m + \frac{1}{n}\right) N_K N_1 N_5\right) . \tag{5.63}$$

The angular momentum of these configurations is independent of the parameter m and still given by (5.58). For $m = 0$ one recovers the configurations discussed in the previous section. The harmonic functions for a configuration obtained using spectral flow are

$$\begin{aligned} H^0 &= h^0 - \tfrac{Q_n}{r} + \tfrac{Q_n}{r_+}\,, & H_0 &= h_0 + \tfrac{(mn+1)(mn)^2 Q_K Q_1 Q_5}{Q_n^2 r} - \tfrac{(mn+1)^2 mn Q_K Q_1 Q_5}{Q_n^2 r_+}\,, \\ H^1 &= h^1 + \tfrac{(mn+1)Q_K}{r} - \tfrac{mnQ_K}{r_+}\,, & H_1 &= h_1 - \tfrac{(mn)^2 Q_1 Q_5}{Q_n r} + \tfrac{(mn+1)^2 Q_1 Q_5}{Q_n r_+}\,, \\ H^2 &= h^2 - \tfrac{mnQ_1}{r} + \tfrac{(mn+1)Q_1}{r_+}\,, & H_2 &= h_2 + \tfrac{(mn+1)mnQ_K Q_5}{Q_n r} - \tfrac{(mn+1)mnQ_K Q_5}{Q_n r_+}\,, \\ H^3 &= h^3 - \tfrac{mnQ_5}{r} + \tfrac{(mn+1)Q_5}{r_+}\,, & H_3 &= h_3 + \tfrac{(mn+1)mnQ_K Q_1}{Q_n r} - \tfrac{(mn+1)mnQ_K Q_1}{Q_n r_+}\,. \end{aligned} \tag{5.64}$$

As before, one can choose the asymptotic moduli such that $h_0 = -1, \quad h^1 = h^2 = h^3 = 1, \; h_2 = h_3 = 0$. The remaining constants are determined by (5.32) to be

$$h_1 = -h^0 = \frac{(2mn+1)Q_1 Q_5 Q_n}{(mn+1)mnQ_K Q_1 Q_5 + Q_K Q_n^2}\,. \tag{5.65}$$

For the constraint (5.37) on the distance one finds a rather complicated expression

$$\begin{aligned} \frac{1}{a} &= \frac{1}{Q_K Q_1 Q_5\left((mn+1)^2(mn)^2 Q_1 Q_5 + Q_n^2\right)}\Big(Q_n^4 - Q_n^2\left(Q_1 Q_5 + (mn+1)(2Q_1 Q_5 - Q_K(Q_1+Q_5))\right) \\ &\quad + (mn+1)^2(mn)^2 Q_1 Q_5 (Q_K Q_1 + Q_K Q_5 + Q_1 Q_5)\Big)\,. \end{aligned} \tag{5.66}$$

5.2.4 Polarity and flow trees

It will be now be discussed that the considered configurations are four-dimensional 'polar' states. As discussed already extensively in this thesis, the relevant quantity for establishing whether a total charge system $\Gamma_{\rm tot}$ is polar, is the 'reduced' D0 brane charge

$$\hat{q}_0 = q_0 - \frac{1}{2} D^{AB} q_A q_B \,, \tag{5.67}$$

where $D^{AB} = (D_{ABC} p^C)^{-1}$. If $\hat{q}_0 > 0$, the states are polar and no single-centered black hole solutions carrying these charges exist. This means that the states considered here, are polar if one chooses positive fluxes on the branes. For $n = 1$, when there is only one D6 and one anti-D6 brane, $\hat{q}_0$ reaches its maximal value for a given p^1, p^2, p^3 charge. The quantity $\hat{q}_0$ is invariant under spectral flow transformations (5.47), hence the charge configurations with D0 charge (5.63) are also polar. We inspected the existence of split flow trees for these configurations in order to be able to infer the existence of the corresponding BPS state. We were able to show that the single centered flow reaches a wall of marginal stability at a point $z_{\rm split}$ in moduli space before reaching the crash point z_0, where the single centered flow ends. At the marginal stability wall, the flow branches into two flows representing the D6 and anti D6 centers, which reach their attractor points without encountering any more marginal stability walls. A schematic depiction of the split flow is given in figure 5.3.

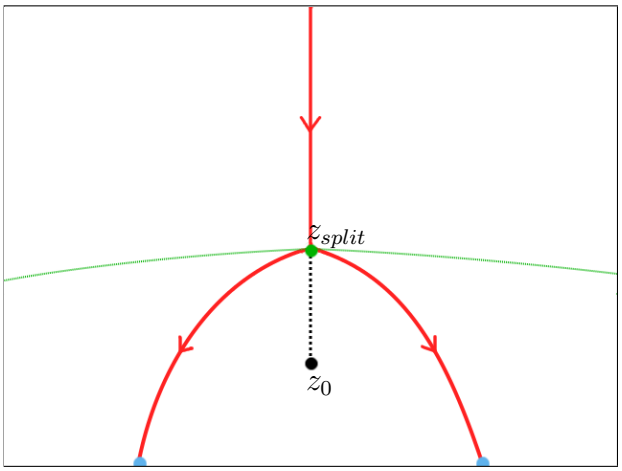

Figure 5.3: Schematic drawing of the split flow tree for our representative charge system. The flow coming in from the top (red line) reaches the wall of marginal stability (green line) at the split point z_{split} (green) before it would reach the crash point z_0 (black). One also sees the single flows for each center starting from the split point until they reach the boundary of moduli space (blue). The existence of those states is clear in the light of the previous chapter.

A crucial simplification is that, by doing the spectral flow transformation (5.47), one can equivalently examine the flow tree for a charge $e^S\Gamma$ at a shifted B-value $B + S$. When, by shifting the asymptotic value of the B-field, one does not cross any walls of marginal

stability, one can simply fix the asymptotic B-field to a convenient value and choose a charge vector $e^S\Gamma$ such that the analysis becomes simple. This was possible for the considered configurations, provided that one chooses the background Kähler moduli large enough. The reason for this is that walls of marginal stability between two charges can only run all the way to infinity for a 'core-halo pair' of D-branes (Halos can only carry D2-D0 brane charge, any other charge configuration will automatically be a core, see [1] for definitions and a more in-depth treatment of these concepts). Luckily, one is always dealing with core constituents here. From now on, the asymptotic B-field will be taken to be zero and an appropriate charge vector $e^S\Gamma$ is chosen.

One can pick a charge representative by giving some convenient value to the spectral flow parameter m in the general charge configuration (5.63). It can be taken to have the value[5] $m = -\frac{1}{2n}$. This leads to the total charge

$$\Gamma_{\rm tot} = \left(0, N_K, N_1, N_5, 0, 0, 0, \frac{N_K N_1 N_5}{4n^2}\right) . \tag{5.68}$$

This obviously is a pure D4-D0 system. As discussed above, one chooses the background moduli to have purely imaginary and very large values, $z_\infty = (iy^1_\infty, iy^2_\infty, iy^3_\infty)$. The single centered flow runs along the imaginary z-axes until the crash point is reached where the holomorphic central charge (5.31) vanishes. This happens at the point

$$z_0 = i\sqrt{\frac{\hat{q}_0}{3N_K N_1 N_5}}(N_K, N_1, N_5) = i\frac{1}{\sqrt{12n^2}}(N_K, N_1, N_5) . \tag{5.69}$$

Next one can check whether the flow hits a wall of marginal stability. The charges at the centers read

$$\begin{aligned} \Gamma_1 &= \left(-n, \frac{N_K}{2}, \frac{N_1}{2}, \frac{N_5}{2}, -\frac{N_1 N_5}{4n}, -\frac{N_K N_5}{4n}, -\frac{N_K N_1}{4n}, \frac{N_K N_1 N_5}{8n^2}\right) , \\ \Gamma_2 &= \left(n, \frac{N_K}{2}, \frac{N_1}{2}, \frac{N_5}{2}, \frac{N_1 N_5}{4n}, \frac{N_K N_5}{4n}, \frac{N_K N_1}{4n}, \frac{N_K N_1 N_5}{8n^2}\right) . \end{aligned} \tag{5.70}$$

One easily sees that the real parts of the central charges are equal, whereas the imaginary parts have opposite signs. Thus, the wall will be hit when $\mathrm{Im}(\mathrm{Z}_1) = \mathrm{Im}(\mathrm{Z}_2) = 0$. One finds

$$z_{\rm split} = i\sqrt{\frac{3}{4n^2}}(N_K, N_1, N_5) . \tag{5.71}$$

As $\sqrt{\frac{3}{4n^2}} > \sqrt{\frac{1}{12n^2}}$ this means that the wall of marginal stability is always reached before the single flow crashes. The single centered flows for the fluxed D6 brane centers terminate at the boundary of moduli space in the supergravity approximation. Nevertheless they correspond to states in the BPS spectrum of string theory and higher derivative corrections

[5] As the flow tree analysis takes place within supergravity, one can ignore charge quantization restrictions for the moment.

are expected to yield regular attractor points: the reader finds explanations on this as well as numerous examples for (fluxed) D6 branes on a Calabi-Yau, in chapter 4.

A further simple check also shows that the necessary stability criterion [1, 60] $\langle \Gamma_1, \Gamma_2 \rangle \cdot (\arg(Z_1) - \arg(Z_2)) > 0$ is met. This shows that one indeed reaches the wall from the side where the single brane is stable and crosses to the side where the brane decays into a bound state. Recall that this condition can be interpreted as ensuring that tachyonic strings would be present between the two constituent branes on the 'stable' side, in this case above the wall, such that a bound state is formed after tachyon condensation.

5.3 U-duality and fuzzballs in Taub-NUT

In this section, contact is made between the polar solutions constructed above and various horizonless supertube solutions in five noncompact dimensions that are central to the fuzzball proposal advocated by Mathur and collaborators. As a first step, a duality transformation to a type IIB frame is performed, such that the charges and dipole moments carried by the found solutions are the same as the ones carried by the supertubes. Fuzzball solutions in five noncompact dimensions can be seen as Kaluza-Klein (KK) monopole[6] supertubes where the KK monopole charge is sourced along a contractible curve in four noncompact directions. One of the compact directions, which will become S^4 in the conventions used here (recall that $T_1 = S^4 \times S^5$ was chosen), is a Taub-NUT circle which pinches off at every point of the curve. By adding flux to the KK-monopole, one can source the charge of D1 and D5-branes wrapped around the S^4 circle. For a circular curve, one can place this configuration in a Taub-NUT space with a different Taub-NUT circle, S^5 in the present conventions, and interpolate between five and four dimensions by varying the size of S^5. We were able to show that the four-dimensional configurations obtained in this manner are U-dual to the D6-anti D6 polar solutions discussed above.

5.3.1 U-duality to a type IIB frame

First, a U-duality transformation to a type IIB frame is described such that STU-model solutions lift to configurations carrying the charges indicated above. The system is taken to a duality frame where p^0 becomes a Kaluza-Klein monopole charge with Taub-NUT circle S^4, p^1 becomes a Kaluza-Klein monopole charge with Taub-NUT circle S^5, p^2 becomes the charge of a $D1$-brane wrapped on S^4 and p^3 becomes the charge of a $D5$-brane wrapped on $S^4 \times T_2 \times T_3$. This is accomplished by making a U-duality transformation consisting of a T-duality along S^4, followed by S-duality and 4 T-dualities along $T_1 \times T_3$, as illustrated in table 5.2.

This new duality frame will be denoted 'frame B'. In this frame, the vector multiplet scalars z^1, z^2, z^3 represent the complex structure modulus of T_1, the 4d axion-dilaton and the (complexified) Kähler modulus of T_1 respectively. The $U(1)$ fields $\mathcal{A}^0$ and $\mathcal{A}^1$ are

[6]Recall that a Kaluza-Klein monopole in 10D is a (5+1)-dimensional object whose transverse 4-dimensional space has Taub-NUT geometry or, in the case of several centers, a Gibbons-Hawking space.

IIA (frame A)		IIB		IIB		IIB (frame B)
D6 (T^6)		D5		NS5		KK5 $(S^5 \times T_2 \times T_3)$
D4 $(T_2 \times T_3)$	T (S^4)	D5	S	NS5	T (S^4, S^5, T_3)	KK5 $(S^4 \times T_2 \times T_3)$
D4 $(T_1 \times T_3)$	$\longrightarrow$	D3	$\longrightarrow$	D3	$\longrightarrow$	D1 (S^4)
D4 $(T_1 \times T_2)$		D3		D3		D5 $(S^4 \times T_2 \times T_3)$

Table 5.2: U-duality transformation from frame A to frame B

q_0	P (S^4)	p^0	KK5 $(S^5 \times T_2 \times T_3)$
q_1	P (S^5)	p^1	KK5 $(S^4 \times T_2 \times T_3)$
q_2	D5 $(S^5 \times T_2 \times T_3)$	p^2	D1 (S^4)
q_3	D1 (S^5)	p^3	D5 $(S^4 \times T_2 \times T_3)$

Table 5.3: 10D origin of the charges in frame B

Kaluza-Klein gauge fields from the metric components $g_{\mu 4}$ and $g_{\mu 5}$ respectively, while $\mathcal{A}^2$ and $\mathcal{A}^3$ arise from the RR two form components $C_{\mu 4}$ and $C_{\mu 5}$. The 10-dimensional origin of the full set of charges in this frame is given in table C.2. In frame B, the first class of polar solutions with charges (5.49) corresponds to two stacks of n KK monopoles and anti-KK monopoles with Taub-NUT circle S^4 carrying flux-induced charges of D1, D5, momentum and KK monopoles wrapped on the S^4 circle. The more general solutions (5.62) obtained by spectral flow carry momentum along S^4 as well. Such solutions will be smooth, and, as will be shown, have the interpretation of KK monopole supertubes embedded in Taub-NUT space.

5.3.2 Lifting general multi-centered solutions

In order to see what these solutions look like in frame B from the 10-dimensional point of view, one needs to know the reduction formulas of type IIB on a six-torus to the four-dimensional STU-model action (5.16) such that the 4d charges have the interpretation given in table C.2. This is worked out in detail in appendix C. The metric of a general 4d multi-centered solution lifts to a 10D geometry where the T_1 torus is nontrivially fibered over the 4d base:

$$\begin{aligned} ds_{10}^2 &= \frac{1}{\sqrt{b^2 b^3}} ds_4^2 + \sqrt{b^2 b^3}\mathcal{M}_{mn}(dx^m + \mathcal{A}^{m-4})(dx^n + \mathcal{A}^{n-4}) + \sqrt{\frac{b^2}{b^3}} ds^2_{T_2 \times T_3}\,, \\ ds_4^2 &= -\frac{2}{\Sigma}(dt + \omega)^2 + \frac{\Sigma}{2} d\vec{x}^2\,, \\ \mathcal{M}_{mn} &= \frac{1}{b^1}\begin{pmatrix} (a^1)^2 + (b^1)^2 & -a^1 \\ -a^1 & 1 \end{pmatrix}, \qquad m, n = 4, 5\,. \end{aligned} \tag{5.72}$$

The dilaton and RR two-form are given by

$$\begin{aligned} e^{2\Phi^{(10)}} &= \frac{b^2}{b^3}\,, \\ C^{(10)} &= \frac{1}{2}C_{\mu\nu}dx^\mu dx^\nu + a^3(dx^4-\mathcal{A}^0)\wedge(dx^5-\mathcal{A}^1) \\ &\quad -dx^4\wedge\mathcal{B}^2 - dx^5\wedge\mathcal{A}^3 + \frac{1}{2}(\mathcal{A}^0\wedge\mathcal{B}^2+\mathcal{A}^1\wedge\mathcal{A}^3)\,, \\ da^2 &= -(b^2)^2\star F\,, \\ F &= dC + \frac{1}{4}(\mathcal{A}^0\wedge\mathcal{G}^2+\mathcal{B}^2\wedge\mathcal{F}^0+\mathcal{A}^1\wedge\mathcal{F}^3+\mathcal{A}^3\wedge\mathcal{F}^1)\,. \end{aligned} \tag{5.73}$$

where the Hodge $\star$ is to be taken with respect to the 4d metric ds_4^2. It will be useful to rewrite the metric in the form of a lifted solution of 6d supergravity as in [118, 158, 159], where the 6d part of the metric is written as a fibration over a 4d Gibbons-Hawking base space. If both p^0 and p^1 are nonzero, both the S^4 and S^5 are nontrivially fibered, and one can choose either circle to be the fibre in the Gibbons-Hawking geometry. Here, the S^5 is chosen to be this fibre, so that the Gibbons-Hawking base space is spanned by the coordinates (r,θ,ϕ,x^5). The metric can be rewritten in the form

$$\begin{aligned} ds^2 &= -\frac{1}{HF}(dt+k)^2 + \frac{F}{H}\left(dx^4 - s - \frac{1}{F}(dt+k)\right)^2 + Hds^2_{\rm GH} + \sqrt{\frac{\kappa_2}{\kappa_3}}ds^2_{T_2\times T_3}\,, \\ ds^2_{\rm GH} &= \frac{1}{H^1}(dx^5+\mathcal{A}^1_D)^2 + H^1 d\mathbf{x}^2\,. \end{aligned} \tag{5.74}$$

where one has defined

$$\begin{aligned} F &= \left(H_2\frac{H_3}{H^1} - H_0\right)\,, \\ H &= \frac{\sqrt{\kappa_2\kappa_3}}{H_1}\,, \\ k &= \omega + \frac{LH^1 - 2\kappa_2\kappa_3}{\sqrt{2}H^0(H^1)^2}(dx^5+\mathcal{A}^1_D) \\ &= \omega + \frac{1}{H_1}\left(H_I H^I - 2H_1H^1 - \frac{2H_0H_2H_3}{H^1}\right)(dx^5+\mathcal{A}^1_D)\,, \\ s &= -\mathcal{A}^0_D + \frac{H^0}{H^1}(dx^5+\mathcal{A}^1_D)\,. \end{aligned} \tag{5.75}$$

These expressions will now be used to find the lift of the four-dimensional polar configurations.

5.3.3 Lift of polar states without D0 charge

The lift of our configurations (5.49) that do not contain D0 charge will first be discussed in frame A. In frame B these correspond, according to table C.2, to two stacks of n KK

monopoles and anti-KK monopoles with Taub-NUT circle S^4, which carry flux-induced D1, D5 and KK monopole charges, wrapped on the S^4 circle. It will be shown that, from a 10D point of view, these charges precisely correspond to the Kaluza-Klein monopole supertubes in Taub-NUT space that were constructed by Bena and Kraus in [143].

The harmonic functions of the solution are given by (5.51, 5.55, 5.56), where the normalizations in the current duality frame should be taken to be, according to (5.23),

$$\begin{array}{ll} Q_n = \frac{nR_4}{2}\,, & Q_K = \frac{N_K R_5}{2}\,, \\ Q_1 = \frac{(2\pi)^4 g\alpha'^3}{2R_5 V_{T_2\times T_3}} N_,\,. & Q_5 = \frac{g\alpha'}{2R_5} N_5\,. \end{array} \tag{5.76}$$

The constraint on the distance between the centers (5.57) can also be written as

$$Q_n = \sqrt{Q_1 Q_5 \tilde{H}^1}\,, \tag{5.77}$$

with $\tilde{H}^1 = 1 + \frac{Q_K}{a}$. One finds the lift of this class of solutions to 10 dimensions in duality frame B by plugging these expressions into (5.74). Making a coordinate transformation $x^4 \to x^4 + t$, the metric becomes

$$\begin{aligned} ds^2 &= \frac{1}{\sqrt{H^2 H^3}}\left[-(dt+k)^2 + (dx^4 - s - k)^2\right] + \sqrt{H^2 H^3} ds^2_{\rm TN} + \sqrt{\frac{H^2}{H^3}} ds^2_{T_2\times T_3}\,, \\ ds^2_{\rm TN} &= \frac{1}{H^1}(R_5 d\psi + Q_K \cos\theta d\phi)^2 + H^1 d\mathbf{x}^2\,. \end{aligned} \tag{5.78}$$

where the angle ψ has been defined as $x^5 = R_5\psi$. From the ten-dimensional point of view, the constraint (5.77) on the distance between the centers arises from requiring smoothness of the metric [143], while the condition that Σ is real implies the absence of closed timelike curves [150]. The one-forms k and s have components along ϕ and ψ and, using the distance constraint (5.77), can be written as

$$\begin{array}{ll} k_\psi = \frac{R_5 Q_n Q_K}{2a r_+ \tilde{H}^1 H^1}\left[r_+ - r - a - \frac{2ar}{Q_K}\right]\,, & k_\phi = \frac{Q_n Q_K}{2a r_+ \tilde{H}^1}\left[r_+ - r - a + \frac{r-a-r_+}{H^1}\cos\theta\right]\,, \\ s_\psi = \frac{R_5 Q_n}{r r_+ H^1}\left[r - r_+ - \frac{r r_+}{Q_K \tilde{H}^1}\right]\,, & s_\phi = \frac{Q_n}{r_+}\left[a + \frac{r_+ - r - \frac{r_+}{\tilde{H}^1}}{H^1}\cos\theta\right]\,. \end{array} \tag{5.79}$$

Using (5.73), one can show that the dilaton and RR three-form take the form

$$\begin{aligned} e^{2\Phi} &= \frac{H^2}{H^3}\,, \\ F^{(3)} &= d\left[\frac{1}{H^2}(dt+k)\wedge(dx^4 - s - k)\right] - \star_4 d(H^3)\,, \end{aligned} \tag{5.80}$$

where the Hodge star $\star_4$ is to be taken with respect to the Taub-NUT metric ds^2_{TN}. As was argued, the above solutions represent the lift of a two-centered KK-monopole anti-monopole system in frame B (or a D6 anti-D6 system in frame A), where the Taub-NUT

circle for these KK monopoles is the S^4. The KK monopoles sit at a radial distance r_+ while the anti-monopoles sit at the origin. At the position of these centers, the S^4 circle should pinch off. This is not so obvious in the 10D form of the metric (5.78), so this point will be illustrated in more detail. The coefficient in front of the $(dx^4)^2$ term in the metric (5.78) is $1/\sqrt{H^2H^3}$. This factor goes to zero at $r = r_+$ but stays finite at $r = 0$, so it is not obvious that there is a KK anti-monopole source at the origin. Nevertheless, there should be such a source since the total KK monopole charge has to balance out, and it should be located at the origin because of symmetry reasons. The resolution to this puzzle lies in the fact that the six-dimensional metric still contains a factor of the six-dimensional dilaton $e^{\Phi^{(6)}}$. This factor is given by $e^{\Phi^{(6)}} = \frac{1}{b_2 b_3}$, and hence the factor that measures the size of the S^4 is $b_2 b_3/\sqrt{H^2H^3}$. One can easily check that this factor indeed goes to zero both in $r = 0$ and $r = r_+$. This is illustrated in figure 5.4.

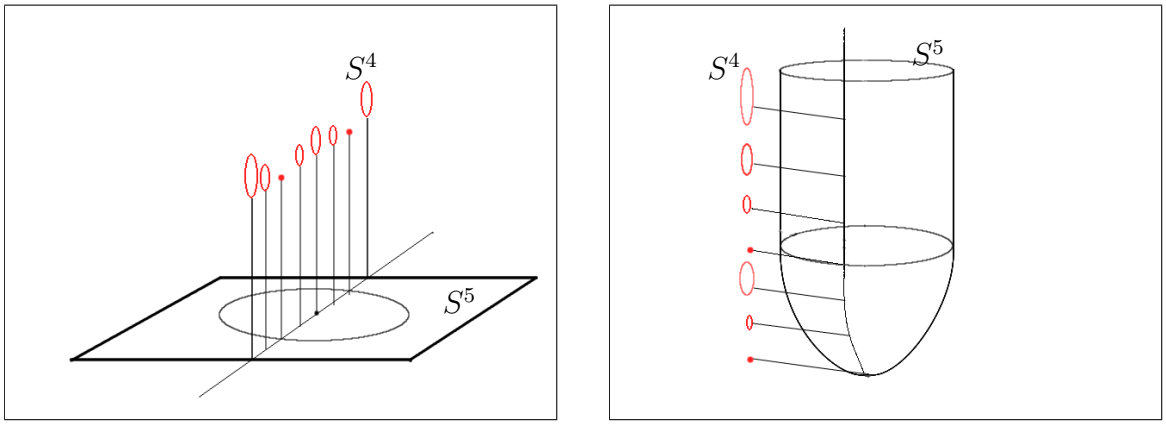

Figure 5.4: Left: The black circle represents a KK monopole supertube with a circular profile of radius a in 5 dimensions. At every point of the curve, the internal circle S^4 (drawn in red) pinches off to zero size. Right: After placing another KK monopole wrapped on S^4 in the origin, the asymptotic geometry becomes $\mathbb{R}^4 \times S^5$. As argued in the text, the S^4 circle pinches off along the curve as well as in the origin.

These are precisely the solutions constructed by Bena and Kraus [143][7]. They represent Kaluza-Klein monopole supertubes, which have been embedded into a Taub-NUT space which has the asymptotic spatial geometry $\mathbb{R}^3 \times S^5$. By varying the radius R_5 of the circle S^5 one can interpolate between solutions in 4 and in 5 noncompact dimensions; this is the '4d-5d connection' [68, 69]. The 5d solutions one obtains in this way are highly symmetric fuzzball solutions where the curve that defines the supertube is circular.

[7]To make contact with the conventions in [143], one has to make a further coordinate transformation $\phi \to -\phi, \theta \to \pi - \theta$.

5.3.4 4d-5d connection and 5d fuzzball geometries

Let this be illustrated in more detail. One takes the $R_5 \to \infty$ limit keeping the following quantities fixed:

$$2rR_5 \equiv \tilde{r}^2\,, \qquad 2aR_5 \equiv \tilde{a}^2/n^2\,. \tag{5.81}$$

After taking this limit, the p^1 charge N_K of the configuration becomes a deficit angle and one obtains a configuration embedded in an orbifold space $\mathbb{R}^4/\mathbb{Z}_{N_K}$. We therefore specialized to the case $N_K = 1$, so that we obtained solutions in asymptotically flat space. One defines charges $\tilde{Q}_1, \tilde{Q}_5$, which remain finite in the limit (5.81) and are the correctly normalized D1- and D5-brane charges in 5 noncompact dimensions:

$$\begin{aligned} \tilde{Q}_1 &= 2R_5 Q_1 = \frac{g(2\pi)^4\alpha'^3 N_1}{V_{T_2\times T_3}}\,, \\ \tilde{Q}_5 &= 2R_5 Q_1 = g\alpha' N_5\,. \end{aligned} \tag{5.82}$$

The constraint (5.57) on the distance between the centers then reduces to

$$R_4 = \frac{\sqrt{\tilde{Q}_1\tilde{Q}_5}}{\tilde{a}}\,. \tag{5.83}$$

The solution (5.79, 5.80) can, in this limit, be written as a fuzzball solution with a circular profile function [120–123]:

$$\begin{aligned} ds^2 &= \frac{1}{\sqrt{H^2H^3}}\left[-(dt+k)^2 + (dx^4 - s - k)^2\right] + \sqrt{H^2H^3}d\mathbf{x}^2 + \sqrt{\frac{H^2}{H^3}}ds^2_{T_2\times T_3}\,, \\ e^{2\Phi} &= \frac{H^2}{H^3}\,, \\ F^{(3)} &= d\left[\frac{1}{H^2}(dt+k)\wedge(dx^4 - s - k)\right] - \star_4 d(H^3)\,, \end{aligned} \tag{5.84}$$

where the harmonic functions are given by

$$\begin{aligned} H^2 &= 1 + \frac{\tilde{Q}_5}{L}\int_0^L \frac{dv}{|\mathbf{x}-\mathbf{F}|^2}\,, \\ H^3 &= 1 + \frac{\tilde{Q}_5}{L}\int_0^L \frac{|\dot{\mathbf{F}}|^2 dv}{|\mathbf{x}-\mathbf{F}|^2}\,, \end{aligned} \tag{5.85}$$

and the one-foms k, s take the form

$$\begin{aligned} s &= \frac{\tilde{Q}_5}{L}\int_0^L \frac{dvF^a}{|\mathbf{x}-\mathbf{F}|^2}dx^a\,, \\ s + k &= -\star_4\, ds\,. \end{aligned} \tag{5.86}$$

Here, $\mathbf{x}$ represents Cartesian coordinates on $\mathbb{R}^4$ which, in terms of the coordinates $\tilde{r}, \theta, \phi, \psi$ introduced earlier, are given by

$$\begin{aligned} x^1 &= \tilde{r}\cos\tfrac{\theta}{2}\cos\left(\psi+\tfrac{\phi}{2}\right), & x^3 &= \tilde{r}\sin\tfrac{\theta}{2}\cos\left(\psi-\tfrac{\phi}{2}\right), \\ x^2 &= \tilde{r}\cos\tfrac{\theta}{2}\sin\left(\psi+\tfrac{\phi}{2}\right), & x^4 &= \tilde{r}\sin\tfrac{\theta}{2}\sin\left(\psi-\tfrac{\phi}{2}\right). \end{aligned} \tag{5.87}$$

The profile function $\mathbf{F}(v)$ describes a circular profile in the $x^1 - x^2$ plane:

$$\begin{aligned} F^1 &= \tfrac{\tilde{a}}{n}\cos\tfrac{2\pi n}{L}v, & F^3 &= 0\,, \\ F^2 &= \tfrac{\tilde{a}}{n}\sin\tfrac{2\pi n}{L}v, & F^4 &= 0\,. \end{aligned} \tag{5.88}$$

where $L \equiv \frac{2\pi\tilde{Q}_5}{R_4}$. The averaged length of the tangent vector to the profile should be proportional to the D1-brane charge:

$$Q_1 = \frac{Q_5}{L}\int_0^L |\dot{\mathbf{F}}|^2 dv\,. \tag{5.89}$$

As a consistency check, one can easily see that this is the case using the constraint (5.83). It is also interesting to discuss how the 5d angular momenta are related to quantum numbers in 4d. Solutions in five noncompact dimensions can have 2 independent angular momenta J_{12} in the $x^1 - x^2$-plane and J_{34} in the $x^3 - x^4$-plane. These are related to the R-symmetry generators J^3 and $\bar{J}^3$ in the dual CFT as $J_{12} = -(J^3 + \bar{J}^3)$, $J_{12} = -(J^3 - \bar{J}^3)$. From the parametrization (5.87) one can see that J^3 comes from a linear momentum in four dimensions while $\bar{J}^3$ is proportional to the four-dimensional angular momentum J_z. This leads to the dictionary between the charges that was anticipated in (5.13). More specifically, the solutions above have $J_{12} = \frac{N_1 N_5}{n}$, $J_{34} = 0$, such that

$$J^3 = \bar{J}^3 = -\frac{N_1 N_5}{2n}. \tag{5.90}$$

5.3.5 Spectral flow and fuzzball solutions with momentum

In subsection 5.2.3, solutions were considered that were obtained by a spectral flow transformation labeled by a parameter m that had the effect of adding D0-charge (5.63). In the dual frame B, these will carry nonzero momentum charge P on the S^4 circle. The harmonic functions and constraint on the distance were given in (5.64, 5.66). When one takes the special case $Q_1 = Q_5$, substituting in (5.74) gives a solution with constant dilaton which can be embedded in minimal 6-dimensional supergravity [159]. This solution precisely matches the solutions constructed in [144] representing fuzzball geometries with momentum placed in a Taub-NUT space.

One can again take the 5d limit $R_5 \to \infty$ as discussed above. Again taking $N_K = 1$ to get solutions in flat space, one obtains the five-dimensional fuzzball solutions with momentum which were constructed in [139–142]. These solutions were originally obtained by

applying a spectral flow transformation to the five-dimensional solutions without momentum (5.86). They carry the following 5d charges

$$\begin{array}{ll} J^3 = -\frac{N_1 N_5}{2}\left(2m+\frac{1}{n}\right), & \bar{J}^3 = -\frac{N_1 N_5}{2n}, \\ P = N_1 N_5 m\left(m+\frac{1}{n}\right), & \end{array} \tag{5.91}$$

where P denotes the momentum on the S^4 circle. The flux quantization discussed in paragraph 5.2.3 imposes that the parameter m should be an integer.

5.4 Microscopic interpretation

The microscopic interpretation of the solutions we considered will now be discussed both from the 4d and 5d point of view. One can start with the configurations (5.49) without D0-charge in frame A. It was shown that these arise through the 4d-5d connection, from 5d fuzzball solutions with circular profile, carrying macroscopic angular momentum $J_{12} = N_1 N_5/n$, and placed in a Taub-NUT geometry. A first question is whether one should regard these solutions as zero-entropy constituents of a spinning black hole or of a black ring in five dimensions. In the present context, the latter is the only possibility, since a black hole of the desired charge (if it exists as a BPS solution in type II on a torus) cannot be placed in Taub-NUT space in a supersymmetric manner and therefore the 4d-5d connection cannot be applied to it. Indeed, if it could, the resulting 4d configuration would be a small black hole with charges $(0, N_K, N_1, N_5, N_1 N_5/n, 0, 0, 0)$. This is however a polar charge for which a single-centered black hole solution cannot exist, even including higher derivative corrections. Hence our four dimensional solutions should be seen as coming from small black ring microstates in five dimensions. This interpretation also corresponds to the one argued in [102, 122, 160, 161]. It is worth pointing out that that the above argument does not rule out the existence of a 5d supersymmetric spinless ($J_{12} = J_{34} = 0$) small black hole placed at the center of Taub-NUT space. Indeed, the resulting 4d configuration would have pure D4-charge $(0, N_K, N_1, N_5, 0, 0, 0, 0)$, which is not a polar charge ($\hat{q}_0 = 0$), and therefore could give rise to a single-centered small black hole when higher derivative corrections are taken into account.

In the following, it is discussed, which states in the dual CFT correspond to the configurations (5.49) from the 5d point of view. As mentioned in the context of introducing the Strominger-Vafa black hole in chapter 2, the D1-D5 CFT is a deformation of a symmetric product CFT with target space $(T_2 \times T_3)^{N_1 N_5}/S_{N_1 N_5}$ (see [162] for a review). For present purposes, one can consider the theory at the orbifold point. The states considered are closely related to chiral primary operators denoted by σ_n^{--} with quantum numbers $L_0 = J^3 = \bar{L}_0 = \bar{J}^3 = \frac{n-1}{2}$. One can construct operators $U(\alpha)$ which generate a left-moving spectral flow with an integer parameter α:

$$\begin{aligned} U(\alpha) L_0 U(\alpha)^{-1} &= L_0 - \alpha J^3 + \alpha^2 \frac{c}{24} \\ U(\alpha) J^3 U(\alpha)^{-1} &= J^3 - \alpha \frac{c}{12} \end{aligned} \tag{5.92}$$

where the central charge is $c = 6N_1N_5$. Similar generators of right-moving spectral flow with parameter $\tilde{\alpha}$ will be denoted by $\tilde{U}(\tilde{\alpha})$. The CFT states corresponding to (5.49) are ground states in the R sector given by

$$U(1)\tilde{U}(1)(\sigma_n^{--})^{\frac{N_1N_5}{n}}|0\rangle. \tag{5.93}$$

They carry the quantum numbers

$$\begin{array}{ll} L_0 = \frac{N_1N_5}{4}\,, & \bar{L}_0 = \frac{N_1N_5}{4}\,, \\ J^3 = -\frac{N_1N_5}{2n_-}\,, & \bar{J}^3 = -\frac{N_1N_5}{2n}\,, \\ P = L_0 - \bar{L}_0 = 0\,. & \end{array} \tag{5.94}$$

The above states belong to a 'microcanonical' ensemble of R ground states at fixed D1-charge N_1, D5-charge N_5, and angular momenta[8] $J_{12} = N_1N_5/n,\ J_{34} = 0$. When $n \gg 1$, J_{12} is sufficiently far from the maximal value N_1N_5, and there is an exponential degeneracy of states carrying these quantum numbers, leading to a microscopic entropy [161]

$$S_{\rm micro} = 2\sqrt{2}\pi\sqrt{N_1N_5 - J} = 2\sqrt{2}\pi\sqrt{N_1N_5(1-\frac{1}{n})}\,. \tag{5.95}$$

On the basis of general arguments [163], it is expected that, after including higher derivative corrections to the effective action, a black ring solution with a matching macroscopic entropy exists. It is an open problem to explicitly compute such corrections in toroidal compactifications, unlike the case where the four-torus $T_2 \times T_3$ is replaced with K_3, [102, 160, 164].

When a small black ring is placed in Taub-NUT space with one unit of NUT charge and the radius of the Taub-NUT circle is decreased, one obtains a 4d configuration consisting of two centers. One center, coming from the wrapped ring itself, becomes a small black hole in 4d, while the other center, coming from the Taub-NUT charge, is a KK monopole carrying zero entropy [102,160]. In the duality frame A, the first center is a small $D4-D2$ black hole with charge $(0, 0, N_1, N_5, N_1N_5/n, 0, 0, 0)$ and entropy given by (5.95), the second center is a pure D4-brane with charge $(0, 1, 0, 0, 0, 0, 0, 0)$. Because these charges are not parallel, the combined system carries macroscopic angular momentum $J_z = -N_1N_5/n$. Therefore one can view our 4d polar D6-anti D6 configurations (5.49) as zero-entropy constituents of this two-centered configuration.

A similar discussion can be led for the solutions (5.62) carrying D0-charge in frame A. Their CFT counterparts are related to (5.93) by an additional left-moving spectral flow with parameter $2m$:

$$U(2m+1)\tilde{U}(1)(\sigma_n^{--})^{\frac{N_1N_5}{n}}|0\rangle. \tag{5.96}$$

They carry the quantum numbers that were anticipated in (5.12):

$$\begin{array}{ll} L_0 = N_1N_5\left(m^2 + \frac{m}{n} + 1/4\right)\,, & \bar{L}_0 = \frac{N_1N_5}{4}\,, \\ J^3 = -\frac{N_1N_5}{2}\left(2m + \frac{1}{n}\right)\,, & \bar{J}^3 = -\frac{N_1N_5}{2n}\,, \\ P = L_0 - \bar{L}_0 = N_1N_5 m\left(m + \frac{1}{n}\right)\,. & \end{array} \tag{5.97}$$

[8] This is a different ensemble from the one, where the angular momenta are not fixed, used in the context of the OSV conjecture in chapter 3.

In the CFT, the parameters n and m should be quantized such that n is a divisor of N_1N_5 and m is an integer. This matches with the conditions found from charge quantization in the corresponding D-brane configurations. These states are part of an ensemble of CFT states with fixed D1-D5 charges, angular momenta J^3, $\bar{J}^3$ and momentum P. This ensemble is obtained by the ensemble of zero momentum ground states discussed above by acting with the spectral flow operator $U(2m)$. The degeneracy is then again given by (5.95).

5.5 Discussion

In this chapter, the identification of four-dimensional multi-centered D-brane configurations that correspond to a class of fuzzball solutions in five noncompact dimensions was presented, under the 4d-5d connection. In a type IIA duality frame where all the charges come from D6-D4-D2-D0 branes, the relevant 4d configurations are two-centered D6-anti D6 solutions with fluxes corresponding to polar states.

The fuzzball solutions considered here were highly symmetric, where the profile function that defines the solution is taken to be a circular curve in the x^1-x^2 plane in the coordinates (5.87). It is intereseting to comment on the fate of more general fuzzball solutions under the 4d-5d connection. A fuzzball solution arising from a generic curve will typically not have enough symmetry to be written as a torus fibration over a four-dimensional base as in (5.73) and can hence not be given a four-dimensional interpretation. However, according to the proposed dictionary between microstates and fuzzball solutions in [165,166], the subclass of fuzzball solutions that semiclassically represent eigenstates of the R-symmetry group should possess $U(1)\times U(1)$ symmetry and be represented by (possibly disconnected) circular curves in the x^1-x^2 and x^3-x^4 planes in the coordinates (5.73). Such solutions have isometries along the directions $\partial/\partial\phi$ and $\partial/\partial\psi$ as well as along the Taub-Nut direction $\partial/\partial x^4$, and should therefore be the lift of axially symmetric solutions in four dimensions. When the quantum numbers are chosen appropriately, these would describe other constituents of the 4-dimensional 2-centered system with entropy (5.95). It would be interesting to explore this ensemble of four-dimensional configurations.

It is also interesting to comment on the relation between the present work and black hole deconstruction [55]. In four dimensions, say in frame A, multi-centered 'scaling' solutions exist with centers so close that their throats have 'melted' together and which are asymptotically indistinguishable from single centered solutions. Such solutions can carry the same charges as a large single-centered D4-D0 black hole, and can be seen as a deconstruction of such a black hole into zero-entropy constitutents. The scaling solutions consist of a 'core' D6 anti-D6 system with flux, and a 'halo'of D0-brane centers added to it (again, see [1] for more details on the formalism of 'cores' and 'halos'). The scaling limit consists of taking the total D0-charge to be parametrically larger than the magnetic charge $p^1p^2p^3$. The entropy of the black hole in this limit can be understood by treating the D0-branes as probes and counting the supersymmetric ground states of the probe quantum mechanics [56]. The 'core' D6 anti-D6 system in these configurations is precisely the same kind that we studied and mapped to 5d fuzzball solutions. Indeed, for the special values

$n = 1,\ m = -1/2$ of the parameters one obtains the following charges at the centers

$$\begin{aligned}\Gamma_1 &= \left(-1, \frac{N_K}{2}, \frac{N_1}{2}, \frac{N_5}{2}, -\frac{N_1N_5}{4}, -\frac{N_KN_5}{4}, -\frac{N_KN_1}{4}, \frac{N_KN_1N_5}{8}\right), \\ \Gamma_2 &= \left(1, \frac{N_K}{2}, \frac{N_1}{2}, \frac{N_5}{2}, \frac{N_1N_5}{4}, \frac{N_KN_5}{4}, \frac{N_KN_1}{4}, \frac{N_KN_1N_5}{8}\right). \end{aligned} \tag{5.98}$$

These are precisely the charges that appear in the core of the scaling solutions in [55]. It seems natural to expect that, for the other values of these parameters m and n, our configurations can serve as the core system for the deconstruction of a black hole with added D2-charge.

The relation to deconstruction could have interesting implications in five dimensions as well. If one takes a scaling solution in four dimensions, dualizes it to frame B and takes the 4d-5d limit, one should end up with a configuration carrying the charges of a large D1-D5-P Strominger-Vafa [63] black hole. The scaling limit implies that one will have $P \gg N_1N_5$, which is equivalent to the Cardy limit $\Lambda_0 \ll c$ where the CFT microstate counting is performed. Therefore such configurations would be candidates for describing typical microstates of the D1-D5-P black hole, and it would be interesting to study such solutions in more detail. It is not clear whether such configurations could rightly be called 'fuzzball' geometries for the D1-D5-P black hole, as they will not be smooth near the centers where the harmonic functions describing the momentum diverge. As argued in [45], treating the momentum as coming from giant graviton probes, the number of ground states would be of the right order to explain the entropy.

Concluding discussion

The metaphor developed in this final chapter explains the specific research context of this thesis as well as the author's results by drawing an analogy between black holes in string theory and humans in microbiology. To be more specific, it suggests a 'black hole genome project' in analogy to the human genome project.

This final discussion is aimed at a broad audience and should be understandable for a reader turning to these pages directly from the introduction, but it should also provide a final glance at – and hopefully an interesting interpretation of – the content of chapters 3-5 also for more specialized readers who have read parts or all of the thesis. This discussion is divided into two sections:

- The first one gives a metaphoric interpretation of the research context of this thesis. Two ideas on the quantum nature of black holes stand at the center. This part may be seen as a layman's guide to the most important parts of chapter 3 and section 5.1.

- The second section gives an interpretation of the results obtained during the author's Ph.D. studies. From the viewpoint of the metaphor, future directions of research should become clear. This section can be seen as a layman's guide to the chapters 4 and 5, the chapters containing the author's main technical results.

The specific research context of this thesis

Two ideas on the quantum nature of black holes

The author's research fits into the context of two bigger research programs, both involving stunning ideas about the quantum nature of black holes.

- The first idea has originally been formulated within a four-dimensional compactification of string theory, and conjectures the wave function for (a specific type of) black holes to be of a certain form. The reader will find a short explanation of what is meant by a 'wave function of a black hole' in the next paragraph.

- The second idea has been formulated and researched in five-dimensional compactifications of string theory. This research program focusses on finding gravitational microstates of black holes, allowing a gravitational explanation to be given of the

entropy of a black hole. These gravitational microstates are not black holes, they are rather called fuzzballs. If this conjecture turns out to be the right path, black holes do not really exist, but they rather appear as an 'average picture' of these microstates (this will be explained in more detail).

Wave functions for black holes

The 'quantum behavior' of the world seems to involve the awkward fact that a system (e.g. a particle) does not behave in one specific way, but it rather realizes 'several parallel states', or as the system evolves with time, 'parallel existences'. One refers to this fact as that of a *quantum* system behaving as a superposition of possible *classical* states. Only when an observer performs a measurement, one of these states (or existences) is selected from the lot, forcing the quantum entity into a classical pattern of behavior. Building upon this, the reader is provided with an idea of the notion of a wavefunction. Putting matters into very simple words, a wavefunction is a mathematical object in which all possible states of a system appear, weighted with the probability of their appearance, should an observer perform a measurement. A wave function is denoted as $|\Psi\rangle$. Thus, for example, for Schrödinger's cat, the wavefunction might be written as $|\Psi_{\text{cat}}\rangle = \sqrt{p}_1|\text{alive}\rangle + \sqrt{p}_2|\text{dead}\rangle$, where the numbers p_1, p_2 stand for probabilities to measure dead (p_2) or alive (p_1). Before moving on to discuss a wavefunction for a black hole, another concept with which the reader should become familiarized is the *uncertainty* related to quantum systems. A concept known as 'Heisenberg's uncertainty principle' might be called a basic fact in quantum theories. When describing e.g. a particle as a 'quantum', highlighting both particle- and wave-nature of the object, one cannot simultaneously gain a direct knowledge both of the exact position of the particle and the speed and direction at which the particle is traveling. One can intuitively imagine that the measurement of the position forces the speed and direction of the particle into a 'blurry uncertainty' – a sum of a whole lot of possibilities (a superposition). Should one however decide to measure the speed and direction of a (moving) particle, the exact position becomes 'blurry' and 'uncertain'. This may serve as some intuition on the uncertainty of quantum mechanics: there is always this dichotomy between so-called 'conjugate' aspects to the behavior of the system under study. This hopefully again provides the reader with a taste of how weird the quantum world has revealed itself to be; in this case this is an example of how measurements always affect the system on which a measurement is performed: there is no such thing as an *external and neutral observer*. The observer is, at least for a certain extent, 'observing himself'.

The OSV conjecture

In 2004, a paper written by three well-known string theorists appeared (Ooguri, Strominger and Vafa), in which the authors formulated a conjecture now known as the 'OSV conjecture'. Although the following is not really accurate, it should allow the reader to get a grip on some main ideas. This conjecture is formulated for a very special class of black holes. Namely, various branes of different charges are chosen to realize the various

single microstates of a black hole. Some branes can be interpreted as being magnetically charged, whereas others as carrying electric charge. The black hole is made from a superposition of all sorts of brane states, carrying various magnetic and electric charges. All states are chosen to have in common however, that they carry the same magnetic charge, while all different branes are used carrying all possible electric charges. One might even go as far as interpreting magnetic versus electric charge for a black hole as analagous to position versus momentum for a particle [9]. For the kind of black hole one is describing, one can imagine having measured the magnetic charge of a black hole, but dealing with a completely 'blurry, uncertain' quantum object, carrying a whole lot of possible electric charges. The OSV conjecture states that the wave function of such a (fixed magnetic charge, superposition of all possible electric charges) black hole is given by the topological string partition function $|\psi_{\text{blackhole}}\rangle = \mathcal{Z}_{\text{top}}$. So, somehow topological string theory seems to describe microstates of black holes and allows them to be enumerated.

What does the word 'topological' mean?

For a space to be 'topological' is a weaker statement than for a space to allow the performing of distance measurements. In this case, an extrinsic definition of the concept will be advocated. The topological structure of a space expresses something very coarse, yet powerful in mathematics. Should one for example consider a donut as a 'space' (a geometry on which to perform calculations), one finds that when squeezing or stretching the donut (that is, if one does not rip the donut apart), the 'distances' between different parts of the donut change, however the topological properties remain unchanged. For example, it remains true that there is one hole in the middle. It is best to imagine, that topological traits of a space remain invariant under pulling, stretching or squeezing a space: they are invariant under 'rubber-like' deformations.

So what is topological string theory?

Topological string theory is a more simple (but still complicated) version of string theory which one might imagine as the backbone of a 'full' string theory. Most of the states (the flesh) are not described, only the states which are invariant under rubber-like deformations are included (the bone): the topological states of the spectrum. Of course the simplicity of the theory lies in this fact that only a small fraction of all states (states might be read as particles, or more generally, branes, in this context) that exist in the 'full string theory' can be found within topological string theory. The theory only studies a 'mathematically well-behaved' backbone of the full theory, without the flesh, yet very interesting, as it does contain some 'key information'. Topological string theory (at least the case of interest) is six-dimensional, and describes a part of the states living in the six extra dimensions. The core of the matter in this context lies in the fact, that one can use

[9] Some intuition on this, also including some connecting thoughts on the corresponding duality for topological string theory, is beautifully described in the original publication, [89].

this theory to compute sets of numbers counting 'topological' brane states, and this leads right back to the core of the matter: degeneracies of black holes.

Before moving on to explain a slightly different topic, it seems fair to reveal some limits of the considered setup to the reader. First of all, the class of black holes that is discussed here, is very special. These black holes are, in the jargon of physics, extremal. This is a restriction on charge in relation to mass, and at the same time they are supersymmetric. This means that they are only toy models, and are certainly not a model for the black holes one supposes to be out there, in the middle of our galaxy, or in neighboring star systems. At the same time, the black holes which are addressed by the OSV conjecture are somewhat special from the point of view of string theory, as one has chosen to use specific brane charges (keeping the magnetic charge fixed, summing over electric charges – one can also choose to study different black hole models): this is by no means the only possible setup to perform studies. The ideas are promising, but in relation to understanding a quantum black hole in a neighboring star system properly, the reader should imagine these studies to be simple playgrounds in which to hopefully qualitatively understand some essential features upon which to build more realistic studies. Having said this, it is time to move on to present the second research program to which some of the author's work is linked.

Fuzzballs instead of black holes

The second research program was initiated by Mathur and his collaborators, and is situated (mostly) in five-dimensional compactifications of string theory. The picture that arises from the original theoretical models of black holes, starting with the solution to Einstein's equations of general relativity, found by Schwarzschild around 1915, is a singularity (more or less a point in the universe), where all the matter of a black hole is concentrated, surrounded by an event horizon – recall that the event horizon is the boundary where the region 'of no return' starts. As established in the 1970's by Hawking and collaborators, a black hole does not exist forever, but it radiates away energy, thereby losing mass. The radiation can be imagined to leave the black hole at the event horizon, and one would therefore expect that it never interacted with the matter located in the black hole itself – as the latter is separated in space from the event horizon. Recall that this naive picture of a black hole is a dot in the universe surrounded (at a distance called the Schwarzschild radius) by a shell called the event horizon. This leads upon closer consideration to the fact that information about the black hole is lost. In other words, a black hole radiating away completely is a mechanism to destroy information, a loss of entropy. But that contradicts one of the older and well-known laws of thermodynamics, namely that the total entropy in the universe never decreases. It is this issue that apparently inspired Mathur and collaborators to propose, that knowledge of quantum gravity alters this picture of black holes. Rather, the matter inside a black hole should be spread out (imagine it as a sort of foam). In fact, the black hole should be thought of as a superposition of microstates that are all of a sort where the matter is not concentrated in a point. When averaging over all of these geometries, the former picture of a black hole arises as an artefact, an effective way of looking at the system. Individually, the single microstates do not contain

a singularity (where the matter would be localized in a tiny point), and they are therefore referred to as 'smooth'. These microstates have been given the name 'fuzzballs', probably referring to the 'fuzzy quantum matter' (a sort of foam) spread out somewhere in the region between the would-be singularity at the center and the event horizon of the system. If one takes the fuzzball idea seriously, a black hole is not really a black hole, but only seems to be one. Actually, matter *can* leave the region that seems to be an event horizon (therefore the hole is not really 'black'), but statistically speaking it takes so long that it appears not to be able to do so. The research program also involves a proposal of how branes carrying integer charges are automatically split up into so-called fractional branes inside the fuzzball states. Apparently, this allows a denser packing of matter (and therefore entropy) than in any other way. Just like a diamond might be interpreted as an extremely dense packed lattice, a black hole, or rather the superposition of fuzzballs might be interpreted as the diamond of the universe: the most dense packaging of matter and information possible. One might think of them as entropy maximizing objects, and the fuzzball decomposition of the picture (the microscopic explanation of the macroscopic object) offers a way of understanding how this maximization is possible. This concludes an overview on the research context and is followed by a presentation of the author's research and how it fits in.

The black hole genome project

The author's research presented in this thesis can be metaphorically interpreted as a pursuit of a 'black hole genome project'. This black hole genome project in string theory might be seen as a analagous to the human genome project in microbiology. In fact, black hole genome project goes at bit far, the results in this thesis might rather be translated into the statement that genomes analagous to those of fruit flies are analyzed: namely, genomes for point particles. In microbiology, studying simpler genomes (e.g. of the fruit fly, of yeast, or of 'roundworms') can be seen as warm-up exercises for understanding the human genome, and in the same way, the genome of a point particle can be seen as a 'toy model' for the black hole case. It is time to take a closer look at the metaphor for the genome of a black hole.

Polar states: the chromosomes of black holes

The 'partition function' of a black hole (of the type discussed, modeled with fixed magnetic charge, and various 'possible' electric charges) is a mathematical object consisting of an infinite sum of terms. Each term corresponds to a specific electric charge, and comes with a number, counting the number of possible states with the given charges. It is easiest to explain this more concretely, by giving a (strongly) simplified example. Imagine a black hole with magnetic charge (this number is just randomly chosen for the example) '1000', and various electric charges 1,2,3,... The black hole can thus be in the state with magnetic/electric charge 1000/1, but it could also be in any other state, e.g. 1000/200.

The quantum nature of the black hole lies in the superposition of these possibilites. The partition function $\mathcal{Z}$ (partition functions are normally denoted with this letter) counts all possible states of the black hole. It could be that there are 100 (this number was again chosen at random for this example) possible states for the black hole with charges 1000/1 (magnetic charge 1000 / electric charge 1). These one-hundred states might arise from different ways of distributing the electric charge across the magnetic charged brane. Say, there could be 200 states with charge 1000/2. Again, this number '200' arises from the various possibilites of distributing the two electric charges across the magnetic brane, and so on and so forth. In this case, the partition function for this black hole would be something like $\mathcal{Z} = 100q + 200q^2 + ...$, where the dots indicate that an infinite number of terms follow (for example, a term such as $15'000q^{20}$, which would mean that there are 15'000 possible states for a black hole with charge 1000/20). The number in front of a term counts the number of states with a specific charge, while the exponent of the variable q counts the electric charge of the state.

- The first crucial point in all of this however is, that it turns out that a partition function is determined completely purely through mathematical knowledge about the whole system by a finite set of terms, which are called *polar states*. In the example considered it might be the case, that one only needs to know the first two terms (the 100 and the 200), and the rest would automatically be determined. One would then automatically know that the series (e.g.) continues with $550q^3 + 800q^4 + ...$ This would e.g. imply that one could *predict* that there are 550 possible states for the black hole to have charge 1000/3, without having to count them.

- A second crucial point is, that (almost) all polar states are realized exclusively as multicentered bound states. *This means that the existence of (almost) all such polar microstates can be inferred from examining split attractor flow trees.*

These properties of black hole partition functions and the polar states were used by Denef and Moore in 2007 to reformulate and refine the OSV conjecture stated above.

This leads to the suggested metaphor. For comparison, in microbiology, one is interested in the complete molecular structure of organisms. It is however sufficient to know the 'genetic code', in this case, one can (e.g. for humans or fruit flies) analyze the pairs of chromosomes and classify all possible genes. There are a finite total number of chromosomes, which come in so-called 'homologous pairs', one chromosome from each parent for each pair. Humans for example have 23 such pairs. Other organisms have a different number of chromosomes, and in the same way the total number of polar states is different for various D-particles (in this thesis there are particles e.g. with seven polar states, check 4.2, but there is also an example with two polar states, check section 4.4) [10]. It is suggested to think of polar states as chromosome pairs for black holes (or D-particles). When these polar states are realized as bound states, they are modeled by a bound state of two

[10]Note that the 'D' in D-particles stands for the fact that the particles are geometrically modeled by 'D'-branes wrapped around extra dimensions (this will be explained more in the next paragraph).

higher-dimensional branes, which are 'glued' together by strings. Each of these branes can be thought of as a chromosome. Topological string theory computes numbers which count all possible states of such branes, they do in some sense classify the genome stored on one such 'parent chromosome'.

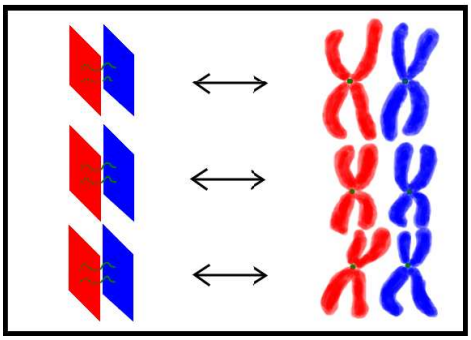

Figure 5.5: **Polar states as black hole chromosomes:** Left: A polar state is a bound state of higher-dimensional D-branes. One 'mother' and one 'father' brane are glued together by tachyonic strings. Right: Chromosomes of organisms such as humans or fruit flies come in ('homologous') pairs, one from each parent. Note that the chromosomes in this figure have been doubled, which is not really accurate, but the reader will be more familiar with this picture (see the explanations on meiosis for further details).

Point particles: the fruit fly of quantum gravity

Having discussed the models of black holes above, it is easy to explain how one obtains the toy model point particles analyzed in this thesis. One just lowers the magnetic charge, say in the example from 1000 to 1. As the mass of the system is tied to the total charge, it turns out that such a system does not have enough mass anymore to form a black hole, but it is just a point particle. A point particle however of which one has measured the magnetic charge and which is realized as a 'blurry superposition' carrying various electric charges, and also a 'geometrized' point particle of which the entropy is modeled by the D-branes wrapped around extra dimensions. One can also refer to such a particle as a 'D-particle', since the 'inner' degrees of freedom / the entropy of the particle reside within the different possible states of the D-branes wrapped in the extra dimensions. In the light of the previous paragraph, this suggests interpreting these D-particles as analogous to fruit flies. Studying the partition functions for these particles is meant to be an instructive exercise to gain a better understanding of black holes and their partition functions.

If one chooses minimal magnetic charge *one*, all polar states are in fact realized as perfect pairs. Enumerating all polar states using split flow trees and the set of numbers computed by topological string theory allows the writing down of exact mathematical expressions for a couple of D-particles. A few such partition functions were known from studies by Gaiotto, Strominger and Yin in 2006 and 2007, derived using a different technique, and also working with a different 'window into string theory'. In a collaboration with Andrés Collinucci, [3], the author has derived such an example using the techniques explained here, namely using

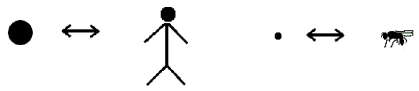

Figure 5.6: **Genomes in string theory vs. genomes in microbiology:** Left: The black hole genome appearing in polar states vs. humane genome appearing in chromosome pairs. Right: Simpler study models; the D-particle genome realized as polar states vs. the fruit fly genome appearing in pairs of chromosomes.

split attractor flow trees to establish the existence of polar states, and using a different set of numbers computed by topological string theory to enumerate the 'parent chromosome' D-branes. In addition, non-trivial checks on the method were performed on non-polar states (which are fully determined when all polar states are known), by also enumerating such states using the same techniques. For this partition function, exact agreement with the previous studies was found. It turned out however for non-polar states, that in order to obtain exact results in general, a refinement of the computation prescription needed to be developed. This will be the topic of the next paragraph. In another collaboration with Walter Van Herck, [4], more partition functions were derived, and in fact, it was shown that the refined prescription to enumerate the number of states is in fact correct, and also alters some results on polar states, correcting one of the partition functions found by Gaiotto, Strominger and Yin.

Meiosis and crossing-over for black holes

The degeneracy of a specific polar state is naively obtained by multiplying three numbers: the number of states of the first 'parent brane', the number of 'gluing strings', and the number of states of the second 'parent brane': this means that the total number of states is assumed to *factorize into three factors*.

The analogy that will be made between this effect and an effect appearing in the meiosis in biology requires the introduction of a few concepts. First of all, recall that for example a human has 23 'homologous' [11] chromosome pairs: a total of 46 chromosomes. As each chromosome has a 'partner', one speaks of a diploid organism. Chromosomes carry many different genes, which again allow variations, called alleles. For example, a gene for eye color could have an allele 'blue', but also an allele 'green', etc. In reality, several genes will affect an appearance such as eye color, but things are kept as simple as possible in the current explanation. Not all genetic information is actually expressed, only a certain part of it is really used. One might call this a specific state, belonging to the chromosome. For example, a certain chromosome might allow for a billion different expressions, of which one is rezlied at a specific moment in time. For the metaphor consider these billion states as the microstates, the 'inner degeneracy' of the chromosome. The question one might ask is, how many possible states a generation can pass on to the next. Naively one might

[11] The word homologous stands for non-identical, but carrying the same genes.

just count the possible 'states' of the father chromosome pair, and multiply this with the number of possible states of the mother chromosome pair (of course, this will be done for each chromosome pair, separately). This is however not quite accurate, as there will also be states, which one can imagine to be analogous to the special states of a constituent in a D-brane bound state, as discussed previously. In order to understand this, some explanations of the phenomenon of meiosis are needed.

Meiosis is an important mechanism for organisms performing sexual reproduction (such as humans, fruit flies, or more generally, 'eukaryots'). Within the process of reproduction, genetic variability plays an important role. Put very simply, a good mixture of the possible genes is an evolutionary factor for success. In meiosis, also called reductional divison, genetic material is selected in order to pass it on to a next generation. Meiosis is also called 'reductional division', and basically consists of two cell divisions. Before the meiosis starts, the human chromosomes are duplicated. For each pair, both the mother and the father chromosome have been duplicated. To make this more concrete, consider the example of a meiosis for humans. The two cell divisions, referred to as meiosis I and meiosis II, proceed as follows:

- Meiosis I: The (duplicated) homologous chromosome pairs line up, and are split into two. This means, that two cells are created (known as the daughter nuclei I), carrying 23 duplicated chromosomes each. Note that the (duplicated) mother and father chromosome pairs have been distributed randomly, amongst these two daughter cells. This means, that a cell could (for example) contain 14 mother and 9 father chromosomes (and vice versa). This random selection of chromosomes from the parents is one factor responsible for genetic variability and is referred to as *interchromosomal recombination*.

- Meiosis II: In a next phase, the duplicated chromosome pairs are pulled apart, and one chromosome is placed in a cell. In this way, four daughter nuclei II are created, each carrying one simple set of 23 chromosomes. A cell of this kind is ready for fertilization (e.g. a sperm cell). Upon fertilization, the next generation receives 23 chromomes from the mother, and 23 chromosomes from the father.

The mechanism of interchromosomal recombination is however not the only factor assuring genetic variability, otherwise one would meet people who resemble each other to a remarkable degree on a regular basis. Namely, in meiosis I, just before the duplicated homologous chromosomes are split into two sets, they are neatly assembled, homologous pairs next to each other. In fact, the pairs are brought into very close vicinity, and a phenomenon called *crossing-over*, also known as *intrachromosomal recombination*, takes place. Crossing-over refers to the process of exchange of pieces of the DNA on pair chromosomes. This means that a piece is cut out on each chromosome, and the piece coming from the homologous partner chromosome is built-in instead. It is at the core of genetic diversity.

Now, the question can be asked: how many possible microstates (in the sense of allele combinations that are actually expressed) can be passed on to the next generation. One might just multiply the number of 'mother states' with the number of 'father states'.

One would in this way however neglect the possibility of 'special states', namely those based on an inherited cell formed by virtue of crossing-over. Without getting involved in any microbiological details, let it be said, that a new combination of the former alleles, resulting from a crossing-over, leads to 'new microstates'. One thus has to deal with the 'special states' (a result from some sort of interaction) separately, and the number of possible states for the next generation does not factorize. One then needs to sum up different combinations.

To reconnect to the author's work, recall that for the polar states, the number of states does not factorize. In this case, the branes never really perform a crossing-over, but the number of tachyonic strings (whose specific existence does depend on both of the branes) gluing the state together jumps. The number of states where the number of tachyonic strings is as expected was called 'generic states', and the states on a brane giving rise to a bound state with a different number of gluing strings were called 'special states'. To make this concrete, again consider the simple toy-example introduced above, and imagine that a polar state with magnetic charge 1 and electric charge 2. It was said before that this polar state had a degeneracy of 200, and imagine that this number came from e.g. 25*4*2, where 25 is the number of states of the mother brane, 4 is the number of tachyonic strings, and 2 is the number of father brane states. The procedure developed in this thesis might tell you that there are actually five tachyonic strings stretching between the branes for 2 of the 25 mother brane states, and that the correct total number of states is therefore 23*4*2+2*5*2: in other words, the number of states does not factorize, and although there are obvious differences, one might denote this as a form of crossing-over, as the generic/special division does depend on both parent branes, it is therefore a reflection of a form of interaction between them.

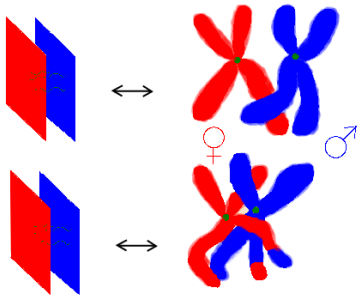

Figure 5.7: **Polar states, non-factorization and crossing-over:** The number of gluing strings between two branes is not independent of the states in which the two branes reside. This ruins factorization of the total number of states for such a polar term. In meiosis, homologous pairs of chromosomes are lined up and can exchange pieces of their DNA (intrachromosomal recombination). This phenomenon is called crossing-over and is depicted for the lower pair of chromosomes. This means that the number of (possibilities to express the) genes, passed on to the next generation is not a simple product of possible gene / allele combinations of each parent.

Fuzzball chromosomes

A slightly different direction of research is presented in chapter 5 of this thesis. This chapter is based on a collaboration with Joris Raeymaekers, Bert Vercnocke and Walter Van Herck, [5]. A connection was established between the four-dimensional context of polar states and the five-dimensional fuzzball program on black holes. Namely, we found an explicit map between specific polar states and a set of fuzzball geometries. It could be interesting to also model black holes in five dimensions, using a fixed 'magnetic charge' and varying over all possible 'electric charges'. In a far-reaching sense, the research in chapter 5 might therefore be interpreted as a pointer to 'fuzzball chromosomes'. In any case, it does relate 'polar states' in four dimensions to the type of geometries investigated in five dimensions, in the context of the fuzzball research program.

The research presented in this thesis can be seen as a step towards a black hole / fuzzball genome project. It is a task for the future to study more D-particles in order to establish a more general picture of 'generic' and 'special' states of a constituent within a bound state. It is especially interesting to see what can be learned from this refined procedure to count D-particle microstates about black holes and, building on the developed connection, about fuzzballs. As a simple goal one can state the finding of the meiosis for black holes / fuzzballs. More generally, one would like to classify the genome of black holes / fuzzballs and gain a better understanding of the wavefunctions describing these objects of crucial importance within a theory of quantum gravity.

Appendix A

Basic definitions, conventions and notation

Dimensions
Throughout this thesis, a capital D is used to indicate the total spacetime of a theory, whereas a small d is used for indicating spacetime dimensions for a compactified theory.

Metrics in 10D or 11D are denoted with a capital G whereas metrics in 4d or 5d are denoted with a small g.

Partition functions and central charges
For distinction, partition functions are consistently denoted by a calligraphic $\mathcal{Z}$, whereas central charges are always denoted by an ordinary Z.

A.1 Compendium on Calabi-Yau manifolds

Some basic properties of Calabi-Yau manifolds

On a complex manifold $\mathcal{M}$, one calls a metric g that satisfies $g_{ij} = g_{\bar{i}\bar{j}} = 0$ a Hermitian metric. As a consequence it can be written as $g = g_{i\bar{j}} dz^i \otimes d\bar{z}^{\bar{j}} + g_{\bar{i}j} d\bar{z}^{\bar{i}} \otimes dz^j$. A complex manifold allows a complex structure $J : T\mathcal{M} \to T\mathcal{M}$, $J^2 = -\mathbf{1}$. The hermiticity condition can also be expressed as $g(J(v_1), J(v_2)) = g(v_1, v_2)$. Given a Hermitian metric on a complex manifold, one can define a $(1,1)$-form according to

$$\mathcal{J} = i g_{i\bar{j}} dz^i \otimes d\bar{z}^{\bar{j}} - i g_{\bar{i}j} d\bar{z}^{\bar{i}} dz^j = i g_{i\bar{j}} dz^i \wedge d\bar{z}^{\bar{j}}. \tag{A.1}$$

If this form is closed, $d\mathcal{J} = 0$, it is called a Kähler form, and the manifold is called a Kähler manifold. This allows stating a definition for a Calabi-Yau manifold. In the following, dimension always stands for *complex dimension*.

Definition: Calabi-Yau manifold
A d-dimensional Calabi-Yau manifold is a compact, complex Kähler manifold with $SU(d)$ holonomy.

Sometimes this definition is relaxed, and one allows a holonomy group $G \subset SU(d)$. The strict $SU(d)$ condition is then called 'proper $SU(d)$ holonomy'. There are a number of equivalent definitions. Instead of using the definition through the holonomy of the metric, one could have used either one of the following definitions. A CY d-fold is a compact d-complex-dimensional Kähler manifold with:

- trivial canonical bundle, or, equivalently, a globally defined holomorphic $(d, 0)$-form,
- vanishing first Chern class $c_1 = 0$,
- a Ricci-flat metric (Ricci tensor zero $R_{i\bar{j}} = 0$), even though such a metric is in fact not explicitly known for almost any CY-manifold (this is equivalent according to the Calabi-Yau theorem stated below).

The reader can find simple proofs for the equivalence of these definitions e.g. in [167]. When reading this thesis, it probably seems most straightforward to stick to the definition including the vanishing of the first Chern class.

According to the famous conjecture by Calabi from 1954, proven by Yau in 1976:

Calabi-Yau theorem:
A complex Kähler manifold with vanishing first Chern class (a Calabi-Yau manifold) and with Kähler form J allows one unique Ricci-flat metric, whose Kähler form J' is in the same cohomology class as J.

The restriction on the general Kähler geometry simplifies the cohomology a lot. Namely, it determines various cohomology groups to be one-dimensional, reflected in the Hodge numbers $h^{(0,0)} = h^{(d,0)} = h^{(0,d)} = h^{(d,d)} = 1$, and some others are equal to zero. As the case $d = 3$ is of most interest, the Hodge diamond of a CY-3-fold X shall be written out.

Dolbeault cohomology groups dimensions of a Calabi-Yau 3-fold	
$H^0(X) = H^{(0,0)}(X)$	1
$H^1(X) = H^{(1,0)}(X) \oplus H^{(0,1)}(X)$	$0 \quad 0$
$H^2(X) = H^{(2,0)}(X) \oplus H^{(1,1)}(X) \oplus H^{(0,2)}(X)$	$0 \quad h^{(1,1)} \quad 0$
$H^3(X) = H^{(3,0)}(X) \oplus H^{(2,1)}(X) \oplus H^{(1,2)}(X) \oplus H^{(0,3)}(X)$	$1 \quad h^{(2,1)} \quad h^{(2,1)} \quad 1$
$H^4(X) = H^{(3,1)}(X) \oplus H^{(2,2)}(X) \oplus H^{(1,3)}(X)$	$0 \quad h^{(1,1)} \quad 0$
$H^5(X) = H^{(3,2)}(X) \oplus H^{(2,3)}(X)$	$0 \quad 0$
$H^6(X) = H^{(3,3)}(X)$	1

Basis for the even degree cohomology $H^{2*}(X)$ of a Calabi-Yau

The full even degree integer cohomology of X is

$$H^{2*}(X, \mathbb{Z}) = H^0(X, \mathbb{Z}) \oplus H^2(X, \mathbb{Z}) \oplus H^4(X, \mathbb{Z}) \oplus H^6(X, \mathbb{Z}), \tag{A.2}$$

and the basis is denoted by

$$(D_0, D_A, \tilde{D}^A, \omega), \tag{A.3}$$

where $A = 1, ..., h^{(1,1)}$. It was conciously introduced as the notation for the integer degree cohomology, as this is mainly used in this thesis. When working in the pure supergravity limits to the theories, one works with real cohomologies, $H^k(X, \mathbb{R})$, and one could of course use the same notation for that basis, too. In the following, the shorthand notation $H^k(X) = H^k(X, \mathbb{Z})$ will be adapted.

For $H^2(X, \mathbb{Z})$ the basis elements D_A $(A = 1, ..., h^{(1,1)})$ are introduced.Define also $D_{ABC} = \int_X D_A \wedge D_B \wedge D_C$, which is at the same time the intersection number belonging to two-cycles. One can use a dual basis $\tilde{D}_B$ for $H^4(X)$ such that $\int_X D_A \wedge \tilde{D}^B = \delta^B{}_A$, where of course $\tilde{D}^A = \sum_{B,C} D^{BC} D_B \wedge D_C$, using $D^{BC} := (\sum_A D_{ABC})^{-1}$.

Basis for the even degree homology $H_{2*}(X)$ of a Calabi-Yau

For the homology, one can use the Poincaré dual cycles as a basis. A hat is used to denote a Poincaré dual element. Recall that a Poincaré dual cycle $C = \hat{D} \in H^{6-k}(X)$ to a form $D \in H^k(X)$ is defined through the relation

$$\int_X D \wedge \omega = \int_C \omega. \tag{A.4}$$

Thus, one can denote the basis for $(0, 2, 4, 6)$-cycle classes in $H_{2*}(X)$, with $(1 = \hat{\omega}, \hat{\tilde{D}}^A, \hat{D}_A, X = \hat{1})$. As this is obviously not a convenient notation, the dual basis will be written as

$$(1, D^A, \tilde{D}_A, \tilde{D}_0). \tag{A.5}$$

Note the subtle difference in where the indices stand, when comparing cohomology and homology. Integrating forms over cycles of the appropriate dimension yields the relations

$$\begin{aligned} \int_{D^B} D_A &= \delta^B_A, \\ \int_{\tilde{D}_B} \tilde{D}^A &= -\delta^A_B. \end{aligned}$$

Basis for the odd degree cohomology $H^3(X)$ of a Calabi-Yau

For the cohomology $H^3(X)$ one can choose a real symplectic basis (α_I, β^I), $(I = 1, ..., h^{(2,1)})$:

$$\int_X \alpha_I \wedge \beta^J = \delta_I{}^J. \tag{A.6}$$

Basis for the odd degree homology $H_3(X)$ of a Calabi-Yau

In complete analogy to what was stated for the even degree cohomology, for the dual homology, the symplectic basis (A^I, B_J) with $I, J = 1, ..., h^{(2,1)}$ is used. This basis is formed with Poincaré dual 3-cycle classes. To avoid confusion, explicitly note that β^I is Poincaré dual to A_I, and α_I is Poincaré dual to B^I. The intersection numbers thus read

$$\begin{aligned} A^I \cap B_J &= -B_J \cap A^I = \delta^I_J, \\ A^I \cap A^J &= B_I \cap B_J = 0, \end{aligned} \tag{A.7}$$

and the pairing of cohomology and homology elements is given by

$$\begin{aligned} \int_{A^J} \alpha_I &= \int \alpha_I \wedge \beta^J = \delta^J_I, \\ \int_{B_J} \beta^I &= \int \beta^I \wedge \alpha_J = -\delta^I_J. \end{aligned} \tag{A.8}$$

As a side remark: note that it is exactly the group $\mathrm{Sp}(2h^{(2,1)} + 2, \mathbb{Z})$ that preserves these properties.

Algebraic Calabi-Yau varieties

This part of the appendix introduces some key concepts from algebraic geometry, Calabi-Yau spaces as algebraic varieties and characteristic classes from the viewpoint of the framework of algebraic geometry set up with algebraically closed fields [1]. Studying algebraic CY spaces is very convenient because this allows working with explicit examples.

Chern classes

The total Chern class $c(X) = \sum_{i=0}^{n} c_i(X)$ and the individual Chern classes $c_i(X)$ of a space X are defined as the Chern classes of the tangent bundle T_X. If the bundle T_X is differentiable, one can define the curvature of a connection A, $F = dA + A \wedge A$, and define the total Chern class from the viewpoint of differential geometry, according to

$$\begin{aligned} c(T_X) = & c(X) = \det(1 + \frac{i}{2\pi} F), \\ = & 1 + \frac{i}{2\pi} \mathrm{Tr} F + ... \\ = & 1 + c_1(T_X) + c_2(T_X) + ... \end{aligned} \tag{A.9}$$

The i-th Chern class of a bundle can be interpreted as an obstruction to the existence of $(n-i+1)$ everywhere complex linearly independent vector fields, and lies in the cohomology group $H^{2i}(X)$ of the base space X.

[1] Throughout this thesis this algebraically closed field will be the complex numbers $\mathbb{C}$.

The Hirzebruch-Riemann-Roch index theorem gives as an elegant way to compute the Euler characteristic of a Calabi-Yau manifold using the Chern character and the Todd class,

$$\chi(X) = \sum_i (-1)^i b^i = \int_X \mathrm{ch}(X)\mathrm{td}(X). \tag{A.10}$$

Weighted projective spaces and one modulus CYs

A *weighted projective space* $WC\mathbb{P}^N_{\vec{w}} = WC\mathbb{P}^N_{w_0,w_1,...,w_N}$ is defined as a space of N-tuples $(x_0 : ... : x_N) \in \mathbb{C}$. The space has homogeneous coordinates

$$(x_0 : ... : x_N) \equiv (\lambda^{w_0} x_0 : ... : \lambda^{w_N} x_N) \neq (0 : ...0), \tag{A.11}$$

$(\forall \lambda \in \mathbb{C}^*)$.

One can now embed a subspace X as a variety through the vanishing locus of n *quasi-homogeneous* polynomials $p_1, ..., p_n$. Such a polynomial p_i satisfies

$$p_i(\lambda^{w_0} x_0 : ... : \lambda^{w_N} x_N) = \lambda^{d_i} p_i(x_0 : ... : x_N), \tag{A.12}$$

where d_i denotes the degree of the polynomial p_i. Subvarieties are consistently defined in this way, if the corresponding polynomials are transversal meaning that the matrix $(\frac{\partial p_i}{\partial x_j})$ has a constant rank n, and they are called *complete intersections*.

The *adjunction formula* states a relation between the canonical bundle K_X of a hypersurface H, the normal bundle N_X and the canonical bundle of the ambient space A, $K_A|_H$. More precisely, the latter denotes the restriction of the canonical bundle to the hypersurface H. It is based on the exact sequence

$$0 \to T_X \to T_A|_X \to N_X \to 0. \tag{A.13}$$

The Whitney sum formula then allows to express the total Chern class of a hypersurface as

$$c(T_A|_X) = c(T_X)c(N_X). \tag{A.14}$$

This can be used to construct CY varieties as follows. Denote the pullback of the Kähler form of the ambient space to the subvariety X by H. The adjunction formula then reads

$$\prod_{i=0}^{N}(1 + w_i H) = c(X) \cdot \prod_{j=1}^{n}(1 + d_j H). \tag{A.15}$$

The first Chern class of X thus reads

$$c_1(X) = (\sum_{i=1}^{N} w_i - \sum_{j=1}^{n} d_j)H, \tag{A.16}$$

which requires one to set

$$\sum_{i=1}^{N} w_i = \sum_{j=1}^{n} d_j \tag{A.17}$$

in order to obtain a CY. Having chosen the order of the polynomials defining a complete intersection, one can easily calculate all the Chern classes and also the Euler character of X, using the standard normalization for a weighted projective space

$$\int_{WC\mathbb{P}^N_{\vec{w}}} H^N = \frac{1}{\prod_{j=0}^N w_i}. \tag{A.18}$$

A simple model which is also used in this thesis extensively, is obtained by taking just one polynomial p to define a hypersurface X in $C\mathbb{P}^4$. The previous equation leads to

$$c(X) \cdot (1 + dH) = (1 + H)^5|_X = 1 + 5H + 10H^2 + 10H^3, \tag{A.19}$$

from which one reads off that in order for the first Chern class $c_1(X)$ of X to vanish, one needs to choose a degree five polynomial $d = 5$. The Calabi-Yau variety constructed in this way is known as the *quintic*. One automatically also obtains $c_2(X) = 10H^2$ and $c_3 = -40H^3$. By the Hirzebruch-Riemann-Roch theorem A.10, one now computes the Euler character as an integral over the top Chern class

$$\chi(X) = \int_X c_3(X) = -40 \int_X H^3 = -200. \tag{A.20}$$

Appendix B

Area code case studies on the quintic

This part of the appendix contains a more detailed study of the area code belonging to two different charge systems on the quintic. As in [51], the w-plane is used to graphically represent the region of moduli space of interest. The w-coordinate is related to the complex structure modulus ψ by $w = \frac{\ln(|\psi|+1)}{\ln(2)}\frac{\psi}{|\psi|}$. The w-plane is a fivefold cover of moduli space, and the normalization is chosen such that the five conifold point copies lie at $w = e^{2ni\pi/5}$ for $(n = 0, ..., 4)$. In the illustrations in the appendix, beginning with figure B.1, threshold walls are printed in black, walls of marginal stability for the first split in blue, and flow branches in green, the five copies of the conifold point in red. A wall of marginal stability between a D6-core and a D2-D0-halo will be printed as a dotted red line.

The state $\Delta q = 1$, $\Delta q_0 = -2$ on the quintic

This section covers the area code of the non-polar system with $\hat{q}_0 \approx -0.31$. Recall that this charge system can be described as a D4-brane with half a unit of worldvolume of flux turned on, additional worldvolume flux dual to a degree one rational curve, and one $\overline{\text{D0}}$. This corresponds to the total charge $\Gamma = H + \frac{7}{10}H^2 + \frac{11}{60}H^3$. One finds two different basic types of split flow trees for this charge configuration.

The first will be called a **type A**-split, and it comes in two variants. These splits come with three centers: a D6 with worldvolume flux H, a $\overline{\text{D6}}$ with a D2 wrapped on a degree one rational curve, and a $\overline{\text{D0}}$. The two variants correspond to the placing of the background on the two sides of the $\overline{\text{D0}}$-threshold wall [1].

- If one starts above the TH wall, the $\overline{\text{D0}}$ remains on the D6-side after the first split (and then splits off to run towards the LCS point): this is denoted the *type A1* variant. An example can be found on the left-hand side in figure B.1. Schematically:

$$\begin{aligned}(D4_{C_1}/\overline{\text{D0}}) &\rightarrow (D6/\overline{\text{D0}}) + (\overline{\text{D6}}/D2)\\ &\rightarrow (D6) + (\overline{\text{D0}}) + (\overline{\text{D6}}/D2).\end{aligned}$$

[1] The 'incoming branch' of the flow tree does not cross the $\overline{\text{D0}}$-TH wall.

- When one starts the flow tree below the TH wall, the $\overline{\text{D0}}$ binds to the $\overline{\text{D6}}$-D2 after the first split: this is referred to as the *type A2* variant, and an example can be found on the right-hand side in figure B.1. Schematically:

$$\begin{aligned}(D4_{C_1}/\overline{\text{D0}}) &\rightarrow (D6) + (\overline{\text{D6}}/D2/\overline{\text{D0}}) \\ &\rightarrow (D6) + (\overline{\text{D6}}/D2) + (\overline{\text{D0}}).\end{aligned}$$

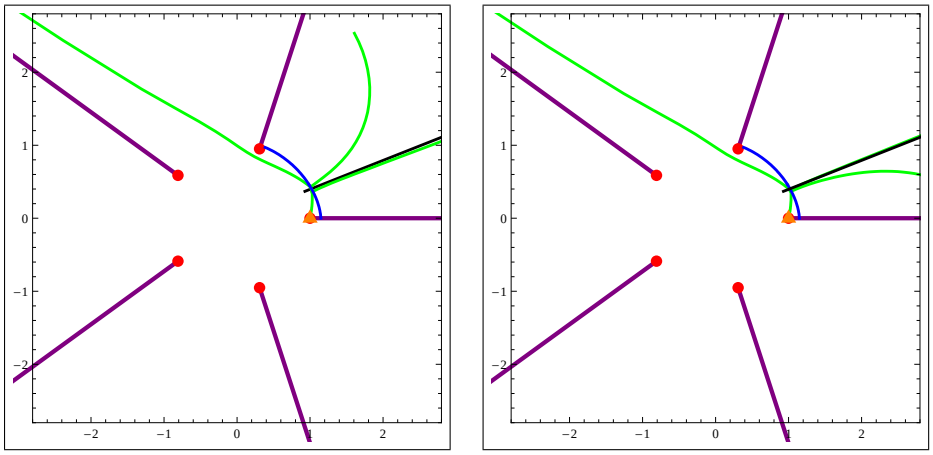

Figure B.1: **Left: Type A1 split.** A split flow tree with the background above the threshold wall. The incoming branch reaches a wall of marginal stability and splits into D6-$\overline{\text{D0}}$ and $\overline{\text{D6}}$-D2. The $\overline{\text{D6}}$-D2-branch then flows off to an attractor point outside of the fundamental wedge, not shown in the figure. The D6 and the $\overline{\text{D0}}$-brane split just slightly below the wall after which the $\overline{\text{D0}}$ flows off to the LCS point, and the D6 (with one unit of worldvolume-flux) flows to a copy of the conifold point. **Right: Type A2 split.** A split flow tree with the background below the threshold wall. The incoming branch reaches a wall of marginal stability and splits into D6 and $\overline{\text{D6}}$-D2-$\overline{\text{D0}}$, after which the D6 flows to a copy of the conifold point. The $\overline{\text{D0}}$ split off and heads towards the LCS point, while the $\overline{\text{D6}}$-D2 runs off towards an attractor point outside of the fundamental wedge, again not shown in the figure.

The second basic type of split will be called a **type B**-split and also comes with three endpoints. However, this time, the D6 with flux H and the $\overline{\text{D6}}$ do not carry any curves, and their flow branches each end on a copy of the conifold point. After the first split, the D2-D0 charge is on the $\overline{\text{D6}}$-side, and then leaves the $\overline{\text{D6}}$ at the second split point. Schematically:

$$\begin{aligned}(D4_{C_1}/\overline{\text{D0}}) &\rightarrow (D6) + (\overline{\text{D6}}/D2/\overline{\text{D0}}) \\ &\rightarrow (D6) + (\overline{\text{D6}}) + (D2/\overline{\text{D0}}).\end{aligned}$$

The important message is that the existence of this type of split is not influenced by the threshold wall. [2]

[2]It does however require the $\overline{\text{D6}}$(core)-D2-D0 (halo) branch to reach the core-halo wall in order to be

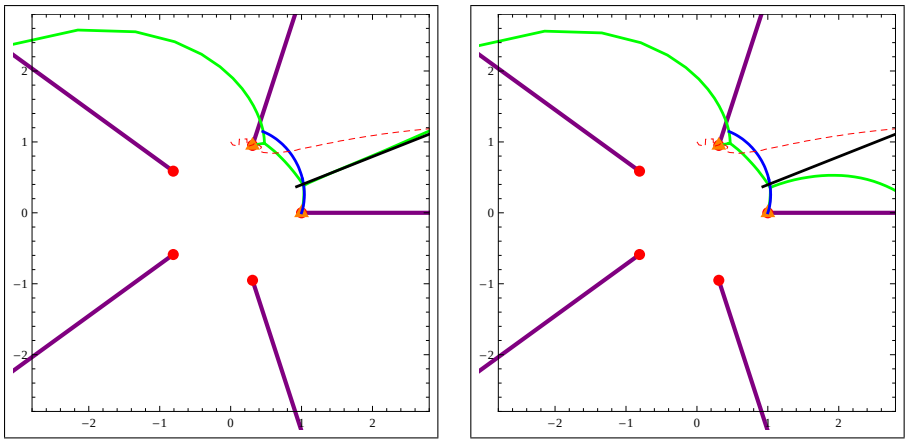

Figure B.2: **Left: Type B split with background above TH wall.** A type B split with the background chosen above the threshold wall (and not too close to the conifold point). The charge splits into D6 and $\overline{\text{D6}} - D2 - \overline{\text{D0}}$. The D6-branch flows to a copy of the conifold point. The D2-D0 halo particle then splits off from the $\overline{\text{D6}}$ and flows off towards its attractor point outside of the fundamental wedge. The $\overline{\text{D6}}$ also flows towards a copy of the conifold point. **Right: Type B split with background below TH wall.** Example of a type B split flow tree with the background chosen below the threshold wall.

Below the threshold wall the total index for this charge system is easy to calculate:

$$\Omega = \Omega_{A2} + \Omega_B = (-1)^1 \cdot 2 \cdot N_{\text{DT}}(0,0) \cdot N_{\text{DT}}(1,2) = -1'138'500. \tag{B.1}$$

Note that the DT-invariant $N_{\text{DT}}(1,2)$ counts all the $\overline{\text{D6}}$-D2-D0 states, so this is the appropriate enumeration for both the type A2 and the B flow trees. Had one not found the type B flow trees, one would have been overcounting the states by using the DT invariant to enumerate the number of BPS states belonging to the $\overline{\text{D6}}$-branch.

Above the threshold wall, one finds a split flow tree of type A1 contributing, which is enumerated as follows:

$$\Omega_{A1} = (-1)^1 \cdot 2 \cdot N_{\text{DT}}(0,1) \cdot N_{\text{DT}}(1,1) = -1'150'000. \tag{B.2}$$

However, one also has a type B flow tree above the wall, which explains why the two naively equivalent indices, B.1 and B.2, do not match. The apparent discrepancy lies in the fact, that, below the threshold wall, $N_{\text{DT}}(1,2)$ counts both the A2 and the B flow trees. Therefore the all flow trees starting below the threshold wall are taken care of by this index.

When taking the background value of the modulus to start above the wall, the index with $N_{\text{DT}}(0,1) \cdot N_{\text{DT}}(1,1)$ only counts the A1 split. One still needs to account for the

able to perform the second split (recall that the core-halo wall is plotted as a dotted red line in figure B.2), which is the case if one does not start too close to the copy of the conifold point lying on the upper branch cut boundary of the fundamental wedge. This latter fact would eventually lead to another topological sector for the final area code of this charge system, but this subtlety will be ignored.

B split, which also exists in this sector of the moduli space. In principle, one would not directly know how to enumerate the type B split directly, but in this case one does know that the total index cannot jump when crossing a wall of threshold stability. Therefore, one can conclude that the type B split has to contribute $+11'500$ to the index above the wall, allowing to also state $-1'138'500$ as the total index when placing the background modulus above the threshold wall.

The state $\Delta q = 2$, $\Delta q_0 = -2$ on the quintic

In this section, the area code for the system with $\hat{q}_0 \approx -1.11$ is discussed. The total charge can be obtained by considering a (pure fluxed) D4 with additional flux dual to a degree two rational curve as well as one bound $\overline{\text{D0}}$. This yields the total charge $\Gamma = H + \frac{9}{10}H^2 - \frac{1}{60}H^3$. One finds three different flow trees for this system. Two of these and their area code behave completely analogously to the system B, discussed previously. The only difference to the previous case study is, that one is always dealing with a degree two instead of a degree one curve, and as a consequence of this difference in charge, the corresponding but analogous walls are slightly different.

One can again list the **type A** flow trees, two variants between which a threshold wall interpolates.

- Above the TH wall, the $\overline{\text{D0}}$ remains on the D6-side after the first split (and then splits off to run towards the LCS point): this is denoted the *type A1* variant. Such a split flow can be seen on the left-hand side in figure B.3. Schematically:

$$\begin{aligned}(D4_{C_1}/\overline{\text{D0}}) &\rightarrow (D6/\overline{\text{D0}}) + (\overline{\text{D6}}/D2)\\ &\rightarrow (D6) + (\overline{\text{D0}}) + (\overline{\text{D6}}/D2).\end{aligned}$$

- Below the TH wall, the $\overline{\text{D0}}$ binds to the $\overline{\text{D6}}$-D2 after the first split: this is referred to as the *type A2* variant. Such a split flow can be seen on the right-hand side in figure B.3. Schematically:

$$\begin{aligned}(D4_{C_1}/\overline{\text{D0}}) &\rightarrow (D6) + (\overline{\text{D6}}/D2/\overline{\text{D0}})\\ &\rightarrow (D6) + (\overline{\text{D6}}/D2) + (\overline{\text{D0}}).\end{aligned}$$

Again, there is also a **type B** flow tree, the only difference to the previous case study lies in the charge of the halo. As this is straightforward, it will not be discussed here.

However, there is a third type of flow tree for this charge system, which will be called **type C**. It is extremely convenient to analyze this charge configuration in a background where it is realized as a split flow with two end points. This specific realization of type C split will be called a *type C1*. The first center corresponds to a D6-brane with flux $2H$ as well as a $\overline{\text{D2}}$ wrapped on a degree *three* rational curve. The second center corresponds to a $\overline{\text{D6}}$ with flux H. The type C1 split flow tree requires the background to be 'very close' to the wall of marginal stability between the two centers. An example of what is meant by 'close' can be seen in figure B.4.

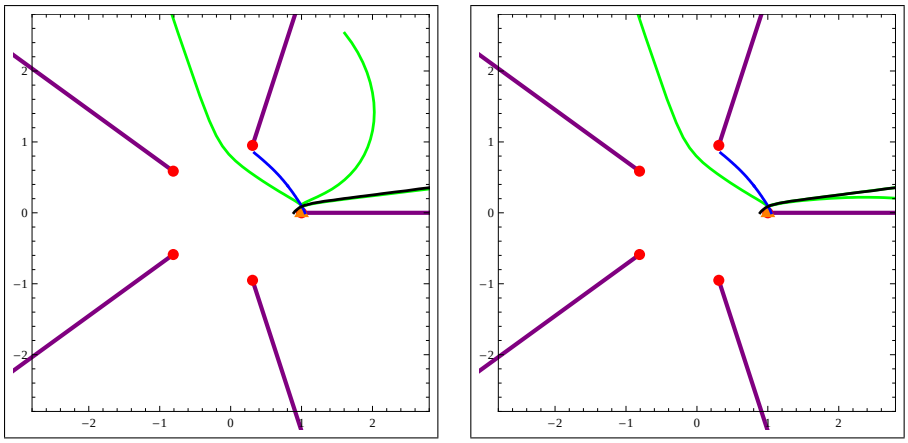

Figure B.3: **Left: Type A1 split.** A split flow tree with the background above the threshold wall. The incoming branch reaches a wall of marginal stability and splits into D6-$\overline{\text{D0}}$ and $\overline{\text{D6}}$-D2. The $\overline{\text{D6}}$-D2-branch then flows off to an attractor point outside of the fundamental wedge, not shown in the figure. The D6 and the $\overline{\text{D0}}$-brane split just slightly below the wall after which the $\overline{\text{D0}}$ flows off to the LCS point, and the D6 (with flux H) flows to a copy of the conifold point. **Right: Type A2 split.** A split flow tree with the background below the threshold wall. The incoming branch reaches a wall of marginal stability and splits into D6 and $\overline{\text{D6}}$-D2-$\overline{\text{D0}}$, after which the D6 flows to a copy of the conifold point. The $\overline{\text{D0}}$ splits off and heads towards the LCS point, while the $\overline{\text{D6}}$-D2 runs off towards an attractor point outside of the fundamental wedge.

However, when one moves the background further 'upwards in the figure' / 'further away' from the wall of marginal stability, the first split point travels upwards 'on the wall of marginal stability'. At some point, this first split point would seemingly cross the upper branch cut boundary of the fundamental wedge. This means that a topology change takes place. The index of BPS states is not allowed to jump, but flow trees can develop new branches. In the background region, where one finds the type C1 split flow tree, there is no single flow. However, by moving the background to the right, the incoming branch runs over the upper branch cut and then flows to an attractor point: a single flow enters the spectrum. This means that this topology change can be thought of as a trade-off between the C1 split flow tree and a single flow (and possibly also new, different split flow trees). The contribution to the total index of BPS states cannot jump, when a topology change occurs. This example fits in nicely with the interpretations of [51]. Running this topology change in reverse, one could state: Starting in the background with the single flow, one crosses a branch cut when trying to 'pull the flow through the conifold singularity', and one actually creates a new branch of the flow tree.

To conclude, taking the background very 'close to the wall of marginal stability' between the D6- and the $\overline{\text{D6}}$-center, and also 'close to the branch cut' (the upper boundary of the fundamental wedge), the total index for this charge reads:

$$\Omega = \Omega_B + \Omega_{C1} = \Omega_B + (\Omega_C - \Omega_{C2}) = 124'762'875 + 317'206'375 = 441'969'250. \quad \text{(B.3)}$$

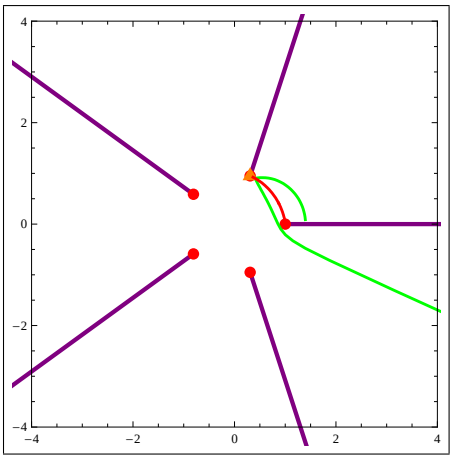

Figure B.4: **Type C1 split.** After the first split, the $\overline{\text{D6}}$ flows to a copy of the conifold point, and the D6 with a D2 on a degree three rational curve runs off to an attractor point outside of the fundamental wedge.

This index has to remain invariant when varying the background modulus without crossing a wall of marginal stability. According to the preceding remarks, one can see this as an interpolation between different topological sectors of moduli space (check figure B.5).

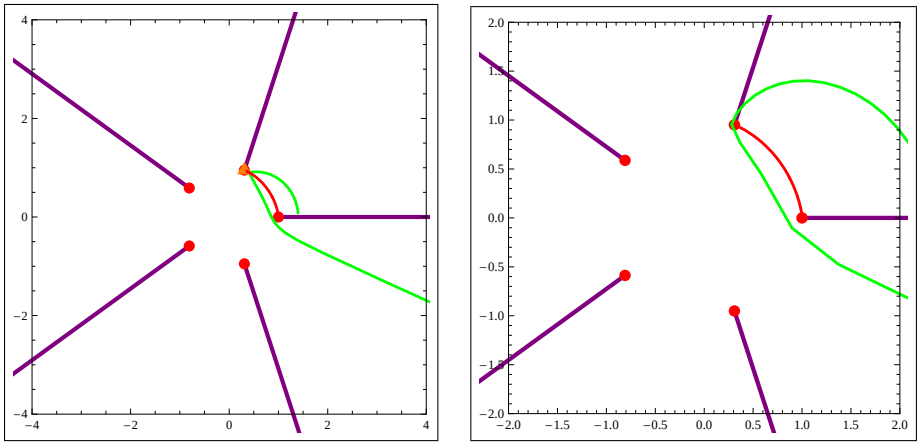

Figure B.5: Topology change for the type C split. **Left: Type C1.** The charge supports a split flow tree. The first center is a D6 with flux $2H$ and a $\overline{\text{D2}}$ wrapped on a degree three rational curve. The second center is a $\overline{\text{D6}}$ with flux H. As one moves the background modulus 'upwards' ('further away' from the marginal stability wall), the first split point also moves upwards, until it hits the branch cut boundary. **Right: Type C2, a single flow.** If one moves the background 'too far' upwards or 'too far' to the right, the incoming branch hits the branch cut before reaching the wall of marginal stability. Instead, this flow reaches an attractor point: a single flow enters the spectrum which is not supported in the background region where one finds the split flow on the left-hand side.

Appendix C

Dimensional reduction and truncation to the STU model

This part of the appendix contains the dimensional reduction of type II supergravity to 4d by compactification on T^6 as well as the truncation to the bosonic STU model action (5.16) in the duality frame B. It will be convenient to first reduce to an intermediate duality frame, which one can call frame $\tilde{B}$, where the $U(1)$ fields are labeled as $\mathcal{A}^0, \mathcal{A}^1, \mathcal{B}_2, \mathcal{A}^3$ and the charges are labeled as $(p^0, p^1, \tilde{p}^2, p^3, q_1, \tilde{q}_2, q_1, q_0)$. The 10D interpretation of the charges in frame $\tilde{B}$ is given in table C.1.

The frame $\tilde{B}$ differs from the frame B of table C.2 by an electromagnetic duality transformation on the $U(1)$ field $\mathcal{B}^2$. where P refers to momentum. It suffices to restrict attention to a truncated IIB action containing only the metric, dilaton and RR 3-form:

$$S = \frac{1}{(2\pi)^7 \alpha'^4} \int d^{10}x \sqrt{-G^{(10)}} \left[e^{-2\Phi^{(10)}} \left(R^{(10)} + 4\partial_M \Phi^{(10)} \partial^M \Phi^{(10)} \right) - \frac{1}{12} F^{(10)}_{MNP} F^{(10)\,MNP} \right] . \tag{C.1}$$

A trivial dimensional reduction over the four-torus $T_2 \times T_3$ ir performed, while allowing the torus T_1 to be nontrivially fibered over the four-dimensional base. One can start by flipping the sign of $\Phi^{(10)}$ and making a Weyl transformation (as one does in S-duality) such that all terms in (C.1) have an $e^{-2\Phi^{(10)}}$ factor in front. One can then perform the dimensional reduction of this sector as discussed in [168]. The conventions used here match

q_0	$P(S^4)$	p^0	$KKmon(S^4)$
q_1	$P(S^5)$	p^1	$KKmon(S^5)$
$\tilde{q}_2$	$D1(S^4)$	$\tilde{p}^2$	$D5(S^4)$
q_3	$D1(S^5)$	p^3	$D5(S^5)$

Table C.1: The interpretation of the charge in an intermediate frame $\tilde{B}$.

q_0	P (S^4)	p^0	KK5 $(S^5 \times T_2 \times T_3)$
q_1	P (S^5)	p^1	KK5 $(S^4 \times T_2 \times T_3)$
q_2	D5 $(S^5 \times T_2 \times T_3)$	p^2	D1 (S^4)
q_3	D1 (S^5)	p^3	D5 $(S^4 \times T_2 \times T_3)$

Table C.2: 10D origin of the charges in frame B

those of [169]. The following reduction ansatz is imposed

$$\begin{aligned}
\Phi^{(10)} &= -\Phi - \frac{1}{4}\ln\det\hat{G}_{mn} - \frac{1}{4}\ln\det\hat{G}_{ij}\,,\\
G^{(10)}_{\mu\nu} &= (\det\hat{G})^{-1/4}\left(e^{\Phi}G_{\mu\nu} + 2\beta^2 e^{-\Phi}\mathcal{A}^{m-4}_{\mu}\mathcal{A}^{n-4}_{\nu}\hat{G}_{mn}\right)\,,\\
G^{(10)}_{\mu n} &= \sqrt{2}\beta(\det\hat{G})^{-1/4}e^{-\Phi}\hat{G}_{np}\mathcal{A}^{p-4}_{\mu}\,,\\
G^{(10)}_{mn} &= (\det\hat{G})^{-1/4}e^{-\Phi}\hat{G}_{mn}\,,\\
G^{(10)}_{ij} &= (\det\hat{G})^{-1/4}e^{-\Phi}\hat{G}_{ij}\,,\\
C^{(10)}_{\mu\nu} &= C_{\mu\nu} + 2\beta^2\hat{C}_{45}(\mathcal{A}^0_{\mu}\mathcal{A}^1_{\nu} - \mathcal{A}^1_{\mu}\mathcal{A}^0_{\nu}) + \beta^2(\mathcal{A}^0_{\mu}\mathcal{B}_{2\nu} - \mathcal{B}_{2\mu}\mathcal{A}^0_{\nu}) + \beta^2(\mathcal{A}^1_{\mu}\mathcal{A}^3_{\nu} - \mathcal{A}^3_{\mu}\mathcal{A}^1_{\nu})\,,\\
C^{(10)}_{\mu 4} &= \sqrt{2}\beta(\mathcal{B}_{2\mu} + \hat{C}_{45}\mathcal{A}^1_{\mu})\,,\\
C^{(10)}_{\mu 5} &= \sqrt{2}\beta^2(\mathcal{A}^3_{\mu} - \hat{C}_{45}\mathcal{A}^0_{\mu})\,,\\
C^{(10)}_{mn} &= \hat{C}_{mn}\,.
\end{aligned} \tag{C.2}$$

Here, $M, N = 0, \ldots, 9;\ m, n = 4, 5,\ i, j = 6, \ldots 9$ and x^4, x^5 are taken to parametrize S_4, S_5 respectively. The matrix $\hat{G}_{ij}$ is a constant metric on $T_2 \times T_3$ and the matrices $\hat{G}_{mn}, \hat{C}_{mn}$ can be conveniently parametrized as

$$\begin{aligned}
\hat{G}_{mn} &= b_3 \begin{pmatrix} \frac{a_1^2+b_1^2}{b_1} & -\frac{a_1}{b_1} \\ -\frac{a_1}{b_1} & \frac{1}{b_1} \end{pmatrix}\,,\\
\hat{C}_{mn} &= \begin{pmatrix} 0 & a_3 \\ -a3 & 0 \end{pmatrix}\,,\\
e^{-2\Phi} &= b_2\,.
\end{aligned} \tag{C.3}$$

The two-form $C_{\mu\nu}$ can be dualized in four dimensions to give another scalar $\tilde{a}_1$:

$$da_2 = b_2^2 \star F\,, \tag{C.4}$$

where the Hodge $\star$ is to be taken with respect to the 4D metric $G_{\mu\nu}$ and the three-form field strength F is defined as

$$F = dC + \frac{\beta^2}{2}\left(\mathcal{A}^0 \wedge \mathcal{G}^2 + \mathcal{B}^2 \wedge \mathcal{F}^0 + \mathcal{A}^1 \wedge \mathcal{F}^3 + \mathcal{A}^3 \wedge \mathcal{F}^1\right)\,. \tag{C.5}$$

From the above expressions it is clear that $z^1 = a_1 + ib_1$ is the complex structure modulus of T_1, $z^2 = a_2 + ib_2$ is the 4D axion-dilaton and $z^3 = a_3 + ib_3$ is the complexified Kähler modulus of T_1.

In these variables, one finds the 4d action

$$\begin{aligned} S &= \frac{1}{16\pi G_4}\int d^4x\sqrt{-G}\Big[R - 2\sum_{A=1}^{3}\frac{\partial_\mu \tilde{z}^A \partial^\mu \bar{\tilde{z}}^A}{(\tilde{z}^A - \bar{\tilde{z}}^A)^2} \\ &\quad + \frac{\beta^2}{2}\mathrm{Im}\tilde{\mathcal{N}}_{IJ}\mathcal{F}^I_{\mu\nu}\mathcal{F}^{J\,\mu\nu} + \frac{\beta^2}{4}\mathrm{Re}\tilde{\mathcal{N}}_{IJ}\epsilon^{\mu\nu\rho\sigma}\mathcal{F}^I_{\mu\nu}\mathcal{F}^J_{\rho\sigma}\Big], \end{aligned} \tag{C.6}$$

after performing the dimensional reduction, with the matrix $\tilde{\mathcal{N}}$ given by

$$\mathrm{Re}(\tilde{\mathcal{N}}) = \begin{pmatrix} 0 & 0 & -a_2 & 0 \\ 0 & 0 & 0 & -a_2 \\ -a_2 & 0 & 0 & 0 \\ 0 & -a_2 & 0 & 0 \end{pmatrix},$$

$$\mathrm{Im}(\tilde{\mathcal{N}}) = \begin{pmatrix} -\frac{b_2\left(a_1{}^2+b_1{}^2\right)\left(a_3{}^2+b_3{}^2\right)}{b_1 b_3} & \frac{a_1 b_2\left(a_3{}^2+b_3{}^2\right)}{b_1 b_3} & -\frac{a_1 a_3 b_2}{b_1 b_3} & \frac{a_3 b_2\left(a_1{}^2+b_1{}^2\right)}{b_1 b_3} \\ \frac{a_1 b_2\left(a_3{}^2+b_3{}^2\right)}{b_1 b_3} & -\frac{b_2\left(a_3{}^2+b_3{}^2\right)}{b_1 b_3} & \frac{a_3 b_2}{b_1 b_3} & -\frac{a_1 a_3 b_2}{b_1 b_3} \\ -\frac{a_1 a_3 b_2}{b_1 b_3} & \frac{a_3 b_2}{b_1 b_3} & -\frac{b_2}{b_1 b_3} & \frac{a_1 b_2}{b_1 b_3} \\ \frac{a_3 b_2\left(a_1{}^2+b_1{}^2\right)}{b_1 b_3} & -\frac{a_1 a_3 b_2}{b_1 b_3} & \frac{a_1 b_2}{b_1 b_3} & -\frac{b_2\left(a_1{}^2+b_1{}^2\right)}{b_1 b_3} \end{pmatrix}.$$

The 4-dimensional Newton constant G_4 is given by

$$G_4 = \frac{8\pi^6(\alpha')^4 g^2}{(2\pi)^2 R_4 R_5 V_{T_2\times T_3}}, \tag{C.7}$$

where g denotes the string coupling in 10 dimensions.

To go to the duality frame B of table C.2, where the $U(1)$ fields are labeled as $\mathcal{A}^0, \mathcal{A}^1, \mathcal{B}^2, \mathcal{A}^3$ and the charges are labeled as $(p^0, p^1, p^2, p^3, q_1, q_2, q_3, q_0)$, one has to perform an electromagnetic duality on the field $\mathcal{B}_2$. After this duality, the action takes the form (5.16) with the matrix $\mathcal{N}$ related to $\tilde{\mathcal{N}}$ given above by a symplectic transformation

$$\mathcal{N} = (C + D\tilde{\mathcal{N}})(A + B\tilde{\mathcal{N}})^{-1}, \tag{C.8}$$

with

$$A = D = \begin{pmatrix} 1 & 0 & 0 & 0 \\ 0 & 1 & 0 & 0 \\ 0 & 0 & 0 & 0 \\ 0 & 0 & 0 & 1 \end{pmatrix}; \quad B = -C = \begin{pmatrix} 0 & 0 & 0 & 0 \\ 0 & 0 & 0 & 0 \\ 0 & 0 & -1 & 0 \\ 0 & 0 & 0 & 0 \end{pmatrix}. \tag{C.9}$$

Explicitly, one finds

$$\begin{aligned}
\mathrm{Re}(\mathcal{N}) &= -\begin{pmatrix} 2\,a_1\,a_2\,a_3 & -(a_2\,a_3) & -(a_1\,a_3) & -(a_1\,a_2) \\ -(a_2\,a_3) & 0 & a_3 & a_2 \\ -(a_1\,a_3) & a_3 & 0 & a_1 \\ -(a_1\,a_2) & a_2 & a_1 & 0 \end{pmatrix}, \\
\mathrm{Im}(\mathcal{N}) &= -\begin{pmatrix} b_1b_2b_3+\frac{b_1b_2a_3^2}{b_3}+\frac{b_1b_3a_2^2}{b_2}+\frac{b_2b_3a_1^2}{b_1} & -\frac{a_1\,b_2\,b_3}{b_1} & -\frac{a_2\,b_1\,b_3}{b_2} & -\frac{a_3\,b_1\,b_2}{b_3} \\ r-\frac{a_1\,b_2\,b_3}{b_1} & \frac{b_2\,b_3}{b_1} & 0 & 0 \\ -\frac{a_2\,b_1\,b_3}{b_2} & 0 & \frac{b_1\,b_3}{b_2} & 0 \\ -\frac{a_3\,b_1\,b_2}{b_3} & 0 & 0 & \frac{b_1\,b_2}{b_3} \end{pmatrix}.
\end{aligned}$$

This is indeed the standard form of the matrix $\mathcal{N}$ in the STU-model derived from the prepotential through (5.17). The $U(1)$ field $\mathcal{B}_2$ is related to the $\mathcal{A}^I$ through

$$d\mathcal{B}_2 = \mathrm{Im}\mathcal{N}_{2J} \star \mathcal{F}^J + \mathrm{Re}\mathcal{N}_{2J}\mathcal{F}^J\,. \tag{C.10}$$

Summarized, the reduction formulae read

$$\begin{aligned}
e^{2\Phi^{(10)}} &= \frac{b^2}{b^3}\,, \\
ds_{10}^2 &= \frac{1}{\sqrt{b^2b^3}}ds_4^2 + \sqrt{b^2b^3}\mathcal{M}_{mn}(dx^m+\sqrt{2}\beta\mathcal{A}^{m-4})(dx^n+\sqrt{2}\beta\mathcal{A}^{n-4}) + \sqrt{\frac{b^2}{b^3}}ds^2_{T_2\times T_3}\,, \\
\mathcal{M}_{mn} &= \frac{1}{b^1}\begin{pmatrix} (a^1)^2+(b^1)^2 & -a^1 \\ -a^1 & 1 \end{pmatrix}, \\
C^{(10)} &= \frac{1}{2}C_{\mu\nu}dx^\mu dx^\nu + a^3(dx^4-\sqrt{2}\beta\mathcal{A}^0)\wedge(dx^5-\sqrt{2}\beta\mathcal{A}^1) \\
&\quad -\sqrt{2}\beta\,dx^4\wedge\mathcal{B}^2 - \sqrt{2}\beta\,dx^5\wedge\mathcal{A}^3 + \beta^2\left(\mathcal{A}^0\wedge\mathcal{B}^2+\mathcal{A}^1\wedge\mathcal{A}^3\right), \\
da_2 &= (b_2)^2\star F\,, \\
F &= dC + \frac{\beta^2}{2}(\mathcal{A}^0\wedge\mathcal{G}^2+\mathcal{B}^2\wedge\mathcal{F}^0+\mathcal{A}^1\wedge\mathcal{F}^3+\mathcal{A}^3\wedge\mathcal{F}^1)\,.
\end{aligned} \tag{C.11}$$

Appendix D

Nederlandse samenvatting

Lezers interesseren zich voor verschillende aspecten van deze thesis. Evenals dit in het begin van de introductie werd gedaan, zal ook hier hulp worden verleend aan de lezer bij zijn zoektocht, en (in het ideale geval) tonen waar hij meer informatie kan vinden over onderdelen die hem bijzonder interesseren.

Drie delen van deze thesis zijn niet alleen toegankelijk voor de natuurkundige, maar voor iedereen:

1. *De introductie*: in de introductie verklaart de auteur de algemene context waarin zijn onderzoek mag worden gesitueerd. Ten eerste wordt het onderzoeksgebied 'snaartheorie' geschetst. Dit wordt gevolgd door een klein overzicht met betrekking tot het onderwerp 'zwarte gaten'. De lezer vindt in deze Nederlandse samenvatting veel inhoudelijke overeenstemming met de introductie; de laatste gaat echter iets dieper in op dezelfde onderwerpen.

2. *De conclusies*: Terwijl de meer gespecialiseerde lezer aparte en meer wetenschappelijke introducties, samenvattingen en discussies kan vinden aan het begin en het einde van elk hoofdstuk, zijn de conclusies bedoeld om begrijpelijk te zijn voor een meer uitgebreid publiek. Met name wordt het door de auteur verrichte onderzoek middels een metafoor geduid. Het onderzoek over zwarte gaten wordt vergeleken en analoog geschetst aan het bestuderen van genomen in de microbiologie. De gemaakte analogieën zijn geenszins perfect, maar ze maken het mogelijk om het werk van de auteur vanuit een intuitieve benadering in een eenvoudige taal aan de lezer over te brengen.

3. *De Nederlandse samenvatting in de appendix*: (Dit is waar de lezer zich nu bevindt.)

Het hoofddeel van deze thesis bestaat uit vijf hoofdstukken. De eerste drie introduceren de context in vaktaal, waarin het onderzoek van de auteur zijn plaats vindt. Deze hoofdstukken verschijnen in de volgorde naarmate van specialisatie van de behandelde onderwerpen, lopend van algemeen naar meer specifiek. De twee daarop volgende hoofdstukken (4 en 5) omschrijven de belangrijkste onderzoeksresultaten van de auteur.

Allereerst zal de algemene context van dit onderzoek worden uiteengezet (snaartheorie en zwarte gaten), gevolgd door een meer specifieke metaforische interpretatie van de resultaten die de auteur heeft gevonden. Ten slotte vindt men vanaf D.3 in de Nederlandse samenvatting ook een meer gedetailleerd overzicht over de specifieke inhoud van deze thesis.

D.1 Snaartheorie en zwarte gaten

Men zou misschien het historische verschijnsel 'unificatie' (het verklaren van verschillende fysische fenomenen door gemeenschappelijke onderliggende wetten) als een drijfveer kunnen beschouwen voor de zoektocht naar een kwantumtheorie van alle vier bekende fysische krachten. De huidige situatie omtrent de unificatie van theorieën binnen de theoretische fysica zou als volgt kunnen worden samengevat:

- *De microkosmos*: De drie krachten (waaronder elektromagnetisme) die de microkosmos overheersen, worden allemaal omschreven door middel van kwantumveldentheorieën. Deeltjes krijgen in deze theorieën de interpretatie van propagerende storingen van kwantumvelden, en alle deeltjes vallen in één van de twee fundamentele klassen: fermionen, met een halftallige spin (een kwantummechanisch draaimoment): bijvoorbeeld een elektron, én bosonen, met een heeltallige spin: bijvoorbeeld een foton.

- *De macrokosmos*: De zwakste van de krachten, de gravitatie, is de enige die op heel grote ruimteschaal een rol speelt. Gravitatie wordt omschreven door de Algemene Relativiteitstheorie, een klassieke veldentheorie, die ongeveer tussen 1907 en 1916 door Albert Einstein werd ontwikkeld.

Men zou graag willen beschikken over een theorie, die zowel de micro- als de macrokosmos kan omschrijven. Snaartheorie is daarvoor een veelbelovende kandidaat. In een poging om snaartheorie te onderscheiden van pre-snaar natuurkunde, kan de paradigma-verschuiving worden gebruikt van een punt-deeltje naar een snaar (een object met een dimensie meer). Alle deeltjes welke in de microkosmos bestaan zijn dan verschillende modes van een fundamentele, vibrerende snaar. Dit is vergelijkbaar met de manier waarop een toon ontstaat op een viool. Dit voorstel onderstreept de gemeenschappelijke oorsprong van deeltjes. In 1995 werden echter verschillende ontdekkingen gedaan die de overheersende rol van de snaar zouden relativeren. Het blijkt namelijk, dat snaartheorie noodzakelijkerwijs ook objecten van verschillende andere dimensies (naast 0-dimensionale punt-deeltjes en 1-dimensionale snaren) bevat, aan welke de naam 'branen' werd gegeven. Een punt-deeltje (0-braan) en een snaar (1-braan) zijn dus alleen speciale gevallen binnen een rijk spectrum van objecten, waaronder er ook hoger dimensionale objecten zoals 2-branen, 3-branen, etc. kunnen worden gevonden. Een voor menigeen vreemd verschijnsel, zeker voor wie er de eerste keer mee wordt geconfronteerd, is, dat snaartheorie een totaal aantal van 10 of 11 dimensies vereist. Dit is noodzakelijk voor haar innerlijke consistentie. De lezer kan zich de voorstelling maken, dat een andere keuze voor het totaal aantal dimensies direct zou impliceren, dat vele berekeningen onzin opleveren, in de zin dat de gevonden resultaten oneindig zijn. Dit

betekent wederom, dat een snaartheoreticus gedwongen is om een verbinding te scheppen tussen de 10 (of 11)-dimensionale wereld op het papier en de 4-dimensionale ruimtetijd welke men in het dagelijkse leven ondervindt. Een gebruikelijke werkwijze is om zes dimensies 'compact' (dat wil zeggen heel klein) te kiezen, en de vier dimensies, welke men in het dagelijkse leven ervaart, groot te houden.

Een kwantumveldentheorie van alle vier krachten, daaronder ook de kwantumgraviteit, wordt onder meer belangrijk, als men de natuurkunde van het heel vroege universum wil omschrijven, maar ook als men modellen van zwarte gaten wil ontwikkelen. Het onderzoek dat in deze thesis wordt omschreven, richt zich op de zwarte gaten, zoals ze kunnen worden beschouwd binnen het kader van de snaartheorie. Hieronder zal daarom meer uitleg over zwarte gaten worden gegeven.

Het breekpunt van de kwantumgravitatie: zwarte gaten

Zwarte gaten als theoretische entiteiten werden tijdens de eerste wereldoorlog ontdekt door Karl Schwarzschild. Zulk een zwart gat is een oplossing van de Einstein vergelijkingen van de Algemene Relativiteitstheorie (ART), die gravitatie omschrijft als de kromming van de ruimtetijd. In het bijzonder dwingt een massief object de ruimtetijd in zijn nabijheid te krommen. De term 'zwart gat' heeft betrekking op een gebied van de ruimtetijd dat zo dicht wordt gekoloniseerd door materie, dat de ruimtetijd daardoor een dusdanig sterke kromming ervaart, dat er uit dat gebied geen ontkomen meer is. De 'rechte banen' in zo een gekromde ruimtetijd-achtergrond leiden namelijk niet weg van het zwart gat. Dit is net zoals een rechte baan in de 4-dimensionale ruimtetijd voor een planeet in de buurt van een ster een cirkelvormige beweging is, en niet, zoals men misschien zou kunnen verwachten, die planeet gewoon laat wegglijden van de ster: dit laat zien hoe de 4-dimensionale, geometrische herinterpretatie van de gravitatiekracht werkt. Dit geldt ook voor de snelst bewegende entiteit binnen het universum: het licht. Omdat geen licht van een zwart gat wordt uitgezonden, lijkt het object ook zwart. Ergens in de buurt van een zwart gat is er een zone waar geen ontsnappen meer mogelijk is, genoemd 'waarnemingshorizon'.

In de jaren zeventig van de 20e eeuw maakten Stephen Hawking en medewerkers de voorspelling dat de hoeveelheid aan onzekerheid, die met de daadwerkelijke toestand van een zwart gat verbonden is, proportioneel is met het oppervlak van de waarnemingshorizon. Deze onzekerheid wordt in de natuurkunde entropie genoemd, en wordt gemeten door het aantal toestanden in welke zich een zwart gat zou kunnen bevinden. Dit zou men graag ook expliciet willen verklaren door alle mogelijke 'microtoestanden' van een zwart gat te vinden. Het klassieke beeld van een zwart gat is alleen een zwarte bal zonder verdere kenmerken. Daarom is het een belangrijk doel binnen een theorie van kwantumgravitatie om de entropie van een zwart gat microscopisch te verklaren. Dit zou inhouden om voor een bepaalde entropie van een zwart gat (dat wil zeggen een bepaald oppervlak van de waarnemingshorizon) alle microscopische toestanden te vinden, om zo alle mogelijkheden, welke voorspeld worden door de entropie-berekeningen, ook te zien. Binnen de snaartheorie is dit voor een bepaalde klasse van zwarte gaten ook gebeurd. Zwarte gaten binnen de snaartheorie (ten minste de supersymmetrische, die binnen de snaartheorie beter zijn

begrepen) kunnen gemodelleerd worden door branen op de 'extra' (opgewonden, compacte) dimensies te zetten, zodanig dat men een punt (of iets wat een beetje groter wordt dan een punt) observeert vanuit een vierdimensionaal perspectief. De verschillende mogelijkheden om deze branen op de extra dimensies te zetten levert dan de (microscopisch verklaarde en 'geometriseerde') entropie van een zwart gat op.

Gespleten attractor stromen

Het concept van 'gespleten attractor stromen', dat in de titel van deze thesis opduikt, vergt enige verklaring. Er werd al gezegd dat zwarte gaten binnen de snaartheorie door branen worden gemodelleerd die om extra dimensies worden gewikkeld. Dit laat toe om te verklaren dat een speciale klasse van zwarte gaten de geometrie van de extra dimensies sterk beperkt. Om een zwart gat te modelleren kan men namelijk de vorm en de grootte van de extra dimensies op een oneindige afstand van het zwarte gat kiezen, maar het zwarte gat eist dan een bepaalde geometrie op alle eindige afstanden van het zwarte gat zelf, in het bijzonder ook bij de waarnemingshorizon. Zou men een licht andere geometrie op oneindige afstand kiezen, blijft de geometrie bij de waarnemingshorizon invariant. Er bestaan specifieke grootheden die de geometrie bij de waarnemingshorizon 'meten', en die worden bij de horizon naar attractor-waarden gedreven. Daarom spreekt men ook over het attractor-mechanisme voor zwarte gaten. Zou men deze waarden voor de geometrieën in beeld brengen, in functie van een radiële coördinaat (een simpel zwart gat is radiaal-symmetrisch), dan vormen de waarden een lijn (in de ruimte van mogelijke 'veld-waarden'), beginnend bij de waarde op oneindige afstand, en eindigend bij het attractor punt. Deze lijn noemt men ook, om dit van de nog te bespreken gespleten attractor stromen te onderscheiden, een 'enkele stroom'.

Het blijkt echter dat ook zwarte gaten met meerdere centra, zogenaamde multicenter zwarte gaten, van groot belang zijn binnen de snaartheorie. Zulke multicenter zwarte gaten zijn gebonden toestanden van 'gewone' zwarte gaten (gewoon betekent hier: met één centrum). Een gelijkaardig attractor mechanisme is ook van toepassing op deze multicenter zwarte gaten, maar een 'stroom-lijn', beginnend bij de waarde op oneindige afstand, splitst (misschien zelfs meerdere keren). Er bestaat één 'eind-tak' per centrum, dat eindigt bij een met het centrum geassocieerd attractorpunt. Voor elk centrum omschrijft het attractor punt (de 'vorm of grootte' van) de geometrie van de extra dimensies bij de waarnemingshorizon. De grafische representaties van de geometrieën worden 'gespleten attractor stromen' genoemd, en er bestaat een vermoeden dat ze een bestaanscriterium vormen voor multicenter zwarte gaten. Eén klasse van multicenter zwarte gaten speelt een bijzonder belangrijke rol in deze thesis. Deze zullen als chromosomen van zwarte gaten worden geduid binnen de aangekondigde metafoor, waarvan gebruik zal worden gemaakt om het onderzoek van de auteur te bediscussiëren. Deze opmerking onderstreept het belang van gespleten attractor stromen voor dit werk.

D.2 Het genoomproject voor zwarte gaten

De metafoor die nu zal worden uiteengezet, verklaart het door de auteur verrichte onderzoek door een analogie te trekken tussen zwarte gaten binnen de snaartheorie en mensen binnen de microbiologie. Meer specifiek wordt er een voorstel gedaan van een 'genoomproject voor zwarte gaten', dat analoog is aan het menselijke genoomproject. Dit deel kan worden gezien als een voor een leek toegankelijke uiteenzetting van de hoofdstukken 3 tot 5.

Dit doctoraatsproject is gericht op het opdoen van verdere kennis over zwarte gaten. In het bijzonder werden systemen van zwarte gaten onderzocht in compactificaties van type II snaartheorieën. Het verrichte onderzoek valt binnen de context van twee grotere onderzoeksprogramma's, die allebei verbazingwekkende uitspraken doen over de kwantumnatuur van zwarte gaten.

Golffuncties voor zwarte gaten

In 2004 verscheen een publicatie van drie snaartheoretici (Ooguri, Strominger en Vafa), waarin dat de auteurs een vermoeden formuleerden, welke nu bekend staat onder de naam 'OSV hypothese'. Hoewel de volgende omschrijvingen niet volledig correct zijn, zou het voor de lezer een paar centrale ideeën begrijpbaar moeten maken. Het vermoeden is geformuleerd voor een heel specifieke klasse van zwarte gaten. Met name zijn het zwarte gaten, die met verschillend geladen branen worden gemodelleerd. Terwijl sommige braan-ladingen als magnetisch worden beschouwd, gelden andere als elektrisch. Een zwart gat is dusdanig gebouwd, dat het als superpositie van verschillende microtoestanden kan worden gerealiseerd, waarbij de totale magnetische lading voor alle toestanden vast wordt gehouden, terwijl alle mogelijke elektrische ladingen worden gerealiseerd.

In de afgelopen jaren is duidelijk geworden dat multicenter zwarte gaten centraal zijn voor de notie van entropie van zwarte gaten. Gespleten attractor stroom technieken werden ontwikkeld om het bestaan van multicenter zwarte gaten te onderzoeken, of – microscopisch – om het bestaan van gebonden toestanden van snaren en branen te onderzoeken. Het onderzoek kan in een bredere context van twee vermoedens worden gezet. De eerste is de 'OSV hypothese', die een relatie tussen de partitie functie van een zwart gat en de topologische snaren schept. De tweede is het 'fuzzball voorstel' dat een voorstel doet over de kwantumgravitationele natuur van zwarte gaten, dat hopelijk een resolutie zal blijken te zijn van de informatie paradox voor zwarte gaten. De OSV hypothese stelt dat de golffunctie van zo'n zwart gat (magnetische lading vast, variabele elektrische lading) wordt gegeven door de partitiefunctie van de topologische snaartheorie, $|\psi_{\text{blackhole}}\rangle = \mathcal{Z}_{\text{top}}$. Dus telt blijkbaar, op welke manier dan ook, topologische snaartheorie microtoestanden van zwarte gaten. (De lezer die meer wil weten over wat het woord 'topologisch' en in het bijzonder ook 'topologische snaartheorie' betekent, wordt geadviseerd om in de 'concluding discussion' te lezen, waar hij meer details zal vinden.)

Fuzzballs in plaats van zwarte gaten

Het tweede grote onderzoeksprogramma werd door Mathur en zijn medewerkers begonnen, en wordt vooral in vijf-dimensionale compactificaties van snaartheorieën bestudeerd. Het beeld van zwarte gaten, dat wordt gesuggereerd door de Algemene Relativiteitstheorie, zoals bijvoorbeeld door de Schwarzschild-oplossing, is een singulariteit (min of meer een puntje binnen het universum), waarin al de materie die een zwart gat vormt, is geconcentreerd. Dit puntje wordt dan (op een eindige afstand) omrand door de waarnemingshorizon. Zoals in de jaren zeventig werd aangetoond door Hawking en zijn medewerkers, bestaat een zwart gat echter niet voor altijd, maar het straalt en verliest daardoor materie. Men kan zich voorstellen dat de straling het zwart gat bij de waarnemingshorizon verlaat en dat zij daarom ook nooit met de materie in een directe wisselwerking kwam – dit omdat de materie op een afstand zit van de waarnemingshorizon. Dit betekent wederom dat het stralen van een zwart gat een mechanisme zou opleveren om informatie in het universum te vernietigen, een stelling die een directe tegenspraak oplevert met de tweede hoofdwet van de thermodynamica, namelijk dat de totale entropie binnen het universum alleen toe- en nooit afneemt. Het was deze ontdekking die Mathur blijkbaar de inspiratie heeft geleverd om het voorstel te doen, dat kennis van de kwantumgravitatie deze visie zal veranderen. Men zou zich volgens het fuzzball-voorstel een zwart gat beter kunnen voorstellen als een verzameling van materie, die binnen de waarnemingshorizon over het hele gebied is verspreid. Volgens het fuzzballprogramma moet men zich een zwart gat voorstellen als een superpositie van microtoestanden, welke allemaal zodanig zijn bepaald, dat de materie niet in een punt is gelokaliseerd. Als men over alle geometrieën middelt, ontstaat een zwart gat zoals men zich dat op de conventionele manier voorstelt, als een soort artefact van deze middelings-procedure, als een 'effectieve' omschrijving van het systeem. Alle individuele microstoestanden bevatten geen singulariteit (waar de materie zou gelokaliseerd zijn). Ze worden daarom ook 'glad' genoemd. Deze microtoestanden hebben de naam 'fuzzballs' gekregen (wat op hun 'fuzzy', kwantum-natuur wijst). De fuzzball-materie is verspreid is over het hele gebied tussen het midden van het systeem en de waarnemingshorizon. Als men het fuzzball-idee serieus neemt, is een zwart gat niet echt een zwart gat, maar lijkt er alleen één te zijn. In feite kan materie namelijk altijd het door de waarnemingshorizon omgrensde gebied verlaten, alleen gebeurt dit statistisch gesproken zo langzaam, dat het lijkt alsof de materie niet in staat zou zijn dat te doen.

Het genoomproject voor zwarte gaten

Het door de auteur verrichte onderzoek mag metaforisch worden beschouwd als een streven naar een 'genoomproject voor zwarte gaten'. Dit project binnen de snaartheorie zou als analoog kunnen worden bekeken aan het menselijke genoomproject binnen de microbiologie. De in deze thesis gepresenteerde resultaten kunnen beter worden vertaald naar een ontdekking van genomen voor fruitvliegen. Het bestuderen van eenvoudigere organismen binnen de microbiologie (e.g. de fruitvlieg) kan als opwarm-oefening worden bekeken voor het vormen van een beter begrip van het genoom voor mensen. Op dezelfde manier kan het

bestuderen van een simpeler, maar analoog gevormd systeem (tegenover een zwart gat), in dit geval een puntdeeltje, tot beter begrip leiden van het 'genoom voor zwarte gaten'.

Polaire toestanden: de chromosomen van zwarte gaten

De partitiefunctie van een zwart gat (van het type met vaste magnetische lading en verschillende mogelijke elektrische ladingen) is een wiskundig object, dat uit oneindig veel termen bestaat (zie wederom voor een nauwkeurigere verklaring van deze noties in de 'concluding discussion'). Hierover kan men twee cruciale conclusies trekken.

- De eerste cruciale vaststelling is, dat een partitiefunctie volledig wordt bepaald door een eindig aantal termen, welke de polaire toestanden worden genoemd.
- De tweede cruciale vaststelling houdt in dat bijna alle polaire toestanden alleen door multicenter toestanden worden gerealiseerd.

Dit betekent, dat de vraag naar het bestaan van bijna alle polaire microtoestanden kan worden beantwoord door het bestuderen van gespleten attractor stromen. Deze vaststellingen werden door Denef en Moore in 2007 gebruikt om een herformulering (en een nauwkeurigere formulering) van de OSV conjecture te vinden.

Dit maakt de weg nu vrij om de aangekondigde metafoor uiteen te zetten. Om te vergelijken: de interesse binnen de microbiologie is gericht op de complete moleculaire structuur van organismes. Het is echter voldoende om de genetische code te kennen; men kan namelijk in dit geval (bijvoorbeeld voor mensen of voor fruitvliegen) alléén naar de chromosomen kijken en deze analyseren om alle genen te klassificeren. Er bestaan in totaal een eindig aantal chromosomen, welke in zogenaamde 'homologe paren' optreden, waaronder één chromosoom afkomstig is van elke ouder. Mensen vertonen bijvoorbeeld 23 paren van chromosomen. Andere organismes hebben een verschillend aantal chromosomen, en op dezelfde manier hebben verschillende deeltjes of zwarte gaten binnen de snaartheorie een verschillend aantal polaire toestanden. Daarom wordt voorgesteld om polaire toestanden als chromosomen van zwarte gaten (of puntdeeltjes) te interpreteren. Als deze polaire toestanden worden omschreven als gebonden toestanden, worden ze gemodelleerd door een gebonden toestand van D-branen, die worden samengelijmd door snaren. Elk van die twee branen kan worden beschouwd als een chromosoom. Topologische snaartheorie telt toestanden van zo'n braan, en klassificeert dus het genoom op een chromosoom.

Hoe kan men dus de resultaten van deze thesis interpreteren? Ten eerste werd het genoom van verschillende puntdeeltjes binnen de snaartheorie bestudeerd, en exacte resultaten werden gevonden. Dit gebeurde door het bestuderen van polaire toestanden (dit zijn altijd gebonden toestanden van twee puntdeeltjes) middels gespleten attractor stromen. Ten tweede werd in deze thesis ontdekt, dat het totaal aantal toestanden, dat met een gebonden polaire toestand overeenkomt, niet als een product mag worden berekend, dat wil zeggen: niet als het product van het totaalantaal toestanden van een centrum, vermenigvuldigd met het totaal aantal toestanden van het andere centrum, maal het aantal

toestanden van de snaren, die de twee centra aan elkaar vastlijmen. Bij een nadere studie blijkt namelijk, dat de toestanden van de twee centra niet totaal onafhankelijk zijn, en er een soort wisselwerking van de twee centra plaatsvindt. Dit wordt in de metafoor als een intrachromosomale recombinatie binnen de meiose geinterpreteerd (meer daarover in de 'concluding discussion').

Een ander deel van de onderzoeksresultaten die in deze thesis werden gepresenteerd, vormt een samenhang tussen de twee geschetste grotere onderzoeksprogramma's. In hoofdstuk vijf wordt een afbeelding van vier-dimensionale polaire toestanden op vijf-dimensionale fuzzball-geometrieën uitgelegd. Dit kan vanuit de metafoor worden beschouwd als een uitleg over wat men zou kunnen bedoelen met 'chromosomen voor fuzzballs' (indien men zou beslissen om een bepaalde klasse van fuzzballs te bestuderen: vaste magnetische lading en verschillende elektrische ladingen).

D.3 Inhoudelijk overzicht van deze thesis

Introductie
In de introductie vindt de lezer eenvoudige verklaringen voor het situeren van deze thesis en verder ook discussies over theorie en experiment omtrent het onderwerp van zwarte gaten heden ten dage. Drie van de vijf aansluitende hoofdstukken leiden vanuit de grondbeginselen van de snaartheorie naar een punt waarop het afgewerkte onderzoek van de auteur aansluit.

Hoofdstuk 1: Compactificaties van de snaartheorie
Het eerste hoofdstuk zet de algemene context uiteen van het onderzoek binnen de snaartheorie. Compactificaties van type II snaartheorieën (met een bijzondere aandacht voor compactificaties op Calabi-Yau variëteiten) worden gepresenteerd vanuit het perspectief van wereldvlakken van snaren, maar ook vanuit het ruimtetijd-perspectief van de laag-energetische type II supergravitatie. De effectieve vier-dimensionale supergravitaties, hun veld-inhoud en geometrieën worden doelmatig bediscussiëerd. Ook worden een paar relevante beginselen voor branen en meer algemeen voor het supersymmetrische spectrum van toestanden in type II snaartheorieën besproken.

Hoofdstuk 2: Zwarte gaten in de snaartheorie en gespleten attractor stromen
Het tweede hoofdstuk leidt de lezer, die inmiddels bekend is met zwarte gat oplossingen, naar het modelleren van zwarte gaten met branen binnen de snaartheorie. Het attractor mechanisme evenals de techniek van gespleten attractor stromen wordt in detail uitgelegd. De essentie van dit hoofdstuk vormt de discussie van de 'split attractor flow conjecture', welke het vermoeden bevat (opgesteld door Frederik Denef en medewerkers), dat gespleten attractor stromen bestaanscriteria zijn en een classificatie toestaan voor gebonden (BPS) toestanden, niet alleen binnen de supergravitatie, maar ook binnen de hele snaartheorie. Op het einde van het hoofdstuk wordt entropie van zwarte gaten besproken.

Hoofdstuk 3: Topologische snaren, gespleten toestanden en spiegelsymmetrie
Een korte introductie en overzicht omtrent de belangrijkste principes van de topologische snaartheorie vormen het begin van het derde hoofdstuk. Daarna wordt de reeds genoemde 'OSV hypothese' gepresenteerd, die een verbinding legt tussen partitiefuncties van zwarte gaten en van de topologische snaartheorie. De centrale technieken voor het tellen van braan-toestanden voor de twee centra van gebonden toestanden, zoals door Denef en Moore ontwikkeld, worden toegelicht. Het hoofdstuk wordt afgerond met een presentatie van de gebruikte spiegelsymmetrie, die een gelijkwaardigheid postuleert van type IIA snaartheorie op een Calabi-Yau variëteit en van type IIB snaartheorie op een andere, zogenaamde spiegel-Calabi-Yau variëteit.

Hoofdstuk 4: Elliptic genera, gespleten attractor stromen en Donaldson-Thomas partitions
Het vierde hoofdstuk toont de vermoedelijk belangrijkste resultaten van het afgesloten onderzoek afkomstig uit samenwerkingen met Andrés Collinuci en Walter Van Herck. Objecten worden gemodelleerd met type IIA of IIB snaartheorie-compactificaties op Calabi-Yau variëteiten. Er worden Calabi-Yau's gekozen welk als hypervlakken in 'gewogen projectieve ruimtes' worden ingebed. Aan de ene kant worden voor een punt-deeltje met minimale magnetische (D4-braan) lading en variërende elektrische (D2/D0-braan) lading op een aantal Calabi-Yau's alle polaire toestanden geteld met attractor stromen en Donaldson-Thomas invarianten. Aan de andere kant worden verschillende niet-triviale consistentie-checks doorgevoerd voor niet-polaire toestanden. Voor kleine ladingen spelen instanton-correcties voor de centrale ladingen een belangrijke rol. Exacte centrale ladingen voor bepaalde braansystemen worden met spiegelsymmetrie gefundeerd. Vanuit een onnozele manier van kijken factoriseren moduliruimtes voor tachyonische snaren, die de twee centra aan elkaar vastknopen. De niet-triviale fibratiestructuur van de moduliruimte van een gebonden toestand wordt uitgelegd en verfijnde indices worden berekend. Een veelheid aan exacte resultaten wordt op deze manier gereproduceerd. De resultaten onderbouwen het ontwikkelde raamwerk en leveren sterk bewijsmateriaal voor een sterke versie van de 'split attractor flow tree conjecture' van Denef en Moore. Bovendien staat deze behandeling toe om 'partitions' van Donaldson-Thomas invarianten in te brengen, die tussen algemene en speciale D6-D4-D2-D0 (de ladingen van de verschillende centra) toestanden onderscheiden.

Hoofdstuk 5: 5d Fuzzball geometrieën en 4d polaire toestanden
Dit hoofdstuk presenteert onderzoeksresultaten die in samenwerking met Joris Raeymaekers, Bert Vercnocke en Walter Van Herck werden gevonden. Er werd samenhang aangetoond tussen multicenter zwarte gaten in 4d type IIA compactificaties, waarvan het bestaan door gespleten attractor stromen werd onderzocht, en 5d fuzzball geometrieën in type IIB compactificaties.

Concluding discussion
De lezer kan in deze slotbeschouwing een metaforische interpretatie vinden van het door

de auteur verrichte onderzoek. Dit stuk vertoont veel overeenkomsten met delen van de voorliggende Nederlandse samenvatting, maar bevat meer detail.

Appendix
De appendix houdt aan de ene kant vele korte definities van wiskundige structuren in, die in deze thesis voorkomen. Aan de andere kant worden enkele zeer technische berekeningen getoond, die echter voor het begrip van de hoofdtekst niet essentieel zijn. Daaronder vindt men in detail enkele bijzonder ingewikkelde attractor stromen en het tellen van overeenkomstige microtoestanden van braanladingen op de quintic Calabi-Yau. Bovendien is er een dimensionele reductie te vinden, die in het kader van het fuzzball-onderzoek werd toegepast. Ten slotte vindt de lezer voorliggende Nederlandse samenvatting.

Acknowledgments

First and foremost, my thanks goes to my Ph.D. promoter, Walter Troost. Let me thank you Walter, for giving me this great opportunity to write my Ph.D. on a topic within string theory, for leaving me the freedom and having the trust in my abilities to perform research independently on the topics of my interest; for sharing your valuable advice and intuition on physics and on other matters, especially in this last phase of my studies, but also for making me aware of the fact that seemingly easy questions in physics are the truly difficult ones, and finding answers to these brings us further. Thanks for providing me with an opportunity to experience life in another country, to learn and even to teach in another language, thereby working for a professor who is the kind of teacher every student wishes to have.

I also want to express my gratitude towards the person I have had more discussions on and shared more topics within physics than with anyone else: Andrés Collinucci. Thank you, Andrés, for supporting me throughout my Ph.D. studies, for being a great friend during these years, and at the same time the more experienced, valuable research colleague. Thank you for your feedback on my thesis, for our numerous discussions about physics and about our common passion for cultures and languages. Without you, I would never have become the physicist I believe to be.

Thank you Frederik, for confronting me with the topics of research, which led to the igniting of an initial spark which turned into a flame, that kept me going for the length of my Ph.D. studies. You pointed me in a particular direction and let me build on a small part of the wide ground you had prepared. Thanks for your feedback on parts of my research.

Also, thank you very much, Joris, for inspiring me as a researcher, and for letting me be one of your fellow researchers; for pointing me in an additional research direction within my Ph.D. studies, for sharing your experience in the field, and for your patience when waiting for some of my calculations. It was always a huge pleasure working with you.

Thank you also to the Ph.D. jury members, who have not been already mentioned: Toine, Mark and Désiré, I am thankful for your interest in my Ph.D., and for your helpfulness over the years at the institute. Special thanks goes to the external jury members, Stefan Vandoren and Markus Reineke, who made special efforts to find time and interest for my Ph.D. studies. Your participation in my preliminary defense is very much appreciated.

Thank you, Bert and Walter – it was always a great pleasure working with you. Thanks Bert, Jan and Walter, for sharing the years at the institute, as work colleagues and as friends, the numerous jokes, impressions and sketches we shared will remain a wonderful

memory of these years. Thanks to all three of you, for the time you took to give me feedback on my thesis in this last phase of my Ph.D., and on top of this for the invaluable discussions on physics and on life beyond physics. Let me also thank all other members of the institute, for your support, and for all the good times at the institute.

There are also people outside the physics community, without whose help this Ph.D. would not be what it is.

First of all, thank you Marielle, for joining me in life in Belgium, for supporting me during my studies, and for putting up with my long working hours. You were and still are the sunshine of my life. It is a blessing to know that we will continue our common path, and that we will add to the many places in Europe we have come to share in our hearts.

My thanks also goes to my mother: for your support, your valuable advice during sometimes stressful times, the inspiration you gave me to find translations for some of my ideas into more accessible terms, your interest in my research, and for the many hours you invested in helping me with usage of the beautiful English language, which is your (but also, if to a lesser extent, my) native mother tongue. I also want to thank my mother's wonderful husband, Arthur. Thank you both, for providing a homebase in the Netherlands, and Arthur, for your genuine support and advice, for your help with and guidance on practical problems, for being one (if not my main) teacher in the beautiful Dutch language, and also for your kind help with my Dutch summary.

Let me also thank my father in Switzerland, as well as his lovely wife, Aliya, for providing a homebase in Switzerland, your interest in my work, sharing your experience on writing Ph.D.'s, your sincere advice, and beyond that for many other forms of support.

Equally, I would like to thank Marielle's family, especially her parents, Johanna and Heinz Peter. Thank you for the tranquility and sense of balance you spread, for providing a second homebase in Switzerland, for your sincere advice and for other valuable support.

My thanks to my grandmother for her continuing interest in my studies, her general support, and for providing yet another homebase, this time in the United Kingdom.

Finally, I mention just a few of my many dear friends, who have marked their presence during these years, specifically in connection with my Ph.D. First of all, thank you Kay, not only for your numerous hours of support with my various little daily problems (the most prominent of which are probably the famous Linux problems), but also for being a great friend. Thank you Simon, for your valuable friendship, for your positive attitude and your complete belief in me and my capabilities, and of course, for your beautiful black hole illustrations for the poster I presented in Dalfsen, 2009. Thank you Alex, for being a great friend, for sharing time and numerous discussions on people, culture and on ideals and how they might match reality.

There are more people, without naming them explicitly, to whom I cannot give the credit they deserve, but I hope they know, that they are in my heart, just the same as the people named above. No doubt I have left someone out whom I should have named, but doubtless a dear person will also have slipped from your mind at the wrong moment too, at some point. If you feel left out, do not hesitate to tell me off. I will humbly apologize, and promise to try and make it up to you by inviting you for a glass of wine and forcing you to listen to what kind of research I engaged in during my Ph.D. studies.

Bibliography

[1] F. Denef and G. W. Moore, "Split states, entropy enigmas, holes and halos," hep-th/0702146.

[2] M. Kontsevich and Y. Soibelman, "Stability structures, motivic donaldson-thomas invariants and cluster transformations," arXiv/0811.2435.

[3] A. Collinucci and T. Wyder, "The elliptic genus from split flows and Donaldson-Thomas invariants," 0810.4301.

[4] W. Van Herck and T. Wyder, "Black Hole Meiosis," 0909.0508.

[5] J. Raeymaekers, W. Van Herck, B. Vercnocke, and T. Wyder, "5D fuzzball geometries and 4D polar states," 0805.3506.

[6] M. B. Green and J. H. Schwarz, "Anomaly Cancellation in Supersymmetric D=10 Gauge Theory and Superstring Theory," *Phys. Lett.* **B149** (1984) 117–122.

[7] E. Cremmer, B. Julia, and J. Scherk, "Supergravity theory in 11 dimensions," *Phys. Lett.* **B76** (1978) 409–412.

[8] J. Polchinski, "Dirichlet-Branes and Ramond-Ramond Charges," *Phys. Rev. Lett.* **75** (1995) 4724–4727, hep-th/9510017.

[9] E. Witten, "Bound states of strings and p-branes," *Nucl. Phys.* **B460** (1996) 335–350, hep-th/9510135.

[10] M. Gutperle and A. Strominger, "Spacelike branes," *JHEP* **04** (2002) 018, hep-th/0202210.

[11] K. Hori *et al.*, "Mirror symmetry,". Providence, USA: AMS (2003) 929 p.

[12] P. Candelas, P. S. Green, and T. Hubsch, "FINITE DISTANCES BETWEEN DISTINCT CALABI-YAU VACUA: (OTHER WORLDS ARE JUST AROUND THE CORNER)," *Phys. Rev. Lett.* **62** (1989) 1956.

[13] P. Candelas, P. S. Green, and T. Hubsch, "Rolling Among Calabi-Yau Vacua," *Nucl. Phys.* **B330** (1990) 49.

[14] B. R. Greene, "String theory on Calabi-Yau manifolds," hep-th/9702155.

[15] A. Van Proeyen, "Structure of supergravity theories," hep-th/0301005.

[16] G. Nordstrom, "On the possibility of unifying the electromagnetic and the gravitational fields," *Phys. Z.* **15** (1914) 504–506, physics/0702221.

[17] G. Nordstrom, "On a theory of electricity and gravitation," physics/0702222.

[18] G. Nordstrom, "On a possible foundation of a theory of matter," physics/0702223.

[19] T. Kaluza, "On the Problem of Unity in Physics," *Sitzungsber. Preuss. Akad. Wiss. Berlin (Math. Phys.)* **1921** (1921) 966–972.

[20] O. Klein, "Quantum theory and five-dimensional theory of relativity," *Z. Phys.* **37** (1926) 895–906.

[21] B. de Wit, P. G. Lauwers, and A. Van Proeyen, "Lagrangians of N=2 Supergravity - Matter Systems," *Nucl. Phys.* **B255** (1985) 569.

[22] L. Andrianopoli *et al.*, "N = 2 supergravity and N = 2 super Yang-Mills theory on general scalar manifolds: Symplectic covariance, gaugings and the momentum map," *J. Geom. Phys.* **23** (1997) 111–189, hep-th/9605032.

[23] K. Behrndt, I. Gaida, D. Lust, S. Mahapatra, and T. Mohaupt, "From type IIA black holes to T-dual type IIB D-instantons in N = 2, D = 4 supergravity," *Nucl. Phys.* **B508** (1997) 659–699, hep-th/9706096.

[24] T. W. Grimm and J. Louis, "The effective action of type IIA Calabi-Yau orientifolds," *Nucl. Phys.* **B718** (2005) 153–202, hep-th/0412277.

[25] A. Strominger, "SPECIAL GEOMETRY," *Commun. Math. Phys.* **133** (1990) 163–180.

[26] P. Candelas and X. de la Ossa, "MODULI SPACE OF CALABI-YAU MANIFOLDS," *Nucl. Phys.* **B355** (1991) 455–481.

[27] P. S. Aspinwall, "K3 surfaces and string duality," hep-th/9611137.

[28] B. Craps, F. Roose, W. Troost, and A. Van Proeyen, "Special Kaehler geometry: Does there exist a prepotential?," hep-th/9712092.

[29] B. Craps, F. Roose, W. Troost, and A. Van Proeyen, "What is special Kaehler geometry?," *Nucl. Phys.* **B503** (1997) 565–613, hep-th/9703082.

[30] B. Craps, F. Roose, W. Troost, and A. Van Proeyen, "The definitions of special geometry," hep-th/9606073.

[31] V. Cortes, "Special Kaehler manifolds: a survey," `math/0112114`.

[32] D. V. Alekseevsky, V. Cortes, and C. Devchand, "Special complex manifolds," *Journal of Geometry and Physics* **42** (2002) 85.

[33] D. S. Freed, "Special Kaehler manifolds," *Commun. Math. Phys.* **203** (1999) 31–52, `hep-th/9712042`.

[34] S. Ferrara, J. Scherk, and B. Zumino, "Algebraic Properties of Extended Supergravity Theories," *Nucl. Phys.* **B121** (1977) 393.

[35] C. Faber and R. Pandharipande, "Hodge integrals and gromov–witten theory," 1998.

[36] M. R. Douglas, "Branes within branes," `hep-th/9512077`.

[37] G. T. Horowitz and A. Strominger, "Black strings and P-branes," *Nucl. Phys.* **B360** (1991) 197–209.

[38] A. W. Peet, "TASI lectures on black holes in string theory," `hep-th/0008241`.

[39] K. S. Stelle, "Lectures on supergravity p-branes," `hep-th/9701088`.

[40] K. S. Stelle, "An introduction to p-branes,". Given at APCTP Winter School on Dualities of Gauge and String Theories, Seoul and Sokcho, Korea, 17-28 Feb 1997.

[41] G. W. Moore, "Arithmetic and attractors," `hep-th/9807087`.

[42] G. W. Moore, "Attractors and arithmetic," `hep-th/9807056`.

[43] F. Denef, "Supergravity flows and D-brane stability," *JHEP* **08** (2000) 050, `hep-th/0005049`.

[44] E. Witten and D. I. Olive, "Supersymmetry Algebras That Include Topological Charges," *Phys. Lett.* **B78** (1978) 97.

[45] J. Raeymaekers, "Near-horizon microstates of the D1-D5-P black hole," *JHEP* **02** (2008) 006, `0710.4912`.

[46] S. Ferrara, R. Kallosh, and A. Strominger, "N=2 extremal black holes," *Phys. Rev.* **D52** (1995) 5412–5416, `hep-th/9508072`.

[47] S. Ferrara, G. W. Gibbons, and R. Kallosh, "Black holes and critical points in moduli space," *Nucl. Phys.* **B500** (1997) 75–93, `hep-th/9702103`.

[48] A. Strominger, "Massless black holes and conifolds in string theory," *Nucl. Phys.* **B451** (1995) 96–108, `hep-th/9504090`.

[49] P. Fre, "Supersymmetry and first order equations for extremal states: Monopoles, hyperinstantons, black holes and p- branes," *Nucl. Phys. Proc. Suppl.* **57** (1997) 52–64, hep-th/9701054.

[50] T. Mohaupt, "Black hole entropy, special geometry and strings," *Fortsch. Phys.* **49** (2001) 3–161, hep-th/0007195.

[51] F. Denef, B. R. Greene, and M. Raugas, "Split attractor flows and the spectrum of BPS D-branes on the quintic," *JHEP* **05** (2001) 012, hep-th/0101135.

[52] B. Bates and F. Denef, "Exact solutions for supersymmetric stationary black hole composites," hep-th/0304094.

[53] F. Denef, "(Dis)assembling special Lagrangians," hep-th/0107152.

[54] J. de Boer, F. Denef, S. El-Showk, I. Messamah, and D. Van den Bleeken, "Black hole bound states in AdS_3xS^2," 0802.2257.

[55] F. Denef, D. Gaiotto, A. Strominger, D. Van den Bleeken, and X. Yin, "Black hole deconstruction," hep-th/0703252.

[56] D. Gaiotto, A. Strominger, and X. Yin, "Superconformal black hole quantum mechanics," *JHEP* **11** (2005) 017, hep-th/0412322.

[57] D. Gaiotto, A. Simons, A. Strominger, and X. Yin, "D0-branes in black hole attractors," hep-th/0412179.

[58] J. de Boer, S. El-Showk, I. Messamah, and D. V. d. Bleeken, "Quantizing N=2 Multicenter Solutions," 0807.4556.

[59] F. Denef, "On the correspondence between D-branes and stationary supergravity solutions of type II Calabi-Yau compactifications," hep-th/0010222.

[60] F. Denef, "Quantum quivers and Hall/hole halos," *JHEP* **10** (2002) 023, hep-th/0206072.

[61] M. R. Douglas, "D-branes, categories and N = 1 supersymmetry," *J. Math. Phys.* **42** (2001) 2818–2843, hep-th/0011017.

[62] J. M. Bardeen, B. Carter, and S. W. Hawking, "The Four laws of black hole mechanics," *Commun. Math. Phys.* **31** (1973) 161–170.

[63] A. Strominger and C. Vafa, "Microscopic Origin of the Bekenstein-Hawking Entropy," *Phys. Lett.* **B379** (1996) 99–104, hep-th/9601029.

[64] J. M. Maldacena, A. Strominger, and E. Witten, "Black hole entropy in M-theory," *JHEP* **12** (1997) 002, hep-th/9711053.

[65] J. de Boer, "Large N Elliptic Genus and AdS/CFT Correspondence," *JHEP* **05** (1999) 017, hep-th/9812240.

[66] T. Eguchi, H. Ooguri, A. Taormina, and S.-K. Yang, "Superconformal Algebras and String Compactification on Manifolds with SU(N) Holonomy," *Nucl. Phys.* **B315** (1989) 193.

[67] T. Kawai, Y. Yamada, and S.-K. Yang, "Elliptic genera and N=2 superconformal field theory," *Nucl. Phys.* **B414** (1994) 191–212, hep-th/9306096.

[68] D. Gaiotto, A. Strominger, and X. Yin, "New connections between 4D and 5D black holes," *JHEP* **02** (2006) 024, hep-th/0503217.

[69] D. Gaiotto, A. Strominger, and X. Yin, "5D black rings and 4D black holes," *JHEP* **02** (2006) 023, hep-th/0504126.

[70] M. Marino, R. Minasian, G. W. Moore, and A. Strominger, "Nonlinear instantons from supersymmetric p-branes," *JHEP* **01** (2000) 005, hep-th/9911206.

[71] A. Strominger, "Macroscopic Entropy of $N = 2$ Extremal Black Holes," *Phys. Lett.* **B383** (1996) 39–43, hep-th/9602111.

[72] M. Shmakova, "Calabi-Yau Black Holes," *Phys. Rev.* **D56** (1997) 540–544, hep-th/9612076.

[73] R. Minasian, G. W. Moore, and D. Tsimpis, "Calabi-Yau black holes and (0,4) sigma models," *Commun. Math. Phys.* **209** (2000) 325–352, hep-th/9904217.

[74] C. Vafa, "Black holes and Calabi-Yau threefolds," *Adv. Theor. Math. Phys.* **2** (1998) 207–218, hep-th/9711067.

[75] R. Dijkgraaf, J. M. Maldacena, G. W. Moore, and E. P. Verlinde, "A black hole farey tail," hep-th/0005003.

[76] R. Minasian and G. W. Moore, "K-theory and Ramond-Ramond charge," *JHEP* **11** (1997) 002, hep-th/9710230.

[77] D. S. Freed and E. Witten, "Anomalies in string theory with D-branes," hep-th/9907189.

[78] J. Manschot, "On the space of elliptic genera," *Commun. Num. Theor. Phys.* **2** (2008) 803–833, 0805.4333.

[79] D. Gaiotto and X. Yin, "Examples of M5-brane elliptic genera," *JHEP* **11** (2007) 004, hep-th/0702012.

[80] A. Dabholkar, F. Denef, G. W. Moore, and B. Pioline, "Precision counting of small black holes," *JHEP* **10** (2005) 096, hep-th/0507014.

[81] E. Witten, "Topological Sigma Models," *Commun. Math. Phys.* **118** (1988) 411.

[82] R. Dijkgraaf, H. L. Verlinde, and E. P. Verlinde, "Notes on topological string theory and 2-D quantum gravity,". Based on lectures given at Spring School on Strings and Quantum Gravity, Trieste, Italy, Apr 24 - May 2, 1990 and at Cargese Workshop on Random Surfaces, Quantum Gravity and Strings, Cargese, France, May 28 - Jun 1, 1990.

[83] D. Maulik, N. Nekrasov, A. Okounkov, and R. Pandharipande, "Gromov-witten theory and donaldson-thomas theory, i," 2003.

[84] D. Maulik, N. Nekrasov, A. Okounkov, and R. Pandharipande, "Gromov-witten theory and donaldson-thomas theory, ii," 2004.

[85] R. Dijkgraaf, C. Vafa, and E. Verlinde, "M-theory and a topological string duality," `hep-th/0602087`.

[86] R. Gopakumar and C. Vafa, "M-theory and topological strings. I," `hep-th/9809187`.

[87] R. Gopakumar and C. Vafa, "M-theory and topological strings. II," `hep-th/9812127`.

[88] A. Iqbal, N. Nekrasov, A. Okounkov, and C. Vafa, "Quantum foam and topological strings," *JHEP* **04** (2008) 011, `hep-th/0312022`.

[89] H. Ooguri, A. Strominger, and C. Vafa, "Black hole attractors and the topological string," *Phys. Rev.* **D70** (2004) 106007, `hep-th/0405146`.

[90] G. Lopes Cardoso, B. de Wit, and T. Mohaupt, "Corrections to macroscopic supersymmetric black-hole entropy," *Phys. Lett.* **B451** (1999) 309–316, `hep-th/9812082`.

[91] G. Lopes Cardoso, B. de Wit, and T. Mohaupt, "Deviations from the area law for supersymmetric black holes," *Fortsch. Phys.* **48** (2000) 49–64, `hep-th/9904005`.

[92] G. Lopes Cardoso, B. de Wit, and T. Mohaupt, "Macroscopic entropy formulae and non-holomorphic corrections for supersymmetric black holes," *Nucl. Phys.* **B567** (2000) 87–110, `hep-th/9906094`.

[93] G. Lopes Cardoso, B. de Wit, and T. Mohaupt, "Area law corrections from state counting and supergravity," *Class. Quant. Grav.* **17** (2000) 1007–1015, `hep-th/9910179`.

[94] G. Lopes Cardoso, B. de Wit, J. Kappeli, and T. Mohaupt, "Supersymmetric black hole solutions with R**2 interactions," `hep-th/0003157`.

[95] G. Lopes Cardoso, B. de Wit, J. Kappeli, and T. Mohaupt, "Stationary BPS solutions in N = 2 supergravity with R**2 interactions," *JHEP* **12** (2000) 019, hep-th/0009234.

[96] G. Lopes Cardoso, B. de Wit, J. Kappeli, and T. Mohaupt, "Examples of stationary BPS solutions in N = 2 supergravity theories with R**2-interactions," *Fortsch. Phys.* **49** (2001) 557–563, hep-th/0012232.

[97] G. Lopes Cardoso, B. de Wit, J. Kappeli, and T. Mohaupt, "BPS black holes with R**2-interactions," *Nucl. Phys. Proc. Suppl.* **102** (2001) 187–193.

[98] D. Gaiotto, A. Strominger, and X. Yin, "From AdS(3)/CFT(2) to black holes / topological strings," *JHEP* **09** (2007) 050, hep-th/0602046.

[99] D. Gaiotto, A. Strominger, and X. Yin, "The M5-brane elliptic genus: Modularity and BPS states," *JHEP* **08** (2007) 070, hep-th/0607010.

[100] C. Beasley *et al.*, "Why Z(BH) = —Z(top)—**2," hep-th/0608021.

[101] J. de Boer, M. C. N. Cheng, R. Dijkgraaf, J. Manschot, and E. Verlinde, "A farey tail for attractor black holes," *JHEP* **11** (2006) 024, hep-th/0608059.

[102] A. Dabholkar, N. Iizuka, A. Iqubal, and M. Shigemori, "Precision microstate counting of small black rings," *Phys. Rev. Lett.* **96** (2006) 071601, hep-th/0511120.

[103] D. Shih and X. Yin, "Exact Black Hole Degeneracies and the Topological String," *JHEP* **04** (2006) 034, hep-th/0508174.

[104] P. Candelas, X. C. De La Ossa, P. S. Green, and L. Parkes, "A pair of Calabi-Yau manifolds as an exactly soluble superconformal theory," *Nucl. Phys.* **B359** (1991) 21–74.

[105] D. Joyce, "On counting special Lagrangian homology 3-spheres," *Contemp. Math.* **314** (2002) 125–151, hep-th/9907013.

[106] M. Vonk, "A mini-course on topological strings," hep-th/0504147.

[107] M. Marino, "Les Houches lectures on matrix models and topological strings," hep-th/0410165.

[108] M. Marino, "Chern-Simons theory and topological strings," *Rev. Mod. Phys.* **77** (2005) 675–720, hep-th/0406005.

[109] A. Neitzke and C. Vafa, "Topological strings and their physical applications," hep-th/0410178.

[110] B. Pioline, "Lectures on on black holes, topological strings and quantum attractors," *Class. Quant. Grav.* **23** (2006) S981, hep-th/0607227.

[111] B. R. Greene and C. I. Lazaroiu, "Collapsing D-branes in Calabi-Yau moduli space. I," *Nucl. Phys.* **B604** (2001) 181–255, hep-th/0001025.

[112] A. Klemm, M. Kreuzer, E. Riegler, and E. Scheidegger, "Topological string amplitudes, complete intersection Calabi-Yau spaces and threshold corrections," *JHEP* **05** (2005) 023, hep-th/0410018.

[113] M.-x. Huang, A. Klemm, and S. Quackenbush, "Topological String Theory on Compact Calabi-Yau: Modularity and Boundary Conditions," hep-th/0612125.

[114] R. P. Thomas, "A holomorphic casson invariant for calabi-yau 3-folds, and bundles on k3 fibrations," *JOUR.DIFF.GEOM.* **54** (2000) 367.

[115] E. Witten, "Supersymmetry and Morse theory," *J. Diff. Geom.* **17** (1982) 661–692.

[116] P. Candelas, M. Lynker, and R. Schimmrigk, "Calabi-Yau Manifolds in Weighted P(4)," *Nucl. Phys.* **B341** (1990) 383–402.

[117] H. Elvang, R. Emparan, D. Mateos, and H. S. Reall, "A supersymmetric black ring," *Phys. Rev. Lett.* **93** (2004) 211302, hep-th/0407065.

[118] I. Bena and N. P. Warner, "One ring to rule them all ... and in the darkness bind them?," *Adv. Theor. Math. Phys.* **9** (2005) 667–701, hep-th/0408106.

[119] H. Elvang, R. Emparan, D. Mateos, and H. S. Reall, "Supersymmetric black rings and three-charge supertubes," *Phys. Rev.* **D71** (2005) 024033, hep-th/0408120.

[120] J. M. Maldacena and L. Maoz, "De-singularization by rotation," *JHEP* **12** (2002) 055, hep-th/0012025.

[121] O. Lunin and S. D. Mathur, "AdS/CFT duality and the black hole information paradox," *Nucl. Phys.* **B623** (2002) 342–394, hep-th/0109154.

[122] O. Lunin and S. D. Mathur, "Statistical interpretation of Bekenstein entropy for systems with a stretched horizon," *Phys. Rev. Lett.* **88** (2002) 211303, hep-th/0202072.

[123] O. Lunin, J. M. Maldacena, and L. Maoz, "Gravity solutions for the D1-D5 system with angular momentum," hep-th/0212210.

[124] S. D. Mathur, "The fuzzball proposal for black holes: An elementary review," *Fortsch. Phys.* **53** (2005) 793–827, hep-th/0502050.

[125] S. D. Mathur, "The quantum structure of black holes," *Class. Quant. Grav.* **23** (2006) R115, hep-th/0510180.

[126] S. D. Mathur, "What Exactly is the Information Paradox?," *Lect. Notes Phys.* **769** (2009) 3–48, 0803.2030.

[127] K. Skenderis and M. Taylor, "The fuzzball proposal for black holes," *Phys. Rept.* **467** (2008) 117–171, 0804.0552.

[128] S. D. Mathur, "Fuzzballs and the information paradox: a summary and conjectures," 0810.4525.

[129] S. W. Hawking, "Particle Creation by Black Holes," *Commun. Math. Phys.* **43** (1975) 199–220.

[130] O. Lunin and S. D. Mathur, "Metric of the multiply wound rotating string," *Nucl. Phys.* **B610** (2001) 49–76, hep-th/0105136.

[131] S. R. Das and S. D. Mathur, "Excitations of D-strings, Entropy and Duality," *Phys. Lett.* **B375** (1996) 103–110, hep-th/9601152.

[132] S. D. Mathur, "Emission rates, the correspondence principle and the information paradox," *Nucl. Phys.* **B529** (1998) 295–320, hep-th/9706151.

[133] B. D. Chowdhury and S. D. Mathur, "Non-extremal fuzzballs and ergoregion emission," *Class. Quant. Grav.* **26** (2009) 035006, 0810.2951.

[134] V. Balasubramanian, J. de Boer, S. El-Showk, and I. Messamah, "Black Holes as Effective Geometries," *Class. Quant. Grav.* **25** (2008) 214004, 0811.0263.

[135] H. Elvang, R. Emparan, D. Mateos, and H. S. Reall, "Supersymmetric 4D rotating black holes from 5D black rings," *JHEP* **08** (2005) 042, hep-th/0504125.

[136] I. Bena, P. Kraus, and N. P. Warner, "Black rings in Taub-NUT," *Phys. Rev.* **D72** (2005) 084019, hep-th/0504142.

[137] K. Behrndt, G. Lopes Cardoso, and S. Mahapatra, "Exploring the relation between 4D and 5D BPS solutions," *Nucl. Phys.* **B732** (2006) 200–223, hep-th/0506251.

[138] J. Ford, S. Giusto, A. Peet, and A. Saxena, "Reduction without reduction: Adding KK-monopoles to five dimensional stationary axisymmetric solutions," *Class. Quant. Grav.* **25** (2008) 075014, 0708.3823.

[139] O. Lunin, "Adding momentum to D1-D5 system," *JHEP* **04** (2004) 054, hep-th/0404006.

[140] S. Giusto, S. D. Mathur, and A. Saxena, "3-charge geometries and their CFT duals," *Nucl. Phys.* **B710** (2005) 425–463, hep-th/0406103.

[141] S. Giusto, S. D. Mathur, and A. Saxena, "Dual geometries for a set of 3-charge microstates," *Nucl. Phys.* **B701** (2004) 357–379, hep-th/0405017.

[142] S. Giusto and S. D. Mathur, "Geometry of D1-D5-P bound states," *Nucl. Phys.* **B729** (2005) 203–220, hep-th/0409067.

[143] I. Bena and P. Kraus, "Microstates of the D1-D5-KK system," *Phys. Rev.* **D72** (2005) 025007, hep-th/0503053.

[144] A. Saxena, G. Potvin, S. Giusto, and A. W. Peet, "Smooth geometries with four charges in four dimensions," *JHEP* **04** (2006) 010, hep-th/0509214.

[145] I. Bena and N. P. Warner, "Bubbling supertubes and foaming black holes," *Phys. Rev.* **D74** (2006) 066001, hep-th/0505166.

[146] P. Berglund, E. G. Gimon, and T. S. Levi, "Supergravity microstates for BPS black holes and black rings," *JHEP* **06** (2006) 007, hep-th/0505167.

[147] I. Bena, C.-W. Wang, and N. P. Warner, "The foaming three-charge black hole," *Phys. Rev.* **D75** (2007) 124026, hep-th/0604110.

[148] V. Balasubramanian, E. G. Gimon, and T. S. Levi, "Four Dimensional Black Hole Microstates: From D-branes to Spacetime Foam," *JHEP* **01** (2008) 056, hep-th/0606118.

[149] I. Bena, C.-W. Wang, and N. P. Warner, "Mergers and Typical Black Hole Microstates," *JHEP* **11** (2006) 042, hep-th/0608217.

[150] M. C. N. Cheng, "More bubbling solutions," *JHEP* **03** (2007) 070, hep-th/0611156.

[151] I. Bena, N. Bobev, and N. P. Warner, "Bubbles on Manifolds with a U(1) Isometry," *JHEP* **08** (2007) 004, 0705.3641.

[152] E. G. Gimon and T. S. Levi, "Black Ring Deconstruction," *JHEP* **04** (2008) 098, 0706.3394.

[153] I. Bena, C.-W. Wang, and N. P. Warner, "Plumbing the Abyss: Black Ring Microstates," *JHEP* **07** (2008) 019, 0706.3786.

[154] I. Bena and N. P. Warner, "Black holes, black rings and their microstates," *Lect. Notes Phys.* **755** (2008) 1–92, hep-th/0701216.

[155] M. J. Duff, J. T. Liu, and J. Rahmfeld, "Four-dimensional string-string-string triality," *Nucl. Phys.* **B459** (1996) 125–159, hep-th/9508094.

[156] K. Behrndt, R. Kallosh, J. Rahmfeld, M. Shmakova, and W. K. Wong, "STU black holes and string triality," *Phys. Rev.* **D54** (1996) 6293–6301, hep-th/9608059.

[157] M. Billo *et al.*, "The 0-brane action in a general D = 4 supergravity background," *Class. Quant. Grav.* **16** (1999) 2335–2358, hep-th/9902100.

[158] I. Bena, N. Bobev, and N. P. Warner, "Spectral Flow, and the Spectrum of Multi-Center Solutions," *Phys. Rev.* **D77** (2008) 125025, 0803.1203.

[159] J. B. Gutowski, D. Martelli, and H. S. Reall, "All supersymmetric solutions of minimal supergravity in six dimensions," *Class. Quant. Grav.* **20** (2003) 5049–5078, hep-th/0306235.

[160] N. Iizuka and M. Shigemori, "A note on D1-D5-J system and 5D small black ring," *JHEP* **08** (2005) 100, hep-th/0506215.

[161] V. Balasubramanian, P. Kraus, and M. Shigemori, "Massless black holes and black rings as effective geometries of the D1-D5 system," *Class. Quant. Grav.* **22** (2005) 4803–4838, hep-th/0508110.

[162] J. R. David, G. Mandal, and S. R. Wadia, "Microscopic formulation of black holes in string theory," *Phys. Rept.* **369** (2002) 549–686, hep-th/0203048.

[163] A. Sen, "Extremal black holes and elementary string states," *Mod. Phys. Lett.* **A10** (1995) 2081–2094, hep-th/9504147.

[164] A. Dabholkar, N. Iizuka, A. Iqubal, A. Sen, and M. Shigemori, "Spinning strings as small black rings," *JHEP* **04** (2007) 017, hep-th/0611166.

[165] K. Skenderis and M. Taylor, "Fuzzball solutions and D1-D5 microstates," *Phys. Rev. Lett.* **98** (2007) 071601, hep-th/0609154.

[166] I. Kanitscheider, K. Skenderis, and M. Taylor, "Holographic anatomy of fuzzballs," *JHEP* **04** (2007) 023, hep-th/0611171.

[167] V. Bouchard, "Lectures on complex geometry, Calabi-Yau manifolds and toric geometry," hep-th/0702063.

[168] J. Maharana and J. H. Schwarz, "Noncompact symmetries in string theory," *Nucl. Phys.* **B390** (1993) 3–32, hep-th/9207016.

[169] A. Sen, "Strong - weak coupling duality in four-dimensional string theory," *Int. J. Mod. Phys.* **A9** (1994) 3707–3750, hep-th/9402002.